
THE UNIVERSITY
*of* EDINBURGH

This thesis has been submitted in fulfilment of the requirements for a postgraduate degree (e.g. PhD, MPhil, DClinPsychol) at the University of Edinburgh. Please note the following terms and conditions of use:

This work is protected by copyright and other intellectual property rights, which are retained by the thesis author, unless otherwise stated.
A copy can be downloaded for personal non-commercial research or study, without prior permission or charge.
This thesis cannot be reproduced or quoted extensively from without first obtaining permission in writing from the author.
The content must not be changed in any way or sold commercially in any format or medium without the formal permission of the author.
When referring to this work, full bibliographic details including the author, title, awarding institution and date of the thesis must be given.

# The role of heat shock protein 90 in modulating ischemia-reperfusion injury in the kidney

**Stephen O'Neill**

PhD – The University of Edinburgh – 2015

# Contents

**Preface** ..... **i**
**Acknowledgements** ..... **ii**
**Abstract** ..... **iii**
**Chapter 1: Introduction** ..... **6**
1.1 End-stage renal disease ..... 6
1.2 Kidney transplantation ..... 6
1.3 DCD transplantation ..... 9
1.4 Ischemia-reperfusion injury ..... 11
1.5 Acute ischemic kidney injury ..... 11
1.6 Preconditioning ..... 12
1.7 Other therapies ..... 12
1.8 The potential for synergy of treatments and emerging therapies ..... 15
1.9 Heat shock proteins ..... 16
1.9.1 Heat shock response ..... 18
1.9.2 Hsp regulation ..... 19
1.10 Hsp90 ..... 21
1.11 Hsp90 inhibitors ..... 22
1.11.1 Routes of administration and dosing regimens ..... 25
1.11.2 Toxicity profile of Hsp90 inhibitors ..... 26
1.11.3 Isoform-selective Hsp90 inhibitors ..... 27
1.11.4 AT13387 ..... 28
1.12 The role of Hsps in modulating IRI in the kidney ..... 30
1.13 Mechanisms of protection offered by Hsp90 inhibition ..... 32
1.13.1 The inhibition of pro-inflammatory transcription factors ..... 32
1.13.2 The up-regulation of anti-inflammatory proteins ..... 35
1.14 Cellular and molecular mechanisms of protection by Hsp70 ..... 37
1.14.1 Correction of protein conformation ..... 39
1.14.2 Intracellular protection and cytoskeletal stabilisation ..... 39
1.14.3 Anti-inflammatory effects ..... 40
1.14.4 Requirement in autophagy ..... 41
1.14.5 Anti-apoptotic effects ..... 41

1.14.6 Influence on the phenotype of mononuclear phagocytes ..... 42
1.15 Pharmacological modulation of Hsp70 expression ..... 43
1.16 The role of immunity and TLR4 ..... 44
1.16.1 TLR4 and renal IRI ..... 45
1.17 Hsp90 inhibitors and immune regulation ..... 47
1.17.1 Interaction of Hsp and TLRs ..... 48
1.17.2 Extracellular Hsp70 and potential pro-inflammatory effects ..... 50
1.18 Inflammaging ..... 51
1.19 Hsp90 and maintenance of vascular tone ..... 52
1.20 Lymphocytes and renal IRI ..... 53
1.20.1 Tregs and renal IRI ..... 54
1.20.2 Hsp70 interaction with Tregs in renal IRI ..... 55
1.21 Translational perspective ..... 60
1.21.1 Preconditioning and prevention of IRI ..... 60
1.21.2 Enhancing recovery following IRI ..... 63
1.22 Summary ..... 66
1.23 Hypotheses ..... 68
1.23.1 In vitro ..... 68
1.23.2 In vivo ..... 68
**Chapter 2: Materials and methods ..... 69**
2.1 Cell culture ..... 69
2.2 Animals ..... 69
2.3 Drugs ..... 70
2.4 Reagents ..... 70
2.5 Transfection ..... 71
2.6 Western blot ..... 71
2.7 Flow Cytometry ..... 72
2.8 ELISA ..... 72
2.8.1 Phosphorylated IκBα (S32/S36) ELISA ..... 72
2.8.2 Hsp70 ELISA ..... 73
2.9 Assays ..... 73
2.9.1 Luciferase assay ..... 73
2.9.2 Crystal violet cell viability assay ..... 73

2.9.3 SEAP assay ..... 74
2.10 Human cytokine array panel ..... 74
2.11 Renal IRI model ..... 75
2.12 Renal transplantation model ..... 76
2.13 Tissue collection ..... 76
2.14 Lung Digestion and cytometric analysis ..... 77
2.15 BAL analysis ..... 77
2.16 Immunohistochemistry ..... 78
2.17 Scoring of morphological kidney injury ..... 78
2.18 Serum creatinine determination ..... 79
2.19 Murine cytokine array panel ..... 79
2.20 Real-time reverse transcriptase–PCR ..... 80
2.21 Statistical analysis ..... 80
2.22 Power calculation ..... 80
**Chapter 3: AT13387 represses TLR4-mediated NF-κB activation resulting in reduced pro-inflammatory cytokine release ..... 83**
3.1 Background ..... 83
3.2 HEK293 cells do not express TLR4 ..... 83
3.3 Endotoxin-free hyaluronan is a sterile TLR4-specific ligand in HEK293 cells expressing TLR4 ..... 87
3.4 AT13387 and 17-DMAG pre-treatment leads to repression of TLR4-mediated NF-κB activation ..... 91
3.5 Pre-treatment with AT13387 and 17-DMAG leads to loss of the IKK complex ..... 93
3.6 IKKα is degraded by autophagy following treatment with AT13387 and 17-DMAG ..... 95
3.7 AICAR partially restores NF-κB activity in AT13387 and 17-DMAG pre-treated cells following hyaluronan stimulation ..... 98
3.8 AT13387 and 17-DMAG pre-treatment reduces TLR4-mediated pro-inflammatory cytokine release ..... 100
3.9 Pre-treatment with AT13387 and 17-DMAG reduces non-TLR4-specific activation ..... 102
3.10 Pre-treatment with AT13387 and 17-DMAG reduces non-sterile NF-κB activation ..... 107
3.11 Summary ..... 112
3.12 Discussion ..... 112

3.12.1 Limitations ..... 112
3.12.2 Variability ..... 113
3.12.3 Reproducibility ..... 114
**Chapter 4: AT13387 enables cellular survival following oxidative stress ..... 115**
4.1 Background ..... 115
4.2 Oxidative stress reduces cell viability ..... 115
4.3 Hsp90 inhibition increases cell viability following oxidative stress ..... 117
4.4 Summary ..... 119
4.5 Discussion ..... 119
4.5.1 Limitations ..... 119
4.5.2 Variability ..... 120
4.5.3 Reproducibility ..... 120
**Chapter 5: AT13387 leads to induction of renal Hsp70 in mice ..... 121**
5.1 Background ..... 121
5.2 AT13387 increases Hsp70 expression in the kidney of FVB/n mice ..... 121
5.3 AT13387 increases Hsp70 expression in the kidney of Balb/c and Balb/c SCID mice ..... 125
5.4 Summary ..... 127
5.5 Discussion ..... 127
5.5.1 Limitations ..... 127
5.5.2 Variability ..... 128
5.5.3 Reproducibility ..... 128
**Chapter 6: AT13387 pre-treatment results in functional and morphological protection from renal IRI ..... 129**
6.1 Background ..... 129
6.2 Establishing a renal IRI model in FVB/n mice ..... 129
6.3 AT13387 pre-treatment reduces functional and morphological kidney injury following renal IRI in FVB/n mice ..... 132
6.4 AT13387 pre-treatment reduces the expression of TLR4 and inflammatory chemokines in the kidney following renal IRI ..... 136
6.5 Summary ..... 139
6.6 Discussion ..... 139
6.6.1 Limitations ..... 139
6.6.2 Variability ..... 140

6.6.3 Reproducibility ..... 141
**Chapter 7: The protection afforded from renal IRI by AT13387 is lymphocyte-dependent ..... 143**
7.1 Background ..... 143
7.2 AT13387 reduces renal IRI in Balb/c mice but not Balb/c SCID mice ..... 143
7.3 Tregs in the spleen following AT13387 treatment ..... 148
7.4 T-lymphocytes in the kidney following renal IRI ..... 151
7.5 Summary ..... 154
7.6 Discussion ..... 154
7.6.1 Limitations ..... 154
7.6.2 Variability ..... 155
7.6.3 Reproducibility ..... 156
**Chapter 8: AT13387 reduces lung injury secondary to renal IRI ..... 157**
8.1 Background ..... 157
8.2 Renal IRI causes secondary lung injury ..... 157
8.3 AT13387 increases Hsp70 expression in the lung ..... 158
8.4 Establishing the model for assessing lung injury following pre-treatment with AT13387 and renal IRI ..... 161
8.5 AT13387 reduces lung injury secondary to renal IRI ..... 165
8.6 Summary ..... 170
8.7 Discussion ..... 170
8.7.1 Limitations ..... 170
8.7.2 Variability ..... 171
8.7.3 Reproducibility ..... 171
**Chapter 9: Recipient treatment with AT13387 reduces renal IRI in transplantation ..... 173**
9.1 Background ..... 173
9.2 Recipient treatment with AT13387 is feasible in a renal transplant model 173
9.3 AT13387 reduces secondary lung injury in renal transplantation ..... 176
9.4 Summary ..... 180
9.5 Discussion ..... 180
9.5.1 Limitations ..... 180
9.5.2 Variability ..... 181
9.5.3 Reproducibility ..... 181

**Chapter 10: Discussion ..... 183**
10.1 Background ..... 183
10.2 *In vitro* data ..... 183
10.2.1 Chapter 3 ..... 183
10.2.2 Chapter 4 ..... 187
10.3 *In vivo* data ..... 189
10.3.1 Chapter 5 ..... 189
10.3.2 Chapter 6 ..... 190
10.3.3 Chapter 7 ..... 192
10.3.4 Chapter 8 ..... 196
10.3.5 Chapter 9 ..... 197
10.4 Published evidence ..... 200
10.5 Context ..... 202
10.6 Summary ..... 206
**References ..... 207**
**Abbreviations ..... 227**
**Presentations of data from this thesis ..... 229**
**Publication of data from this thesis ..... 230**

# Figures

Figure 1.1 The number of renal transplants from each transplant source and the total number on the transplant list at the end of each year in the UK ..... 8

Figure 1.2 HSF1 regulation by Hsp90 ..... 20

Figure 1.3 Structure of Hsp90 inhibitors..... 24

Figure 1.4 Structure of AT13387 ..... 29

Figure 1.5 Repression of TLR4-mediated NF-κB activation by Hsp90 inhibition ... 34

Figure 1.6 Hsp70 induction by Hsp90 inhibition..... 36

Figure 1.7 Mechanisms of Hsp70 mediated protection from renal IRI ..... 38

Figure 1.8 Putative pathway of Hsp-regulation of Hsp70, Treg expansion and suppression of renal IRI ..... 58

Figure 3.1 TLR4 flow cytometry on HEK293 cells..... 85

Figure 3.2 TLR4 flow cytometry on TLR4 transfected HEK293 cells..... 86

Figure 3.3 Luciferase assay to determine NF-κB activity following NF-κB transfection and hyaluronan stimulation in HEK293 and HEK293-TLR4 cells 88

Figure 3.4 SEAP assay to determine NF-κB activity following a ligand dose response assay using hyaluronan stimulation in HEK293-TLR4-NF-κB cells . 89

Figure 3.5 SEAP assay to determine NF-κB activity following hyaluronan stimulation with and without the presence of polymyxin B in HEK293-TLR4-NF-κB cells ..... 90

Figure 3.6 NF-κB activity determined by SEAP assay following pre-treatment with AT13387 or 17-DMAG and hyaluronan stimulation in HEK293-TLR4-NF-κB cells ..... 92

Figure 3.7 IKKα, IKKβ and NEMO levels on Western blotting following AT13387 or 17-DMAG pre-treatment and hyaluronan stimulation in HEK293-TLR4-NF-κB cells ..... 94

Figure 3.8 IKKα, IKKβ and NEMO levels on Western blotting following AT13387 or 17-DMAG treatment with and without pre-incubation/presence of AICAR in HEK293-TLR4-NF-κB cells ..... 96

Figure 3.9 IKKα, IKKβ and NEMO levels on Western blotting following AT13387 or 17-DMAG pre-treatment with and without pre-incubation/presence of AICAR and hyaluronan stimulation in HEK293-TLR4-NF-κB cells ..... 97

Figure 3.10 SEAP assay to determine NF-κB activity following pre-treatment with AT13387 or 17-DMAG with and without pre-incubation/presence of AICAR and hyaluronan stimulation in HEK293-TLR4-NF-κB cells..... 99

Figure 3.11 Cytokine expression following AT13387 or 17-DMAG pre-treatment and hyaluronan stimulation in HEK293-TLR4-NF-κB cells..... 101

Figure 3.12 Luciferase assay to determine NF-κB activity following NF-κB transfection and a ligand dose response assay using TNFα stimulation in HEK293 cells ..... 103

Figure 3.13 Luciferase assay to determine NF-κB activity following NF-κB transfection, pre-treatment with AT13387 or 17-DMAG and TNFα stimulation in HEK293 cells ..... 104

Figure 3.14 ELISA to determine phosphorylated IκBα levels following pre-treatment with AT13387 or 17-DMAG and TNFα stimulation in HEK293-TLR4-NF-κB cells ..... 105

Figure 3.15 SEAP assay to determine NF-κB activity following pre-treatment with AT13387 or 17-DMAG and TNFα stimulation in HEK293-TLR4-NF-κB cells ..... 106

Figure 3.16 SEAP assay to determine NF-κB activity following a ligand dose response assay using LPS stimulation in HEK293-TLR4-NF-κB cells ..... 108

Figure 3.17 SEAP assay to determine NF-κB activity following pre-treatment with AT13387 or 17-DMAG and LPS stimulation in HEK293-TLR4-NF-κB cells ..... 109

Figure 3.18 IKKα, IKKβ and NEMO levels on Western blotting following AT13387 or 17-DMAG pre-treatment and LPS stimulation in HEK293-TLR4-NF-κB cells ..... 110

Figure 3.19 Cytokine expression following AT13387 or 17-DMAG pre-treatment and LPS stimulation in HEK293-TLR4-NF-κB cells..... 111

Figure 4.1 Cell viability determined by crystal violet assay following oxidative stress with hydrogen peroxide in HEK293-TLR4 cells ..... 116

Figure 4.2 Crystal violet assay to determine cell viability following pre-treatment with AT13387 or 17-DMAG and oxidative stress with hydrogen peroxide in HEK293-TLR4 cells ..... 118

Figure 5.1 Renal Hsp70 expression following AT13387 or vehicle treatment on ELISA in FVB/n mice ..... 122

Figure 5.2 Renal Hsp70 expression following AT13387 or vehicle pre-treatment in the control kidney on ELISA in FVB/n mice ..... 123

Figure 5.3 Renal Hsp70 expression following vehicle treatment in the outer stripe of the outer medulla of the kidney on immunohistochemistry in FVB/n mice .... 124

Figure 5.4 Renal Hsp70 expression following AT13387 treatment in the outer stripe of the outer medulla of the kidney on immunohistochemistry in FVB/n mice 124

Figure 5.5 Renal Hsp70 expression following AT13387 or vehicle pre-treatment in the control kidney on ELISA in Balb/c and Balb/c SCID mice ..... 126

Figure 6.1 Serum creatinine 24 h following renal IRI in FVB/n mice ..... 131

Figure 6.2 Serum creatinine following AT13387 or vehicle pre-treatment and 24 h following renal IRI in FVB/n mice ..... 133

Figure 6.3 Tubular necrosis score following AT13387 or vehicle pre-treatment and 24 h following renal IRI in FVB/n mice ..... 134

Figure 6.4 Morphological kidney injury following pre-treatment with vehicle and 24 h following renal IRI in FVB/n mice ..... 135

Figure 6.5 Morphological kidney injury following pre-treatment with AT13387 and 24 h following renal IRI in FVB/n mice ..... 135

Figure 6.6 Renal TLR4 expression following AT13387 or vehicle pre-treatment and 24 h following renal IRI in FVB/n mice ..... 137

Figure 6.7 Renal cytokine expression following AT13387 or vehicle pre-treatment and 24 h following renal IRI in FVB/n mice ..... 138

Figure 7.1 Serum creatinine following AT13387 or vehicle pre-treatment and 24 h following renal IRI in Balb/c and Balb/c SCID mice ..... 145

Figure 7.2 Tubular necrosis score following AT13387 or vehicle pre-treatment and 24 h following renal IRI in Balb/c mice ..... 146

Figure 7.3 Morphological kidney injury following pre-treatment with vehicle and 24 h following renal IRI in Balb/c mice ..... 147

Figure 7.4 Morphological kidney injury following pre-treatment with AT13387 and 24 h following renal IRI in Balb/c mice ..... 147

Figure 7.5 Foxp3 expression on immunohistochemistry in the spleen of Balb/c mice following vehicle treatment ..... 149

Figure 7.6 Foxp3 expression on immunohistochemistry in the spleen of Balb/c mice following AT13387 treatment ..... 149

Figure 7.7 Splenic Foxp3 expression on immunohistochemistry following AT13387 or vehicle treatment in Balb/c mice ..... 150

Figure 7.8 Renal CD3 expression on immunohistochemistry following vehicle pre-treatment and 24 h following renal IRI in Balb/c mice ..... 152

Figure 7.9 Renal CD3 expression on immunohistochemistry, following AT13387 pre-treatment and 24 h following renal IRI in Balb/c mice ..... 152

Figure 7.10 Renal CD3 expression on immunohistochemistry following AT13387 or vehicle pre-treatment and 24 h following renal IRI in Balb/c mice ..... 153

Figure 8.1 Hsp70 expression in the lung 6 h following AT13387 or vehicle treatment on ELISA in Balb/c mice ..... 159

Figure 8.2 Hsp70 expression in the lung up to 24 h following AT13387 or vehicle treatment on ELISA in Balb/c mice ..... 160

Figure 8.3 Renal Hsp70 expression following AT13387 or vehicle pre-treatment in the control kidney on ELISA in Balb/c SCID mice ..... 162

Figure 8.4 Serum creatinine following AT13387 or vehicle pre-treatment and 24 h following renal IRI in Balb/c SCID mice ..... 163

Figure 8.5 BAL cell count following AT13387 or vehicle pre-treatment and 24 h following renal IRI in Balb/c SCID mice ..... 164

Figure 8.6 Interstitial neutrophils in the lungs following AT13387 or vehicle pre-treatment and 24 h following renal IRI in Balb/c SCID mice ..... 166

Figure 8.7 BAL cell differential following AT13387 or vehicle pre-treatment and 24 h following renal IRI in Balb/c SCID mice ..... 167

Figure 8.8 BAL cytospin following vehicle pre-treatment and 24 h following renal IRI in Balb/c SCID mice ..... 168

Figure 8.9 BAL cytospin following AT13387 pre-treatment and 24 h following renal IRI in Balb/c SCID mice ..... 168

Figure 8.10 BAL following AT13387 or vehicle pre-treatment and 24 h following renal IRI in Balb/c SCID mice ..... 169

Figure 9.1 Tubular necrosis score in the transplanted kidney following AT13387 or vehicle pre-treatment of recipient Balb/c mice and 24 h following renal transplantation ..... 174

Figure 9.2 Morphological kidney injury in the transplanted kidney following pre-treatment of recipient Balb/c mice with vehicle and 24 h following renal transplantation ..... 175

Figure 9.3 Morphological kidney injury in the transplanted kidney following pre-treatment of recipient Balb/c mice with AT13387 and 24 h following renal transplantation ..... 175

Figure 9.4 BAL cell count following AT13387 or vehicle pre-treatment and 24 h following renal transplantation in Balb/c mice. ..... 177

Figure 9.5 BAL cell differential following AT13387 or vehicle pre-treatment and 24 h following renal transplantation in Balb/c mice ..... 178

Figure 9.6 Interstitial neutrophils in the lungs following AT13387 or vehicle pre-treatment and 24 h following renal transplantation in Balb/c mice ..... 179

# Tables

Table 1.1 Summary of previous and on going clinical trials of pharmacological agents to prevent IRI in renal transplant recipients..... 14

Table 1.2 Summary of the functions of the various mammalian Hsp families..... 17

Table 1.3 Protection in renal transplantation-relevant models associated with Hsp up-regulation ..... 31

Table 2.1 Power calculation for animal experiments..... 82

# Preface

All of the written work herein is my own. Any contribution made by others to the experimental work is acknowledged in the text. This work has not previously been submitted for any other degree or qualification. The heat shock protein 90 inhibitor AT13387, was kindly provided by Astex Pharmaceuticals. No funding was received from Astex Pharmaceuticals for the research performed, and there are no competing financial interests to declare. The research was funded by grants from Tenovus Scotland and The Royal College of Surgeons Edinburgh. The Maurice Wohl Research Fellowship from the Royal College of Surgeons Edinburgh, The Mason Medical Research Trust Fellowship and a Medical Research Council Clinical Research Training Fellowship provided further support in terms of salary and running costs.

Stephen O'Neill

July 2015

# Acknowledgements

This work could not have been completed without the patience, teaching, training and technical support provided by Mr Jim Black and Miss Kathryn Sangster.

I have been fortunate during the course of this research to collaborate with many talented colleagues and I particularly enjoyed working with George Tse and Duncan Humphries who both contributed significantly to the experiments performed in the later chapters of this thesis.

This thesis would not have been possible without the opportunity kindly granted to me by my supervisors, Professor Jeremy Hughes, Professor Jim Ross, Professor Steve Wigmore and most of all Mr Ewen Harrison who has also been an excellent mentor to me during this period. Many thanks for your ideas, knowledge, expertise and encouragement.

Finally, I would like to thank my wife Michelle for her unwavering personal support, advice, humour and care of our beautiful daughter Violet, who continues to inspire me everyday.

Stephen O'Neill

July 2015

# Abstract

Kidney transplantation is the gold standard treatment for end-stage renal disease. Renal ischemia-reperfusion injury is an unavoidable consequence of the transplantation procedure and is responsible for delayed graft function and poorer long-term outcomes.

Pharmacological inhibition of heat shock protein 90 is a preconditioning strategy that has previously been shown to reduce renal ischemia-reperfusion injury. However, the clinical application of heat shock protein 90 inhibitors is limited by their toxicity profile and the exact mechanisms of protection conferred are unknown.

The aims of this thesis were to establish mechanisms of protection offered by these drugs and investigate a less toxic analogue that has the potential to be safely translated into human studies. AT13387 is a novel small molecule heat shock protein 90 inhibitor with a low toxicity profile, which is being evaluated in phase II studies in oncology and therefore has excellent translational potential in the context of transplantation.

Heat shock protein 90 inhibition up-regulates protective heat shock proteins (especially heat shock protein 70) and potentially down-regulates NF-κB activity by disruption of the IκB kinase complex. Toll-like receptor 4 is a further regulator of NF-κB activity and studies have suggested that Toll-like receptor 4 plays a dominant role in mediating kidney damage following ischemia-reperfusion injury.

To explore potential molecular mechanisms of protection, human embryonic kidney cells were pre-treated with AT13387 and exposed to endotoxin-free hyaluronan to stimulate sterile Toll-like receptor 4-specific NF-κB activation. AT13387-treatment resulted in breakdown of IκB kinase, which abolished Toll-like receptor 4-mediated NF-κB activation by hyaluronan. Inhibition of autophagy prevented IκB kinase-α degradation by heat shock protein 90 inhibition and resulted in regain of NF-κB activity by hyaluronan. In subsequent investigations, AT13387 decreased pro-inflammatory cytokine release following hyaluronan stimulation and increased cell viability in an *in vitro* model of oxidative stress.

In mice, AT13387 induced heat shock protein 70 expression in the kidney. AT13387 pre-treatment then significantly reduced kidney injury following renal ischemia-reperfusion injury. In contrast, in severe combined immunodeficient mice, AT13387 no longer reduced kidney injury from renal ischemia-reperfusion injury. This emphasises the potential importance of the adaptive immune system in the protective effect of this agent. This resonates with reports of heat shock protein 70 up-regulation in the context of heat preconditioning, which leads to renal protection from renal ischemia-reperfusion injury that is lymphocyte-dependent.

Secondary lung injury is an additional consequence of renal ischemia-reperfusion injury. In further experiments, pre-treatment with AT13387 again did not reduce kidney injury following renal ischemia-reperfusion injury in severe combined immunodeficient mice. However, AT13387 did reduce secondary lung injury. This lung protective effect may have been related to heat shock protein 70 up-regulation in the lungs by AT13387.

A rationale for enhancing recovery, following renal ischemia-reperfusion injury, by inhibiting heat shock protein 90 was then sought. This investigation was undertaken

in order to broaden the range of the available therapies to a wider group of patients including renal transplant recipients. AT13387 pre-treatment of the recipient mice preceded an isograft renal transplantation with a kidney harvested from a treatment naive mouse and cold stored for 4 hours. Although a significant reduction in tubular necrosis was not demonstrated following AT13387 treatment, the feasibility of the treatment strategy was demonstrated and interestingly lung injury secondary to transplantation was reduced.

This thesis therefore highlights AT13387 as a new agent with the potential of reducing kidney injury and secondary lung injury following renal ischemia-reperfusion injury. The findings also demonstrate that the mechanisms of protection offered by this drug may involve the adaptive immune system. In addition to the induction of heat shock protein 70 expression in the kidney and repression of Toll-like receptor 4-mediated NF-κB signalling through breakdown of IκB kinase.

# Chapter 1: Introduction

## 1.1 End-stage renal disease

End-stage renal disease (ESRD) is defined as an irreversible decline in kidney function that is severe enough to be fatal in the absence of renal replacement therapy (either dialysis or kidney transplantation) [1]. In 2011 the incidence rate of ESRD in the USA was 357 per million population [2], a figure that has risen rapidly and is unlikely to reach steady state for another 20 years [3].

## 1.2 Kidney transplantation

During 2013 the incidence of renal replacement therapy in the UK was 109 per million population and by the end of the year there were 56,940 adult patients receiving renal replacement therapy [4, 5]. Renal transplantation is currently the best available treatment for ESRD as it not only offers freedom from dialysis, it also improves survival, provides better quality of life and is more cost effective [6-9]. Patients who are eligible for a renal transplant but do not have a living donor available must wait for a suitable kidney to be offered from a deceased donor. There were 5881 patients active on the UK kidney transplant waiting list at the end of 2013/2014 and 3233 renal transplants were performed. The UK median waiting time for a renal transplant is over three years [10]. Over the past forty years transplanted kidneys have come primarily from donation after brain death (DBD) donors [11]. Since current donor organ supply falls short of demand, efforts have been made to increase the donor pool using kidneys from donation after circulatory death (DCD) donors. Increases in overall renal transplant number in the last 10 years have been due largely to increases in the use of DCD donors. During 2013/14 in the UK, renal transplantation from DCD donors accounted for 38% of all deceased donor kidney

transplants compared to 7% in 2003/4 [10, 12]. As a result of this increase in DCD donors, and a rise in living donors, the gap between organ supply and demand has actually decreased (Figure 1.1).

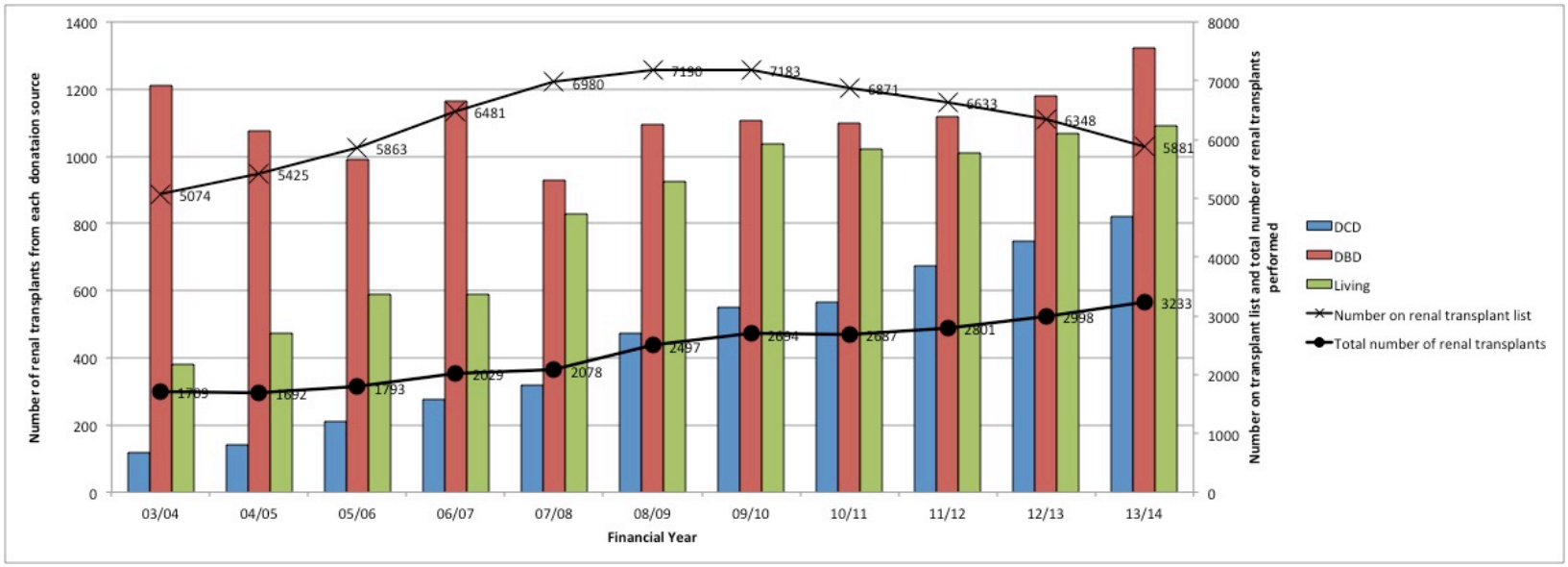


**Figure 1.1 The number of renal transplants from each transplant source and the total number on the transplant list at the end of each year in the UK**

Source: UK Transplant Registry; http://www.organdonation.nhs.uk/statistics/transplant_activity_report/.

Abbreviations: DCD – donation after circulatory death, DBD – donation after brain death.

## 1.3 DCD transplantation

Controlled DCD occurs after death that follows the planned withdrawal of life-sustaining treatments that are felt to be of no overall benefit to a critically ill person who does not fulfill the criteria of brain stem death. This is typically performed in patients on intensive care units who are considered to have suffered a non-recoverable brain injury. Uncontrolled DCD takes place after an unexpected cardiac arrest from which an individual cannot or should not be resuscitated. This usually occurs when a patient sustains an out of hospital cardiac arrest or there is unsuccessful resuscitation, typically in an emergency department. It is associated with even greater ischemic insult to kidneys than controlled DCD. Whilst uncontrolled DCD represents a further potential source of organs, this type of donation is still very rare and until the last year there were no active programs using this source of organs in the UK.

Before controlled DCD takes place, assent is obtained from the donor's family for life-sustaining treatments, including ventilation, to be withdrawn. In UK practice, pre-mortem procedures such as vascular cannulation and heparin administration are prohibited in DCD donors but these maneuvers can be utilised in the United States [13]. After treatment withdrawal, an "agonal" phase with increasing hypotension and hypoxia occurs for a variable time period before circulatory arrest. There is then a 5-minute mandatory standoff period prior to confirmation of death. Following verification of death, the donor is transferred to the operating theatre and a rapid laparotomy is carried out, followed by *in situ* perfusion with cold preservation fluid and organ recovery [14].

In all kidney grafts, the technical process of organ recovery and cold storage, leads to an unavoidable degree of ischemia. The process of DCD organ recovery exposes the kidney to an additional period of warm ischemia during both the agonal phase after

withdrawal of treatment and following circulatory arrest. The subsequent period of cold ischemia, particularly if extended, exacerbates the detrimental effects of warm ischemia, leading to a significantly increased risk of delayed graft function (DGF) following transplantation [15]. It should be noted, that while IRI is a major factor in DGF, it is not considered the principle contributor to early graft loss, which is mainly caused by technical factors or primary non-function. In a Cambridge series of 801 patients who received a kidney-only transplant from a deceased donor, early graft loss within 30 days of transplantation occurred in 50 patients (6.2%). The underlying reasons for early graft loss included primary non-function (20; 2.5%), arterial or venous thrombosis (18; 2.2%), haemorrhage (6; 0.7%) and acute rejection (3; 0.4%) [16].

DGF is usually defined as a need for dialysis during the first week following transplantation, and in the UK occurs in 49% of DCD kidneys compared to 24% of DBD kidneys [15]. Short-term, DGF leads to a requirement for dialysis, prolonged hospitalisation and increased costs [17]. It may also mask features of acute rejection [18]. Longer term, DGF is associated with poorer graft survival including a 41% increased risk of graft loss after 3 years of follow-up [19]. Although it is now recognised that in contrast to DBD kidneys, DGF has no impact on DCD kidney graft survival [20]. Indeed, for first time recipients of kidneys from controlled DCD donors, graft survival and function are equivalent to kidneys from DBD donors [15, 21]. However, in DCD transplantation, a cold ischemic time of more than 12 hours compared to less than 12 hours is associated with 1.5 times risk of graft failure after three years follow up, and importantly only 18% of DCD transplants achieve a cold ischemic time of less than 12 hours [15].

## 1.4 Ischemia-reperfusion injury

Ischemia-reperfusion injury (IRI) is a highly complex and multi-factorial event that involves multiple cell types and numerous biological processes such as cell death, micro-vascular dysfunction, altered transcription and immune activation [22]. IRI is an unavoidable consequence of the transplantation procedure and is responsible for DGF in approximately 25% of kidneys obtained and transplanted from donors with brain stem death and up to 50% of kidneys from donors after cardiac death [23].

Strategies to protect donor kidneys from ischemic injury are lacking and are urgently needed to improve both early and late graft function. In this setting, effective treatments could even lead to expansion of the donor pool by improving the outcome for kidneys severely damaged by ischemia. There is currently no active pharmacological agent used at the time of organ donation to reduce renal IRI, therefore the use of an agent in this clinical setting would be unique.

## 1.5 Acute ischemic kidney injury

The incidence of acute kidney injury is also increasing and represents a significant global health concern [24]. One of the commonest causes for acute kidney injury is renal ischemia, which may result from multiple and often interrelated causes such as hypoperfusion, blood loss and surgery [25]. Apart from supportive renal replacement therapy, no other therapies exist for patients with acute kidney injury. The best treatments presently offered are avoidance of further kidney damage through careful resuscitation, effective treatment of sepsis and avoidance of nephrotoxic medications [26]. In addition, despite anticipated complications, effective preventative strategies prior to predictable renal insults (e.g. elective cardiac surgery) are currently unavailable for patients at high risk of developing post-operative acute kidney injury.

## 1.6 Preconditioning

The concept of treating an organ in order to protect it, prior to a known impending injury is termed *preconditioning* and was first described in the heart by Murry *et al.* in 1986 [27]. Since then many different physical and pharmacological preconditioning strategies have been explored in organ transplantation and in the context of renal IRI. One of the most recent strategies described involves the pharmacological induction of heat shock proteins (Hsps).

## 1.7 Other therapies

Although a number of preconditioning drugs have shown promise in preclinical trials, clinical efficacy has proven harder to demonstrate in phase I/II trials [22]. To date at least 445 studies on IRI have been registered in ClinicalTrials.gov [28]. Despite this level of investigation, relatively few pharmacological therapies have been tested in randomised controlled trials (RCT) in renal transplantation and there is currently no active pharmacological agent used during transplantation to reduce the impact of IRI. The trials performed during the past 25 years are briefly summarised (Table 1.1) [28-41]. An example of a drug that may reduce IRI that is already in clinical use for another condition is heme arginate. It is used in patients to treat porphyria but also leads to up-regulation of heme-oxygenase-1 and reduces renal IRI in aged mice [42]. Since there is patient safety data already available for heme arginate, it has rapidly been translated into a RCT in recipients of deceased donor kidneys (ClinicalTrials.gov Identifier: NCT01430156).

| Author/Year | Trial Design | Participants | N | Method of drug administration | Agent/mechanism | Outcome measure | Follow up | Results |
|---|---|---|---|---|---|---|---|---|
| Schneeberger *et al.* (1989) [29] | Double blind placebo controlled randomised | Deceased donor kidney recipients | 81 | Recipient IV infusion prior to reperfusion | Superoxide dismutase/Free radical scavenger | Early graft function<br>Graft survival<br>Rejection rate | 4 years | No difference in early graft function, significantly better graft survival due to less rejection at 4 years |
| Pollak *et al.* (1993) [30] | Double blind placebo controlled randomised | Deceased donor kidney recipients | 116 | Recipient IV infusion prior to reperfusion and for 1 h after | Superoxide dismutase/Free radical scavenger | Creatinine clearance at 48 h and day 6 | 6 days | No difference |
| Rabl *et al*. (1993) [32] | Open label, placebo controlled, randomised | Any recipient | 30 | Recipient IV infusion prior to reperfusion or shortly after | Omnibionta/Anti-oxidant vitamins | Plasma creatinine at 7 days | 7 days | No difference |
| Noel *et al*. (1997) [33] | Double blind placebo controlled randomised | Deceased donor kidney recipients | 140 | Recipient IV infusion for 48 h starting at induction | Pentoxifylline/Anti-inflammatory | DGF | 1 month | No difference |
| Haug *et al*. (1993) [34] | Phase 1 study, contra-lateral kidney recipient controls | Deceased donor kidney recipients at high risk of DGF | 18 | Recipient IV infusion 1-3 h prior to transplant | Enlimomab/Anti-ICAM1 monoclonal antibody | DGF<br>Graft survival<br>Primary non-function | 2 years | Significantly less DGF, less primary non-function, better graft survival (78% vs. 56% at 2 years). |
| Salmela *et al*. (1999) [35] | Double blind, placebo controlled, randomised | Deceased donor kidney recipients | 262 | Recipient IV injection 3 h before transplant and daily for 6 days after | Enlimomab/Anti-ICAM1 monoclonal antibody | Acute rejection rate<br>DGF<br>1 year survival | 1 year | No difference in any outcome |
| Hladunewich *et al*. (2003) [36] | Double blind, placebo controlled, randomised | Deceased donor kidney recipients with acute renal allograft failure | 43 | Recipient IV injection within 5 h of transplant and twice daily for 6 days | Insulin-like growth factor/Growth factor | Day 7 inulin clearance<br>Need for dialysis<br>Nadir serum creatinine | 6 weeks | No difference in any outcome |
| Fontana *et al*. (2005) [37] | Not reported, active control | Any recipient | 26 | Recipient IV infusion for 48 h post transplant | Dopamine or Fenoldopam (its receptor agonist)/ Improvement of renal blood flow | Day 1 creatinine and ultrasound measured renal vascular resistance | 1 day | No difference in any outcome |
| Shilliday *et al*. (2007) [39] | Cochrane systematic review | Various renal transplant recipients | 724 | Various peri-transplant regimes | Calcium channel blockers/ Vasodilator | DGF<br>Graft survival | Varied 4 weeks to 4 years | Relative risk for DGF 0.55, 95% CI 0.42 to 0.73. No difference in graft loss, mortality or requirement for haemodialysis. |

| | | | | | | | | |
|---|---|---|---|---|---|---|---|---|
| Martinez *et al*. (2010) [38] | Open label, non-placebo controlled randomised | Deceased donor kidney recipients at high risk of DGF | 104 | Recipient IV injection before transplant, at 12 h, 7 and 14 days post op | High dose epoetin beta/Increase tissue oxygen delivery | eGFR at 1 month<br>DGF<br>3 month graft survival | 3 months | No difference in any outcome |
| Trials yet to report | | | | | | | | |
| NCT01442337 | Double blind placebo controlled phase II/III randomised | All recipients stratified by donor risk | Aim 573 | One off recipient IV injection | Diannexin/ Recombinant human Annexin V protein | DGF<br>eGFR at 12 months<br>Graft survival at 12 months<br>Acute rejection rate | 1 year | |
| NCT01794663 | Multi-centre phase II/III, double blind placebo controlled randomised | Recipients at high risk of DGF | Aim 278 | One off IV dose to recipient at start of transplant procedure | OPN-305/Toll-like receptor-specific monoclonal antibody | DGF<br>Acute rejection rate<br>Graft survival 6 months<br>Primary non-function rate | 6 months | |
| NCT01756508<br>NCT01403389 | Open label, non-placebo controlled randomised | Any renal transplant recipient | Aim 40 | One off IV dose to recipient before reperfusion | Eculizumab/ Complement component C5 antibody | Speed of graft warming<br>Daily creatinine decrease first week<br>Doppler graft blood flow<br>One year graft survival<br>One year graft biopsy morphology | 1 year | |
| NCT00802347 | Multi-centre, phase I/II double blind, placebo controlled, randomised | Extended criteria donor kidneys | Aim 374 | Not specified | QPI-1002/ Synthetic SiRNA | DGF | Not specified | |
| ISRCTN49958194 | Multi-centre, double blind, placebo controlled, randomised | Recipients receiving DCD kidneys | Aim 560 | Single dose perfused to the donor kidney via the renal artery during cold perfusion preservation prior to transplantation. | Mirococept/ Complement C1 esterase inhibitor | DGF<br>Renal function and histology at 12 months<br>Acute rejection | 1 year | |
| NCT01430156 | Single-centre, double blind, placebo controlled, randomised | Deceased donor kidney recipients | Aim 40 | IV dose to recipient before transplant procedure and 2 days post-operatively | Heme arginate/ Heme-oxygenase inducer | Heme-oxygenase-1 induction<br>Renal function for 5 days post transplant<br>Renal biopsy on day 5<br>Urinary biomarkers | 5-days | |

**Table 1.1 Summary of previous and on going clinical trials of pharmacological agents to prevent IRI in renal transplant recipients.**

DGF is defined as need for dialysis within the first week unless otherwise stated. Abbreviations: eGFR - estimated glomerular filtration rate.

## 1.8 The potential for synergy of treatments and emerging therapies

It is important to note that the clinical trials performed for pharmacological agents in renal transplantation have been based on one specific treatment strategy, which may have led to the failure of therapies to achieve the desired effect despite inherent efficacy. This could be due to the dosing regimen used or the timing or route of drug delivery [22]. Furthermore, each agent that has been tested in a clinical trial thus far has been thought to inhibit IRI through one specific mechanism. The complexity of IRI may mean that use of a single agent, may not be sufficient in mitigating IRI and future studies may benefit from a therapeutic approach involving a combination of drug treatments [41]. However, given that off-target effects of various agents may be underappreciated, combining regimens could potentially lead to serious adverse events.

Targeting of new IRI pathways that orchestrate injury may also be important [43]. This could include the development of new therapeutic strategies that interfere with regulated cell death and in turn inflammation [44]. It could also involve the investigation of other existing treatments like cyclosporine A, which is a drug that is widely accepted in kidney transplantation due to its immunosuppressive properties but may have additional influence over regulated cell death. Cyclosporine A inhibits mitochondrial permeability transition, which is a process that induces necrotic cell death. Indeed, it has been considered that this potential of cyclosporine A may have already led to a reduction in regulated necrosis, less inflammation and improved graft survival in kidney transplantation [45]. Mitochondrial oxidative damage also occurs early in renal IRI, and may initiate an inflammatory response, therefore another treatment that may be effective is mitochondrial targeted anti-oxidant therapy [46].

## 1.9 Heat shock proteins

Hsps are abundant intracellular proteins that are phylogenetically highly conserved. They occur in constitutive or inducible forms [47]. There are several Hsp families each with specific properties that have been well established. Hsps are subdivided into their respective families according to their molecular weight in kilodaltons [48]. With increasing knowledge, the number of Hsps has greatly expanded resulting in more members being added to the various Hsp families. To enable better classification of Hsps, Kampinga *et al*. (2009) have devised guidelines for the nomenclature of Hsps based on assignments made by the HUGO Gene Nomenclature Committee and used in the National Center of Biotechnology Information Entrez Gene database for the heat shock genes [49].

The various functions of Hsps include; chaperoning of client proteins, regulation of protein complex formation, protein trafficking, refolding of denatured proteins, mitochondrial protein folding and assembly, targeting of misfolded proteins for proteasomal degradation, preventing unfolded protein aggregation and inhibiting apoptosis. To fulfill these diverse roles each Hsp family has unique structural features and domains, but the multi-faceted nature of Hsps is increasingly being recognised and various new roles are being appreciated as the level of understanding increases (Table 1.2) [49, 50].

| Mammalian Hsp family | Principal location | Summary of structural features and domains | Main established functions |
|---|---|---|---|
| Hsp90 | Cytosol | Homodimer with two cytosolic isoforms α and β, dimerization occurs at C-terminal and nucleotide exchange at N-terminal | Chaperone for a multitude of client proteins and regulator of protein complex formation |
| Hsp70 | Cytosol/nucleus/ mitochondria | Consists of a N-terminal (ATPase domain) and a C-terminal substrate binding domain connected by a short flexible linker | Protein trafficking and degradation<br>Refolding of denatured proteins during stress<br>Anti-apoptotic properties |
| Hsp60 | Mitochondria | Arranged as two stacked heptameric rings with three domains (apical, intermediate and equatorial) | Mitochondrial protein folding and assembly |
| Hsp40 | Cytosol/nucleus | J-domain that stimulates the ATPase activity of Hsp70 and C-terminal that loads polypeptides to Hsp70 | Regulates activity of Hsp70<br>Binds non-native protein<br>Processes pro-collagen |
| Hsp27 | Cytosol | Conserved C-terminal and highly variable N-terminal (WDPF domain) | Prevents unfolded protein aggregation |

**Table 1.2 Summary of the functions of the various mammalian Hsp families**

### 1.9.1 Heat shock response

The heat shock response was first discovered in 1962 in *Drosophila* by Ferrucio Ritossa [51] and encompasses the up-regulation of Hsps that are well recognised for cytoprotective activity in a multitude of injury-repair states [52]. A wide range of stressors, including heat, infection, hydrostatic pressure, oxidative stress, chemical insults and ultraviolet radiation induce the heat shock response [53, 54] and crucially this confers protection from subsequent insults [55].

Owing to the generality of this phenomenon, Hsps are often called stress proteins [56]. Furthermore, they have been described as “cellular mechanics” [57] and are commonly referred to as molecular chaperones; since they have been found to play a fundamental role in the correct folding of newly synthesised proteins, the re-folding of proteins that are denatured by various stressors and post-translational translocation of proteins to their sites of action [58]. They are also capable of activating cell signalling pathways [59] and inhibiting caspase-dependent apoptosis [60].

Hsps, therefore, are strongly associated with cellular protection and up-regulation in the clinical setting promises significant benefits. This cellular capability fits well with the clinical concept of preconditioning. Hsps are thus prime therapeutic candidates to be used in the context of predictable injury [61]. Indeed, Hsps, and especially Hsp70, have been extensively studied in this context. Nevertheless, despite extensive experimental investigation, reliable manipulation of Hsp responses for clinical application has thus far remained elusive.

### 1.9.2 Hsp regulation

Heat shock transcription factor 1 (HSF1) is the main regulator of heat shock genes across species [62]. It is found normally in the cytoplasm in an inactive form, bound to a multi-chaperone complex that includes Hsp90 [63]. In order to achieve transcriptional activation, HSF1 must dissociate from this complex, form a homotrimer, move to the nucleus and become hyperphosphorylated [64]. Hsp90 is the primary regulator of HSF1 with binding of Hsp90 to HSF1 maintaining HSF1 in its inactive, compacted form in the cell. In the presence of cellular stress, there is an increased concentration of unfolded proteins [65]. These compete with the Hsp90 multi-chaperone complex allowing free HSF1 to dissociate and be transported to the nucleus where it binds to specific promoter regions with resulting Hsp transcription [63] (Figure 1.1).

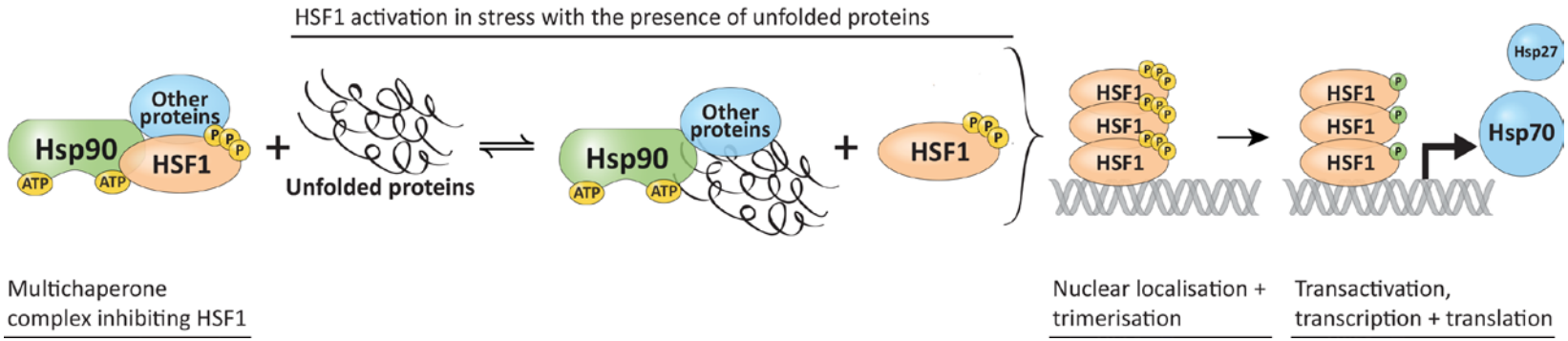


**Figure 1.2 HSF1 regulation by Hsp90**

In its inactive form HSF1 binds to a multi-chaperone complex with Hsp90 in the cell cytoplasm. There is dissociation of the Hsp90 multi-chaperone complex by competition from a stress-induced increase in the concentration of unfolded proteins. As a result, HSF1 is released, moves to the nucleus and becomes hyperphosphorylated. HSF1 then binds to specific promoter regions with resulting Hsp transcription.

## 1.10 Hsp90

The Hsp90 molecular chaperone family is expressed in almost all organisms and under normal conditions Hsp90 accounts for 1-2% of all cellular proteins [66]. As a result, Hsp90 is one of the most plentiful cytoplasmic proteins in the unstressed cell [67]. When a cell is exposed to physiological stressors including heat, hypoxia, acidosis and heavy metals, basal levels can be increased up to 10 times [68, 69].

Hsp90 is a ubiquitous homodimeric molecular chaperone [70] with two cytosolic isoforms termed α and β [71]. Dimerisation occurs when the isoforms form homodimers with the highly conserved C-terminal site of Hsp90 [67].

Hsp90 congregates with other molecular chaperones to form a large protein complex, known as a multi-chaperone complex. This chaperone complex has diverse functions including the prevention of aggregation of unfolded proteins under stressful conditions and regulation of the folding and maturation of a number of signal transduction molecules and receptors [72]. Hsp90 interacts with numerous client proteins in this complex including co-chaperones (such as Hsp70), signal transducers, activators of transcription and potentially IκB kinase (IKK) [73]. However, as an ATP-binding protein [67], Hsp90 is dependent on its intrinsic ATPase activity to be able to fulfil this chaperone purpose [74].

Being a member of the GHKL family of ATPases, Hsp90 exhibits a distinctive N-terminal nucleotide-binding pocket [75]. ATP hydrolysis and ADP/ATP nucleotide exchange in the N-terminal domain induce a conformational change of the protein [67] and are essential for Hsp90 chaperone function [70].

Evidence for a central role of Hsp90 in the regulation of HSF1 includes the observation that Hsp90 inhibitors can activate all steps of the stress protein response. Indeed, activation of HSF1 occurs uniformly in response to all Hsp90 inhibitors currently under clinical evaluation [76]. In this sense, HSF1 is an unusual Hsp90 client protein: other Hsp90-associated proteins become destabilised and degraded by proteolysis on Hsp90 dissociation, while HSF1 is activated leading to Hsp induction [77].

## 1.11 Hsp90 inhibitors

The discovery of geldanamycin marked the initial report of a group of drugs termed the benzoquinone ansamycins. Geldanamycin was first isolated from *streptomyces hygroscopicus* and was identified as having antiprotozoal activity. Herbimycin A was subsequently discovered and was the first of these compounds to be identified as an agent capable of short circuiting the Hsp response [78].

The anti-tumour potential of the benzoquinone ansamycins was soon recognised as first herbimycin [79] and then geldanamycin [80] were shown to inhibit the malignant transformation of fibroblasts by the v-*Src* oncogene. It was further noted that benzoquinone ansamycins prevented the formation of a stable complex between Hsp90 and Src, resulting in Src degradation by the ubiquitin-proteosome pathway [81]. Since this discovery various other oncogenic proteins including HER2, EGFR, mutant ER, HIF1α, Raf-1, AKT and mutant p53 have been identified as requiring functioning Hsp90 in order to exert their effects [82].

While geldanamycin, herbimycin and then radicicol were the first natural Hsp90 inhibitors discovered, their instability and hepatotoxicity limited any clinical

potential [76]. The geldanamycin analogue 17-allylamino-17-demethoxygeldanamycin (17-AAG) was better tolerated and the first of these compounds to be assessed in a clinical trial. A side-chain modification of 17-AAG resulted in the water-soluble geldanamycin analogue, 17-dimethylamino-ethylamino-17-demethoxygeldanamycin (17-DMAG) (Figure 1.3). Since then numerous other smaller molecule Hsp90 inhibitors have been discovered representing some of the most actively pursued cancer drug treatments by the pharmaceutical industry, with at least 17 agents having entered clinical trials [83].

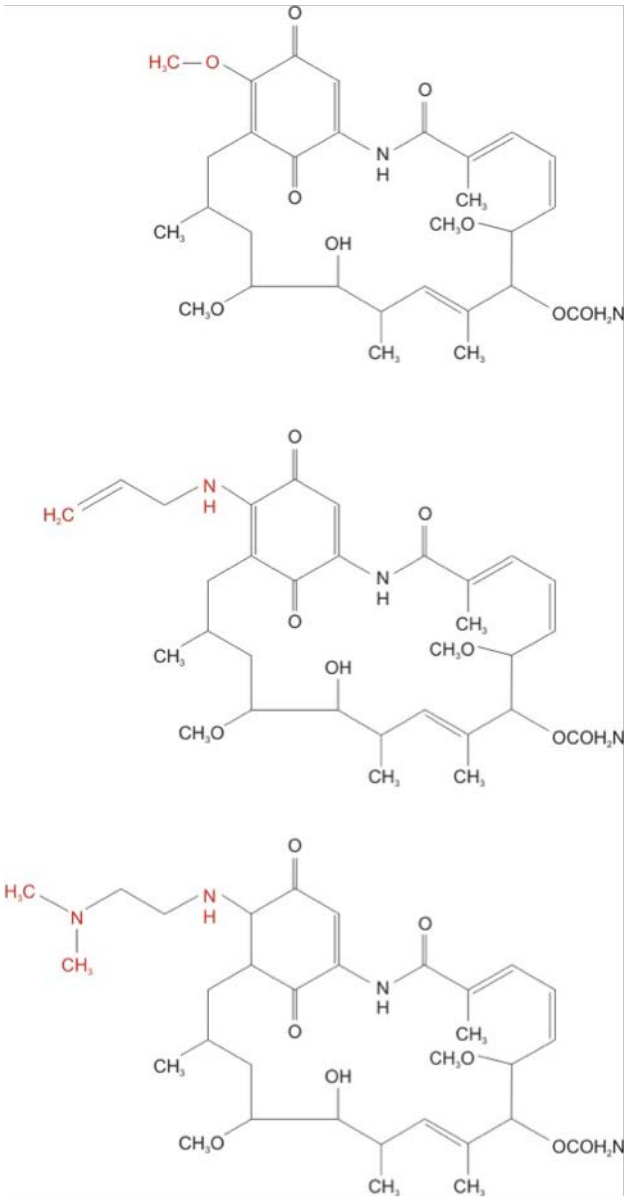


**Figure 1.3 Structure of Hsp90 inhibitors**

The upper structure is geldanamycin, the middle structure is 17-AAG, and the lower structure is 17-DMAG, which has a side chain modification that makes it water-soluble.

Source: Ewen Harrison.

Although cancer treatment has formed the focus of research on Hsp90 inhibitors, therapeutic application has been demonstrated in a number of other disease states [56]. These include renal IRI [84, 85], autoimmune encephalomyelitis [86], sepsis-induced lung injury [70], endotoxin-induced uveitis [87], rheumatoid arthritis [88] and atherosclerosis [73]. In addition, Hsp90 inhibitors are capable of blocking the activity of pro-inflammatory mediators, inhibiting Hsp90-dependent immune pathways [89], attenuating oxidative stress [90], reducing viral replication [91] and treating fungal infection [92]. Moreover, Hsp90 inhibition has therapeutic potential in the treatment of neurodegenerative diseases including Alzheimer's disease, Parkinson's disease, Huntington's disease and motor neurone disease - through prevention of the aggregation and toxicity of misfolded proteins such as amyloid β, tau, α-synuclein, mutant huntingtin and mutant superoxide dismutase-1 [93].

### 1.11.1 Routes of administration and dosing regimens

In the pursuit of Hsp90 inhibitors that are safe for clinical use, a major limitation of 17-AAG is its poor solubility in water. To improve solubility, DMSO in egg phospholipid and cremophor-based formulations were initially developed but required anti-allergenic premedication as well as specialised giving sets for intravenous administration. To overcome these problems, injectable isotonic suspensions, oil-in-water nanoemulsions and newer albumin-bound forms of 17-AAG have emerged to improve solubility and deliver higher concentrations of drug to target sites. 17-DMAG being water-soluble is easier to administer and can be given both intravenously and orally [83].

In a recent phase II study investigating 17-AAG, 11 patients with metastatic, or locally advanced irresectable breast cancer, were given dosing regimens of 220 $mg/m^2$ IV over 2 h on 5 separate days during a 21-day chemotherapy cycle. Five of the study group developed grade 3/4 toxicities, which were primarily hepatic and

pulmonary [94]. In phase I studies of 17-DMAG in patients with advanced solid tumours, the recommended doses for future phase II investigations were found to be 16 mg/m$^2$ x 5 days and 25 mg/m$^2$ x 3 days every 3 weeks administered by hour long intravenous infusion. Similar to 17-AAG, the most common grade 3/4 toxicities encountered with 17-DMAG were hepatic (14%) and pulmonary (9%) [95]. The doses that lead to these significant side effects are high and often at the maximum tolerated level. However, the dose required to give cellular protection is predicted lower and thus associated with less toxicity. For example, doses of 1 mg/kg of geldanamycin, 17-AAG and 17-DMAG have previously conferred renal protection in a mouse model of IRI [84].

### 1.11.2 Toxicity profile of Hsp90 inhibitors

Hsp90 is exploited by cancer cells to sustain oncoproteins including many mutated kinases and transcription factors that are over-expressed in cancer. Hsp90 also buffers cellular stress induced by malignant cells aiding their survival and propagation [76]. Use of Hsp90 inhibitors in the treatment of malignancy therefore does not lead to cancer cell death by cytotoxicity but by targeting and inhibiting these disease-dependent mechanisms e.g. by destabilising oncogenic kinases that are essential for tumour growth [96].

Newer Hsp90 inhibition agents, some of which have good oral bioavailability, lack the hepatotoxic profile of first-generation Hsp90 inhibitors possibly due to an altered quinone moiety and rate of superoxide formation [97]. This allows for repeated administration at higher concentrations. Nevertheless, the Hsp90 chaperone function extends to maintaining normal cellular homeostasis and concerns exist regarding the inhibition of specific Hsp90-dependent cellular mechanisms, at least on a long-term basis, which could be the case with certain chemotherapy regimens [76].

Since the treatment philosophy in organ preconditioning is different to that of cancer therapy, the implications of blocking normal homeostatic functions of Hsp90 are less important when considered in relation to IRI reduction. In this context, an Hsp90 inhibitor is administered on a once only basis at a dose sufficient to up-regulate Hsp70 expression. A two- to three-fold increase in renal Hsp70 in mice given 1 mg/kg of geldanamycin, 17-AAG and 17-DMAG into the peritoneum has previously been demonstrated. Hsp70 expression was maximal at 6 h in mice treated with 17-DMAG, which was significantly earlier than in geldanamycin (8 h) or 17-AAG (16 h) treated groups, perhaps reflecting improved bioavailability as a result of water solubility. No toxic effects were observed over a 2-week period following treatment [84].

Administering the currently available Hsp90 inhibitors at a lower once only dose is unlikely to significantly block the normal homeostatic functions of Hsp90 or lead to the level of toxicity observed in chemotherapy regimens. However, preconditioning agents should ideally not have any harmful side effects, particularly in a DCD setting when the donor is still alive. Therefore a major challenge going forward is to develop less toxic Hsp90 inhibitors that could be safely utilised in human subjects in the setting of renal transplantation.

### 1.11.3 Isoform-selective Hsp90 inhibitors

In addition to the two cytosolic isoforms of Hsp90 termed α and β, two other human isoforms of Hsp90 exist: tumour necrosis factor receptor-associated protein (Trap-1), which is localised to the mitochondria, and glucose-regulated protein, Grp94, which resides in the endoplasmic reticulum. Recently, it has been suggested that the side-effects of Hsp90 inhibitors like geldanamycin, 17-AAG and 17-DMAG may be due to pan-inhibition of Hsp90 and that development of isoform-selectivity may be a means of reducing toxicity. Interestingly, there is also known to be a number of pro-

inflammatory mediators that are Grp94-dependent clients, including Toll-like receptor 4 (TLR4) [98]. This opens up the possibility that Hsp90 inhibitors may exert a protective effect through Grp94 inhibition. It also highlights the need for newer and more specific Hsp90 inhibitors to be developed.

### 1.11.4 AT13387

AT13387 (Astex Pharmaceuticals) is a novel small molecule Hsp90 inhibitor with activity at nanomolar concentrations and low toxicity profile in phase II studies in oncology [99, 100] (Figure 1.4). In previous studies, pharmacological inhibition of Hsp90 by radicicol, geldanamycin and geldanamycin analogues has been shown to be highly protective in experimental renal IRI in mice [84, 85]. However, given that a drug designed to reduce IRI in renal transplantation has an absolute requirement for low toxicity, AT13387 has much better translational potential in this context [99, 100].

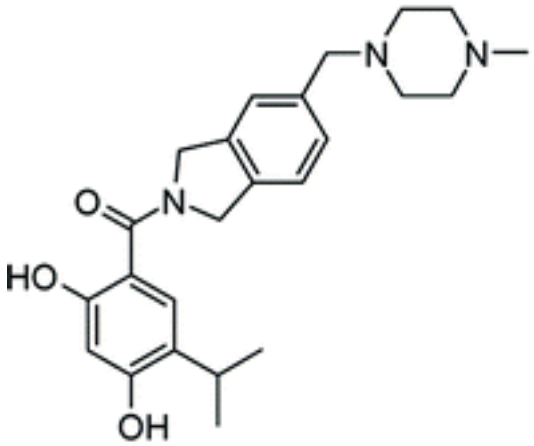


**Figure 1.4 Structure of AT13387**

The structure of AT13387 is unrelated to geldanamycin. Astex Pharmaceuticals developed AT13387 by screening fragments against Hsp90 and optimising hits into leads with inhibitory activities in the low nanomolar range [101]

## 1.12 The role of Hsps in modulating IRI in the kidney

Hsps are crucial regulators of ischemic injury in the kidney. This is affirmed by Zhang *et al.* (2008) who used micro-array analysis to compare gene expression in rat kidneys subjected to IRI. Of the 30,000 genes analysed, Hsp70 gene product up-regulation was greatest (43-fold), followed by Hsp27 (12-fold) and hemeoxygenase-1 (10-fold) [102].

Increasing evidence supports a role for Hsps during the recovery from renal ischemia, especially in the tasks of cellular rescue from apoptotic cell death and cytoskeletal restoration [61]. Pioneering work by Perdrizet *et al*. (1993) demonstrated that total body hyperthermia, followed by recovery, caused enhanced Hsp72 production and protected renal allografts from cold and warm ischemia [103, 104]. Since then Hsp induction has been shown to be associated with improved kidney viability and function post IRI in a variety of experimental models [52, 84, 85, 104-118] (Table 1.3).

| Author | Year | Species | Stimulus | Model | Protein | Ref |
|---|---|---|---|---|---|---|
| Perdrizet | 1993 | Swine | Heat | Allograft | Hsp72 | [104] |
| Redaelli | 2001 | Rat | Heat | Isograft | Hsp72/HO-1 | [107] |
| Yang | 2001 | Rat | SA | IRI | Hsp70 | [111] |
| Yang | 2001 | Rat | Cyclosporin | IRI | Hsp70 | [112] |
| Redaelli | 2002 | Rat | Heat | Isograft | Hsp72/HO-1 | [106] |
| Park | 2002 | Mice | Ureteral obstruction | IRI | Hsp25 | [116] |
| Yang | 2003 | Rat | EPO | IRI | Hsp70 | [115] |
| Wagner | 2003 | Rat | Heat | Isograft | HO-1 | [105] |
| Kim | 2005 | Rat | VD3 | IRI | Hsp70 | [114] |
| Suzuki | 2005 | Rat | GGA | IRI | Hsp70 | [108] |
| Jo | 2006 | Rat | Heat | IRI | Hsp70 | [52] |
| Fuller | 2007 | Rat | Glutamine | Isograft | Hsp70 | [109] |
| Harrison | 2008 | Mice | HBA | IRI | Hsp70 | [84] |
| Zhang | 2009 | Rat | Glutamine | IRI | Hsp70 | [110] |
| Stacchiotti | 2010 | Rat | Stannous Chloride | IRI | HO-1 | [117] |
| Yeh | 2010 | Rat | RHP | IRI | Hsp70 | [113] |
| Sonoda | 2010 | Mice | Radicicol | IRI | Hsp70 | [85] |
| Wang | 2011 | Mice | GGA | IRI | Hsp70 | [118] |

**Table 1.3 Protection in renal transplantation-relevant models associated with Hsp up-regulation**

Abbreviations: SA - sodium arsenite, EPO - erythropoietin, VD3 - 1,25-dihydroxyvitamin D3, GGA – geranylgeranylacetone, HBA - Hsp90 binding agent (Hsp90 inhibitor), RHP - repetitive hypoxic preconditioning, HO-1 – hemeoxygenase-1

## 1.13 Mechanisms of protection offered by Hsp90 inhibition

Why Hsp90 inhibition leads to cellular protection in renal IRI is unclear but is likely a consequence of two main effects. NF-κB controls cell survival, immune responses and pro-inflammatory transcription [119, 120]. Firstly, Hsp90 inhibition may be protective by inhibiting the pro-inflammatory effects of NF-κB via disruption of the IKK complex with Hsp90 [73]. Secondly it may lead to release of HSF1 from its repressive multi-chaperone complex with Hsp90, resulting in subsequent up-regulation of anti-inflammatory Hsps, especially Hsp70 [121].

### 1.13.1 The inhibition of pro-inflammatory transcription factors

In the kidney, IRI induces inflammatory mediators such as adhesion molecules, cytokines, and chemokines [122]. These mediators are thought to instigate an inflammatory cascade leading to leukocyte recruitment and microcirculatory compromise with ensuing renal dysfunction.

As many of these mediators have κB-binding regions, their transcriptional regulation is thought to be under the control of NF-κB [123, 124]. Therefore, NF-κB, which is likely to be regulated by Hsp70 and 90 via the IKK complex [125], may be a potential therapeutic target in ischemic renal injury [52] and specifically through the use of Hsp90 inhibitors.

Hsp90 inhibitors prevent nucleotide binding to Hsp90, resulting in client protein destabilisation, deactivation and degradation [126]. IκB is an inhibitory protein that

masks the nuclear localisation signal sequence of NF-κB [70]. Therefore, activation of NF-κB requires phosphorylation and dissociation from IκB by IKK [127]. Although numerous upstream pathways, such as tumour necrosis factor-alpha (TNFα) and TLR4, can lead to NF-κB activation, IKK is a common point of convergence [128], and activation of NF-κB occurs almost ubiquitously via IKK-mediated degradation of IκB [129]

IKK is composed of two protein kinase subunits IKKα, IKKβ as well as the regulatory subunit NEMO [127]. Hsp90 may be needed to stabilise the IKK complex [130] and the use of Hsp90 inhibitors could cause the dissociation of the IKK complex and prevention of NF-κB activation (Figure 1.5) [125].

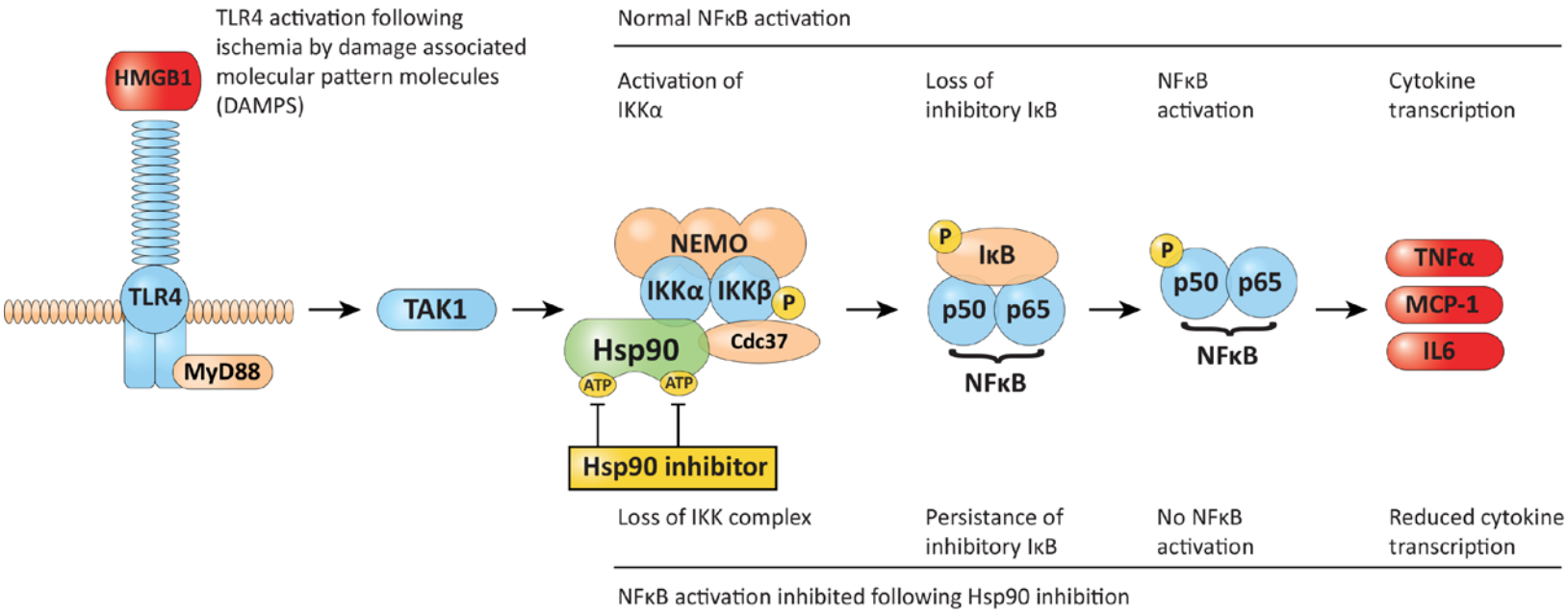


**Figure 1.5 Repression of TLR4-mediated NF-κB activation by Hsp90 inhibition**

Hsp90 inhibition may block TLR4-mediated NF-κB activation by disruption of the IKK complex. The inhibitory action of IκB on p50/p65 is maintained preventing nuclear localisation and transactivation of NF-κB. As a result pro-inflammatory cytokine transcription is reduced.

Indeed, geldanamycin has inhibited TNFα-mediated IKK and NF-κB activation in a number of *in vitro* models [131-135]. Pittet *et al.* (2005) also demonstrated this effectively when observing that heat treatment or sodium arsenite stress induced dissociation of Hsp90 from the IKK complex rendering the IKK complex detergent insoluble. Simultaneously, it was observed that the NF-κB system became impassive to cytokine stimulation [136].

This potential of Hsp90 inhibitors is highly attractive from a translation perspective since it offers a pharmacological strategy to temporarily dampen NF-κB. This is in contrast to ablative strategies targeting IKK that reduce NF-κB mediated inflammation but also prevent subsequent NF-κB mediated protection from apoptosis [137].

### 1.13.2 The up-regulation of anti-inflammatory proteins

Hsp90 inhibitor blockade of the Hsp90 ATP-binding site leads to both degradation of client proteins via a ubiquitin–proteasome-dependent pathway and up-regulation of other Hsps, particularly Hsp70 [121] (Figure 1.6).

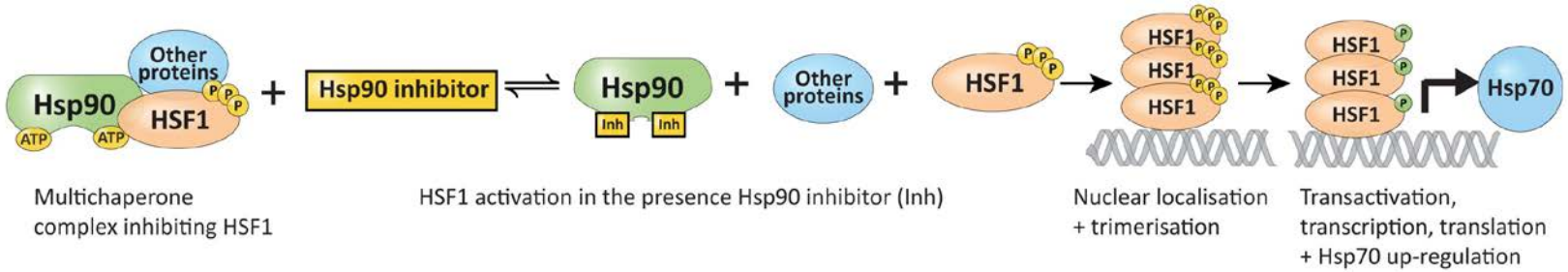


**Figure 1.6 Hsp70 induction by Hsp90 inhibition**

Hsp90 inhibition leads to dissociation of a multi-chaperone complex involving Hsp90 and HSF1. This results in HSF1 release and resultant Hsp70 up-regulation.

During an investigation of lung preconditioning, Pittet *et al.* (2002) showed that treatment of rats with two intraperitoneal doses of the Hsp90 inhibitor geldanamycin induced renal Hsp70 [138]. Harrison *et al*. (2008) also observed this effect and went on to show that use of Hsp90 inhibitors protected primary renal tubular epithelial cells from oxidative stress *in vitro* and conferred functional and morphological protection in a mouse model of kidney IRI [84].

## 1.14 Cellular and molecular mechanisms of protection by Hsp70

The Hsp70 family is capable of protecting cells from lethal heat and other insults [139]. Since Hsp70 prevents protein aggregation and facilitates the refolding of denatured proteins, up-regulating Hsp70 as a preconditioning strategy has been shown to be cytoprotective in a number of organs including the kidney and heart [118, 140-145].

The protective properties of Hsp70 in renal IRI are not fully understood and further putative modes of protection include correction of protein conformation, cytoskeletal stabilisation, anti-inflammatory effects, requirement in autophagy, anti-apoptotic properties, influence over macrophage phenotype and stimulation of regulatory T cells (Tregs) (Figure 1.7).

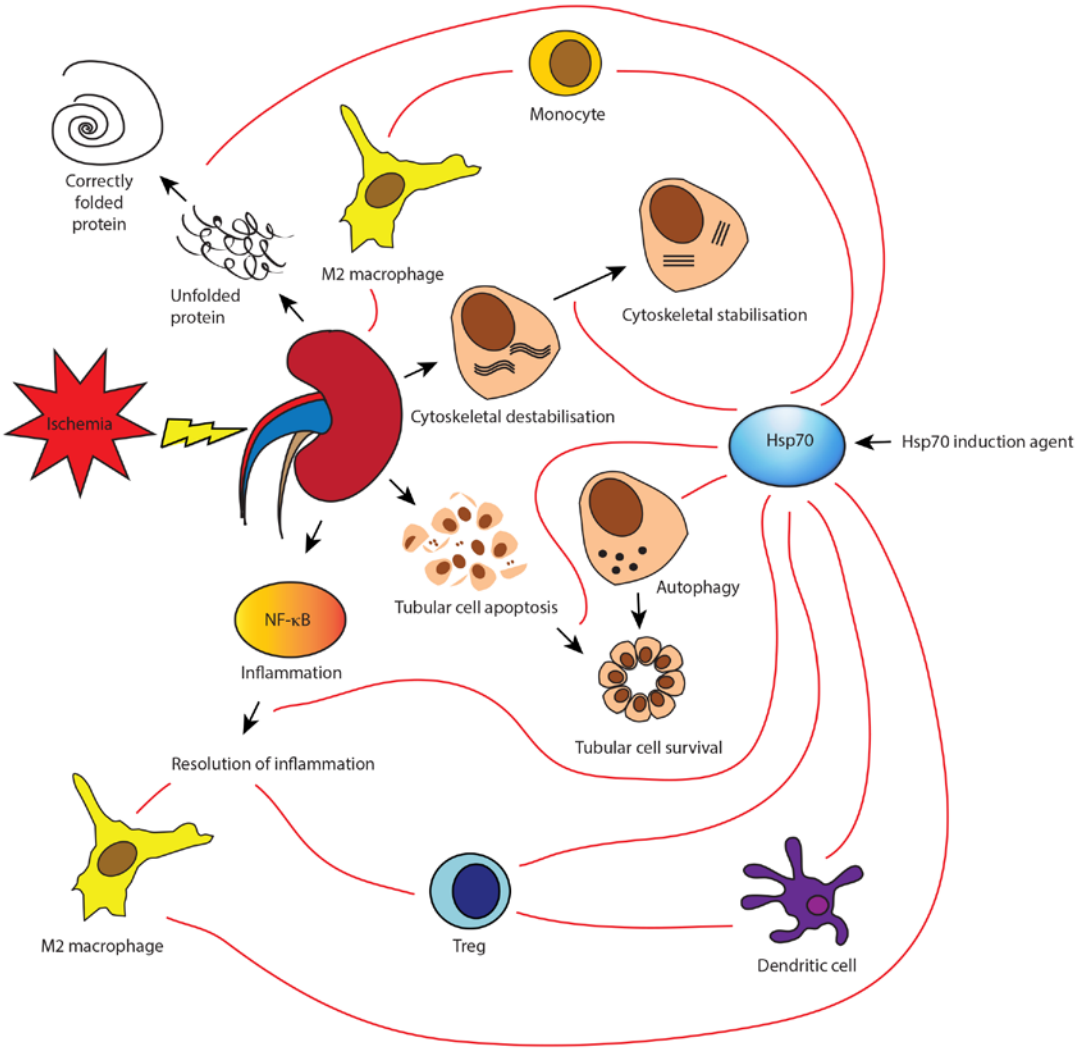


**Figure 1.7 Mechanisms of Hsp70 mediated protection from renal IRI**

Hsp70 induction in IRI may correct cytoskeletal destabilisation, reduce aggregation of unfolded proteins, promote cell survival through autophagy and prevention of apoptosis, and resolve inflammation by interrupting inflammatory signalling and modulating cell behaviour.

### 1.14.1 Correction of protein conformation

Variations in protein location and abnormal protein folding occur in many kidney diseases and are central components of ischemic injury [50]. Hsps exhibit complex protective mechanisms, that can prevent the formation of nonspecific protein aggregates and assist proteins in the acquisition of their native structures [146]. Following cellular injury, Hsps refold damaged proteins, mark irreparably damaged proteins for removal, limit the accumulation of misfolded proteins and aid appropriate folding of nascent proteins [50]. Hsp70 is one of the most highly conserved of these molecular chaperones and its functions encompass regulation of protein transport, prevention of abnormal protein aggregation and resolubilisation of misfolded proteins [61]. Specifically in the injured kidney, Hsps also have a role in the management of protein assembly and stabilisation of multi-protein complexes as well as translocation of proteins to their appropriate intracellular locations [50].

### 1.14.2 Intracellular protection and cytoskeletal stabilisation

Hsps protect cell structure and facilitate survival under conditions that would normally be lethal. Following kidney injury, Hsps may be capable of reducing mitochondrial load, conserving ATP levels, repairing DNA damage, maintaining tight junction integrity and preventing calcium redistribution within the cell [50]. The actin cytoskeleton is also an integral component of the architecture of cells but cellular stresses can lead to major defects [146]. For instance, following renal IRI, renal tubular cells rapidly lose their polarity and the cytoskeleton becomes grossly disrupted. In experimental renal IRI models, Hsps (and in particular Hsp70) play a pivotal role in restoring renal tubular cell cellular polarity and repairing essential proteins that are involved in stabilising cytoskeletal structures [61].

### 1.14.3 Anti-inflammatory effects

It is now recognised that inflammation is perhaps the most critical pathophysiological process involved in the propagation of renal IRI [25]. The exact mechanism by which Hsp70 reduces inflammation remains uncertain but it has been postulated that it may result from IκB stabilisation or prevention of NF-κB p65 translocation [147-151].

Jo *et al*. (2006) who investigated the effect of heat preconditioning in a rat kidney IRI model endorse this theory of protection. In this study, heat preconditioning protected the kidney, induced Hsp70 and suppressed IRI induced NF-κB activation [52]. The administration of quercetin, a widely known but non-specific inhibitor of Hsp70 [152], decreased Hsp70 expression markedly with associated loss of the functional protection from IRI conferred by heat preconditioning. Quercetin treatment was also associated with a reversal of NF-κB suppression [52].

Additionally, Ran *et al.* (2004) demonstrated Hsp70 binding to the coiled-coil domain of NEMO, which prevented the oligomerisation of NEMO and arrangement of the active IKK complex [150]. Weiss *et al.* (2007) observed that Hsp70 disturbed the role of the IKK complex, impairing IκB phosphorylation and degradation and preventing translocation of NF-κB [151]. Another possibility is that Hsp70 leads to ubiquitinisation and proteasomal degradation of certain pro-inflammatory Hsp90 client proteins [70] or dampens inflammation through activation of Tregs [153].

### 1.14.4 Requirement in autophagy

Autophagy is a catabolic process that degrades cytoplasmic components through the action of lysosomes. Autophagy is induced under stress and plays an adaptive role in cell survival. Up-regulation of autophagy in renal tubular cells ameliorates both IRI and cisplatin induced acute kidney injury [154]. Hsp70 is required for autophagy due to many forms of stress [155]. In an immune context, Hsp70 is also associated with autophagy, leading to a preferential uploading of Hsp70 peptides in MHC class II molecules of stressed cells. Tregs then target the conserved Hsp70 peptides that may then be presented in these conditions leading to the repression of inflammation [153].

### 1.14.5 Anti-apoptotic effects

Ischemic injury leads to both necrosis and apoptosis of renal tubular cells, which results in the release of damage associated molecular pattern molecules (DAMPs), which are endogenous ligands released from stressed or damaged cells, and propagation of inflammation [156]. A stressed but not critically injured renal tubular cell may undergo apoptosis and cell death or alternatively the cell can survive and recover function [61]. Another possibility is that the stressed cell may become senescent [157]. This is in contrast to lethally injured cells that inevitably succumb to apoptosis or necrosis and therefore cannot be salvaged [45]. As a consequence, it is the outcome of these stressed but viable cells that would seem the most amenable to cytoprotective interventions [61]. Distinct from necrosis, which is a passive energy-independent mode of cell death, apoptosis is programmed cell death resulting from the engagement of pathways that eventually result in the activation of caspase proteases [45, 158]. Caspase activation is generally considered to be a `point of no return' in this cell death pathway [159].

Hsps interact with important proteins involved in apoptotic pathways and this has crucial consequences for cell survival, proliferation and apoptosis following IRI [160]. For instance in renal IRI, Hsp70 limits apoptosis by controlling the activity of the kinases Akt and glycogen synthase kinase 3β that regulate the activity of the pro-apoptotic protein Bax. This prevents Bax translocation to the mitochondria and activation of caspase 3 [118]. As a result, renal epithelial cells might be rescued from apoptotic cell death following Hsp induction [61]. It is therefore of interest that cortical Hsp70 levels following renal IRI inversely correlate with apoptosis, tubular injury and renal dysfunction [118].

### 1.14.6 Influence on the phenotype of mononuclear phagocytes

Mononuclear phagocytes are pivotally involved at various stages of renal IRI and depending on the phenotype they exhibit and the time point following injury, they can be viewed as either injurious (M1 macrophages) or reparative (M2 macrophages). Hsps appear capable of promoting an anti-inflammatory phenotype in monocytes, which leads to release of anti-inflammatory cytokines such as interleukin-10 (IL-10) and suppression of harmful cytokines including interferon-γ (INF-γ) [153]. Hsps may also influence macrophage phenotype with transcriptomic profiling during the differentiation and polarisation of human macrophages showing distinct patterns of Hsp expression. For example, upon activation to a M1 phenotype a significant up-regulation of members of the Hsp70 family (HspA2 and HspA8) and Hsp90 family (Hsp90AA1) are observed, which suggests their influence over the effector stage of macrophage activation. While in M2 macrophages other members of the Hsp70 (HspA13), Hsp40 (DNAJB5) and Hsp27 (HspBAP1) families are significantly up-regulated [161].

In experimental renal IRI models, preconditioning with heat protects rat kidneys from ischemic damage by inducing Hsp70 and suppressing NF-κB activation. Heat preconditioning also reduces chemokine (C-C motif) ligand 2 (CCL2) expression, which is necessary to attract monocytes to the site of injury [52]. Furthermore, Hsp70 induction by either geranylgeranylacetone or repetitive hypoxic preconditioning reduces macrophage infiltration, protects kidney function, attenuates tubular damage and reduces renal tubular cell apoptosis following renal IRI [108, 113]. The causality of Hsp70 in these observations has been asserted in subsequent investigations that showed reversal of this effect following the addition of the Hsp70 inhibitor, quercetin [108]. However, despite being widely known, quercetin is a non-specific inhibitor of Hsp70 [152] and further investigation of Hsp70 in this context is needed.

## 1.15 Pharmacological modulation of Hsp70 expression

Hsp70 is one of the most frequently studied Hsps because of its potential anti-inflammatory properties and attractiveness as a therapeutic target due to its wide tissue distribution and ability to interact with a multitude of other molecules [153]. Even though Hsp70 is highly inducible, it may not be clinically desirable to generate Hsp70 by a classical heat shock response involving cellular stressors. In addition, physical preconditioning approaches often involve an additional thermal or ischemic injury with potential associated negative consequences. An example is renal ischemic preconditioning, which is thought to confer some of its proposed protection from renal IRI by induction of Hsps, but unfortunately depends on time consuming and often surgeon dependent intra-operative manoeuvers to be implemented in a clinical environment. Local ischemic preconditioning is also not directly applicable to the treatment of the various medical causes of acute kidney injury, such as hypoperfusion and sepsis. In light of this, approaches to induce Hsp70 without the need for preceding cellular stresses have been sought. As such, recent research in this area has begun to focus on pharmacological induction of Hsp70 for potential

therapeutic gain. In the setting of renal IRI, protective Hsp70 overexpression strategies have included the use of reagents such as geranylgeranylacetone [118], glutamine [110], radicicol [85], geldanamycin and geldanamycin analogues [84].

To date these treatments have been used only in murine models of IRI. The main barrier to the translation of these treatments to clinical use is the lack of mechanistic understanding of how Hsp70 induction results in kidney protection. There is also further uncertainty regarding non-specific mechanisms of protection offered by the various pharmacological therapies used thus far. If these issues could be clarified, then Hsp70-inducing drugs could be developed further or newer, more highly specific and less toxic medications could be designed.

## 1.16 The role of immunity and TLR4

TLRs are a family of trans-membrane proteins, named after the *Drosophila* protein Toll with which they share structural homology [162]. TLRs are highly conserved germline-encoded pattern recognition receptors [163] that are central to immune responses [156] including NF-κB regulation [164].

It is now appreciated that TLRs not only represent the major pattern recognition receptors across species but that they also recognise specific endogenous DAMPs that have been transformed from their native state or gathered in non-physiological sites or abnormal amounts during tissue injury [165].

Ischemic injury is thought to lead to necrosis and apoptosis of renal tubular cells leading to production of DAMPs [156]. These are recognised by local TLRs and

promote inflammation through the production of cytokines and chemokines, and enrolment of immune cells that propagate the initial injury [156].

TLRs may be expressed by kidney tubular epithelial cells and mesangial cells in response to insults such as IRI [166]. Kim *et al.* (2005) demonstrated that rat kidneys subjected to IRI showed enhanced TLR mRNA and protein expression [167] and there is growing experimental evidence emerging to suggest that engagement of TLRs by endogenous ligands may be a key trigger of inflammation following ischemia in the kidney [168].

### 1.16.1 TLR4 and renal IRI

As shown by *in situ* hybridisation, TLR4 is constitutively expressed at the RNA level on renal epithelium and this expression is enhanced upon IRI [169]. In mice subjected to renal ischemia, TLR4 expression is especially amplified at sites most susceptible to IRI, such as in the proximal renal tubules at the cortical-medullary junction [168]. This expression is independent of pathogen invasion and TLR4 appears to recognise endogenous molecules that are exposed during cellular injury and extracellular matrix remodelling [166]. To date, a number of proposed endogenous ligands for TLR2 and TLR4 have been found in ischemic renal tissue, including high mobility group box 1 (HMGB1) protein, hyaluronan, biglycan [168] and Hsp70 [167].

*In vivo* experiments have confirmed reduced organ injury in kidney IRI in transgenic mice missing TLR4 or the TLR4-related scaffolding protein MyD88 [170, 171]. Results of experiments by Pulskens *et al.* (2008) also show lower levels of chemokines and inflammatory cells, less renal injury and more preserved renal function following IRI in TLR4-/- mice as compared to wild types [170]. Wu *et al.*

(2007) used chimeric mice to show that TLR4 expressed specifically on tubular epithelium is an important modulator of ischemic injury [168], while Chen *et al.* (2011) extended this role of TLR4 into the endothelium of the kidney and demonstrated that leucocytes release IL-6 when TLR4 receptors are stimulated by HMGB1 release from injured cells [172]. In a rat model, Liu *et al.* (2010) showed that inhibition of TLR4 by the drug Eritoran, a structural analogue of the lipid A portion of lipopolysaccharide (LPS), attenuated inflammatory signalling cascades in renal IRI [173].

Similarly, in the case of TLR2, Leemans *et al.* (2005) [174] and Shigeoka *et al*. (2007) [175] both demonstrated that parenchymal cell deficiency of this receptor dramatically limited kidney injury following IRI, and diminished the associated renal inflammation. In further studies, Rusai *et al.* (2010) found that a double genetic deletion of TLR2 and TLR4 conferred only similar protection to single deletions of TLR2 or TLR4 [176].

This collective body of research suggests that TLR4 signalling plays a dominant role in mediating kidney damage following IRI [168, 172], with at least three major cell types (epithelia, endothelia and leukocytes) being identified as expressing TLR4 at various times during ischemic kidney injury [172]. Moreover, it has been demonstrated that for the classical response to ischemia to occur there is an absolute necessity for TLR4 in these cells [168, 172, 177].

This experimental research also appears to translate to the clinical situation, as a recent study in humans confirmed the role of the donor TLR4 and HMGB1 interaction in kidney transplant IRI [178]. This is in keeping with previous suggestions that kidneys from deceased donors may experience an increased

ischemic injury in response to danger signals provided by the recipient's innate immune system [179].

## 1.17 Hsp90 inhibitors and immune regulation

Although IRI typically occurs in a sterile environment, activation of innate and adaptive immune responses occurs and contributes to injury, including activation of pattern recognition receptors such as TLRs [22]. A number of key signalling proteins that are Hsp90 clients play important roles in the cellular activation of both innate and adaptive immune responses. Therefore, a rationale exists for targeting Hsp90-dependent pathways in immune-mediated diseases [89].

In rats, 17-AAG has been shown to halt the development of LPS induced autoimmune uveitis by inhibiting activation of multiple signalling molecules that mediate the TLR4-induced pro-inflammatory cytokine response in retinal cells [87].

Likewise, Dello Russo *et al*. (2006) demonstrated that 17-AAG blocked pro-inflammatory TLR4 activation *in vitro* and dramatically decreased disease incidence and severity in an experimental model of autoimmune encephalitis [86]. More recently, Yun *et al.* (2011) used a synthetic Hsp90 inhibitor, EC144, to prevent LPS-mediated TLR4 signalling in RAW 264.7 cells through inhibition of ERK1/2, MEK1/2, JNK, and p38 MAPK but not NF-κB [89].

The above evidence suggests that inhibiting Hsp90 function may be applicable to treatment of autoimmune diseases, but whether TLR4 signalling can be similarly

targeted in IRI remains uncertain and to date the interaction between Hsp and TLRs (a controversial area in the literature) is yet to be fully delineated.

### 1.17.1 Interaction of Hsp and TLRs

Members of the heat shock protein family, including Hsp60, 70, 72, 90 and gp96, are capable of inducing production of pro-inflammatory cytokines via CD14/TLR2 and CD14/TLR4 receptor complex-mediated signal transduction pathways [180]. Ohashi *et al.* (2000) found that the pro-inflammatory signalling of human Hsp60 was dependent on a functional TLR4 [181]; whereas Vabulas *et al.* (2002) defined Hsp70 as an endogenous stimulus for the Toll/IL-1 receptor signal pathway that engages TLR2 and TLR4 [182].

In an experimental study investigating cardiac IRI, it was shown that extracellular Hsp70 plays a role in IRI by TLR4-dependent mechanisms and that recombinant Hsp70 induced NF-κB activation as well as the expression of TNFα, IL1β and IL-6 [183]. In the context of renal IRI, Kim *et al.* (2005) suggested that enhanced TLR mRNA and protein expression in a rat model of IRI was due to endogenous TLR ligand levels of Hsp70 within tubular cells [167].

The mechanism by which Hsp produce cellular activation through TLR2- and TLR4-dependent mechanisms is not well understood, and there is continuing debate regarding the importance of interactions between Hsps and TLRs [171].

It has been argued that early investigations identifying Hsps as TLR-ligands were the result of contamination with pathogenic ligands, since the reported cytokine effects

of Hsps *in vitro* were similar to pathogen-associated molecular pattern molecules, such as LPS from Gram-negative bacteria [162]. Since then, a number of *in vitro* techniques have evolved to nullify the risk of LPS contamination including protein expression in eukaryotic hosts, chaperone treatment with polymyxin B, neutralising monoclonal antibodies and acyloxyacyl hydrolase. Other techniques include the use of various controls, including chaperone antibodies, mutants of the chaperone and LPS itself. If the latter is used, transcriptional micro-array analysis is effective at determining differences in response. Finally, purity can also be tested with a limulus assay, mass spectrometry and SDS-PAGE [184].

There is also research that highlights other trans-membrane receptors such as CD91 and LOX-1 as the principle Hsp70 receptor. This evidence may call into question the importance of Hsp and TLR interaction. On the other hand, the implication of Hsp70 signalling through multiple germline-encoded immune receptors may serve to further underline the potential importance of Hsp70 in immune-regulation [185].

Either way, *in vivo* Hsp and TLR interactions that have been well described cannot be explained by contamination. Therefore, another argument against Hsp and TLR interaction has evolved and suggests that molecules bound to, or chaperoned by, Hsps can activate TLRs, rather than the Hsp molecules themselves [186].

Despite these arguments, it has been shown that dying cells often undergo the stress protein response, leading to lysis and release of Hsp into the extracellular space [187]. This is thought to be able to activate not only inflammatory but also immune responses [188]. Conversely, Hsp60 has been reported as being translocated to the surface of apoptosing cells as a recognition element for phagocytotic clearance, thereby attenuating an inflammatory response [189]. In addition, HSF1 has been identified as a transcriptional repressor with a role in the counter-regulation of

cytokine gene transcription [190]. As a result the pro-immune effects of extracellular Hsp have been described as being countered by the intracellular stress protein response in what is now known as a dichotomy of effects, which is best depicted in the case of Hsp70 [188].

### 1.17.2 Extracellular Hsp70 and potential pro-inflammatory effects

Hsp70, like Hsp90, has immune regulation properties with both pro- and anti-inflammatory effects [191] and large clinical studies investigating cardiac ischemia have provided inconsistent reports of protective [192, 193] or detrimental [194] effects of this chaperone.

Hsp70 residing in its cytosolic compartment appears to have the ability to decrease pro-inflammatory signalling cascades, thereby down-regulating inflammatory responses. In contrast, extracellular Hsp70 is thought to exhibit powerful immune-stimulatory effects and has therefore been acknowledged as a “chaperokine” [191].

The overall action of Hsp70 on the inflammatory equilibrium is reliant on the cellular compartment in which Hsp70 displays its predominant effect, which depends mainly on the extent of the tissue injury [185].

In general systemic stress, there is reliance on NF-κB, in addition to up-regulation of intracellular Hsp70 in inflammatory cells [195-197]. In this scenario, pro-inflammatory messages via innate immune receptors can be overcome by the intracellular down-regulating action of Hsp70 on NF-κB signalling, thereby reducing the undesirable effects of systemic inflammation [185]. On the contrary, the response

could be pro-inflammatory when in the absence of cytosolic stress, there is a lack of intracellular Hsp70 up-regulation and absence of its down-regulatory effect on NF-κB [185].

This hypothesis is in agreement with the “danger theory” described by Matzinger [198], in which DAMPS such as Hsp are released from damaged cells providing the immune system with a “danger” signal. The response to that hazard is initiated by antigen-presenting cells that identify Hsp via TLRs resulting in up-regulation of NF-κB and activation of pro-inflammatory cytokines [199].

In summary, the novel functions of Hsp70 could depend on its location with intracellular Hsp70 attenuating inflammatory cascades, while Hsp70 released into the extracellular space specifically binds to TLR2 and 4 and produces immune-regulatory effects, including up-regulation of adhesion molecules, co-stimulatory molecule expression, and cytokine and chemokine release [188]. It is predicted that in Hsp90 inhibition intracellular up-regulation of Hsp70 predominates and exerts a protective effect through an as yet unknown mechanism. This theory requires confirmation and a recent review has highlighted that studies aimed at more accurately characterising the molecular pathways activated by Hsp70 are required to determine its overall effect [153].

## 1.18 Inflammaging

There is increasing recognition that processes of repair can become maladaptive in renal IRI. These mechanisms, which include cell-cycle arrest, cellular senescence, pro-fibrogenic cytokine production and activation of pericytes and interstitial myofibroblasts, trigger the onset of progressive fibrotic kidney disease, a process that

mirrors the development of accelerated kidney ageing [200] This ties in with the concept of “inflammaging”, which is a chronic low grade inflammatory process underlying human aging [201]. In diseases with a strong inflammatory component, such as renal IRI, the identification of mechanisms that control age-related inflammation is felt to be important. A particular mechanism of interest is cellular senescence, which can cause chronic inflammation through the senescence-associated secretory phenotype [202]. In terms of the involvement of Hsps in this process, higher levels of intracellular Hsp70 and Hsp90 occur with age and in patients with inflammation, compared to control subjects [203]. Serum concentrations of Hsp70 also decrease with normal aging; with higher levels of Hsp70 associated with inflammation and frailty in elderly patients. As such, it has been hypothesised that Hsp70 in the serum is of benefit during acute short-lived elevation, but is related to negative clinical conditions when chronically elevated [204].

## 1.19 Hsp90 and maintenance of vascular tone

Ramirez *et al*. (2004) showed that Hsp90α and Hsp90β cytsolic isoforms are expressed along the nephron in rats [205]. Ramirez *et al*. (2008) then went on to demonstrate that inhibition of Hsp90 with radicicol in rats reduced renal blood flow and glomerular filtration rate. Since the effect was associated with a reduction in nitric oxide synthesis and increased endothelial nitric oxide synthase phosphorylation, it was suggested that Hsp90 might be a regulator of vascular tone within the kidney [206].

Quantification of total renal blood flow as a measure of effective blood flow can be misleading in renal IRI due to the possibility of ischemic injury being localised to specific areas of microvasculature within the kidney [25]. Nevertheless, the potential

role of Hsp90 in maintaining vascular tone in the kidney could have important implications for use of Hsp90 inhibitors in renal IRI.

Indeed, Barrera-Chimal *et al*. (2014) from the same group have recently identified in renal IRI that endothelial nitric oxide synthase-Hsp90 uncoupling occurs and reduces nitric oxide levels. They were then able to restore endothelial nitric oxide synthase-Hsp90 coupling by intra-renal Hsp90α or Hsp90β transfection prior to renal IRI, which subsequently reduced morphological kidney injury. Although no significant improvement in kidney function was demonstrated, these observations again implicate Hsp90 in regulating the nitric oxide/endothelial nitric oxide synthase pathway and renal vascular tone [207]. As such, a degree of caution may need exercised when inhibiting Hsp90 in renal IRI.

## 1.20 Lymphocytes and renal IRI

Renal IRI is a highly complex form of tissue injury involving many biological processes, including acute inflammation, cell death, microvascular dysfunction, and immune activation together with multiple myeloid and lymphoid cell types that may play a role in both the initiation and the resolution of tissue injury [22, 208]. Although the complex pathophysiology of renal IRI represents a challenge, it also offers an opportunity to manipulate these cellular responses in order to limit injury and facilitate subsequent repair.

In addition to activating innate immune receptors, renal IRI elicits a profound adaptive immune response. T and B lymphocytes are the major effector cells of the adaptive immune system with T cells involved in cell mediated immunity and B cells the humoral response [209]. Evidence suggests that T and B lymphocytes may

amplify kidney injury in renal IRI, in contrast there is also data to suggest that lymphocytes could play a protective role depending on the cell type involved and the stage of injury [210].

Burne *et al*. (2001) demonstrated in a murine renal IRI model, that nu/nu mice (lacking CD4+ and CD8+ T cells) show significantly less kidney injury compared to wild-type mice, with reconstitution of CD4+ T cells but not CD8+ T cells restoring kidney injury to the level of wild-type mice [211]. In the early phase of renal IRI (<24 h) antigen specific activation may play an important role in the propagation of kidney injury by CD4+ T cells following renal IRI [212]. In terms of B-cells, renal IRI studies using RAG-1-/- mice (lacking B and T cells) have shown both renal protection [213] and a similar kidney injury to wild-type controls [214, 215]. Compared to wild types, renal IRI studies using mu MT mice (lacking B cells alone) are also inconsistent with some suggesting less severe injury [216] and others a more severe kidney injury [217].

### 1.20.1 Tregs and renal IRI

CD25 + Foxp3 + Tregs are a pivotal subtype of T-lymphocytes that display potent immunosuppressive properties and can regulate both immunological function and inflammatory injury. In contrast to the possible harmful effects of CD4+/CD8+ lymphocytes, Tregs appear to have a protective role in IRI [22], and specifically during the repair phase of renal IRI [218]. Treg immunodepletion using an anti-CD25 antibody worsens renal IRI [219], and increasing Treg recruitment to the kidney ameliorates renal IRI [220]. The fact that Tregs both inhibit the innate immune injury of renal IRI [221] and are involved in renal repair following renal IRI [218] highlights their potential utility for therapy in patients with ischemic kidney injury.

### 1.20.2 Hsp70 interaction with Tregs in renal IRI

Various preconditioning strategies, including transient ischemia or heat preconditioning, have been used to induce renoprotection from subsequent renal IRI, and it is highly pertinent that previous studies have demonstrated a role for both Tregs and Hsp70 in mediating the protective effect of preconditioning [52, 222]. It is also of interest that Hsp90 inhibition, which leads to Hsp70 induction, has recently been identified as promoting Treg-dependent suppression of autoimmunity [223].

In a very recent publication, Kim *et al*. (2014) [224] examined the role of Hsp70 in the protection from renal IRI afforded by heat preconditioning comprising the heating of mice to 41°C for 15 min, 24 h before the induction of bilateral renal IRI. The level of kidney injury was determined 24 h after surgery. They then presented data supporting the concept that Hsp70, expressed by CD11c + dendritic cells, plays an important role in Treg-mediated protection from renal IRI.

Heat preconditioning of mice provided significant protection from the adverse effects of renal IRI, as previously observed by their group [52], with heat-preconditioned mice exhibiting reduced serum creatinine and less tubular injury. Treg immunodepletion induced by the administration of an anti-CD25 antibody prior to the induction of renal IRI significantly abrogated the protective effect of heat preconditioning. The restoration of the protective effect of heat preconditioning by adoptive transfer of Tregs to anti-CD25-treated mice strongly suggested an important mechanistic role for Tregs, and experiments were therefore undertaken to explore the specific effect of heat preconditioning on Tregs.

Heat preconditioning increased the number of splenic CD4 + CD25 + Tregs and reduced the proliferative response of cultured splenic mononuclear cells to a

mitogenic stimulus. Although Hsp70 expression was noted in spleen, kidney, liver, and lung under basal conditions, Hsp70 expression was increased by heat preconditioning, with CD11c + Hsp70 + dendritic cells evident in the spleen by immunohistochemistry and flow cytometry. Also, *in vitro* treatment of cultured splenocytes with the Hsp70 inducer geranylgeranylacetone increased Hsp70 expression and the proportion of CD4 + cells expressing CD25 [224].

Increased numbers of CD4 + CD25 + Tregs were detected by flow cytometry in enzyme-dissociated kidneys following renal IRI compared with sham kidneys, indicating localisation of Tregs to the injured kidney. Heat preconditioning significantly expanded the intra-renal CD4 + CD25 + Treg population following renal IRI in comparison with control injured kidneys, with increased expression of Foxp3 mRNA also evident [224].

In order to probe the role of Hsp70 in heat preconditioning, Kim and colleagues [224] administered the Hsp70 inhibitor quercetin to mice 3 hours before heat preconditioning. Quercetin decreased Hsp70 expression in splenocytes, reduced the expansion of splenic Tregs, and blocked the protective effect of heat preconditioning in renal IRI. Furthermore, the adoptive transfer of Tregs to quercetin-treated mice restored the protective effects of heat preconditioning. These data suggest that the protective effect of heat preconditioning might be mediated through an interaction between Hsp70 and Tregs. However, because of the lack of specificity of Hsp70 inhibition by quercetin and the possible up-regulation of other anti-inflammatory Hsps by heat preconditioning, Kim *et al*. (2014) [224] undertook further experiments using T cell-deficient nude mice and the adoptive transfer of cells derived from Hsp70 knockout mice.

As previously demonstrated by Burne *et al*. (2001) [211], Kim *et al*. (2014) [224] found that nude mice exhibited reduced injury following renal IRI, with the adoptive transfer of T cells purified from control mice reconstituting injury and significantly increasing serum creatinine. In contrast, the transfer of T cells from heat-preconditioned wild-type mice to nude mice did not increase injury. Importantly, nude mice given T cells from heat-preconditioned Hsp70 knockout mice before renal IRI exhibited increased creatinine and partial reconstitution of injury.

The totality of these data from Kim *et al*. (2014) [224], suggests that heat preconditioning induces renoprotection that is Treg dependent and associated with increased numbers of both splenic and infiltrating renal Tregs. It is suggested that splenic Treg expansion may result from CD11c + Hsp70 + dendritic cells. The administration of Hsp70 inhibitors and inducers as well as adoptive transfer of T cells from heat-preconditioned Hsp70 knockout mice suggest that Hsp70 is important for the generation of injury-limiting Tregs. The study therefore reinforces the capacity of both Tregs and Hsp70 induction to modulate renal IRI, and, since Hsp70 is amenable to pharmacological up-regulation, the findings speculatively suggest translational potential for preventing renal IRI (Figure 1.8).

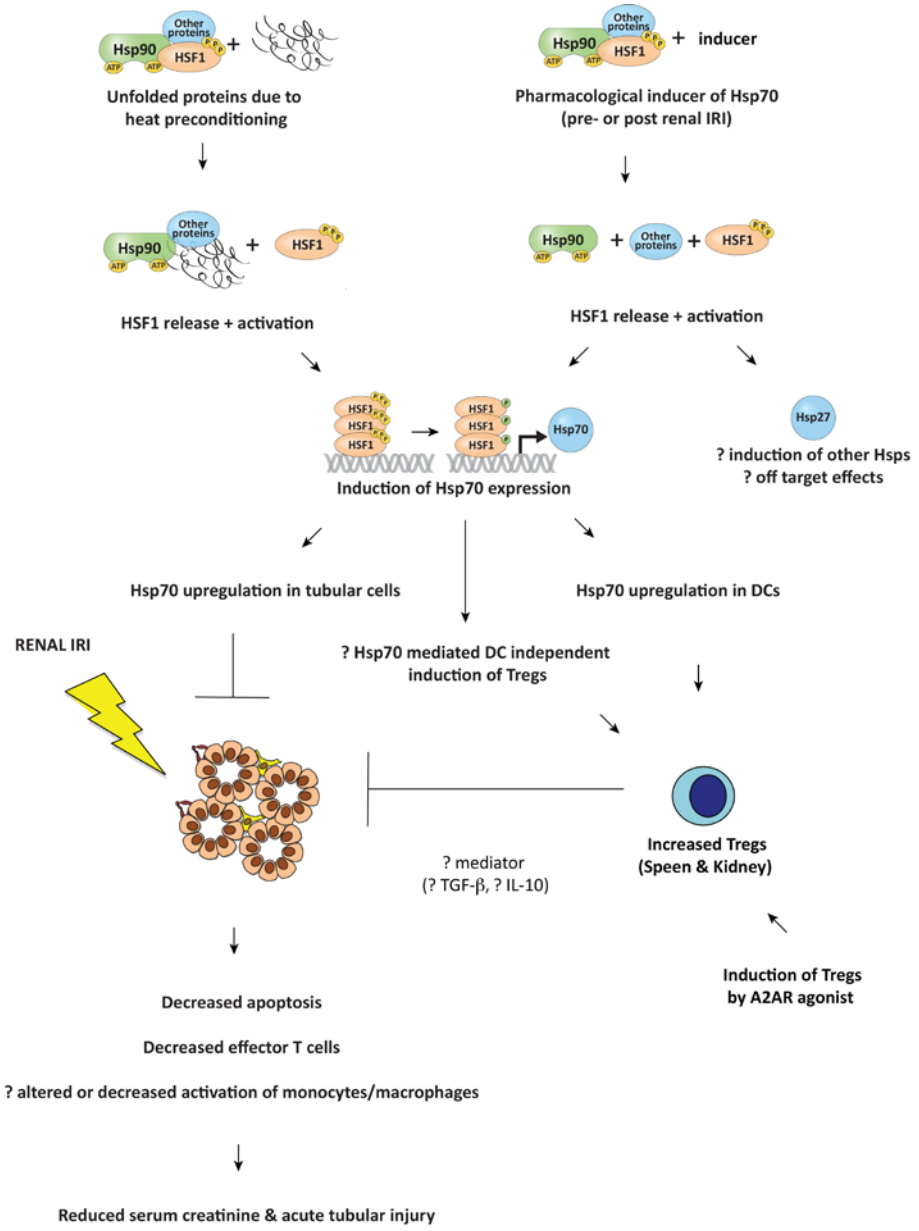


**Figure 1.8 Putative pathway of Hsp-regulation of Hsp70, Treg expansion and suppression of renal IRI**

Schematic diagram illustrating the potential beneficial effects on renal IRI of Hsp70 up-regulation induced by either heat preconditioning or pharmacological agents. Induction of Hsp70 expression in splenic CD11c+ cells induces expansion of Tregs that ameliorate renal injury, as reported by Kim *et al*. (2014) [224]. Tregs may also be induced by adenosine 2A receptor (A2AR) agonists. In addition, Hsp70 induction in renal parenchymal cells, such as tubular epithelial cells, may exert a protective action by limiting cell death. Abbreviations: DCs - dendritic cells, TGF-β - transforming growth factor-β.

The study by Kim *et al*. (2014) also raises a number of questions, and, as ever, there are several caveats to the work. For example, the molecular mechanism underlying the protective effect of Tregs induced by heat preconditioning is unclear, but previous work suggests that IL-10 is an important Treg effector molecule in renal IRI [221]. As such, the role of IL-10-producing Treg type 1 cells should be formally examined. It should also be noted that anti-inflammatory Tregs that protect from renal IRI may also be induced by treatment with an adenosine 2A receptor agonist [225], and it would be of interest to determine whether concurrent Hsp70 induction and treatment with an A2AR agonist or other agents could augment protection.

Increased Hsp70 expression by splenic CD11c + dendritic cells was noted, and it is suggested that these are key to Treg induction. Heat preconditioning also induced renal Hsp70 expression, and it is possible that Hsp70 up-regulation in renal immune cells may also play a role in renal protection. The importance of systemic Hsp70 induction over Hsp70 up-regulation in renal parenchymal cells, renal tubular cells or resident leucocytes could be addressed in a renal transplantation experiment involving systemic Hsp70 induction in the recipient of a non-treated and injured kidney.

Also, Hsp70 present within T cells may physically interact with Foxp3 and directly support survival and proliferation of Tregs and their immunosuppressive function [226] such that CD11c + dendritic cells may not be required. In this regard, it would be interesting to investigate the degree of dependence on CD11c + dendritic cells by ablating CD11c + dendritic cells before pharmacological Hsp70 induction and adoptive T cell transfer.

## 1.21 Translational perspective

### 1.21.1 Preconditioning and prevention of IRI

Despite great improvements in outcome following kidney transplantation, the incidence of graft failure remains high. In the UK, all-cause graft survival after 3 years is 83% for recipients of DCD kidneys and 85% for recipients of DBD kidneys [15]. The shortage of organs for transplantation has led researchers to look for new techniques to expand the donor pool resulting in the increasing use of grafts from expanded criteria and DCD donors [18]. Respectively, these kidneys have worse outcome because of either pre-existent pathology, which renders them more susceptible to IRI, or more prolonged warm ischemic injury during organ recovery.

Transplantation necessitates inflicting an ischemic injury on an organ, but the planned nature of this insult presents an opportunity to act to reduce the magnitude of this injury. There is currently no therapeutic means of treating kidneys destined for transplantation in order to improve post-transplantation function, a process termed *pharmacological preconditioning*. The use of an agent in this clinical setting would therefore be unique. Preconditioning strategies also have the potential to improve the function of substandard organs so that they become suitable for transplantation, thus expanding the donor pool [17].

Debate surrounds the potential benefit of pharmacological strategies over physical preconditioning manoeuvres. In the latter, cellular protection is achieved by repeated temporary interruption of blood flow to an organ or distant site [227]. A pilot study has recently demonstrated a reduction in acute kidney injury after heart surgery following remote ischemic preconditioning of the leg [228]. In transplantation, organ physical preconditioning has been studied almost exclusively in liver and on the

whole, results have been disappointing [229]. Pharmacological preconditioning also has advantages over a physical preconditioning strategy as an ischemic injury with associated negative consequences is avoided and time-consuming, surgeon-dependent intraoperative manoeuvres are not required.

Developing a pharmacological strategy to reduce IRI, the main contributor to DGF after DCD kidney transplantation is therefore highly desirable. The ultimate aim of pharmacological preconditioning is to improve the function of transplanted organs by administering a single dose of an agent to an organ donor prior to organ retrieval. This would prime protective cellular mechanisms in anticipation of the injurious nature of ischemia and reperfusion. In addition, it may be beneficial to treat the organ *ex vivo* with a drug delivered by machine perfusion prior to the implant procedure. However, this may only be applicable to normothermic perfusion strategies since the activity of certain agents may be decreased at the lower temperatures used for hypothermic machine perfusion [230].

Although a number of alternative preconditioning drugs have shown promise in preclinical trials, clinical efficacy has proven harder to demonstrate in phase I/II trials [22]. Preconditioning strategies typically involve direct treatment to the organ donor and/or organ, aiming to reduce injury prior to the onset of ischemia. These other strategies are frequently aimed at treating the organ recipient, which may be more feasible but could also be too late

Donor pre-treatment clearly has much potential because it would allow prevention and treatment of IRI at the earliest stage. However, there are ethical, logistical and organ-specific issues that need resolved before these strategies can be implemented in a clinical environment. These issues revolve around legislation, consent of

donor/recipient and the fear that some preconditioning agents may be beneficial to one organ but not to others [231].

To date using the older Hsp90 inhibitors, geldanamycin and related analogues (17-AAG and 17-DMAG), up-regulation of Hsps together with protection against oxidative injury (in cell culture) and IRI in mice has been demonstrated [84]. Hsp90 inhibition has additionally been shown to induce Hsp70 up-regulation in the liver, lung and heart of mice [84]. Hsp90 inhibitors therefore have potential benefits for all organs retrieved in the multi-organ donor setting. These donors carry huge socioeconomic value and improving early function and longevity of transplanted organs in this setting is a high priority area. This could represent a particular advantage of Hsp90 inhibitors over other agents.

Pharmacological preconditioning occurring in the context of renal transplantation merits particular consideration, as transplantation presents possibilities to promote anti-inflammatory recipient Tregs as well as induce cytoprotective Hsps in the donor kidney before harvesting the organ. However, it is noteworthy that the commonly used immunosuppressive drug mycophenolate mofetil worsens experimental IRI of native kidneys via effects on lymphocytes and renal Treg recruitment [232], though it is unclear whether this is of clinical relevance. Also, the up-regulation of the renal heat-shock response is associated with increased tubular major histocompatibility complex class II expression and immunogenicity [233]. This association may result from the increased action of HSF1 that underlies both endogenous and pharmacologically induced Hsp70 up-regulation. The specificity of both pharmacological inhibitors and inducers of Hsps is a further issue with some drugs; for instance, geldanamycin and its analogs induce both Hsp70 and Hsp27 [84], though this may not be problematic if all the induced Hsps exert a protective action.

Renal IRI is not unique to transplant surgery though, and occurs in variety of different clinical settings including shock, sepsis, exposure to nephrotoxic medications, vascular surgery and cardiothoracic surgery. This leads to an acute ischemic kidney injury, which not only causes potentially life-threatening renal failure, but additionally ignites a pro-inflammatory cascade through the release of inflammatory mediators that lead to a systemic response eventually resulting in remote organ injury and multi-organ failure [234].

Defining a method of inducing protective Hsp expression in transplantation could lead to a reduction of renal IRI in these other allied surgical disciplines as well as opening up avenues of investigation for treatment of non-surgical causes of acute ischemic kidney injury. Preconditioning strategies could be administered before the ischemic insult and are thus of use in patients at risk of renal ischemia or acute kidney injury. For instance, high risk patients (e.g. pre-existing CKD, diabetes, extensive vascular disease etc.) awaiting toxic drug or radiological contrast exposure may also benefit from such preventative measures [61]. Despite this there may be difficulty deciding who should receive such treatments but the development of various predictive models of outcome following diverse interventions may well be able to stratify patients according to the risk of developing acute kidney injury in the future.

### 1.21.2 Enhancing recovery following IRI

Despite evidence that Hsp70 induction after renal IRI can mediate kidney protection [118], current research in this area has focused almost exclusively on preconditioning and to a lesser extent on deploying protective Hsp expression strategies in the recovery from renal IRI. Further investigation of recovery therapy might increase the capacity of these treatments to help patients that have already suffered acute ischemic kidney injury in a native or transplanted kidney. Moreover, treatment of the

transplant recipient may be more translationally feasible due to the ongoing ethical and logistical barriers to pre-treatment of donors [231].

It is anticipated that a greater emphasis on recovery phase therapy may evolve from further understanding of how Hsp70 induction may interact with specific cell types in renal IRI. For instance, confirmation that Hsp70 induction influences circulating or infiltrating immune and inflammatory cells, either involved in the propagation or recovery from IRI would provide stronger evidence that treatment in the recovery stage could also be of benefit. For example, it has been shown that Hsp70 up-regulation by geranylgeranylacetone administered after renal IRI is still protective [118], but it is unknown whether this results from the induction of protective cells such as anti-inflammatory Tregs, or by more direct beneficial effects on renal parenchymal cells, such as tubular cells.

Following transplantation the recipient's circulation continues to carry infiltrating inflammatory cells to the kidney. These circulating inflammatory cells are possible treatment targets due to their ability to either sustain or resolve tissue inflammation [208]. Hsp70 induction may occur in immune cells remote from the kidney following heat shock and plays an important role in mediating protective Treg responses in renal IRI [224]. Consequently, it is predicted that an Hsp70 inducing candidate drug could also modulate infiltrating inflammatory cells or the immune activity of Tregs through a similar systemic effect. There is thus potential for using Hsp70 inducing treatments in recipients prior to transplantation or even after the kidney has been implanted.

These effects have not been unequivocally confirmed as yet and Hsp inducing agents may still have their major impact on renal tubular cells or renal resident leukocytes. As such, Hsp70 induction within the kidney parenchyma itself would be of prime

importance with circulating or infiltrating inflammatory cell populations not representing the key target. In this case, researchers will need to induce protective levels of Hsp70 within renal tubular cells or renal resident inflammatory cells at the earliest possible stage. The focus will therefore remain on preconditioning the kidney, which may slow translational progress in this field particularly in the context of transplantation.

Prior to translation to human disease, there is undoubtedly scope for much future work in this area to determine key cellular and molecular mediators together with an exploration of pharmacological agents that may be used to harness and manipulate the endogenous protection of Tregs and Hsps in an experimental setting. Indeed, this area of research has started to bear fruit in other conditions, such as chronic inflammatory diseases with recent evidence from human trials in arthritis suggesting that exogenous administration of Hsp peptides may exert anti-inflammatory effects via actions on T cells and Tregs [235]. In these studies, Hsp40 and Hsp60 peptides have been shown to modulate T cell responses by inhibiting the division of CD4+ and CD8+ T cells, and promote the production of anti-inflammatory cytokines including IL-10, IL-6 and transforming growth factor-β [153, 235, 236]. This suggests that Hsps may have an important role in preventing or arresting inflammation in renal IRI and thus protecting renal function. It also hints at distinct translational potential for this area of research.

## 1.22 Summary

Pharmacological induction of Hsp expression is an emerging preconditioning strategy aimed at reducing IRI following organ transplantation and other ischemic injuries. The possibility of applying pharmacological agents to induce Hsp70 and prevent renal IRI has significant potential to benefit patients undergoing renal transplantation or at high risk of acute ischemic kidney injury.

Hsp90 inhibitors lead to up-regulation of Hsp expression (especially Hsp70) and potentially block NF-κB activation by disruption of the IKK complex. The importance of TLR4 signalling in mediating kidney damage following IRI is now clear. Hsp90 inhibition is an attractive strategy to reduce TLR4-mediated IRI but as yet remains unproven.

Prior to converting these therapies into a clinical context, an increased mechanistic knowledge of the protection offered by Hsp70 is also required. From a translational standpoint, an enhanced understanding of the inflammatory and immune cell types involved could also broaden the scope of these therapies to wider group of patients, including renal transplant recipients.

Hsp70 induction is protective from renal IRI and it has recently been reported in the context of heat preconditioning that the protective effect of Hsp70 up-regulation in renal IRI is lymphocyte-dependent [118, 224]. Consequently, it is predicted that an Hsp70 inducing candidate drug such as AT13387, could also reduce renal IRI by modulating lymphocyte behaviour. There is thus therapeutic potential for using AT13387 in a recipient prior to transplantation in order to systemically up-regulate

Hsp70 expression in the recipient and modify the recipient's immune response to reperfusion.

## 1.23 Hypotheses

### 1.23.1 In vitro

1. AT13387 represses TLR4-mediated NF-κB activation resulting in reduced pro-inflammatory cytokine release.

2. AT13387 enables cellular survival following oxidative stress.

### 1.23.2 In vivo

1. AT13387 leads to induction of renal Hsp70 in mice.

2. AT13387 pre-treatment results in functional and morphological protection from renal IRI.

3. The protection afforded from renal IRI by AT13387 is lymphocyte-dependent.

4. Recipient treatment with AT13387 reduces renal IRI in transplantation.

# Chapter 2: Materials and methods

## 2.1 Cell culture

Cell lines included Human embryonic kidney cells (HEK293) (European Collection of Cell Cultures, Porton Down, UK, Catalogue No: 85120602), stably transfected HEK293 expressing TLR4 (HEK293-TLR4, Catalogue No: IML-204) and stably co-transfected HEK293 expressing both TLR4 and a secreted alkaline phosphatase (SEAP) reporter under the transcriptional control of NF-κB (HEK293-TLR4-NF-κB, Catalogue No: IML-104MD2CD14) (Imgenex, San Diego, USA). Cells were maintained in Dulbecco's modified eagle's medium (Gibco, Paisley, UK) supplemented with 10% foetal bovine serum, penicillin (50 U/ml), streptomycin (50 μg/ml) and non-essential amino acids (5%). The selection agent for HEK293-TLR4 cells was 10 μg/ml blasticidin (Invivogen, San Diego, CA) and for HEK293-TLR4-NF-κB cells were 10 μg/ml blasticidin, 2 μg/ml puromycin, 200 μg/ml zeocin and 500 μg/ml G418/geneticin (Invitrogen, Carlsbad, CA).

## 2.2 Animals

Male FVB/n mice aged 6-8 weeks and weighing 20-25 g, were used from in-house colonies. Male Balb/c mice and male Balb/c severe combined immunodeficient (SCID) mice aged 6–8 weeks and weighing 20–25 g, were obtained from Harlan Laboratories, Blackthorn, UK. For renal transplantation experiments, slightly older male BALB/c mice aged 10-12 weeks and weighing 25–30 g, were also obtained from Harlan Laboratories, Blackthorn, UK. Mice were caged for a minimum of 7 days before experimentation. Balb/c SCID mice were caged in individually ventilated cages and received sterilised food and water. Other mice were allowed free access to standard chow and water. The mice were kept in a 12:12-h light-dark cycle.

All work involving animals was conducted in accordance with the provisions of the UK Animals (Scientific Procedures) Act 1986, and institutional ethical approval was obtained.

## 2.3 Drugs

The Hsp90 inhibitor AT13387 was kindly provided by Astex Pharmaceuticals [101]. 17-DMAG was purchased from InvivoGen (San Diego, CA). For *in vitro* experiments, stock solutions were formed in Dimethyl sulfoxide (DMSO) (Sigma-Aldridge, Dorset, UK) due to a lack of solubility of the compounds in water. Aliquots were formed from stock solutions to avoid repeated freeze thawing, and were further diluted in culture medium prior to use. Selected doses for *in vitro* experiments ranged from 100 nM to 1000 nM with the lowest effective dose of each drug sought in every experiment and controlled for by an appropriate DMSO vehicle control. The dosing range for AT13387 and 17-DMAG was established from preliminary investigations performed in renal adenocarcinoma cells by Ewen Harrison. Pre-treatment with Hsp90 inhibitors was performed in a time window 2-6 h prior to ligand stimulation or oxidative stress. For *in vivo* experiments AT13387 (80 mg/kg free-base equivalent) was dissolved in (2-Hydroxypropyl)-β-cyclodextrin (2HβC) (Sigma-Aldridge, Dorset, UK), which was prepared in distilled water at 17.5% weight per volume. Mice were treated by intra-peritoneal injection 6-24 h prior to tissue collection or surgery. A 2HβC vehicle-treated group of mice served as the controls.

## 2.4 Reagents

TLR4 grade endotoxin-free hyaluronan was purchased from Enzo Life Sciences (Exeter, UK), polymyxin B from SERVA (Heidelberg, Germany), 5-

aminoimidazole-4-carboxyamideribonucleoside (AICAR) from Cell Signaling Technology (Boston, MA) and TNFα from Peprotech (London, UK). LPS and hydrogen peroxide were purchased from Sigma-Aldridge (Dorset, UK).

## 2.5 Transfection

Transient NF-κB transfections were performed using Fugene HD or Fugene HP (Roche, Lewes, East Sussex, UK) in experiments assessing NF-κB activation in HEK293 cells and HEK293-TLR4 cells, as these cells did not have a stably transfected NF-κB reporter. Transfection efficiency of the NF-κB reporter construct (GL4.32 [luc2P/NF-κB-RE/Hygro]) was controlled by co-transfecting with a control vector (pGL4.73 control vector [hRluc/SV40]) (Promega, Southampton, UK).

## 2.6 Western blot

Western blotting was performed as previously described [237]. Briefly, whole cells extracts were produced and protein concentration determined (BioRad, Hemel Hempstead, UK). Proteins were separated by SDS-PAGE (10% or 15% Tris/HCl gels) and transferred to nitrocellulose (BioRad, Hemel Hempstead, UK). Nitrocellulose membranes were soaked in blocking buffer then primary antibody. Primary antibodies were from the IKK isoform antibody kit (Cell Signaling Technology, Boston, MA). After washing, the membranes were exposed to a horseradish peroxidase-conjugated secondary antibody at a concentration of 1:2000 to 1:5000. Enhanced chemiluminescence reagent (Amersham, Chalfont St Giles, UK) was applied followed by development with autoradiography. Equality of loading was confirmed by probing for β-actin (BD Biosciences, San Diego, CA).

## 2.7 Flow Cytometry

Cells were trypsinised, collected and incubated at room temperature with 2% rabbit serum. Further incubation was then performed with either PBS/0.5% Bovine Serum Albumin (BSA)/0.1% azide (unstained control), mouse IgG1 isotype control antibody (Serotec, Oxford, UK) or purified mouse anti-human TLR4 antibody (BD Pharmingen, San Diego, CA) for test samples (0.5 mg/ml at 1:50 dilution or 0.5 μg per test sample). Cells were washed then incubated with either PBS/0.5% BSA/0.1% azide for unstained controls or fluorescein isothiocyanate (FITC)-conjugated goat anti-mouse IgG (Silenus Laboratories, Victoria, Australia) for IgG1 control samples and TLR4-test samples. Cells were washed again and results acquired on a BD Accuri C6 flow cytometer (BD Biosciences, San Jose, USA).

## 2.8 ELISA

### 2.8.1 Phosphorylated IκBα (S32/S36) ELISA

To measure phosphorylated IκBα in whole cells, a commercially available cell based ELISA that used fluorogenic substrates was performed and analysed as per the manufacturers instructions (R&D Systems, Abingdon, UK). Normalised relative fluorescence units (RFUs) were determined by dividing phosphorylated IκBα fluorescence in each well by the total glyceraldehyde 3-phosphate dehydrogenase (GAPDH) fluorescence in each well. The normalised RFUs were used to establish IκBα phosphorylation, which is an indicator of NF-κB activity. The ELISA was performed 10 minutes following ligand stimulation as per the manufacturers instructions. This reflects the rapid nature of phosphorylated IκBα expression.

### 2.8.2 Hsp70 ELISA

Whole cells extracts were produced from tissue lysates and protein concentrations were determined (BioRad, Hemel Hempstead, UK). Detection of Hsp70 in tissue extracts was then performed using a commercially available ELISA kit according to the manufacturer's instructions (Enzo Life Sciences, Exeter, UK). Sample Hsp70 (ng/ml) was read from a standard curve and normalised to the total protein content of the sample (mg/ml) to establish tissue Hsp70 levels (ng/mg).

## 2.9 Assays

### 2.9.1 Luciferase assay

Luciferase assays were used to investigate NF-κB activity following transient NF-κB transfections in HEK293 and HEK293-TLR4 cells. At 24 hours after transfection and following experimentation, cells were processed for luciferase activity using the Dual-Glo luciferase assay system and Turner Biosystems Modulus Microplate analyser (Promega, Southampton, UK). Firefly luciferase luminescence activity was normalised to that of the co-expressed renilla luciferase to determine the fold induction and indicate NF-κB activity. Maximal signal intensity was achieved when the assay was performed 1 h following ligand stimulation with TNFα and 3 h following ligand stimulation with LPS and hyaluronan.

### 2.9.2 Crystal violet cell viability assay

Cells were split into 6-well plates for experimentation. After experimentation cells were twice washed with 37°C Phosphate Buffered Saline (PBS) then incubated with

0.2% crystal violet solution (2% ethanol in distilled water), which is a solution that stains DNA, for 10 minutes at room temperature. The plate was then twice washed in a large beaker of water. The cell layer was dried upside down on paper towels then solubilised with 1% Sodium Dodecyl Sulfate solution. The plate was agitated on an orbital shaker for 1 h before results were read on a plate reader at 570 nM absorbance. Increasing optical density reflected increased cell density and therefore an increased number of viable cells. Results were normalised to cells left in medium control for the duration of the experiment, which were considered 100% viable.

### 2.9.3 SEAP assay

SEAP assays were used to investigate NF-κB activity in HEK293-TLR4-NF-κB cells as these cells were stably transfected with a SEAP reporter under the transcriptional control of NF-κB. SEAP assays were performed using the SEAPorter assay kit (Imgenex, San Diego, USA). The concentration of SEAP secreted into cell culture supernatant was calculated from a SEAP standard curve and was used to indicate NF-κB activation. The assay was performed 24 h after the addition of ligands as per the manufacturer's instructions in order to allow adequate time for SEAP to be secreted from cells into the culture medium.

## 2.10 Human cytokine array panel

Cell culture supernates were mixed with biotinylated detection antibodies. The sample/antibody mixture was then incubated with a Human Cytokine Array panel (R&D Systems, Abingdon, UK). The panel consisted of a nitrocellulose membrane with capture antibodies for 36 human cytokines spotted on its surface in a duplicate manner. Cognate immobilized capture antibodies on the membrane bound any cytokine/detection antibody complexes present. Following a wash to remove

unbound material, Streptavidin-HRP and chemiluminescent detection reagents were added sequentially followed by development using autoradiography. Light produced at each spot was used to determine the amount of cytokine bound.

## 2.11 Renal IRI model

An established model of warm IRI of the left kidney together with a right nephrectomy was used [238]. This model was preferred to a bilateral ischemia model, as the nephrectomy specimen allowed for confirmation and quantification of AT13387 activity via Hsp70 induction in kidney tissue at the time of surgery in each individual experimental animal. It also more closely mirrors the clinical scenario of a single injured kidney graft in a renal transplant recipient with no other functional nephron mass. The model was designed to inflict a moderate to severe acute tubular injury with zero animal mortality. Mice were anesthetised with an intra-peritoneal injection of Ketamine (75 mg/kg, Vetalar; Pfizer, Kent, UK) and Medetomidine (1 mg/kg, Domitor, Pfizer). A heated mat maintained body temperature with homeostatic control via a rectal temperature probe (Harvard Apparatus, Boston, MA). A mid-line laparotomy was performed for access to both kidneys through a single incision. The right ureter and renal pedicle were ligated then divided. The right kidney was then removed as a control. One half kidney was placed in Methacarn (70% methanol, 20% chloroform, 10% acetic acid) with the other half frozen on dry ice. The pedicle of the left kidney was dissected and occluded using an atraumatic vascular clamp (Micro Serrefine, Fine Science Tools, Linton, UK) for 20 minutes in FVB/n mice and 30 or 32 minutes in Balb/c mice and Balb/c SCID mice since the tolerance of renal IRI was strain dependent. Following removal of the left pedicle clamp, reperfusion was confirmed visually before closure of the abdomen. The anaesthetic was reversed with Atipamezole (1 mg/kg, Antisedan, Pfizer), and a subcutaneous injection of 0.9% saline (25 ml/kg) and Buprenorphine (0.1 mg/kg) was administered. Animals were recovered in an incubator at 29°C until tissue collection 24 h later.

## 2.12 Renal transplantation model

An established model of murine renal transplantation was used to perform isograft renal transplants from Balb/c donors to syngeneic Balb/c recipient mice [239, 240]. To describe the surgical technique briefly, after intraperitoneal administration of the same anesthetic regime used in the renal IRI model, the donor kidney was isolated and perfused with cooled University of Wisconsin solution (Belzer Bridge to Life, Columbia, SC). The donor kidney was stored at 4°C in University of Wisconsin solution for 4 h. Based on the findings of a previous publication, as well as in-house data, this cold ischemic time was anticipated to cause moderate to severe acute tubular necrosis [241]. After unilateral nephrectomy in the recipient, the donor renal artery and renal vein were anastomosed to recipient aorta and inferior vena cava, respectively, with a mean warm ischemic time of 30 minutes. The donor ureter was anastomosed to recipient bladder. The anaesthetic was reversed with Atipamezole (1 mg/kg, Antisedan, Pfizer), and a subcutaneous injection of 0.9% saline (25 ml/kg) and Buprenorphine (0.1 mg/kg) was administered. Animals were recovered in an incubator at 29°C until tissue collection 24 h later. All mice had a single intact native kidney and the model was not transplant-dependent (i.e. the transplanted kidney was not a life-supporting organ [242]).

## 2.13 Tissue collection

Under terminal general anaesthesia, blood was recovered by intra-cardiac puncture, and the serum was stored at -20°C. Kidneys were divided equally in the transverse plane. One half kidney was placed in Methacarn with the other half frozen on dry ice. The spleen was also placed in Methacarn. All frozen tissue was maintained at -80°C until analysis.

## 2.14 Lung Digestion and cytometric analysis

Broncho-alveolar lavage (BAL) was performed with 3 x 0.8 ml ice-cold PBS to remove alveolar cells. Non-adherent cells were then removed from the lung vasculature using 10 ml of PBS flushed through the beating right ventricle after cutting the inferior vena cava to allow exsanguination. Lungs were quickly dissected free and placed into a bijou containing 2 ml of cold Roswell Park Memorial Institute medium (RPMI). After removing the supernatant, lungs were placed in a 1 mg/ml DNAse (Sigma, Dorset, UK) and 10 mg/ml collagenase mix (Roche Diagnostics Ltd, Welwyn Garden City, UK) before being disrupted with scissors and incubated for 1 h at 37°C. Cells were then further released from tissue via vigorous pipetting using a 1 ml syringe. After a spin at 300g for 15 minutes, red cells were lysed using Ammonium-Chloride-Potassium (ACK) lysing buffer (Life Technologies, Paisley, UK) for 5 minutes on ice followed by another wash at 300 g with PBS. Cells were resuspended in PBS, strained using a 40 µm cell strainer (BD Biosciences, UK) and incubated with Fc block (rat anti-mouse CD16/CD32, BD Europe) at 1:100 for 10 minutes at 4°C prior to a wash. The following antibodies were added; FITC-labelled anti-mouse CD11b and Pacific Blue-labelled anti-mouse LY-6G (Biolegend, San Diego, CA) for 30 minutes on ice followed by the addition of FACS lysing solution (BD Biosciences, Oxford, UK). Samples were spun at 350 g for 5 minutes and resuspended in PBS prior to analysis.

## 2.15 BAL analysis

BAL fluid was weighed and subsequent cell counts were adjusted per microliter of BAL fluid collected. Cells were then fixed and stained using a Quick-Diff kit (Reagena, UK) following a cytospin, and differential counts were determined.

## 2.16 Immunohistochemistry

Tissue was fixed in methacarn for 24 h before being mounted in paraffin. Sections were cut and mounted on SuperFrost slides (Fisher Scientific, Pittsburgh, PA). Sections were de-waxed in xylene for 10 minutes and rehydrated through decreasing concentrations of alcohol into distilled water. Endogenous peroxidase was blocked with 3% $H_2O_2$ for 10 minutes followed by washing in distilled water. Antigen retrieval was performed by microwaving sections in 10 mM citrate buffer (pH 6.0) for 15 minutes. Slides were cooled and transferred to Tris Buffered Saline (TBS). Sections were blocked in 10% normal serum of the species the secondary antibody was raised in for 20 minutes. Primary antibody in 10% normal serum was then applied for 1 h at room temperature or overnight at 4 °C. Primary antibodies were as follows: Hsp70 (Enzo Life Sciences, Exeter, UK), CD3 (Dako, Cambridge, UK) and Foxp3 (affymetrix eBioscience, Hatfield, UK). After washing in TBS the sections were exposed to peroxidase-conjugated secondary antibody for 30 minutes. After washing in TBS for 5 minutes, sections were exposed to peroxidase substrate solution (3,3-diaminobenzidine tetrahydrochloride, DAB) (DAKO, Glostrup, Denmark). Following counterstaining with haematoxylin, sections were dehydrated through increasing concentrations of alcohol to xylene, before the cover-slip was mounted. Sections were then examined with light-microscopy. Appropriate primary antibody-only and secondary antibody-only controls were always performed to ensure that non-specific staining was not taking place.

## 2.17 Scoring of morphological kidney injury

Hematoxylin and eosin-stained sections were evaluated for tubulointerstitial injury. A series of non-overlapping fields (x200) were examined by an observer blinded to the sample number. A scoring system based on the proportion of tubules with

necrotic/detached cells was used (tubular necrosis score: 0, none; 1, <30%; 2, 30 – 70%; 3, >70%) [84].

## 2.18 Serum creatinine determination

Plasma samples were prepared from whole blood. Creatinine was determined using the creatininase/creatinase specific enzymatic method described by Borner *et al.* (1979) [243], utilising a commercial kit (Alpha Laboratories Ltd, Eastleigh, UK) adapted for use on a Cobas Fara centrifugal analyser (Roche Diagnostics Ltd, Welwyn Garden City, UK).

## 2.19 Murine cytokine array panel

Kidney protein lysates (200 μg per sample) were mixed with biotinylated detection antibodies. The sample/antibody mixture was then incubated with a mouse cytokine array panel (R&D Systems, Abingdon, UK). The panel consisted of a nitrocellulose membrane with capture antibodies for 40 murine cytokines spotted on its surface in a duplicate manner. Cognate immobilized capture antibodies on the membrane bound any cytokine/detection antibody complexes present. Following a wash to remove unbound material, Streptavidin-HRP and chemiluminescent detection reagents were added sequentially followed by development using autoradiography. Light produced at each spot was used to determine the amount of cytokine bound. Mean gray values were quantified using Image J (National Institutes of Health, USA) [244].

## 2.20 Real-time reverse transcriptase–PCR

For the detection of renal TLR4 expression, RNA was extracted from kidneys and purified by TRIzol (Invitrogen, Life Technologies, Paisley, UK). RNA concentration and quality was determined using a Nanodrop spectrophotometer and Agilent Bioanalyzer. Across all samples the mean 260/280 ratio was 2.06 +/- 0.01, and mean RNA integrity number was 7.9 +/- 0.6. cDNA was synthesized using a $RT^2$ First Strand Kit (Qiagen, Manchester, UK). Real-time PCR was then performed using a $RT^2$ qPCR primer assay for mouse TLR4 (Qiagen, Manchester, UK). GAPDH was used as the reference gene, and was also quantified using a $RT^2$ qPCR primer assay (Qiagen, Manchester UK).

## 2.21 Statistical analysis

Data are presented as mean and standard error of the mean or in standard boxplots with individual results jittered. Statistical comparisons for parametric continuous data were made using student's t-test, one-way analysis of variance (ANOVA) and two-way ANOVA without interaction (using the Tukey's HSD post hoc correction for multiple comparisons). Statistical comparisons for non-parametric data were made using the Mann-Whitney U test. All comparisons were performed in R v3.0.1 (R Foundation for Statistical Computing).

## 2.22 Power calculation

For animal experiments in the renal IRI model, power calculations were performed and the number of mice was kept to a minimum required to answer the research question. Creatinine was selected as the primary outcome measure since it is

objectively measured and less affected by hydration status than blood urea nitrogen. Although creatinine levels are affected by muscle mass and thus differ according to mouse gender and age, all experiments were performed on male mice of the same age. Previous data was used to the estimate effect size for the potential reduction in serum creatinine. Based on the reduction in creatinine in animals treated with Hsp90 inhibitors that underwent contralateral nephrectomy and 30 minutes renal IRI, an effect size of 1.70 was calculated [84]. With $\alpha$ set at 0.05 and $\beta$ set at 0.1 this translated to a required sample size of 9 animals per treatment group [245] (Table 2.1).

| | Creatinine (μmol/l) |
|---|---|
| Test significance level (α) | 0.05 |
| Group 1 mean | 97.8 |
| Group 2 mean | 69.5 |
| Standard deviation | 16.6 |
| Effect size | 1.70 |
| Power (%) | 90 |
| n per group | 9 |

**Table 2.1 Power calculation for animal experiments**

Previous data was used to the estimate effect size for the potential reduction in serum creatinine [84]. Based on the reduction in creatinine in animals treated with Hsp90 inhibitors that underwent contralateral nephrectomy and 30 min renal IRI, an effect size of 1.70 was calculated. This translates to a required sample size of 9 animals per treatment group [245].

# Chapter 3: AT13387 represses TLR4-mediated NF-κB activation resulting in reduced pro-inflammatory cytokine release

## 3.1 Background

As discussed in Chapter 1, Hsp90 may be needed to stabilise IKK [130] and the use of Hsp90 inhibitors could cause dissociation of the IKK complex and prevention of NF-κB activation [125]. Hsp90 inhibition has previously been used to experimentally treat TLR4-mediated autoimmune diseases [86, 87] and reduce TNFα-mediated NF-κB activation [131-135]. However, it remains to be proven whether TLR4 signalling to NF-κB can be similarly targeted by AT13387. This chapter will address the hypothesis that AT13387 represses TLR4-mediated NF-κB activation resulting in reduced pro-inflammatory cytokine release.

## 3.2 HEK293 cells do not express TLR4

HEK293 cells were selected specifically for these experiments since they are easy to grow, transfect efficiently and have previously been reported to lack TLR4 expression [246, 247]. The absence of TLR4 expression by HEK293 cells was confirmed by flow cytometry (Figure 3.1a) [246]. In addition, TLR4 expression was unaltered by exposure to oxidative stress with hydrogen peroxide (Figure 3.1b). This is in contrast to human renal tubular epithelial cells, which express basal levels of TLR4 that are further up-regulated following pro-inflammatory stimulation [248]. Successful TLR4 transfection was validated in HEK293-TLR4 and HEK293-TLR4-NF-κB cell lines by flow cytometry (Figure 3.2a,b). HEK293 and HEK293-TLR4 cells were therefore considered ideal for identifying a suitable TLR4-specific ligand

to explore the *in vitro* hypothesis that AT13387 leads to repression of TLR4-mediated NF-κB activation.

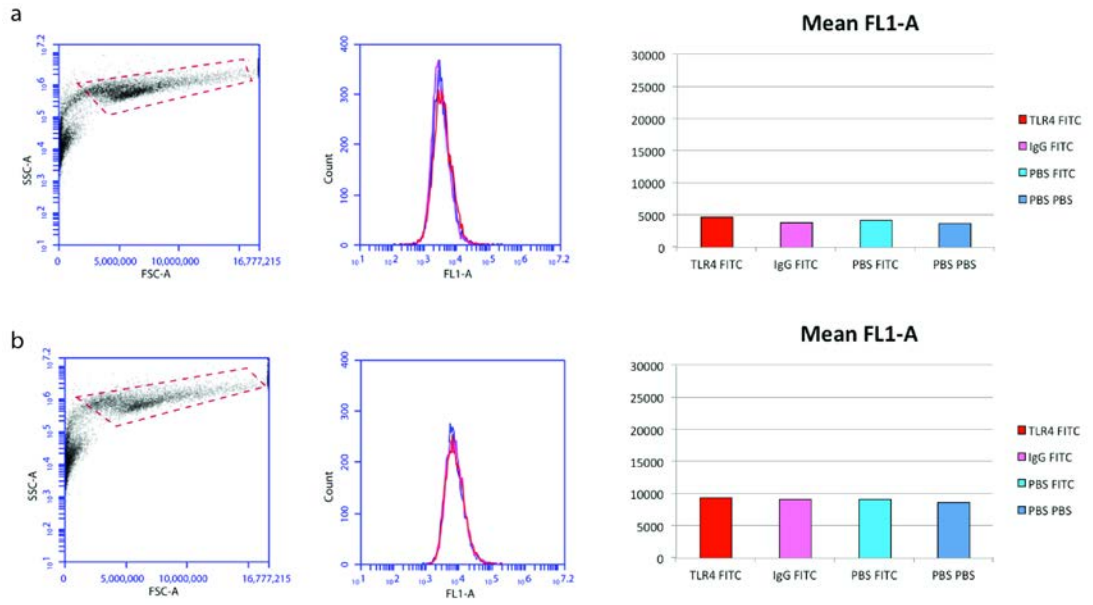


**Figure 3.1 TLR4 flow cytometry on HEK293 cells**

**a) TLR4 expression by HEK293 cells on flow cytometry**. Cells were trypsinised and collected at 50,000 cells per sample. Samples were first incubated at room temperature with 2% rabbit serum for 20 min. Following this a 30 min room temperature incubation was performed with either 50 µl of PBS/0.5% BSA/0.1% azide (unstained control), mouse IgG1 isotype control antibody or purified mouse anti-human TLR4 antibody (0.5 mg/ml at 1:50 dilution or 0.5 µg per test sample). The primary antibodies were washed off with PBS/0.5% BSA/0.1% azide. The cells were then incubated for a further 30 min at room temperature with PBS/0.5% BSA/0.1% azide for unstained controls, and FITC-conjugated goat anti-mouse IgG for IgG1 isotype control antibody samples and TLR4 test samples. The secondary antibodies were washed off with PBS/0.5% BSA/0.1% azide and results were acquired on a BD Accuri C6 flow cytometer. Cells were gated on the basis of forward and side scatter. TLR4 expression in HEK293 cells is represented by the red histograms, IgG-FITC negative control sample by the pink histograms, PBS-FITC negative control sample by the light blue histograms and PBS-PBS negative control sample by the dark blue histograms (n=1).

**b) TLR4 expression by HEK293 cells following oxidative stress on flow cytometry**. Cells were treated with 0.4 mM of Hydrogen Peroxide for 16 h then analysed as per figure 3.1a. The dose of hydrogen peroxide was selected from a dose response assay, and was anticipated to cause oxidative stress without excessive (<10%) cell death (Figure 4.1). TLR4 expression in HEK293 cells is represented by the red histograms, IgG-FITC negative control sample by the pink histograms, PBS-FITC negative control sample by the light blue histograms and PBS-PBS negative control sample by the dark blue histograms (n=1).

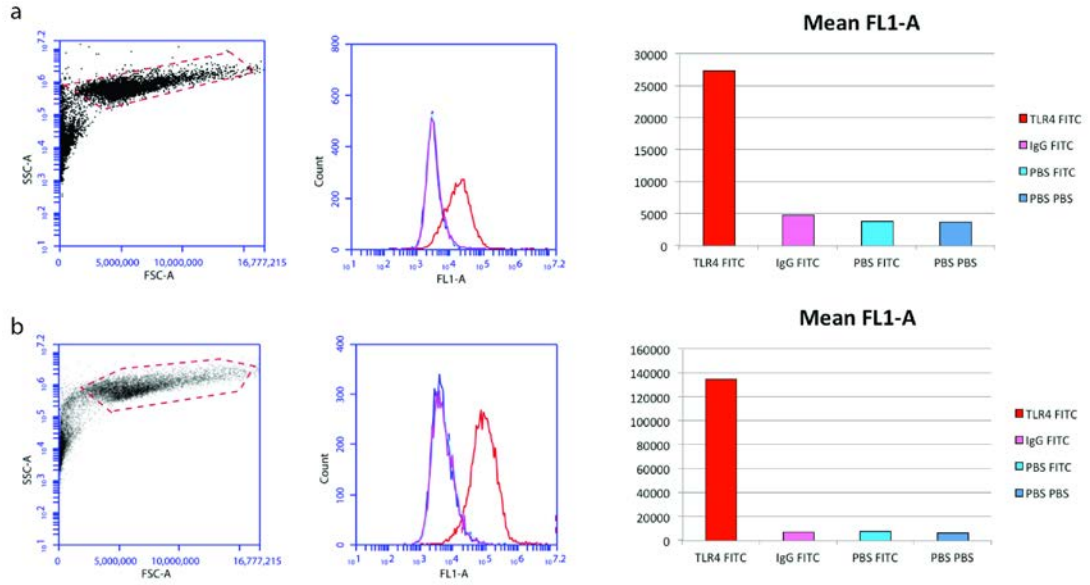


**Figure 3.2 TLR4 flow cytometry on TLR4 transfected HEK293 cells**

**a) TLR4 expression by HEK293-TLR4 cells on flow cytometry**. Cells were analysed as per figure 3.1a. TLR4 expression in HEK293-TLR4 cells is represented by the red histograms, IgG-FITC negative control sample by the pink histograms, PBS-FITC negative control sample by the light blue histograms and PBS-PBS negative control sample by the dark blue histograms (n=1).

**b) TLR4 expression by HEK293-TLR4-NF-κB cells on flow cytometry.** Cells were analysed as per figure 3.1a. TLR4 expression in HEK293-TLR4-NF-κB cells is represented by the red histograms, IgG-FITC negative control sample by the pink histograms, PBS-FITC negative control sample by the light blue histograms and PBS-PBS negative control sample by the dark blue histograms (n=1).

## 3.3 Endotoxin-free hyaluronan is a sterile TLR4-specific ligand in HEK293 cells expressing TLR4

Hyaluronan is a DAMP and a proposed endogenous TLR4 ligand that is released in increasing amounts during the sterile insult that comprises renal IRI [168]. TLR4 was selectively expressed using TLR4-transfected cells (HEK293-TLR4). After ligand stimulation NF-κB activity was assessed by luciferase assay in comparison to TLR4-null cells (HEK293). Following hyaluronan stimulation there was increased NF-κB activity in HEK293-TLR4 cells, but an absence of NF-κB up-regulation in HEK293 cells (HEK293-TLR4 vs. HEK293, $p<0.001$, t-test) (Figure.3.3). This indicates that hyaluronan is a TLR4-specific ligand in HEK293-TLR4 cells. In HEK293-TLR4-NF-κB cells there was also significant NF-κB up-regulation following a TLR4-ligand dose response assay with hyaluronan (Figure 3.4). Furthermore, the level of TLR4-mediated NF-κB activation assessed by SEAP assay following hyaluronan stimulation was not altered by the presence of polymyxin B, a drug that clears endotoxin contamination (Figure 3.5). Therefore, hyaluronan was used to model sterile TLR4-specific NF-κB activation in further experiments.

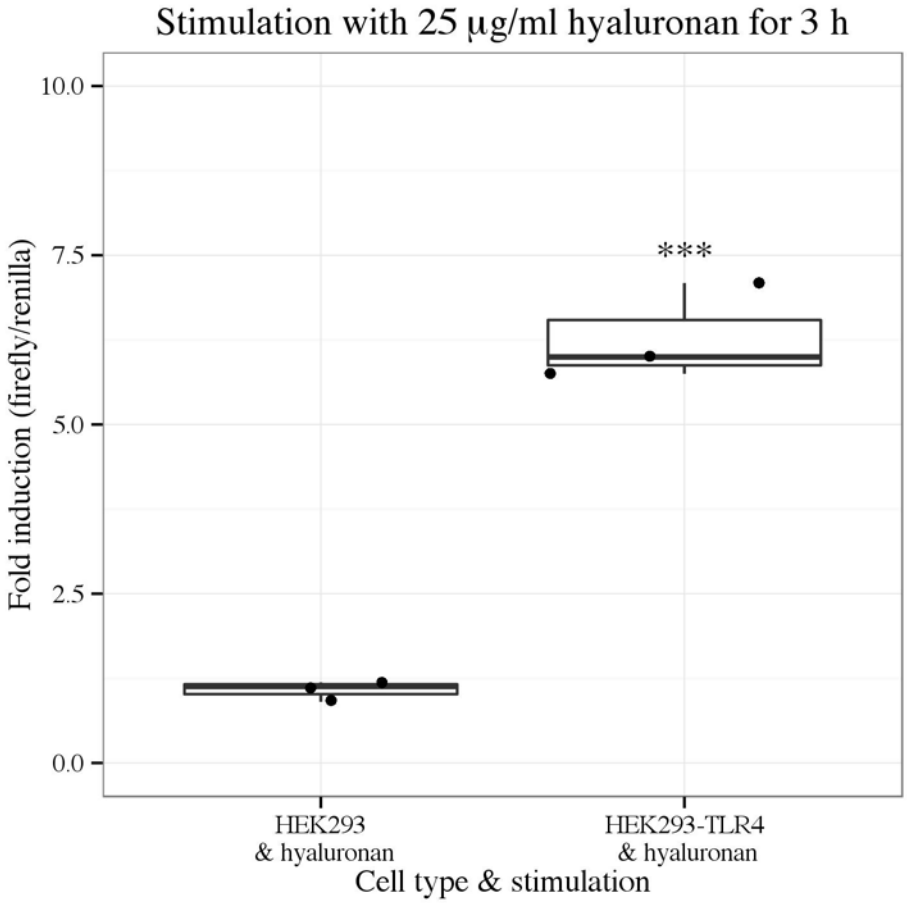


**Figure 3.3 Luciferase assay to determine NF-κB activity following NF-κB transfection and hyaluronan stimulation in HEK293 and HEK293-TLR4 cells**

HEK293 and HEK293-TLR4 cells were divided at a cell density of 100,000 cells in 1 ml of growth medium per well of a 12-well plate. After 24 h, cells were transfected with 0.5 µg pGL4.32 [luc2P/NF-κB-RE/Hygro] plasmid DNA (experimental vector) using a ratio of DNA to Fugene HP of 3:1. A constitutively active control vector (pGL4.73 [hRluc/SV40]) was added at a ratio of experimental to control vector of 100:1. 24 h later, cells were treated with hyaluronan at a dose of 25 µg/ml. After 3 h incubation a luciferase assay was performed to determine firefly activity and renilla activity. Fold induction was calculated from the ratio of firefly to renilla and used to reflect NF-κB activity. Results are presented as 3 independent experiments in a standard boxplot with individual results jittered. The mean fold induction in HEK293 cells was 1.07 +/- 0.09 (standard error of the mean), i.e. there was no increase in NF-κB activity following hyaluronan stimulation. ***$p<0.001$ vs. HEK293 & hyaluronan, t-test.

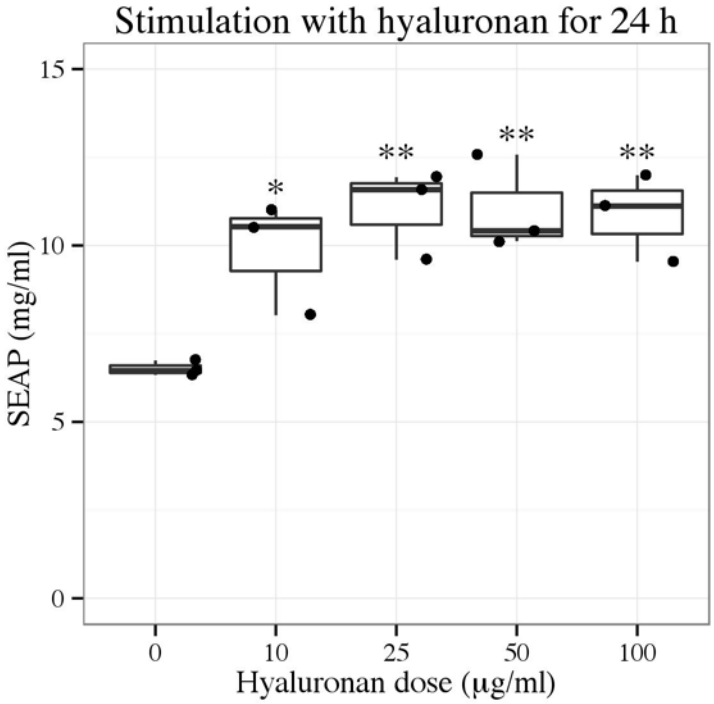


**Figure 3.4 SEAP assay to determine NF-κB activity following a ligand dose response assay using hyaluronan stimulation in HEK293-TLR4-NF-κB cells**

HEK293-TLR4-NF-κB cells were divided at a cell density of 10,000 cells in 100 µl of growth medium per well of a 96-well plate. 24 h later, medium was changed to medium containing hyaluronan at doses ranging from 0 µg/ml to 100 µg/ml. Cells treated with 0 µg/ml of hyaluronan were left in basal conditions in normal culture medium. After 24 h incubation a SEAP assay was performed to determine NF-κB activity. Results are presented from 3 independent experiments in a standard boxplot with individual results jittered. *$p<0.05$ vs. 0 ng/ml hyaluronan and **$p<0.01$ vs. 0 ng/ml hyaluronan, ANOVA.

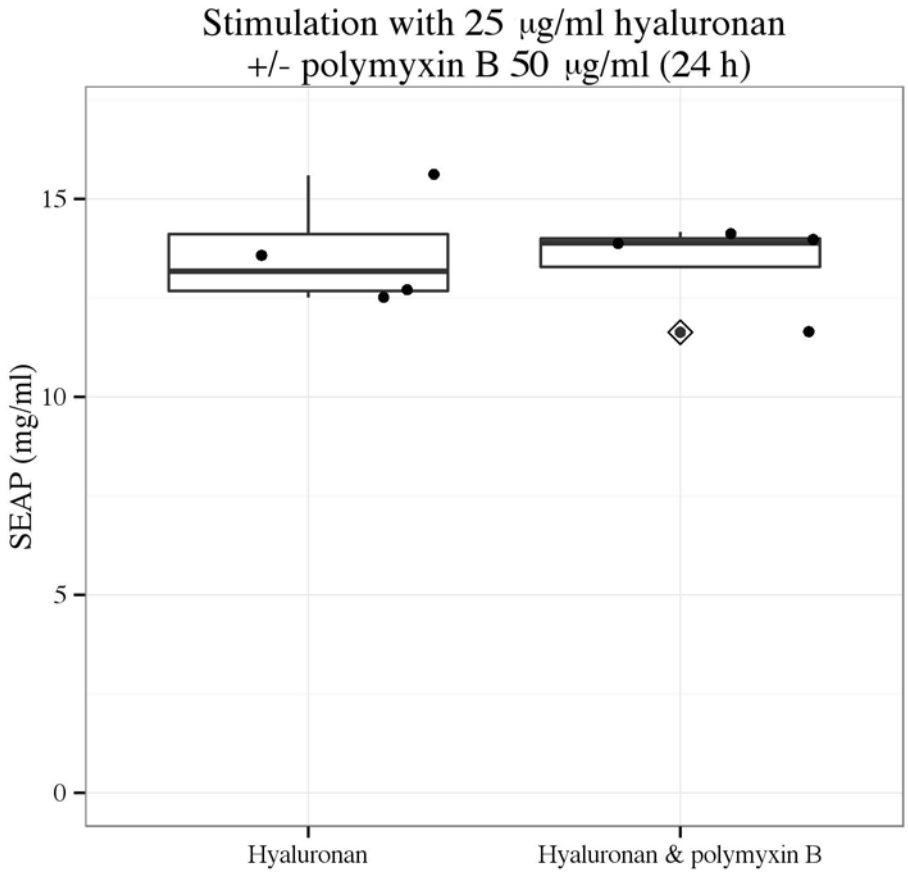


**Figure 3.5 SEAP assay to determine NF-κB activity following hyaluronan stimulation with and without the presence of polymyxin B in HEK293-TLR4-NF-κB cells**

HEK293-TLR4-NF-κB cells were divided at a cell density of 10,000 cells in 100 µl of growth medium per well of a 96-well plate. 24 h later, the medium was changed to medium containing 25 µg/ml of hyaluronan either with or without 50 µg/ml of polymyxin B. After 24 h incubation a SEAP assay was performed to determine NF-κB activity. Results are presented from 4 independent experiments in a standard boxplot with individual results jittered. Outlier data are highlighted by a dot with a diamond in the midline.

## 3.4 AT13387 and 17-DMAG pre-treatment leads to repression of TLR4-mediated NF-κB activation

Hyaluronan was used to test whether pre-treatment with AT13387 and 17-DMAG could lead to a significant reduction in NF-κB activity when mediated by a sterile and highly TLR4-specific stimulus. In HEK293-TLR4-NF-κB cells, pre-treatment with AT13387 and 17-DMAG significantly reduced hyaluronan-mediated NF-κB activity assessed by SEAP assay (AT13387 1000 nM vs. DMSO vehicle, $p<0.001$, 17-DMAG 1000 nM vs. DMSO vehicle, $p<0.001$, AT13387 500 nM vs. DMSO vehicle, $p<0.001$, ANOVA) (Figure 3.6). In fact, pre-treatment with AT13387 reduced NF-κB activity assessed by SEAP assay following hyaluronan stimulation to a level equivalent of cells in basal conditions in normal culture medium (Figure 3.5). In addition, AT13387 was significantly more effective at reducing hyaluronan-mediated NF-κB activity assessed by SEAP assay than 17-DMAG (AT13387 1000 nM vs. 17-DMAG 1000 nM, $p<0.01$, ANOVA) including at a lower dose (AT13387 500 nM vs. 17-DMAG 1000 nM, $p<0.05$, ANOVA). 17-DMAG was ineffective at reducing NF-κB activity at these lower doses. AT13387 therefore had inhibitory efficacy at lower doses than 17-DMAG.

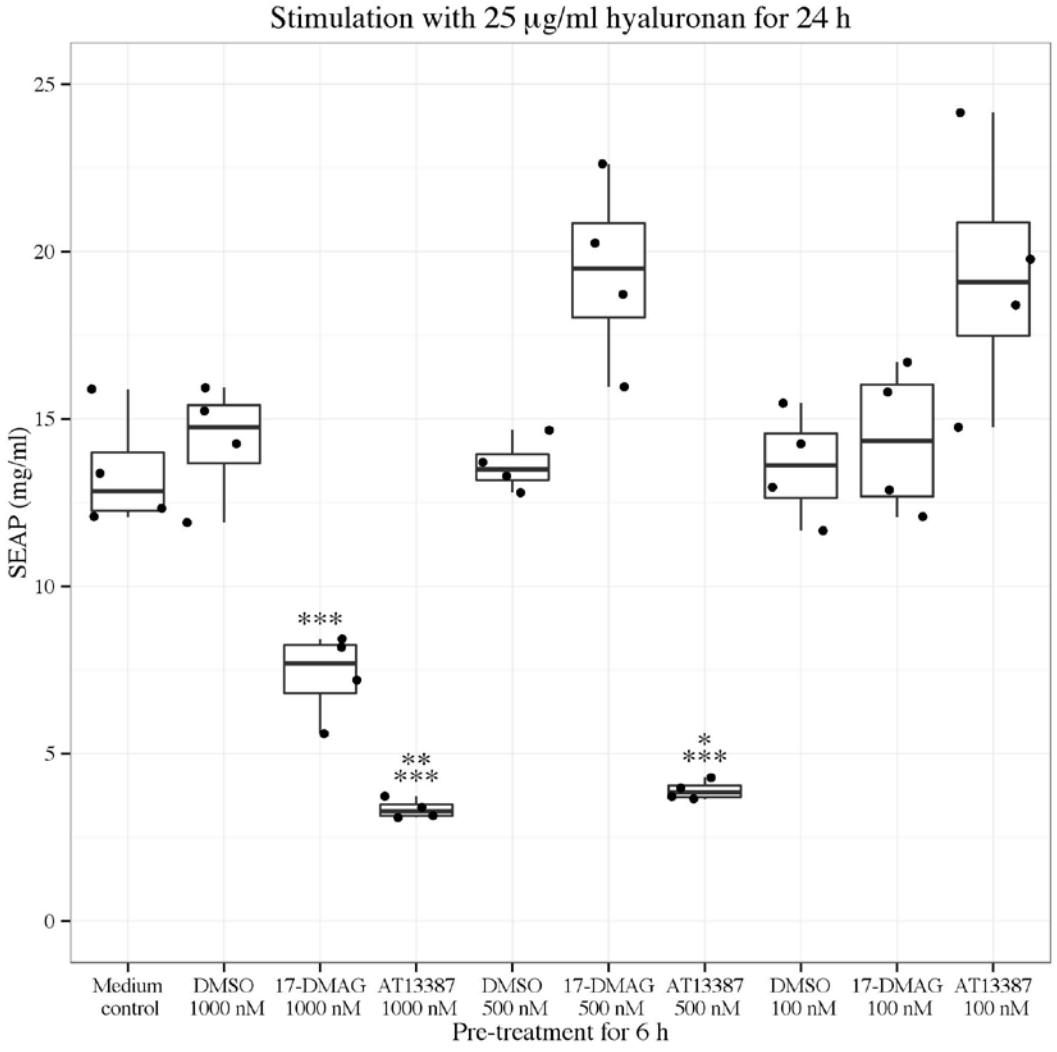


**Figure 3.6 NF-κB activity determined by SEAP assay following pre-treatment with AT13387 or 17-DMAG and hyaluronan stimulation in HEK293-TLR4-NF-κB cells**

HEK293-TLR4-NF-κB cells were divided at a cell density of 10,000 cells in 100 µl of growth medium per well of a 96-well plate. 24 h later, cells were pre-treated with AT13387, 17-DMAG, DMSO vehicle or medium control for 6 h. Hyaluronan was added at a dose of 25 µg/ml for 24 h and a SEAP assay was performed to determine NF-κB activity. Results are presented from 4 independent experiments in a standard boxplot with individual results jittered. *$p<0.05$ vs. 17-DMAG, **$p<0.01$ vs. 17-DMAG and ***$p<0.001$ vs. DMSO vehicle, ANOVA.

## 3.5 Pre-treatment with AT13387 and 17-DMAG leads to loss of the IKK complex

IKK is composed of two protein kinase subunits IKKα and IKKβ as well as the regulatory subunit NEMO [127]. IKK activation leads to the dissociation of NF-κB from IκB and its subsequent activation. Hsp90 inhibition, using pre-treatment with AT13387 and 17-DMAG led to breakdown of the IKK complex on Western blot following hyaluronan stimulation in HEK293-TLR4-NF-κB cells (Figure 3.7).

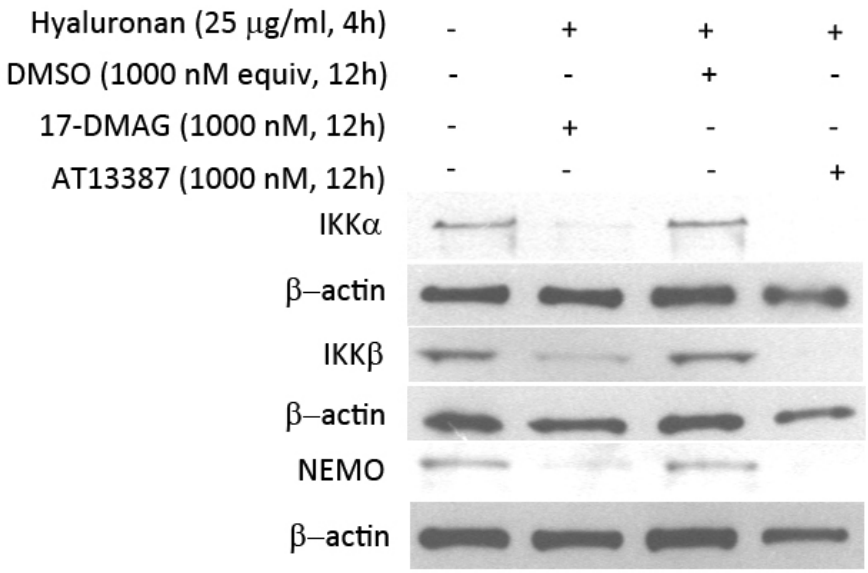


**Figure 3.7 IKKα, IKKβ and NEMO levels on Western blotting following AT13387 or 17-DMAG pre-treatment and hyaluronan stimulation in HEK293-TLR4-NF-κB cells**

HEK293-TLR4-NF-κB cells were divided at a cell density of 500,000 cells in 2 ml of growth medium per well of a 6-well plate. 24 h later, cells were then pre-treated with AT13387, 17-DMAG, DMSO vehicle or medium control for 12 h. With the exception of cells pre-treated with medium control, hyaluronan was added for 4 h. Whole-cell lysates were then prepared and analysed by Western blotting using antibodies to IKKα, IKKβ and NEMO, with β-actin being indicated as a loading control (n=1). Three different β-actin levels are presented because three separate Western blots were performed on the same samples to avoid antibody interactions.

## 3.6 IKKα is degraded by autophagy following treatment with AT13387 and 17-DMAG

Hsp90 inhibition has previously been shown to result in a proteasome-independent and autophagy-mediated degradation of IKK, which can be prevented by the autophagy inhibitor AICAR [249]. In further experiments, pre-incubation with, and the presence of, AICAR prevented IKKα degradation on Western blot by Hsp90 inhibition in HEK293-TLR4-NF-κB cells (Figure 3.8). AICAR also prevented IKKα degradation on Western blot by Hsp90 inhibition in HEK293-TLR4-NF-κB cells following hyaluronan stimulation (Figure 3.9). However, in contrast to the previous study [249], AICAR did not appear to affect the level of IKKβ or NEMO detected on Western blot following Hsp90 inhibition (Figure 3.8 and Figure 3.9).

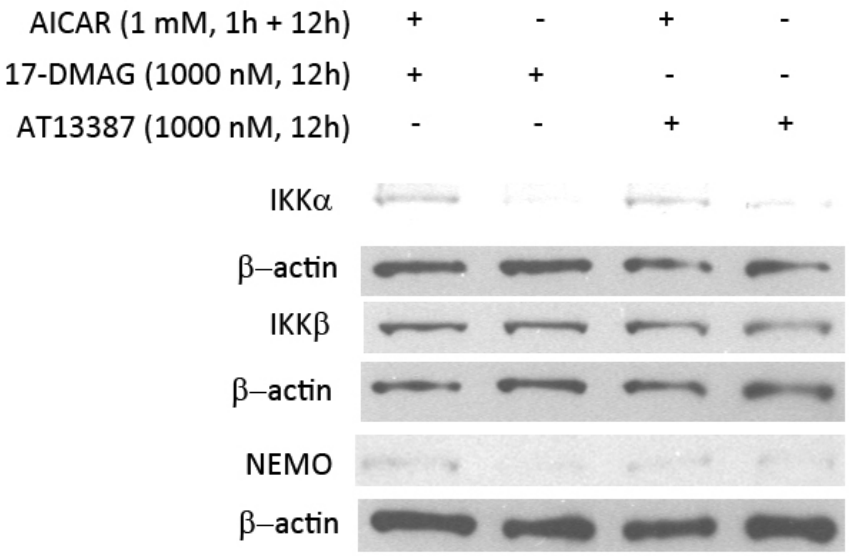


**Figure 3.8 IKKα, IKKβ and NEMO levels on Western blotting following AT13387 or 17-DMAG treatment with and without pre-incubation/presence of AICAR in HEK293-TLR4-NF-κB cells**

HEK293-TLR4-NF-κB cells were divided at a cell density of 500,000 cells in 2 ml of growth medium per well of a 6-well plate. 24 h later, cells were treated with AT13387 or 17-DMAG for 12 h or were pre-incubated with AICAR for 1 h then treated with AT13387 or 17-DMAG in the presence of AICAR for 12 h. Whole-cell lysates were prepared and analysed by Western blotting using antibodies to IKKα, IKKβ and NEMO, with β-actin being indicated as a loading control (n=1). Three different β-actin levels are presented because three separate Western blots were performed on the same samples to avoid antibody interactions.

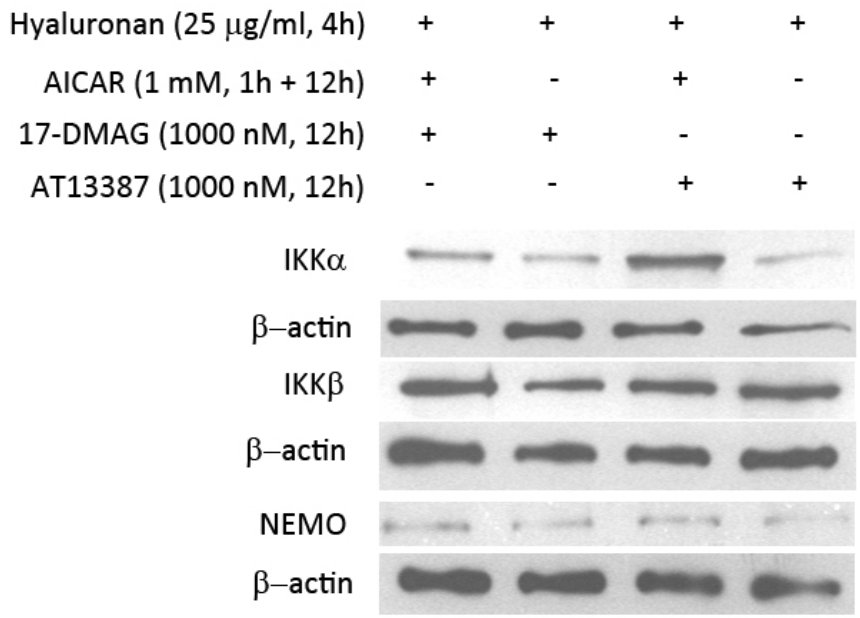


**Figure 3.9 IKKα, IKKβ and NEMO levels on Western blotting following AT13387 or 17-DMAG pre-treatment with and without pre-incubation/presence of AICAR and hyaluronan stimulation in HEK293-TLR4-NF-κB cells**

HEK293-TLR4-NF-κB cells were divided and treated as per figure 3.8. Hyaluronan was then added for 4 h. Whole-cell lysates were prepared and analysed by Western blotting using antibodies to IKKα, IKKβ and NEMO, with β-actin being indicated as a loading control (n=1). Three different β-actin levels are presented because three separate Western blots were performed on the same samples to avoid antibody interactions.

## 3.7 AICAR partially restores NF-κB activity in AT13387 and 17-DMAG pre-treated cells following hyaluronan stimulation

On SEAP assay, pre-incubation and presence of AICAR significantly reduced 17-DMAG but not AT13387-mediated NF-κB repression in HEK293-TLR4-NF-κB cells stimulated with hyaluronan (17-DMAG 1000 nM & AICAR 1 mM vs. 17-DMAG 1000 nM, $p<0.05$, AT13387 1000 nM & AICAR 1 mM vs. AT13387 1000 nM, $p=0.26$, t-test). In these experiments, AT13387 and 17-DMAG were administered at a high dose (1000 nM). There was again marked NF-κB down-regulation and in contrast to earlier results both drugs appeared equally effective at this dose (AT13387 1000 nM vs. DMSO vehicle, $p<0.001$, 17-DMAG 1000 nM vs. DMSO vehicle, $p<0.001$, ANOVA). AICAR alone also led to partial de-activation of TLR4-mediated NF-κB activity by hyaluronan (AICAR 1 mM vs. DMSO 1000 nM, $p=0.06$, t-test) (Figure 3.10).

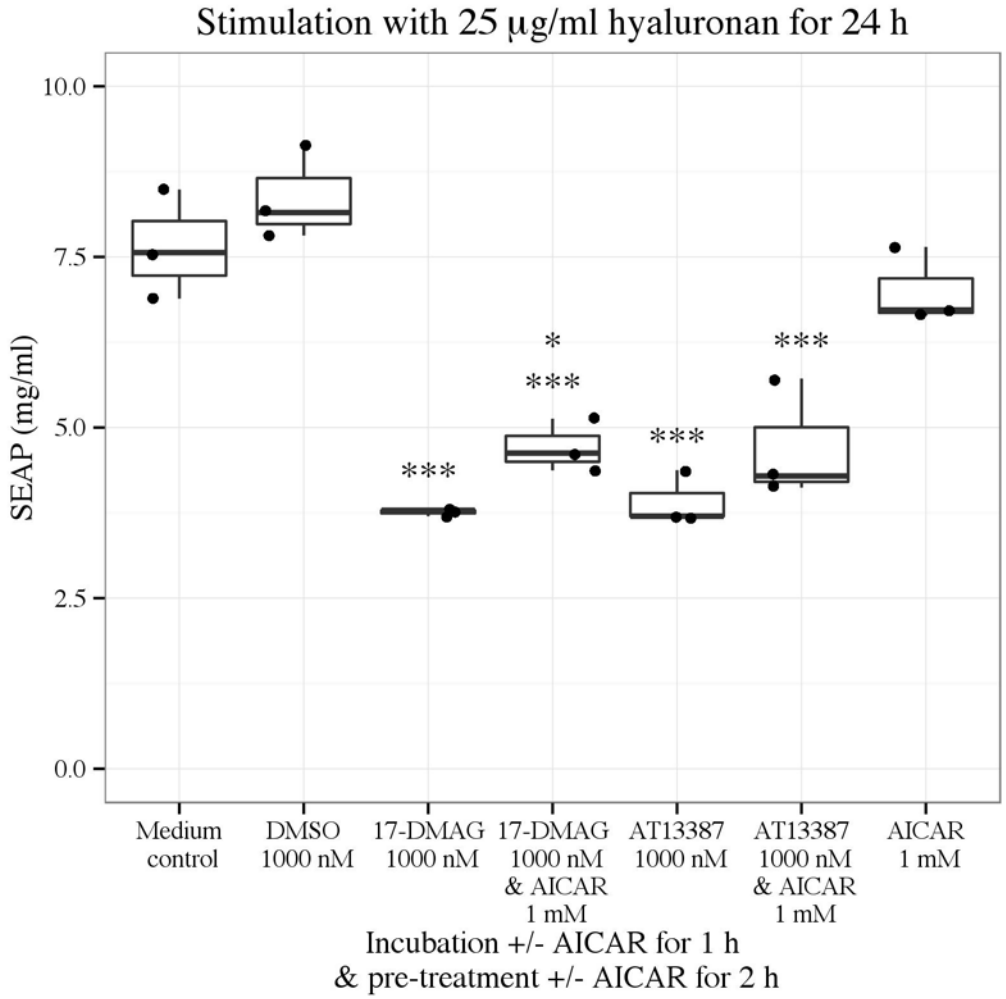


**Figure 3.10 SEAP assay to determine NF-κB activity following pre-treatment with AT13387 or 17-DMAG with and without pre-incubation/presence of AICAR and hyaluronan stimulation in HEK293-TLR4-NF-κB cells**

HEK293-TLR4-NF-κB cells were divided at a cell density of 10,000 cells in 100 µl of growth medium per well of a 96-well plate. 24 h later, cells were pre-incubated with AICAR for 1 h or were left alone. AICAR pre-incubated cells were either pre-treated with AT13387 or 17-DMAG in the presence of AICAR or AICAR alone for 2 h. The non-AICAR incubated cells were then pre-treated with AT13387, 17-DMAG, DMSO vehicle or medium control for 2 h. After which hyaluronan was added at a dose of 25 µg/ml. Following 24 h incubation a SEAP assay was performed to determine NF-κB activity. Results are presented from 3 independent experiments in a standard boxplot with individual results jittered. *$p<0.05$ vs. 17-DMAG, t-test and ***$p<0.001$ vs. DMSO vehicle, ANOVA.

## 3.8 AT13387 and 17-DMAG pre-treatment reduces TLR4-mediated pro-inflammatory cytokine release

The *in vitro* model that was developed simulated the sterile inflammatory environment of renal IRI, but it was unclear what the cytokine response would be like following stimulation with hyaluronan in HEK293 cells. Therefore a cytokine array panel was performed in order to evaluate the expression of a broad range of cytokines. AT13387 and 17-DMAG pre-treatment led to a reduction in the release of cytokines as assessed by cytokine array panel following hyaluronan stimulation. Most notably, there was marked reduction in the expression of the pro-inflammatory chemokine GROα (Figure 3.11). As this was a single array, quantitative analysis was not performed, and all other differentially expressed cytokines must be cautiously interpreted.

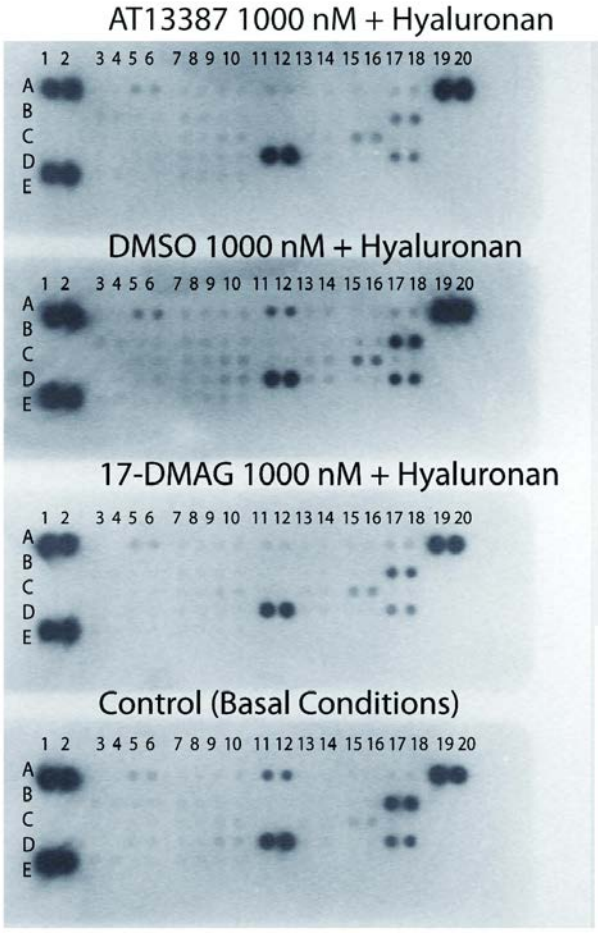


Cytokine Co-ordinates

| Coordinate | Target/Control | Alternate Nomenclature |
|---|---|---|
| A1, A2 | Reference Spot | — |
| A3, A4 | C5/C5a | Complement Component 5/5a |
| A5, A6 | CD40 Ligand | CD154 |
| A7, A8 | G-CSF | CSFβ, CSF-3 |
| A9, A10 | GM-CSF | CSFα, CSF-2 |
| A11, A12 | GROα | CXCL1 |
| A13, A14 | I-309 | CCL1 |
| A15, A16 | sICAM-1 | CD54 |
| A17, A18 | IFN-γ | Type II IFN |
| A19, A20 | Reference Spot | — |
| B3, B4 | IL-1α | IL-1F1 |
| B5, B6 | IL-1β | IL-1F2 |
| B7, B8 | IL-1ra | IL-1F3 |
| B9, B10 | IL-2 | — |
| B11, B12 | IL-4 | — |
| B13, B14 | IL-5 | — |
| B15, B16 | IL-6 | — |
| B17, B18 | IL-8 | CXCL8 |
| C3, C4 | IL-10 | — |
| C5, C6 | IL-12 p70 | — |
| C7, C8 | IL-13 | — |
| C9, C10 | IL-16 | LCF |
| C11, C12 | IL-17 | — |
| C13, C14 | IL-17E | — |
| C15, C16 | IL-23 | — |
| C17, C18 | IL-27 | — |
| D3, D4 | IL-32α | — |
| D5, D6 | IP-10 | CXCL10 |
| D7, D8 | I-TAC | CXCL11 |
| D9, D10 | MCP-1 | CCL2 |
| D11, D12 | MIF | GIF, DER6 |
| D13, D14 | MIP-1α | CCL3 |
| D15, D16 | MIP-1β | CCL4 |
| D17, D18 | Serpin E1 | PAI-1 |
| E1, E2 | Reference Spot | — |
| E3, E4 | RANTES | CCL5 |
| E5, E6 | SDF-1 | CXCL12 |
| E7, E8 | TNF-α | TNFSF1A |
| E9, E10 | sTREM-1 | — |
| E19, E20 | Negative Control | — |

**Figure 3.11 Cytokine expression following AT13387 or 17-DMAG pre-treatment and hyaluronan stimulation in HEK293-TLR4-NF-κB cells**

HEK293-TLR4-NF-κB cells were divided at a cell density of 500,000 cells in 2 ml of growth medium per well of a 6-well plate. 24 h later, cells were pre-treated with AT13387, 17-DMAG, DMSO vehicle or medium control for 6 h. With the exception of medium control pre-treated cells, which were left in basal conditions, hyaluronan was added at a dose of 25 μg/ml. After 24 h incubation a cytokine array panel was performed to determine cytokine expression (n=1).

## 3.9 Pre-treatment with AT13387 and 17-DMAG reduces non-TLR4-specific activation

It has previously been shown *in vitro*, in various cell lines, that Hsp90 inhibition may reduce non-TLR4-specific NF-κB activation mediated by TNFα [131-135]. These results were confirmed in HEK293 cells, where NF-κB activity assessed by luciferase assay increased with TNFα stimulation (Figure 3.12), and pre-treatment with AT13387 and 17-DMAG led to a significant reduction in TNFα-mediated NF-κB activity (AT13387 100 nM vs. DMSO vehicle, $p<0.001$, 17-DMAG 1000 nM vs. DMSO vehicle, $p<0.05$, ANOVA) (Figure.3.13). The results were further validated in HEK293-TLR4-NF-κB cells where pre-treatment with AT13387 and 17-DMAG led to both reduced TNFα-mediated IκBα phosphorylation on ELISA (AT13387 1000 nM vs. DMSO vehicle, $p<0.01$, 17-DMAG 1000 nM vs. DMSO vehicle, $p<0.001$, ANOVA) (Figure 3.14) and NF-κB activation assessed by SEAP assay (AT13387 1000 nM vs. DMSO vehicle, $p<0.001$, 17-DMAG 1000 nM vs. DMSO vehicle, $p<0.001$, ANOVA) (Figure 3.15).

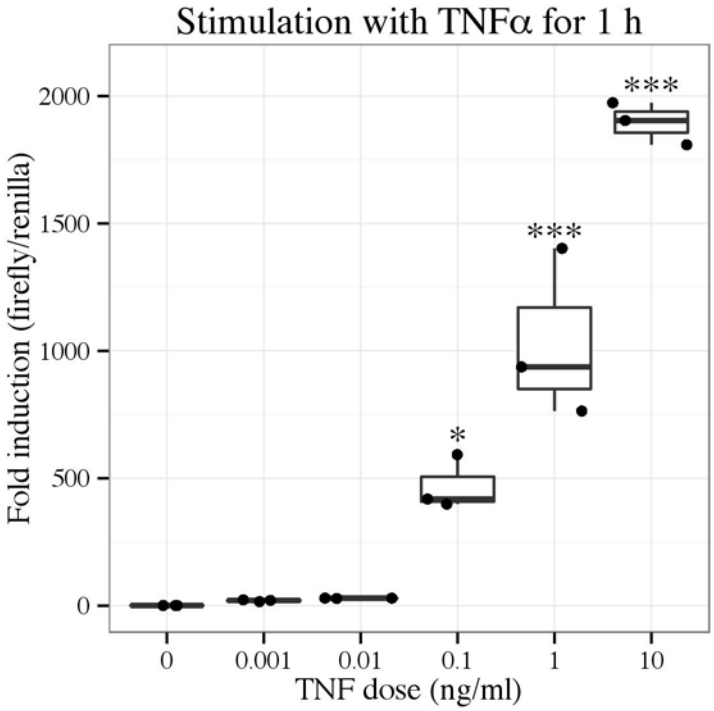


**Figure 3.12 Luciferase assay to determine NF-κB activity following NF-κB transfection and a ligand dose response assay using TNFα stimulation in HEK293 cells**

HEK293 cells were divided at a cell density of 100,000 cells in 1 ml of growth medium per well of a 12-well plate. After 24 h, cells were transfected with 0.5 µg pGL4.32 [luc2P/NF-κB-RE/Hygro] plasmid DNA (experimental vector) using a ratio of DNA to Fugene HD of 5:1. A constitutively active control vector (pGL4.73 [hRluc/SV40]) was added at a ratio of experimental to control vector of 100:1. 24 h later, TNFα was added at doses ranging from 0 ng/ml to 10 ng/ml (as per the manufacturer's instructions) for 1 h. A luciferase assay was then performed to determine firefly activity and renilla activity. Fold induction was calculated from the ratio of firefly to renilla and used to reflect NF-κB activity. Results are presented from 3 independent experiments in a standard boxplot with individual results jittered. *$p<0.05$ vs. 0 ng/ml TNFα and ***$p<0.001$ vs. 0 ng/ml TNFα, ANOVA.

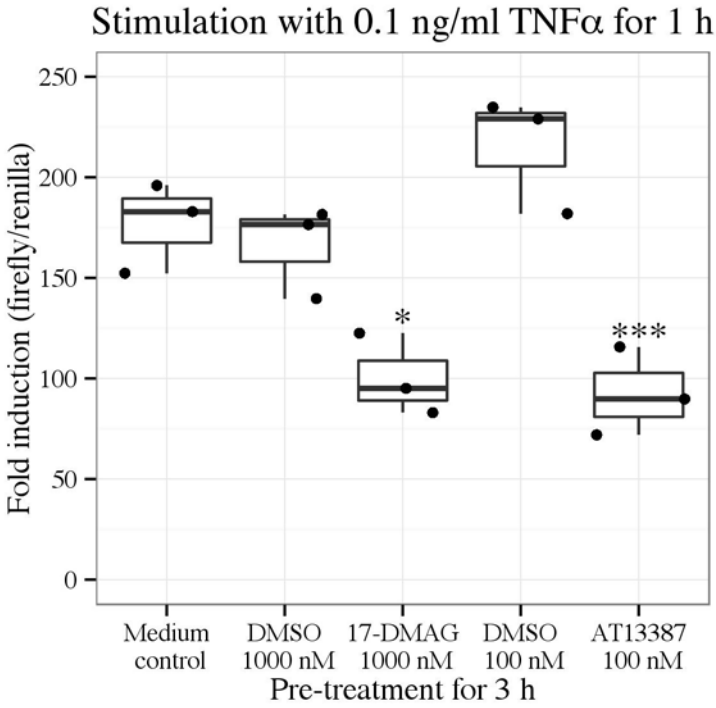


**Figure 3.13 Luciferase assay to determine NF-κB activity following NF-κB transfection, pre-treatment with AT13387 or 17-DMAG and TNFα stimulation in HEK293 cells**

HEK293 cells were divided and transfected as per figure 3.12. 24 h later, cells were pre-treated with AT13387, 17-DMAG, DMSO vehicle or medium control for 3h. TNFα was then added at a dose of 0.1 ng/ml for 1 h. This dose was selected from figure 3.12 as a potentially modifiable level of NF-κB activity. A luciferase assay was then performed to determine firefly activity and renilla activity. Fold induction was calculated from the ratio of firefly to renilla and used to reflect NF-κB activity. Results are presented from 3 independent experiments in a standard boxplot with individual results jittered. *$p<0.05$ vs. DMSO vehicle and ***$p<0.001$ vs. DMSO vehicle, ANOVA.

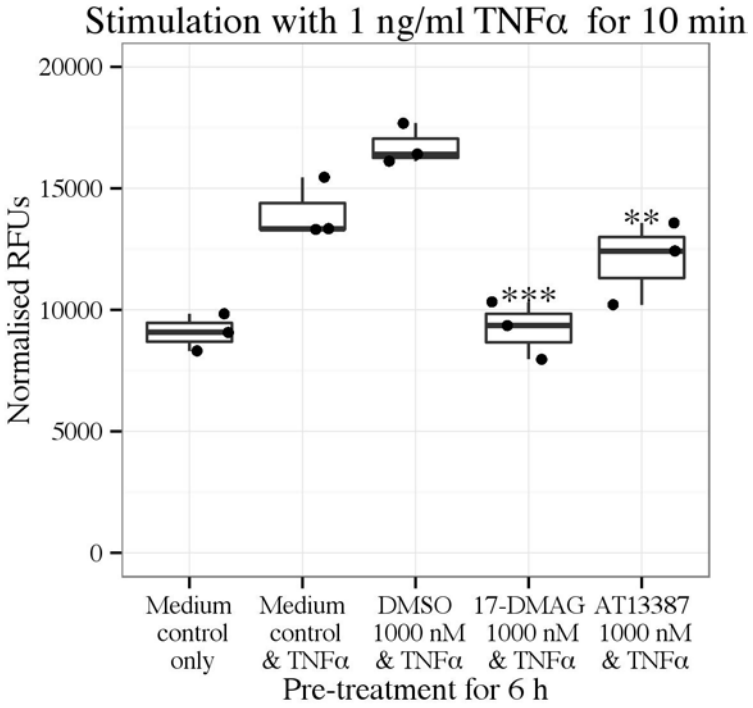


**Figure 3.14 ELISA to determine phosphorylated IκBα levels following pre-treatment with AT13387 or 17-DMAG and TNFα stimulation in HEK293-TLR4-NF-κB cells**

HEK293-TLR4-NF-κB cells were divided at a cell density of 10,000 cells in 100 µl of growth medium per well of a 96-well plate. 24 h later, cells were pre-treated with AT13387, 17-DMAG, DMSO vehicle or medium control for 6 h. TNFα was then added at a dose of 1 ng/ml for 10 min and a phosphorylated IκBα ELISA was performed. The dose of TNFα was increased in this experiment to maximise the possibility of detecting an increase in phosphorylated IκBα. Normalised RFUs (relative fluorescence units) were determined by dividing phosphorylated IκBα fluorescence in each well by the total GAPDH fluorescence in each well. The normalised RFUs were used to establish IκBα phosphorylation, which is an indicator of NF-κB activity. The ELISA was performed 10 minutes following ligand stimulation as per the manufacturers instructions. This reflects the rapid nature of phosphorylated IκBα expression. Results are presented from 3 independent experiments in a standard boxplot with individual results jittered. **$p<0.01$ vs. DMSO vehicle and ***$p<0.001$ vs. DMSO vehicle, ANOVA.

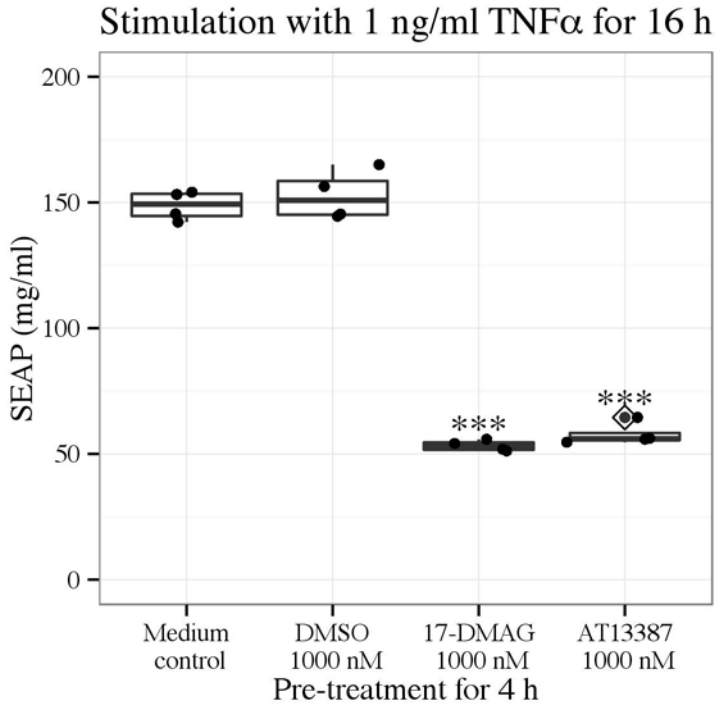


**Figure 3.15 SEAP assay to determine NF-κB activity following pre-treatment with AT13387 or 17-DMAG and TNFα stimulation in HEK293-TLR4-NF-κB cells**

HEK293-TLR4-NF-κB cells were divided at a cell density of 10,000 cells in 100 µl of growth medium per well of a 96-well plate. 24 h later, cells were pre-treated with AT13387, 17-DMAG, DMSO vehicle or medium control for 4 h. TNFα was then added at a dose of 1 ng/ml for 16 h and a SEAP assay was performed to determine NF-κB activity. The dose of TNFα was selected on the basis of the previous experiment (Figure 3.14). Results are presented from 4 independent experiments in a standard boxplot with individual results jittered. Outlier data are highlighted by a dot with a diamond in the midline. ***$p<0.001$ vs. DMSO vehicle, ANOVA.

## 3.10 Pre-treatment with AT13387 and 17-DMAG reduces non-sterile NF-κB activation

It has previously been shown that Hsp90 inhibition can reduce non-sterile LPS-mediated NF-κB activity in human monocytic cell lines [73, 250, 251]. These results were confirmed in HEK293-TLR4-NF-κB cells, where NF-κB activity assessed by SEAP assay increased with LPS stimulation (Figure 3.16), and pre-treatment with AT13387 and 17-DMAG led to a significant reduction in LPS-mediated NF-κB activity (AT13387 1000 nM vs. DMSO vehicle, $p<0.001$, 17-DMAG 1000 nM vs. DMSO vehicle, $p<0.001$, AT13387 100 nM vs. DMSO vehicle, $p<0.05$, ANOVA) (Figure 3.17). Moreover, pre-treatment with AT13387 reduced NF-κB activity assessed by SEAP assay following LPS stimulation to a level equivalent of cells in basal conditions in normal culture medium (Figure 3.16). In further experiments, breakdown of IKK on Western blot was noted following Hsp90 inhibition and LPS stimulation (Figure 3.18). In addition, a reduction in the release of cytokines was noted on cytokine array panel following Hsp90 inhibition and stimulation with LPS (Figure 3.19).

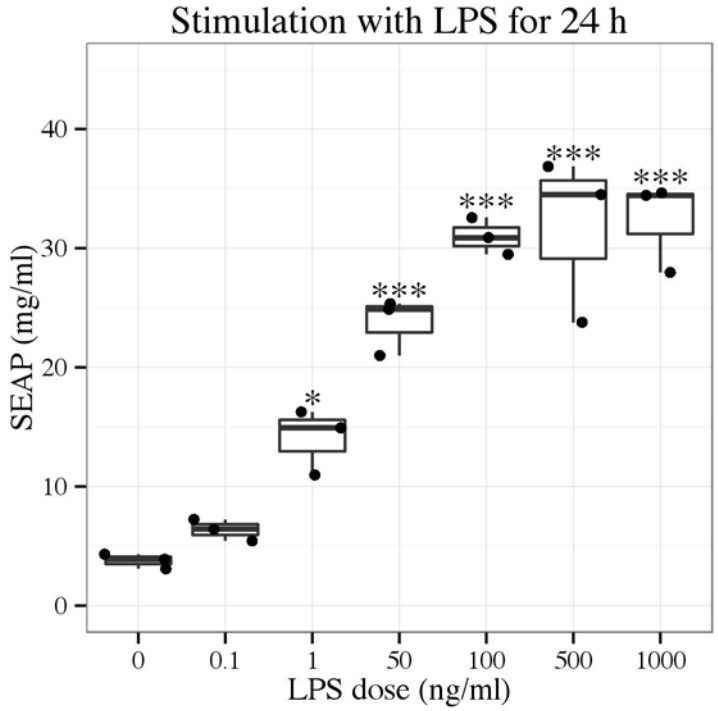


**Figure 3.16 SEAP assay to determine NF-κB activity following a ligand dose response assay using LPS stimulation in HEK293-TLR4-NF-κB cells**

HEK293-TLR4-NF-κB cells were divided at a cell density of 10,000 cells in 100 µl of growth medium per well of a 96-well plate. 24 h later, the medium was changed to medium containing LPS at doses ranging from 0 ng/ml to 1000 ng/ml. Cells treated with 0 ng/ml of LPS were left in basal conditions in normal culture medium. After 24 h incubation a SEAP assay was performed to determine NF-κB activity. Results are presented from 3 independent experiments in a standard boxplot with individual results jittered. *$p<0.05$ vs. 0 ng/ml LPS and ***$p<0.001$ vs. 0 ng/ml LPS, ANOVA.

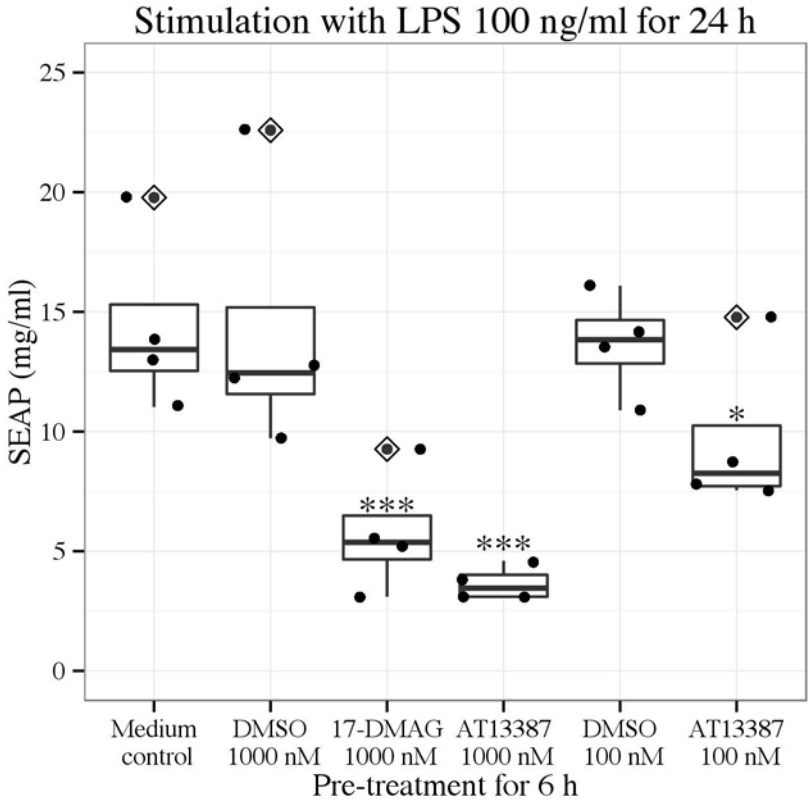


**Figure 3.17 SEAP assay to determine NF-κB activity following pre-treatment with AT13387 or 17-DMAG and LPS stimulation in HEK293-TLR4-NF-κB cells**

HEK293-TLR4-NF-κB cells were divided at a cell density of 10,000 cells in 100 µl of growth medium per well of a 96-well plate. 24 h later, cells were pre-treated with AT13387, 17-DMAG, DMSO vehicle or medium control for 6 h. LPS was then added at a dose of 100 ng/ml for 24 h and a SEAP assay was performed to determine NF-κB activity. Results are presented from 4 independent experiments in a standard boxplot with individual results jittered. Outlier data are highlighted by a dot with a diamond in the midline. *p<0.05 vs. DMSO vehicle and ***p<0.001 vs. DMSO vehicle, ANOVA.

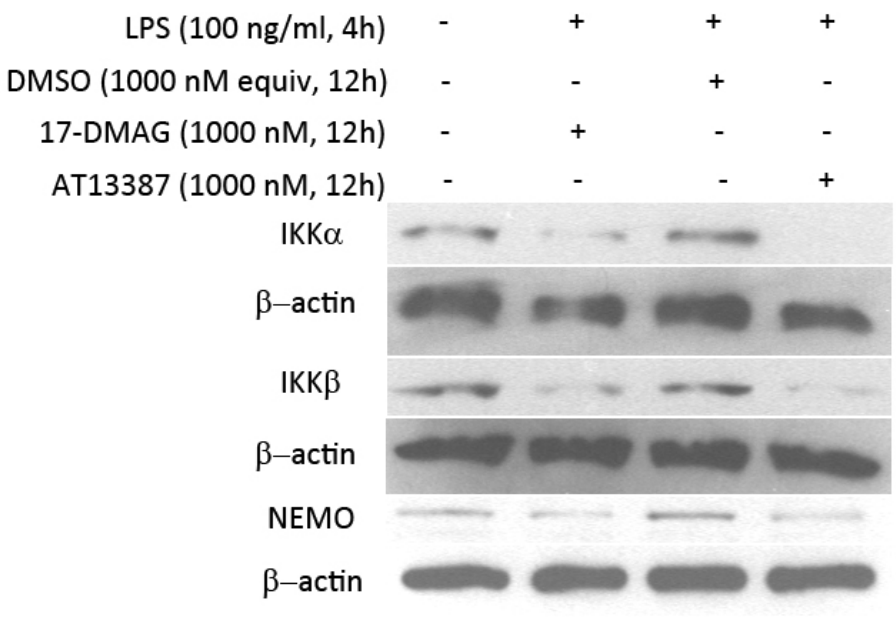


**Figure 3.18 IKKα, IKKβ and NEMO levels on Western blotting following AT13387 or 17-DMAG pre-treatment and LPS stimulation in HEK293-TLR4-NF-κB cells**

HEK293-TLR4-NF-κB cells were divided at a cell density of 500,000 cells in 2 ml of growth medium per well of a 6-well plate. 24 h later, cells were then pre-treated with AT13387, 17-DMAG, DMSO vehicle or medium control for 12 h. With the exception of cells pre-treated with medium control, LPS was added for 4 h. Whole-cell lysates were then prepared and analysed by Western blotting using antibodies to IKKα, IKKβ and NEMO, with β-actin being indicated as a loading control (n=1). Three different β-actin levels are presented because three separate Western blots were performed on the same samples to avoid antibody interactions.

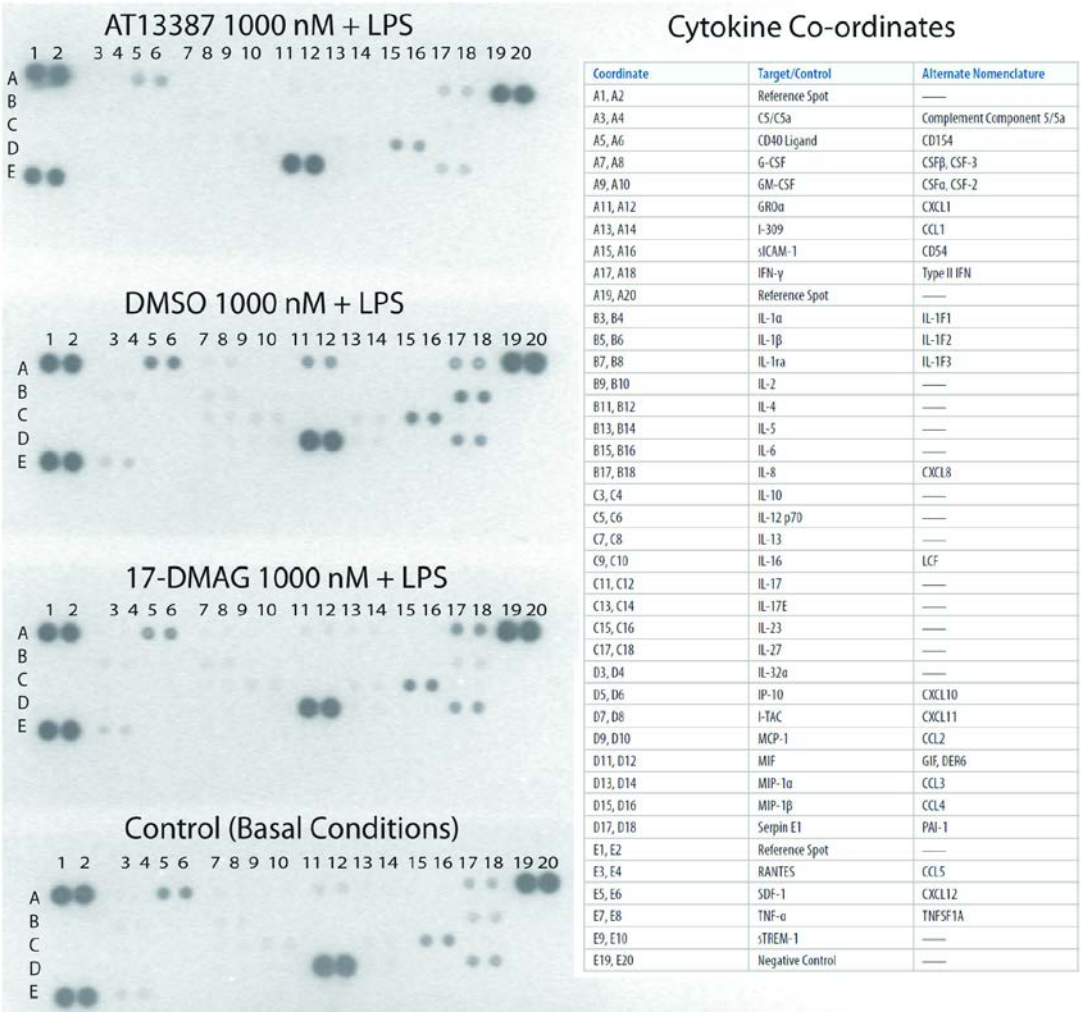


| Coordinate | Target/Control | Alternate Nomenclature |
|---|---|---|
| A1, A2 | Reference Spot | — |
| A3, A4 | C5/C5a | Complement Component 5/5a |
| A5, A6 | CD40 Ligand | CD154 |
| A7, A8 | G-CSF | CSFβ, CSF-3 |
| A9, A10 | GM-CSF | CSFα, CSF-2 |
| A11, A12 | GROα | CXCL1 |
| A13, A14 | I-309 | CCL1 |
| A15, A16 | sICAM-1 | CD54 |
| A17, A18 | IFN-γ | Type II IFN |
| A19, A20 | Reference Spot | — |
| B3, B4 | IL-1α | IL-1F1 |
| B5, B6 | IL-1β | IL-1F2 |
| B7, B8 | IL-1ra | IL-1F3 |
| B9, B10 | IL-2 | — |
| B11, B12 | IL-4 | — |
| B13, B14 | IL-5 | — |
| B15, B16 | IL-6 | — |
| B17, B18 | IL-8 | CXCL8 |
| C3, C4 | IL-10 | — |
| C5, C6 | IL-12 p70 | — |
| C7, C8 | IL-13 | — |
| C9, C10 | IL-16 | LCF |
| C11, C12 | IL-17 | — |
| C13, C14 | IL-17E | — |
| C15, C16 | IL-23 | — |
| C17, C18 | IL-27 | — |
| D3, D4 | IL-32α | — |
| D5, D6 | IP-10 | CXCL10 |
| D7, D8 | I-TAC | CXCL11 |
| D9, D10 | MCP-1 | CCL2 |
| D11, D12 | MIF | GIF, DER6 |
| D13, D14 | MIP-1α | CCL3 |
| D15, D16 | MIP-1β | CCL4 |
| D17, D18 | Serpin E1 | PAI-1 |
| E1, E2 | Reference Spot | — |
| E3, E4 | RANTES | CCL5 |
| E5, E6 | SDF-1 | CXCL12 |
| E7, E8 | TNF-α | TNFSF1A |
| E9, E10 | sTREM-1 | — |
| E19, E20 | Negative Control | — |

**Figure 3.19 Cytokine expression following AT13387 or 17-DMAG pre-treatment and LPS stimulation in HEK293-TLR4-NF-κB cells**

HEK293-TLR4-NF-κB cells were divided at a cell density of 500,000 cells in 2 ml of growth medium per well of a 6-well plate. 24 h later, cells were pre-treated with AT13387, 17-DMAG, DMSO vehicle or medium control for 6 h. With the exception of medium control pre-treated cells, which were left in basal conditions, LPS was added at a dose of 100 ng/ml. After 24 h incubation a cytokine array panel was performed to determine cytokine expression (n=1).

## 3.11 Summary

In this chapter it has been shown that AT13387 represses TLR4-mediated NF-κB activation, which may be an important pro-inflammatory signalling pathway involved in renal IRI. The mechanism of this repression appears to be through a loss of the IKK complex. The further experiments performed with TNFα and LPS suggest that in addition to repressing sterile TLR4-mediated NF-κB activation; Hsp90 inhibition also reduces NF-κB activity from both non-TLR4-specific and non-sterile stimuli.

## 3.12 Discussion

### 3.12.1 Limitations

The fact that the experiments in this chapter were conducted in only one immortalized cell type is the major weakness of the data presented. Immortalized HK2 cells (human cells with the proximal renal tubule the presumed cell type of origin) would have been a potentially useful adjunct to HEK293 cells [252]. The caveat being that the use of HK2 cells, which express basal levels of TLR4, may have been problematic in terms of excluding off target effects (i.e. non-TLR4 effects) of ligands [248]. Furthermore, the fact HK2 cells are also immortalized implies they have undergone genetic and phenotypic alterations that make them different from the cells from which they were derived [253]. The question then becomes whether HK2 cells would accurately model typical kidney cells. Primary renal cells would therefore be an attractive alternative but there are disadvantages to using primary cells, such as modest cell yields and reduced cell viability [254]. There could also have be difficulty with repeated passages, and transfection [255].

### 3.12.2 Variability

In this chapter there were differing levels of SEAP and fold induction between assays, even in control samples, which reflects inter-experimental variability and calls into question the reproducibility of these results. Since intra-experimental results appeared consistent with few outlying data points, and the overall pattern of results were similar, cell passage number at the time of experimentation or imbalances in cell number between experiments could explain this variation. The latter could be secondary to the small volumes of cell suspensions used in 96-well plates. Indeed greater consistency of results was achieved in the cell viability assays reported in the next chapter when larger 6-well plates were utilised. This made it easier to control the consistency of cell concentration across wells.

A further inconsistency was noted in the potency of high dose 17-DMAG at reducing hyaluronan-mediated NF-κB activation. As such, the variability in the 17-DMAG results could represent a batch effect due to use of different stock solutions of 17-DMAG. As AT13387 100 nM and 17-DMAG 500 nM actually increased NF-κB activation on SEAP assay, it could also be suggested that the dose of these drugs is critical to their effect. This is more likely to be a real effect, and there could be complex interactions of different molecules resulting in pro-inflammatory effects of Hsp90 inhibitors under certain conditions (e.g. at low doses), but anti-inflammatory in others (e.g. at high doses). A final consideration of this chapter is that the Western blots using AICAR lacked a medium control and a vehicle control. All samples received Hsp90 inhibitors therefore it is not possible to be certain that Hsp90 inhibition degraded IKK as per the previous Western blots.

### 3.12.3 Reproducibility

In the experiments reported in this chapter, HEK293 cells were not used as an *in vitro* model of typical kidney cells. They were selected specifically for these experiments since they are widely available, deliver reproducible results, transfect efficiently and have previously been reported to lack TLR4 expression [246, 247]. This previously reported phenotype was confirmed on flow cytometry. The main limitations of the flow cytometry data are that the results are only displayed for one experiment. This is similar to the Western blots and cytokine arrays performed later in the chapter. Single experiments do not take into account the potential for variation and do not confirm the reproducibility of the experiments. Despite this concern, the results of Western blots and cytokine arrays were replicated with LPS later in the chapter.

A doubling of fluorescence signal on flow cytometry for TLR4 was noted after oxidative stress with hydrogen peroxide, in comparison to control conditions. This is probably due to variation (as opposed to up-regulation of TLR4) since there was no increase in TLR4 expression above the three negative control samples in either experiment. An additional limitation of this experiment was the lack of verification of the efficacy of hydrogen peroxide. In the next chapter a reduction in cell viability with hydrogen peroxide is demonstrated though. The experiments in the next chapter should also alleviate concerns that DMSO may be exerting toxicity in the experiments performed in this chapter, since there is no reduction in cell viability with DMSO [256]. This is in comparison to cells left in normal culture medium (i.e. medium controls), which are considered 100% viable.

# Chapter 4: AT13387 enables cellular survival following oxidative stress

## 4.1 Background

In Chapter 3, it was shown that AT13387 repressed a pro-inflammatory signalling pathway that may be important in mediating kidney damage following renal IRI. Oxidative stress also leads to cell death and contributes to kidney injury following renal IRI [257, 258]. Hsp90 inhibition with 17-DMAG has previously been used to protect cells from oxidative stress and increase cell viability [84, 90]. However, it remains to be proven whether AT13387 is equally capable of protecting cells from oxidative stress. This chapter will address the hypothesis that AT13387 enables cellular survival following oxidative stress.

## 4.2 Oxidative stress reduces cell viability

Hydrogen peroxide is applied to *in vitro* models to investigate the oxidative stress responses of cells. When administered to cells at a high concentration ($\geq$ 1 mM), hydrogen peroxide causes necrotic cell death [259]. The cytotoxic potency of hydrogen peroxide is dependent on the concentration of hydrogen peroxide used, the ability of the cells to eliminate hydrogen peroxide and the cell concentration [259]. Therefore to achieve greater consistency of results; initial hydrogen peroxide concentration finding experiments were performed in HEK293-TLR4 cells. The cells were split into 6-well plates for experimentation to make it easier to control the consistency of cell concentration across wells. In these initial experiments, incubation with hydrogen peroxide led to a dose-dependent decrease in cell viability in HEK293-TLR4 cells on crystal violet assay (Figure 4.1).

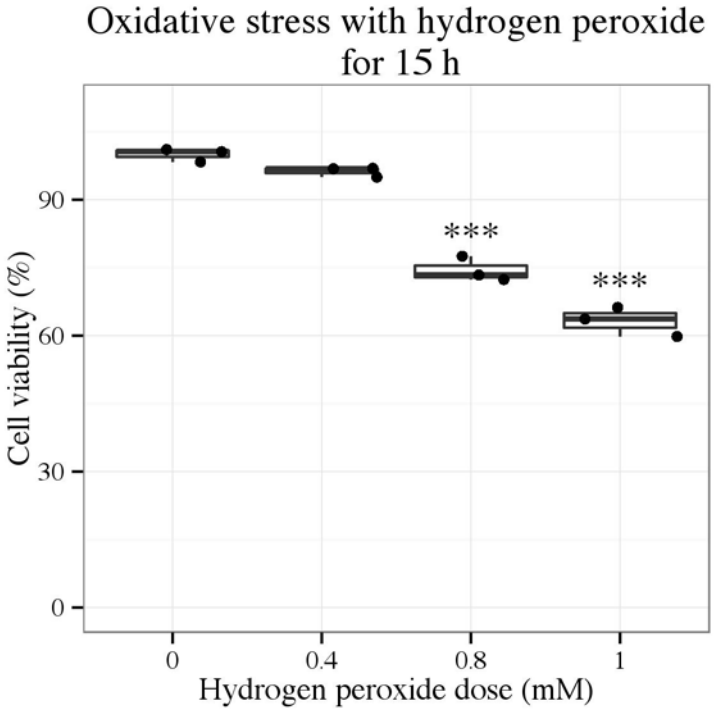


**Figure 4.1 Cell viability determined by crystal violet assay following oxidative stress with hydrogen peroxide in HEK293-TLR4 cells**

HEK293-TLR4 cells were divided at a cell density of 500,000 cells in 2ml of growth medium per well of a 6-well plate. 24 h later, medium was changed and contained hydrogen peroxide at doses ranging from 0 mM to 1 mM. After 15 h incubation a crystal violet assay was performed to determine cell viability. Results are presented from 3 independent experiments in a standard boxplot with individual results jittered. ***$p<0.001$ vs. 0 mM, ANOVA.

## 4.3 Hsp90 inhibition increases cell viability following oxidative stress

In a previous study, pre-treatment of renal adenocarcinoma cells with 17-DMAG protected cell viability in an *in vitro* model of oxidative stress involving hydrogen peroxide [84]. It was found on crystal violet assay in HEK293-TLR4 cells that following pre-treatment with AT13387 and 17-DMAG there was a significant increase in cell viability after incubation with hydrogen peroxide (AT13387 100 nM vs. DMSO vehicle, $p<0.001$, 17-DMAG 100 nM vs. DMSO vehicle, $p<0.01$, ANOVA). In addition, AT13387 was significantly more effective at increasing cell viability than 17-DMAG (AT13387 100 nM vs. 17-DMAG 100 nM, $p<0.05$, ANOVA) (Figure 4.2).

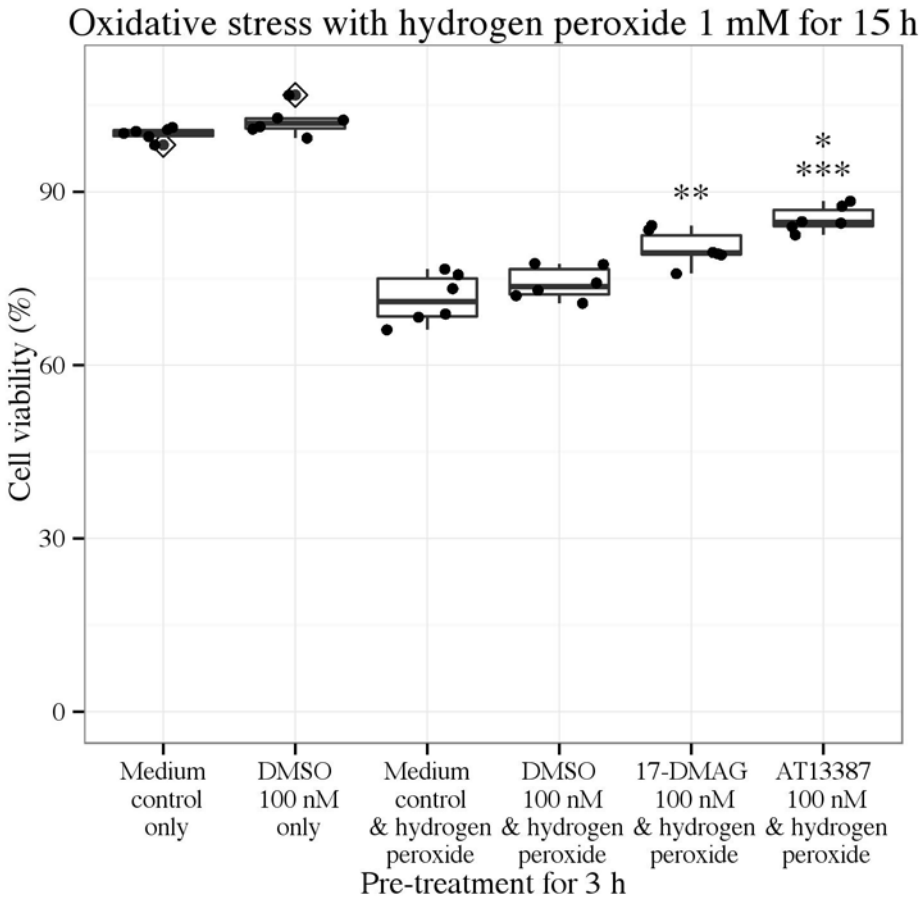


**Figure 4.2 Crystal violet assay to determine cell viability following pre-treatment with AT13387 or 17-DMAG and oxidative stress with hydrogen peroxide in HEK293-TLR4 cells**

HEK293-TLR4 cells were divided at a cell density of 500,000 cells in 2 ml of growth medium per well of a 6-well plate. 24 h later, cells were pre-treated with AT13387, 17-DMAG, DMSO vehicle or medium control for 3 h. The medium was then changed and contained hydrogen peroxide at 1 mM or medium control (DMSO 100 nM only and medium control only). Cells left in medium control for the duration of the experiment were considered 100% viable. After 15 h incubation a crystal violet assay was performed to determine cell viability, which was normalised to the 100% viable cells. Results are presented from 6 independent experiments in a standard boxplot with individual results jittered. Outlier data are highlighted by a dot with a diamond in the midline. *$p<0.05$ vs. 17-DMAG, **$p<0.01$ vs. DMSO vehicle and ***$p<0.001$ vs. DMSO vehicle, ANOVA.

## 4.4 Summary

In this chapter, AT13387 enabled cellular survival in an *in vitro* model involving a cellular insult with hydrogen peroxide. The results in this chapter therefore suggest that in common with other Hsp90 inhibitors, AT13387 may enable cellular survival following oxidative stress and at equivalent doses could actually be more effective than 17-DMAG in this respect.

## 4.5 Discussion

### 4.5.1 Limitations

In this chapter, a crystal violet assay was selected for the measurement of cell viability. The strength of the assay was that it was cheap, had been established in the laboratory and provided consistent results [260]. The major disadvantage was that as a traditional end-point assay it only provided one static result. As such the crystal violet assay did not provide any real-time indication of the kinetic responses of the cells. A real-time assay would have provided more information about the biological status of the cells in terms of cell growth, senescence, morphological changes and apoptosis. An example of a more advanced assay that would provide this data is the. xCELLigence System (ACEA Biosciences, San Diego, CA).

The experiments in this chapter were again performed in only one immortalized cell line; HEK293-TLR4 cells, and involved one type of cell insult. The major weakness of *in vitro* assays of this nature is that they oversimplify the complexity of IRI and evaluate isolated mechanisms of injury [17]. Indeed, oxidative stress is only one aspect of IRI, and there are various other cell culture models of renal IRI that could

supplement the results in this chapter, such as chemical insults and hypoxic injury using hypoxia or anaerobic chambers. Other common criticisms of *in vitro* assays include the use of non-representative cell lines (e.g. cancer cells and non-human cells), and the inability to assess the impact of systemic factors (e.g. cellular infiltration). Developing methods of differentiating human kidney cells from stem cells, adopting co-culture models to evaluate cellular interactions and assessing the effect of multiple cellular insults could overcome these limitations [261, 262].

### 4.5.2 Variability

The effect of hydrogen peroxide is known to depend not only on the concentration of hydrogen peroxide used, but also the cell concentration [259]. For the experiments in this chapter, the cells were split into 6-well plates for experimentation to make it easier to control the consistency of cell concentration across wells. As a result the intra-experimental and inter-experimental variability was minimal.

### 4.5.3 Reproducibility

In the medium control samples there was a consistent level of cell death following the addition of 1 mM of hydrogen peroxide between the two experiments performed in this chapter. Therefore the results are considered consistent and reproducible in the cell line that was selected. It would be of interest to assess the reproducibility of the results in other assays, and in different cell lines.

# Chapter 5: AT13387 leads to induction of renal Hsp70 in mice

## 5.1 Background

In Chapter 4, it was shown in an *in vitro* model that Hsp90 inhibition with AT13387 enabled cellular survival following oxidative stress. However, other potential cellular and molecular mechanisms of protection from renal IRI offered by Hsp90 inhibitors remain to be fully delineated. Defining these is essential for their further development and translation to patients. As discussed in Chapter 1, Hsp90 inhibitors block the ATP-binding site of Hsp90, which releases HSF1 from a repressive multi-chaperone complex involving Hsp90, allowing it to translocate to the cell nucleus and up-regulate Hsp70 [121]. Hsp70 induction is strongly associated with protection from renal IRI [118]. In previous studies, Balb/c mice and Balb/c SCID mice have been shown to increase renal Hsp70 expression following Hsp90 inhibition with 17-DMAG [84, 263]. This chapter will address the hypothesis that AT13387 leads to induction of renal Hsp70 in mice, including FVB/n mice.

## 5.2 AT13387 increases Hsp70 expression in the kidney of FVB/n mice

AT13387 increased renal Hsp70 levels on ELISA in FVB/n mice 6 h following treatment (AT13387 vs. 2HβC vehicle, $p<0.005$, t-test) (Figure 5.1) and at 24 h renal Hsp70 levels remained significantly elevated (AT13387 vs. 2HβC vehicle, $p<0.001$, t-test) (Figure 5.2). Immunohistochemistry showed that in comparison to vehicle treatment, Hsp70 induction following AT13387 treatment was strongest in the outer stripe of the outer medulla of the kidney and was noted predominantly within renal tubular cells (Figure 5.3 and Figure 5.4).

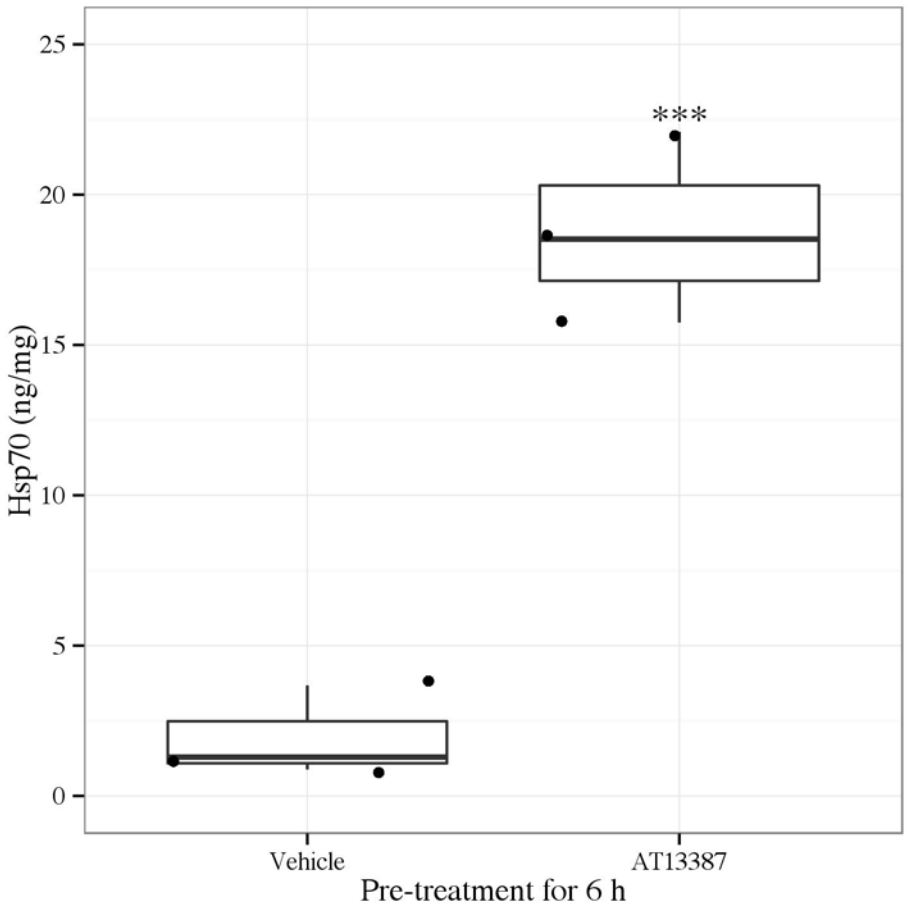


**Figure 5.1 Renal Hsp70 expression following AT13387 or vehicle treatment on ELISA in FVB/n mice**

FVB/n mice were treated with AT13387 or 2HPβC vehicle (n=3 per group) 6 h prior to kidney harvest. Whole-organ lysates were prepared and analysed by an ELISA for Hsp70. Results are presented in a standard boxplot with individual results jittered. **p<0.005 vs. 2HβC vehicle, t-test.

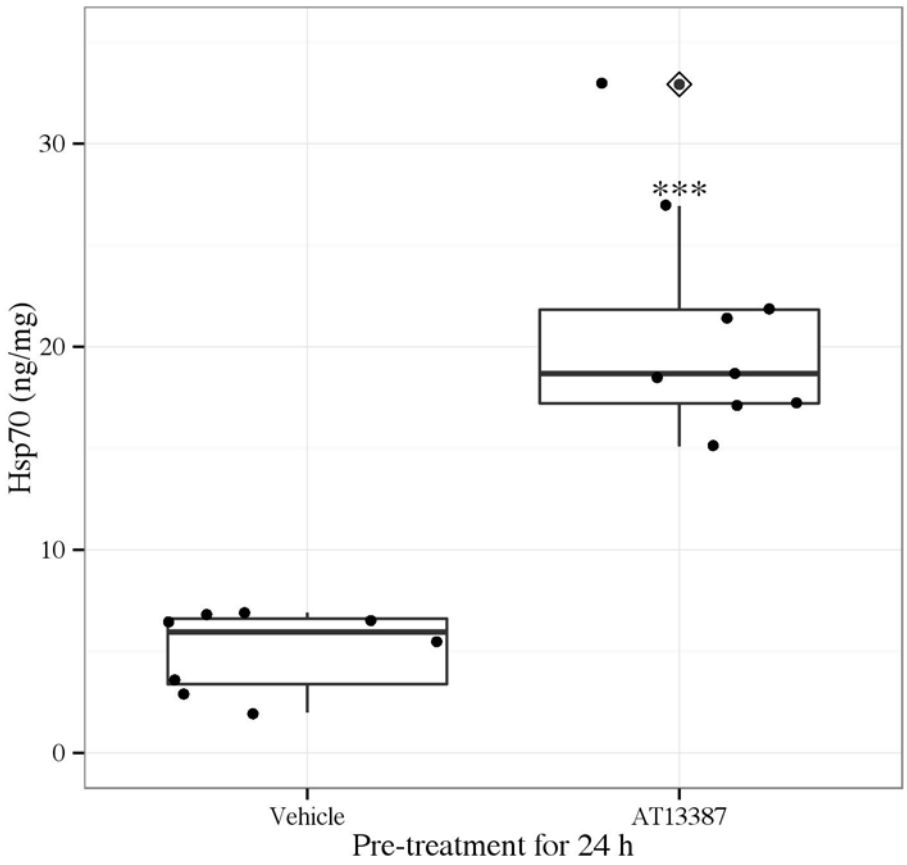


**Figure 5.2 Renal Hsp70 expression following AT13387 or vehicle pre-treatment in the control kidney on ELISA in FVB/n mice**

Mice were pre-treated with AT13387 or 2HβC vehicle (n=9 per group). 24 h later, mice were anaesthetised and underwent right nephrectomy and 20 min of left renal pedicle clamping. Following removal the right (control) kidney was frozen. Whole-organ lysates were later prepared and analysed by an ELISA for Hsp70. Data are displayed for n=8 (instead of 9) in the vehicle group due to a failure processing one control kidney for analysis. Results are presented in a standard boxplot with individual results jittered. Outlier data are highlighted by a dot with a diamond in the midline. ***$p<0.001$ vs. 2HβC vehicle, t-test.

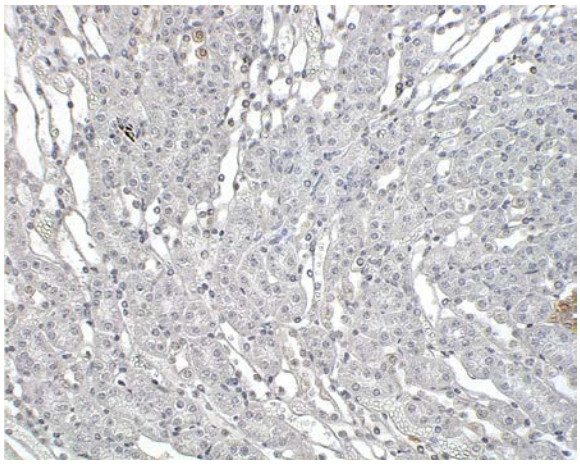

**Figure 5.3 Renal Hsp70 expression following vehicle treatment in the outer stripe of the outer medulla of the kidney on immunohistochemistry in FVB/n mice**

FVB/n mice were treated with 2HPβC vehicle (n=3) 6 h prior to kidney harvest. Sections were later prepared and stained with an antibody to Hsp70. A representative section of the outer stripe of the outer medulla of the kidney at x 100 magnification is shown. There is minimal positive brown staining for Hsp70.

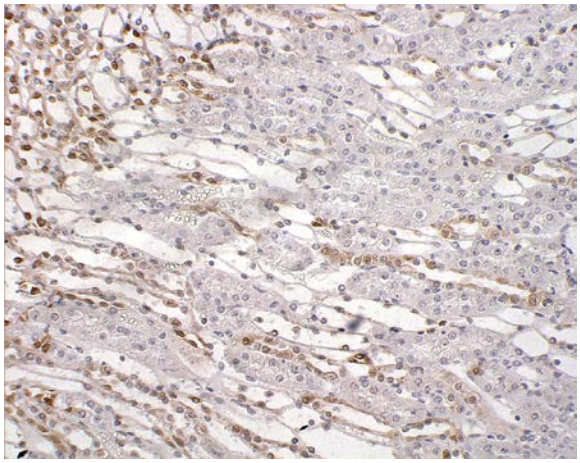

**Figure 5.4 Renal Hsp70 expression following AT13387 treatment in the outer stripe of the outer medulla of the kidney on immunohistochemistry in FVB/n mice**

FVB/n mice were treated with AT13387 (n=3) 6 h prior to kidney harvest. Sections were later prepared and stained with an antibody to Hsp70. A representative section of the outer stripe of the outer medulla of the kidney at x 100 magnification is shown. There is positive brown staining for Hsp70 evident in the renal tubular cells.

## 5.3 AT13387 increases Hsp70 expression in the kidney of Balb/c and Balb/c SCID mice

In comparison to pre-treatment with vehicle, equivalent levels of renal Hsp70 induction on ELISA were observed in Balb/c and Balb/c SCID mice 24 h following pre-treatment with AT13387 (AT13387 vs. 2HβC vehicle, $p<0.001$, t-test) (Figure 5.5).

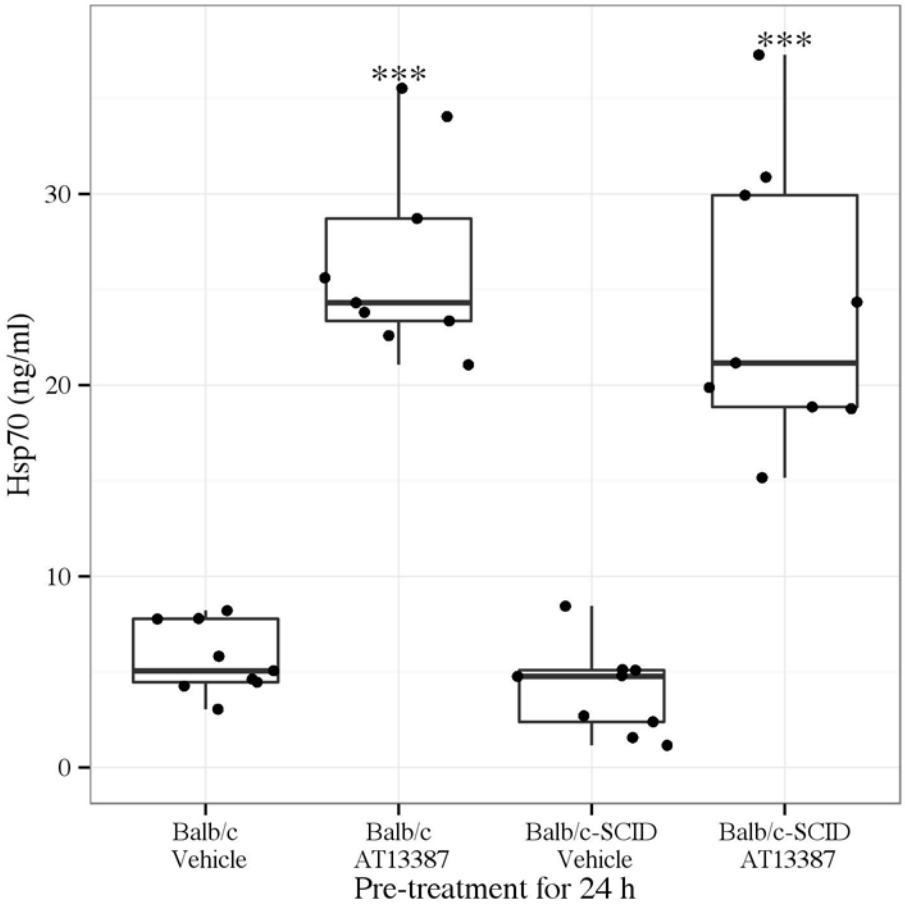


**Figure 5.5 Renal Hsp70 expression following AT13387 or vehicle pre-treatment in the control kidney on ELISA in Balb/c and Balb/c SCID mice**

Mice were pre-treated with AT13387 or 2HβC vehicle (n=9 per group). 24 h later, mice were anaesthetised and underwent right nephrectomy and 30 min of left renal pedicle clamping. Following removal the right (control) kidney was frozen. Whole-organ lysates were later prepared and analysed by an ELISA for Hsp70. Results are presented in a standard boxplot with individual results jittered. ***$p<0.001$ vs. 2HβC vehicle, t-test.

## 5.4 Summary

The results in this chapter show that similar to treatment with 17-DMAG, AT13387 treatment leads to an increase in renal Hsp70 expression in Balb/c and Balb/c SCID mice [84, 263]. AT13387 also leads to the induction of renal Hsp70 in FVB/n mice, which demonstrates that the effect of this drug in mice is not strain dependent.

## 5.5 Discussion

### 5.5.1 Limitations

Assessing for the induction or inhibition of a molecule of interest, is particularly important when using drugs prophylactically prior to the onset of IRI, since it ensures adequate dosing and administration of the protective agent [238] The strengths of the data presented in this chapter are that there was uniform up-regulation of Hsp70 in each experiment, and also across different strains of mice. The results of the ELISA were consistent between experiments, and were also validated using immunohistochemistry. Hsp70 is the most commonly used biomarker of Hsp90 inhibition so this data suggests a consistent effect of AT13387 after 24 h of administration [264]. The weaknesses of this data are the limited sample size (n=3) used in the experiment that assessed Hsp70 levels 6 h after AT13387 treatment. This experiment was performed to give some preliminary data regarding the onset of Hsp90 inhibition with AT13387. A fuller time course experiment could provide additional data on the kinetics of Hsp90 inhibition with AT13387, but was considered beyond the scope of this chapter, as the intention was to treat mice 24 h before renal IRI.

### 5.5.2 Variability

The results presented in this chapter were consistent. A large factor in this consistency was the simplicity of the experiments. The ELISAs were performed on uninjured control kidneys following either organ harvest of nephrectomy. Despite this, certain mice did appear to have greater up-regulation of Hsp70 than others. Indeed, one outlier was noted in the FVB/n group treated with AT13387, but this was the only outlying data point across a total of 59 mice used in this chapter.

### 5.5.3 Reproducibility

There are no significant issues with the reproducibility of the data presented in this chapter. Indeed, the up-regulation of Hsp70 in Balb/c SCID mice is further replicated in Chapter 8.

# Chapter 6: AT13387 pre-treatment results in functional and morphological protection from renal IRI

## 6.1 Background

In Chapter 3, Hsp90 inhibition repressed pro-inflammatory signalling pathways that may be important in renal IRI. Then in Chapter 4, Hsp90 inhibition protected cells from oxidative stress, which is a known consequence of renal IRI [257]. As previously described in Chapter 1, reducing IRI is vital to achieving better outcomes in renal transplantation. It has previously been demonstrated that functional and morphological protection from renal IRI in mice follows pre-treatment with the Hsp90 inhibitors geldanamycin and the geldanamycin-analogues 17-AAG and 17-DMAG [84]. 17-DMAG is the most effective of these agents at reducing renal IRI, and being water-soluble it is easier to administer both intravenously and orally [83, 84]. However, patients poorly tolerate all these older Hsp90 inhibitors. AT13387 has a low toxicity profile in phase II human studies in oncology and should be better tolerated by patients [99, 100]. This chapter will investigate whether there is protection from renal IRI in mice following AT13387 pre-treatment. This chapter therefore addresses the hypothesis that AT13387 pre-treatment results in functional and morphological kidney protection from renal IRI. Injured kidneys are also assessed to evaluate if AT13387 pre-treatment reduces renal TLR4 expression and NF-κB activation following renal IRI

## 6.2 Establishing a renal IRI model in FVB/n mice

In Chapter 5, it was shown that AT13387 induces renal Hsp70 expression across different strains of mice including those on an FVB/n background. FVB/n mice were

available from in-house colonies for use in this thesis. In a previous study utilising the model of IRI described in this thesis, a renal pedicle clamp time of 30 minutes was used to inflict moderate to severe acute tubular injury in Balb/c mice [84]. However, in a further study using the same model in FVB/n mice, a clamp time of 20 minutes was utilised, thus suggesting a strain-dependent difference in the tolerance of these mice to renal IRI [265]. Given these potential differences in ischemic tolerance, an initial model-establishing experiment, testing clamp times of 20 minutes and 25 minutes was performed in FVB/n mice. The former was found to be sufficient to induce renal IRI, as determined by a rise in serum creatinine, comparable to that observed in these previous publications (Figure 6.1) [84, 265].

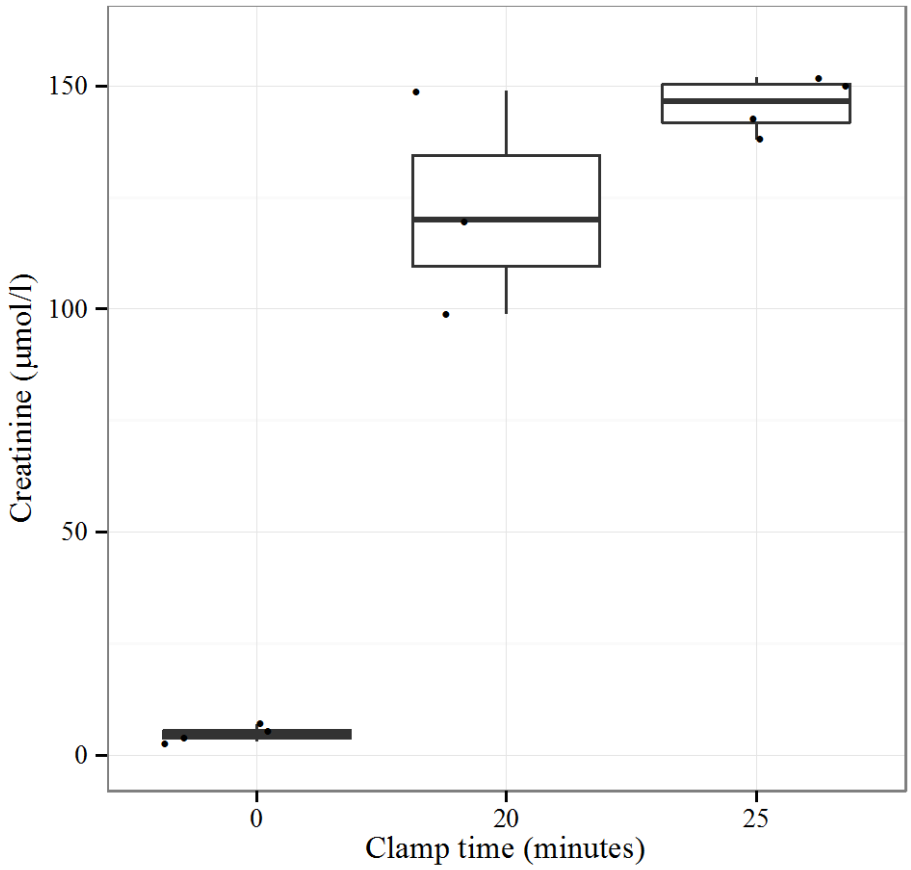


**Figure 6.1 Serum creatinine 24 h following renal IRI in FVB/n mice**

FVB/n mice were anaesthetised and underwent right nephrectomy and 20 or 25 min of left renal pedicle clamping (n=3-4 per group). Control mice (n=4) did not undergo renal pedicle clamping (i.e. clamp time 0 minutes). Following 24 h of recovery, blood was obtained by intra-cardiac puncture and serum creatinine was determined. Results are presented in a standard boxplot with individual results jittered.

## 6.3 AT13387 pre-treatment reduces functional and morphological kidney injury following renal IRI in FVB/n mice

On serum analysis, in comparison to vehicle, AT13387 pre-treatment in FVB/n mice significantly reduced creatinine 24 h following renal IRI (AT13387 vs. 2HβC vehicle, $p<0.05$, t-test) (Figure 6.2). AT13387 pre-treatment in FVB/n mice also reduced tubular necrosis score (AT13387 vs. 2HβC vehicle, $p<0.05$, Mann-Whitney U test) (Figure 6.3) on histological assessment 24 h following renal IRI (Figure 6.4 and Figure 6.5).

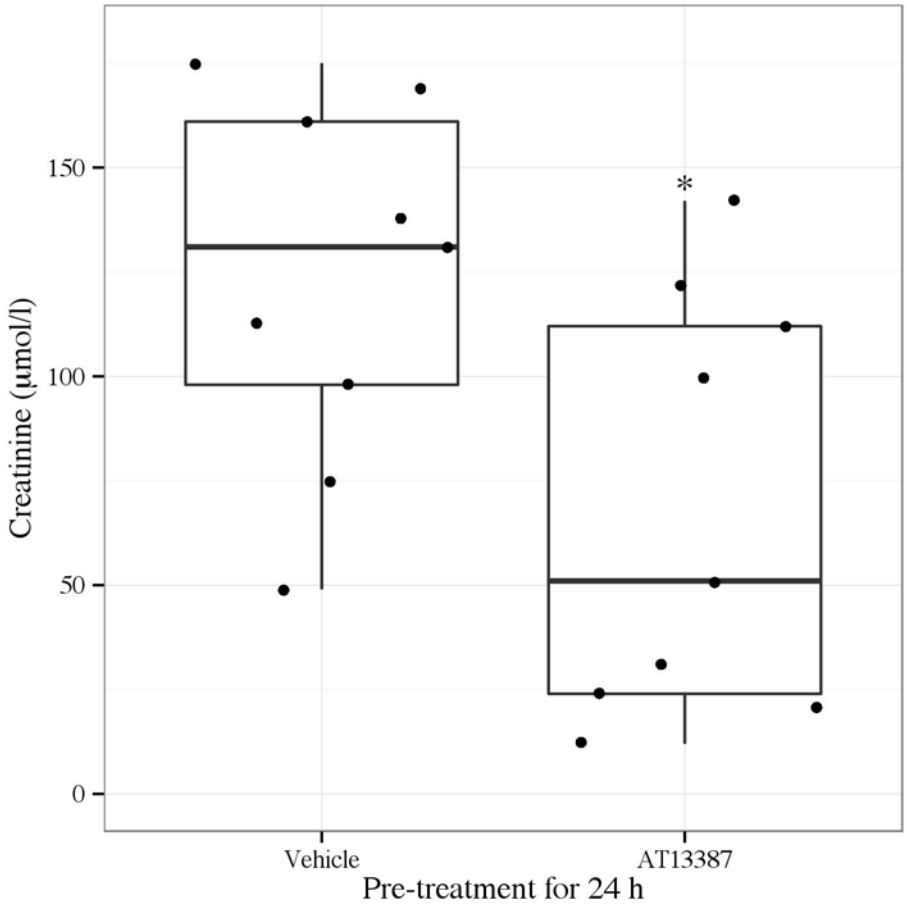


**Figure 6.2 Serum creatinine following AT13387 or vehicle pre-treatment and 24 h following renal IRI in FVB/n mice**

FVB/n mice were pre-treated with AT13387 or 2HβC vehicle (n=9 per group). 24 h later, mice were anaesthetised and underwent right nephrectomy and 20 min of left renal pedicle clamping. Following 24 h of recovery, blood was obtained by intra-cardiac puncture and serum creatinine was determined. Results are presented in a standard boxplot with individual results jittered. *$p<0.05$ vs. 2HβC vehicle, t-test.

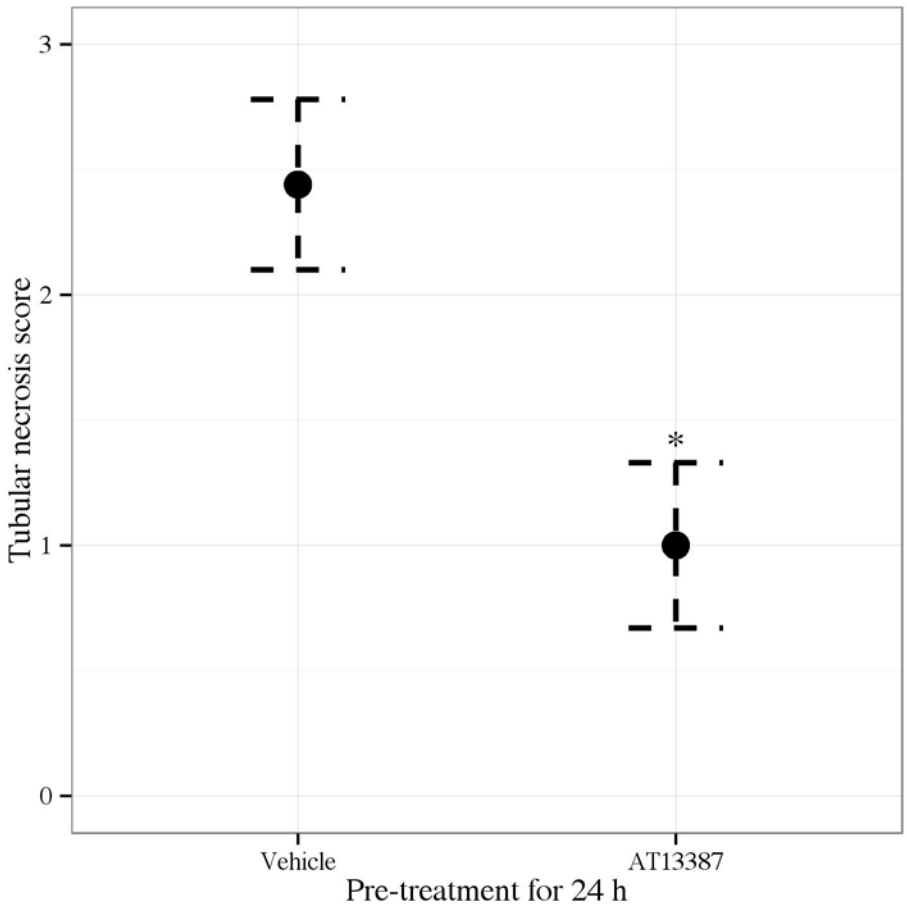


**Figure 6.3 Tubular necrosis score following AT13387 or vehicle pre-treatment and 24 h following renal IRI in FVB/n mice**

FVB/n mice were pre-treated with AT13387 or 2HβC vehicle (n=9 per group). 24 h later, mice were anaesthetised and underwent right nephrectomy and 20 min of left renal pedicle clamping. Following 24 h of recovery, the left kidney was harvested and placed in methacarn. Sections were later prepared and stained with haematoxylin and eosin. A blinded observer then determined the tubular necrosis score. Results are presented as mean and standard error of the mean. *$p<0.05$ vs. 2HβC vehicle, Mann-Whitney U test.

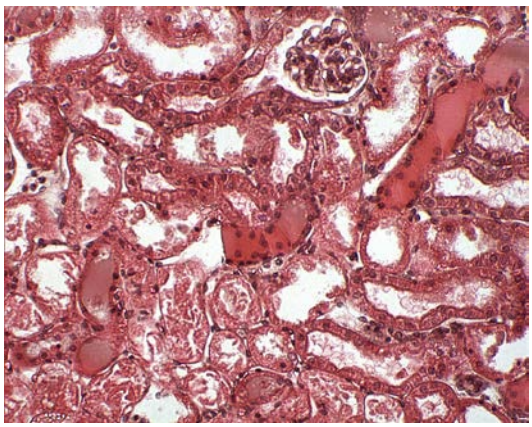

**Figure 6.4 Morphological kidney injury following pre-treatment with vehicle and 24 h following renal IRI in FVB/n mice**

FVB/n mice were pre-treated with 2HβC vehicle (n=9). 24 h later, mice were anaesthetised and underwent right nephrectomy and 20 min of left renal pedicle clamping. Following 24 h of recovery, the left kidney was harvested and placed in methacarn. Sections were later prepared and stained with haematoxylin and eosin. A representative section of kidney cortex at x 200 magnification is shown. There are detached necrotic cells evident.

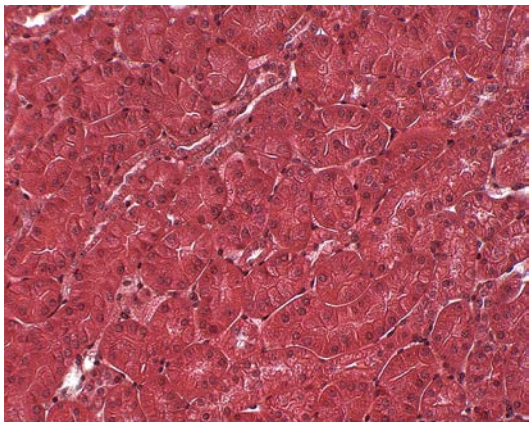

**Figure 6.5 Morphological kidney injury following pre-treatment with AT13387 and 24 h following renal IRI in FVB/n mice**

FVB/n mice were pre-treated with AT13387 (n=9). 24 h later, mice were anaesthetised and underwent right nephrectomy and 20 min of left renal pedicle clamping. Following 24 h of recovery, the left kidney was harvested and placed in methacarn. Sections were later prepared and stained with haematoxylin and eosin. A representative section of kidney cortex at x 200 magnification is shown. Only minimal tubular dilatation is observed.

## 6.4 AT13387 pre-treatment reduces the expression of TLR4 and inflammatory chemokines in the kidney following renal IRI

On PCR analysis, in comparison to vehicle, AT13387 pre-treatment in FVB/n mice significantly reduced renal TLR4 expression 24 h following renal IRI (AT13387 vs. Vehicle, $p<0.01$, Mann-Whitney U test) (Figure 6.6). On cytokine array panel, in comparison to vehicle, AT13387 pre-treatment in FVB/n mice also reduced renal expression of chemokine (C-X-C motif) ligand 1 (CXCL1) and chemokine (C-X-C motif) ligand 2 (CXCL2) 24 h following renal IRI (AT13387 vs. 2HβC vehicle, $p<0.05$, t-test) (Figure 6.7). There were no other significant differences in cytokine or chemokine expression.

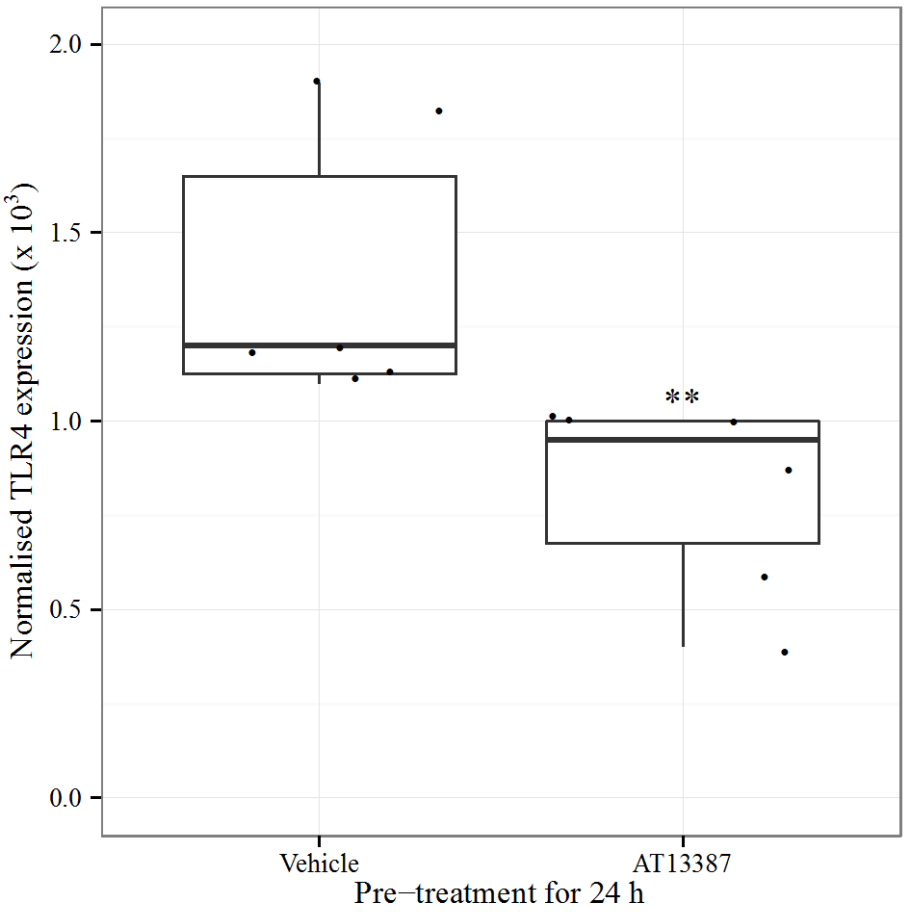


**Figure 6.6 Renal TLR4 expression following AT13387 or vehicle pre-treatment and 24 h following renal IRI in FVB/n mice**

FVB/n mice were pre-treated with AT13387 or 2HβC vehicle (n=6 per group) and underwent renal IRI as per figure 6.2. The left kidney was harvested and stored in RNAlater for 24 h before being frozen. RNA was later extracted and converted to cDNA. PCR was then performed to determine TLR4 expression. TLR4 expression was normalised to GAPDH expression. Results are presented in a standard boxplot with individual results jittered. **p<0.01 vs. 2HβC vehicle, Mann-Whitney U test.

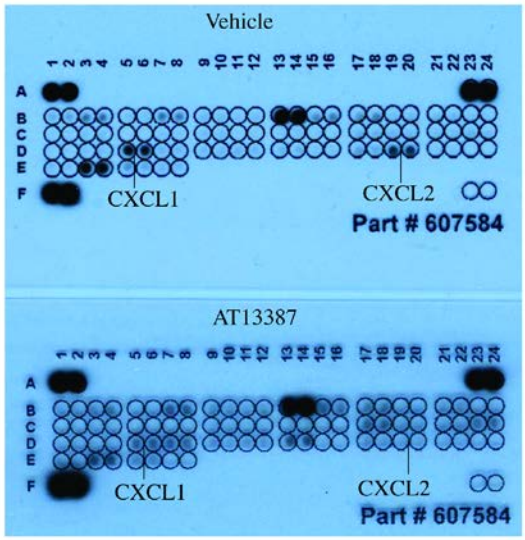


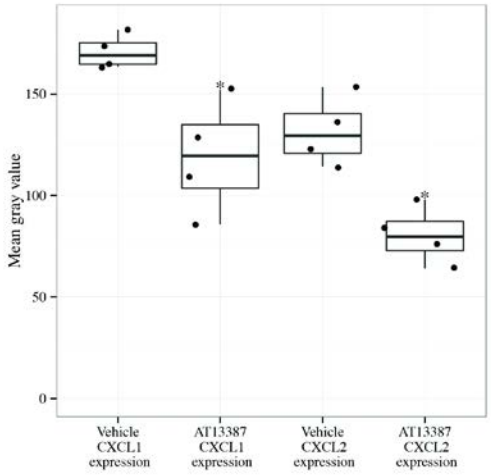


| Coordinate | Target/Control | Alternate Nomenclature |
|---|---|---|
| A1, A2 | Reference Spot | — |
| A23, A24 | Reference Spot | — |
| B1, B2 | BLC | CXCL13/BCA-1 |
| B3, B4 | C5/C5a | Complement Component 5a |
| B5, B6 | G-CSF | — |
| B7, B8 | GM-CSF | — |
| B9, B10 | I-309 | CCL1/TCA-3 |
| B11, B12 | Eotaxin | CCL11 |
| B13, B14 | sICAM-1 | CD54 |
| B15, B16 | IFN-γ | — |
| B17, B18 | IL-1α | IL-1F1 |
| B19, B20 | IL-1β | IL-1F2 |
| B21, B22 | IL-1ra | IL-1F3 |
| B23, B24 | IL-2 | — |
| C1, C2 | IL-3 | — |
| C3, C4 | IL-4 | — |
| C5, C6 | IL-5 | — |
| C7, C8 | IL-6 | — |
| C9, C10 | IL-7 | — |
| C11, C12 | IL-10 | — |
| C13, C14 | IL-13 | — |
| C15, C16 | IL-12 p70 | — |
| C17, C18 | IL-16 | — |
| C19, C20 | IL-17 | — |
| C21, C22 | IL-23 | — |
| C23, C24 | IL-27 | — |
| D1, D2 | IP-10 | CXCL10/CRG-2 |
| D3, D4 | I-TAC | CXCL11 |
| D5, D6 | KC | CXCL1 |
| D7, D8 | M-CSF | — |
| D9, D10 | JE | CCL2/MCP-1 |
| D11, D12 | MCP-5 | CCL12 |
| D13, D14 | MIG | CXCL9 |
| D15, D16 | MIP-1α | CCL3 |
| D17, D18 | MIP-1β | CCL4 |
| D19, D20 | MIP-2 | CXCL2 |
| D21, D22 | RANTES | CCL5 |
| D23, D24 | SDF-1 | CXCL12 |
| E1, E2 | TARC | CCL17 |
| E3, E4 | TIMP-1 | — |
| E5, E6 | TNF-α | — |
| E7, E8 | TREM-1 | — |
| F1, F2 | Reference Spot | — |
| F23, F24 | PBS (Negative Control) | Control (-) |

**Figure 6.7 Renal cytokine expression following AT13387 or vehicle pre-treatment and 24 h following renal IRI in FVB/n mice**

FVB/n mice were pre-treated with AT13387 or 2HβC vehicle (n=4 per group) and underwent renal IRI as per figure 6.2. Following 24 h of recovery, the left kidney was harvested and snap frozen. Protein lysates were later prepared and an array panel was used to determine cytokine expression. The grid describes the cytokines assessed (right panel). A representative array is shown (upper left panel). Mean gray values were quantified using Image J and were used to reflect CXCL1 and CXCL2 expression. Results are presented in a standard boxplot with individual results jittered (lower left panel). *p<0.05 vs. 2HβC vehicle, t-test.

## 6.5 Summary

In this chapter, pre-treatment with AT13387 was found to significantly reduce serum creatinine and tubular necrosis following renal IRI. This chapter has therefore confirmed that similar to previous reports of the protective effect of Hsp90 inhibition in renal IRI [84, 85], AT13387 pre-treatment in mice results in functional and morphological protection of the kidney. CXCL1 and CXCL2 are NF-κB target genes, and the expression of these pro-inflammatory chemokines is NF-κB dependent [266, 267]. The expression of CXCL1 and CXCL2 in the kidney was reduced following renal IRI in mice pre-treated with AT13387. There was also a significant reduction in renal TLR4 expression.

## 6.6 Discussion

### 6.6.1 Limitations

Murine models of IRI typically involve a warm ischemic period of variable duration induced by temporary clamping of the blood supply to the kidneys [238]. Adjusting the clamp time appropriately titrates the level of injury so that acute tubular necrosis occurs in the kidney but without animal suffering or mortality. Establishing a suitable clamp time is a challenge and can be dependent on the mouse strain [268]. Therefore an initial injury titration experiment was performed at the outset of the work involving FVB/n mice. This was across a limited sample size but was sufficient to determine a suitable clamp time to cause an acute rise in serum creatinine but without animal mortality. This was imperative since experiments that utilise survival as an endpoint introduce various confounding factors, such as hyperkalemia [17].

In these experiments, a unilateral kidney ischemia and contra-lateral nephrectomy model was preferred to a bilateral ischemia model, as the nephrectomy specimen allowed for confirmation and quantification of AT13387 activity via Hsp70 induction in kidney tissue at the time of surgery in each individual experimental animal. A single injured kidney is also closer to the clinical scenario of an injured kidney graft in a renal transplant recipient with no other functional nephron mass. While it is appreciated that a similar experiment can be performed in a bilateral ischemia model, using sham mice to confirm adequate dosing, this does not fully exclude inadequate dosing (e.g. from a misplaced injection) in the experimental animals that are being used to determine the primary outcome measure. Another concern is that in the bilateral ischemia model there is a small but inevitable time lag period between clamping the kidney on the contra-lateral side. An absence of sham-operated mice in the experiments in this chapter is a potential weakness, but can be justified by the fact this is an established model, and these sham experiments have previously been performed [84, 238]. In terms of tubular necrosis score, this is a more subjective outcome measure than serum creatinine, which is objectively determined. The use of only one blinded observer was a further weakness, and ideally at least two observers should be used (one of which is a renal pathologist). Although, given the simplicity of the tubular necrosis score adopted, it is felt unlikely that this would have impacted the results significantly.

### 6.6.2 Variability

Serum creatinine, 24 h after surgery, was assessed and while there was a significant reduction in mice treated with AT13387, there were mice in the AT13387 group that appeared more protected than others. This is not explained by surgery being performed on different days, or on different types of mice, as all were from same colony. It is essential to reduce variability in the IRI model by minimising blood loss and controlling temperature carefully, and this spread of data may have been the result of technical issues during the earlier part of the experimental learning curve

[269]. There is also a plateau in the level of injury with increasing clamp times, which leads to a more consistent level of injury when the severity is increased. Therefore it is equally possible that the level of injury induced by 20 minutes of clamping was not on the plateau, and was at a highly modifiable level in terms of serum creatinine reduction. Performing bilateral clamping could potentially have reduced variability, as it is a simpler model to perform. Furthermore, it would be interesting to assess additional markers of kidney function, such as glomerular filtration rate to see whether there is similar variation. Other markers of kidney injury, such as kidney injury molecule-1, and senescence (e.g. p16 and p21) could also be assessed [270, 271].

### 6.6.3 Reproducibility

In the next chapter the protective effect of AT13387 is replicated in Balb/c mice. However, the assessment of injury at only one time point 24 h after surgery means that there is a possibility that AT13387 may be simply delaying the onset of kidney injury. This issue could be addressed in further experiments with a longer recovery period. The potential for 'real-time' measurement of glomerular filtration rate in animals using intravascular optical technology could be another exciting future opportunity in this context, as it would provide immediate and on-going information about renal function after surgery [272, 273].

TLR4 expression in kidneys injured by IRI was assessed by real-time PCR. A significant reduction in TLR4 expression was identified following AT13387 pre-treatment. The NF-κB activation status of kidneys injured by IRI in each group was also assessed in further experiments by cytokine array. The arrays showed a significant reduction in the expression of the NF-κB-dependent chemokines CXCL1 and CXCL2 following AT13387 pre-treatment [266, 267]. This suggests an anti-inflammatory effect of AT13387, and the data is complementary to the *in vitro*

results reported in Chapter 3. However, at just 24 hours following renal IRI, it is likely that protective effect of AT13387 may have involved programmed cell death rather than inflammation [43]. As such, the causality of the reduction in TLR4 and NF-κB expression in the protective effect of AT13387 cannot be assumed from this data. Indeed, the possibility remains that reduced TLR4 and NF-κB expression are simply additional “read outs” of less damage to the kidney. Nevertheless, it has previously been identified that following renal IRI, there is increased expression of CXCL1 and CXCL2. In addition, treatment with neutralizing antibodies to both CXCL1 and CXCL2 significantly improves kidney function within 48 hours of renal IRI [274]. Therefore another area of research worth pursuing is the further development of Hsp90 inhibition with AT13387 to establish the relevance *in vivo* of repressing TLR4-mediated NF-κB activation in renal IRI. This could potentially be achieved through the use of TLR4-/- mice, and is discussed further in Chapter 10.

# Chapter 7: The protection afforded from renal IRI by AT13387 is lymphocyte-dependent

## 7.1 Background

In Chapter 5, it was shown that AT13387 induced Hsp70 expression in the kidney of mice. It has previously been observed that renal Hsp70 induction is associated with protection from kidney injury as a result of renal IRI [118]. In keeping with this observation, in Chapter 6, AT13387 pre-treatment resulted in functional and morphological kidney protection from renal IRI. It has recently been reported in the context of heat preconditioning that the protective effect of Hsp70 up-regulation in renal IRI is lymphocyte-dependent [224]. Consequently, it is predicted that an Hsp70 inducing candidate drug such as AT13387, could similarly reduce renal IRI by modulating lymphocyte behaviour. This chapter addresses the hypothesis that the protection afforded from renal IRI by AT13387 is lymphocyte-dependent.

## 7.2 AT13387 reduces renal IRI in Balb/c mice but not Balb/c SCID mice

Balb/c SCID mice lack adaptive immunity due to a deficiency of mature B and T lymphocyte cells in the peripheral blood and lymphoid organs [275]. Balb/c and Balb/c SCID mice were therefore used to assess the influence of lymphocytes on the effect of AT13387 pre-treatment on kidney injury following renal IRI. Compared to pre-treatment with vehicle, AT13387 pre-treatment in Balb/c mice significantly reduced serum creatinine 24 h following renal IRI (AT13387 vs. 2HβC vehicle, $p<0.05$, t-test) (Figure 7.1). AT13387 pre-treatment in Balb/c mice also reduced tubular necrosis score (AT13387 vs. 2HβC vehicle, $p<0.05$, Mann-Whitney U test) (Figure 7.2) on histological assessment 24 h following renal IRI (Figure 7.3 and

Figure 7.4). However, pre-treatment with AT13387 in Balb/c SCID mice, did not significantly alter serum creatinine in comparison to vehicle pre-treatment 24 h following renal IRI (AT13387 vs. 2HβC vehicle, $p=0.18$, t-test) (Figure 7.1). AT13387 pre-treatment in Balb/c SCID mice also did not reduce tubular necrosis score on histological assessment 24 h following renal IRI (AT13387 vs. 2HβC vehicle, $p=0.10$, Mann-Whitney U test). At 24 h following renal IRI, vehicle treated Balb/c mice had significantly lower serum creatinine levels than vehicle treated Balb/c SCID mice (2HβC Balb/c vehicle vs. 2HβC Balb/c SCID vehicle, $p<0.05$, t-test).

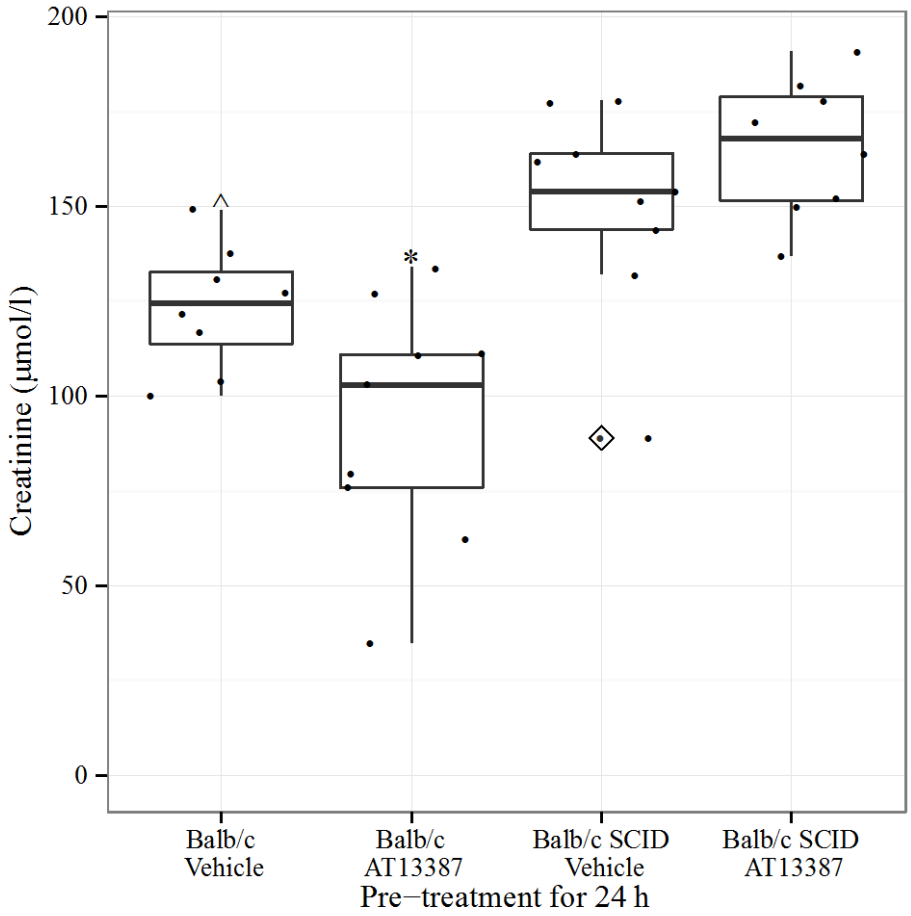


**Figure 7.1 Serum creatinine following AT13387 or vehicle pre-treatment and 24 h following renal IRI in Balb/c and Balb/c SCID mice**

Balb/c and Balb/c SCID mice were pre-treated with AT13387 or 2HβC vehicle (n=9 per group). 24 h later, mice were anaesthetised and underwent right nephrectomy and 30 min of left renal pedicle clamping. Following 24 h of recovery, blood was obtained by intra-cardiac puncture and serum creatinine was determined. Data are displayed for n=8 (instead of 9) in the Balb/c vehicle group because of one intra-operative clamp failure, and n=8 (instead of 9) in the Balb/c SCID AT13387 group because of one inadequate serum sample. Results are presented in a standard boxplot with individual results jittered. Outlier data are highlighted by a dot with a diamond in the midline. ^$p<0.05$ vs. Balb/c SCID 2HβC vehicle, t-test and *$p<0.05$ vs. Balb/c 2HβC vehicle, t-test.

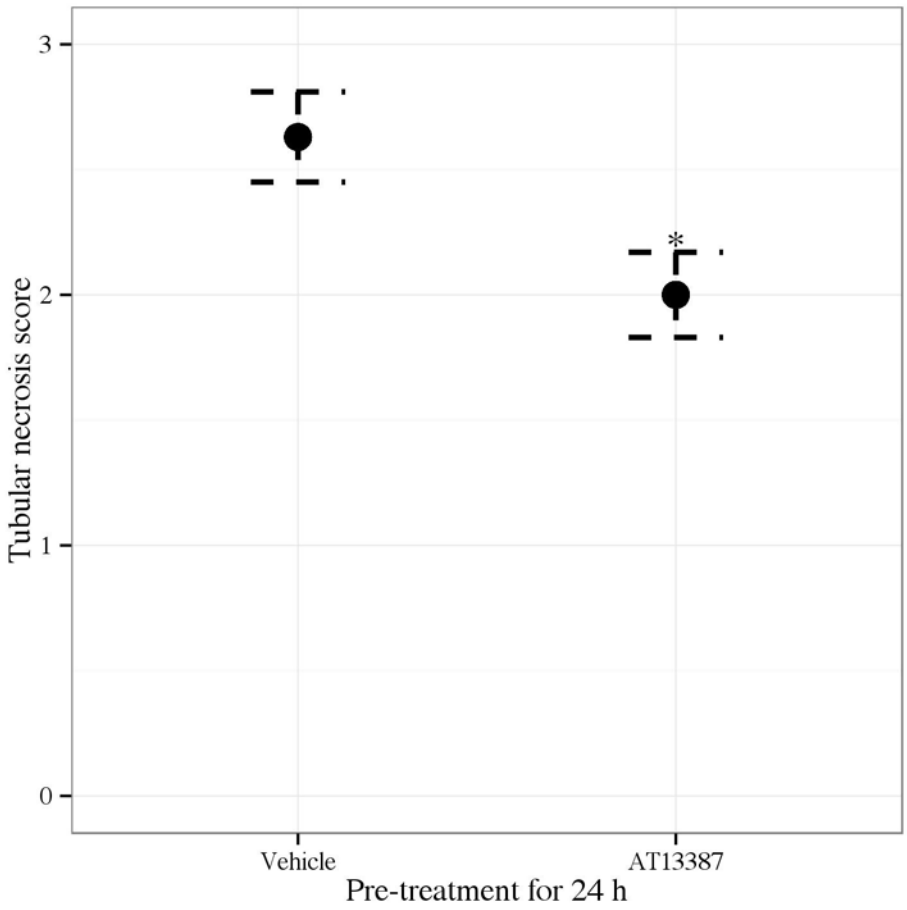


**Figure 7.2 Tubular necrosis score following AT13387 or vehicle pre-treatment and 24 h following renal IRI in Balb/c mice**

Balb/c mice were pre-treated with AT13387 or 2HβC vehicle (n=9 per group). 24 h later, mice were anaesthetised and underwent right nephrectomy and 30 min of left renal pedicle clamping. Following 24 h of recovery, the left kidney was harvested and placed in methacarn. Sections were later prepared and stained with haematoxylin and eosin. A blinded observer then determined the tubular necrosis score. Data are reported for n=8 (instead of 9) in the vehicle group because of one intra-operative clamp failure. Results are presented as mean and standard error of the mean. *$p<0.05$ vs. 2HβC vehicle, Mann-Whitney U test.

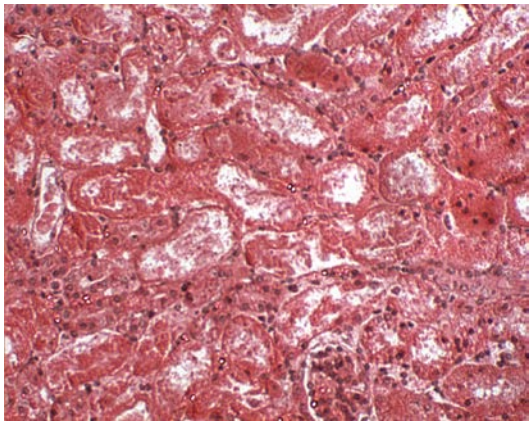

**Figure 7.3 Morphological kidney injury following pre-treatment with vehicle and 24 h following renal IRI in Balb/c mice**

Balb/c mice were pre-treated with 2HβC vehicle (n=9). 24 h later, mice were anaesthetised and underwent right nephrectomy and 30 min of left renal pedicle clamping. Following 24 h of recovery, the left kidney was harvested and placed in methacarn. Sections were later prepared and stained with haematoxylin and eosin. A representative section of kidney cortex at x 200 magnification is shown. There are areas of tubular necrosis and significant tubular cell damage.

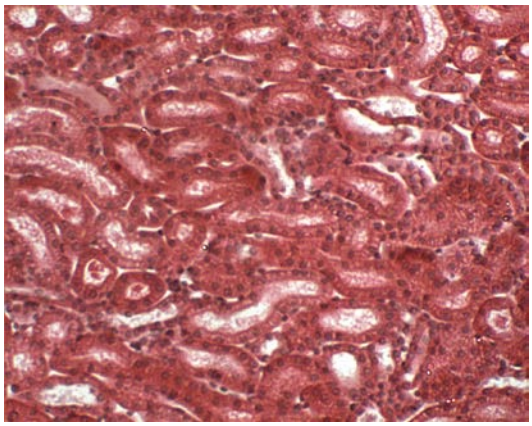

**Figure 7.4 Morphological kidney injury following pre-treatment with AT13387 and 24 h following renal IRI in Balb/c mice**

Balb/c mice were pre-treated with AT13387 (n=9). 24 h later, mice were anaesthetised and underwent right nephrectomy and 30 min of left renal pedicle clamping. Following 24 h of recovery, the left kidney was harvested and placed in methacarn. Sections were later prepared and stained with haematoxylin and eosin. A representative section of kidney cortex at x 200 magnification is shown. There is evidence of tubular dilatation and loss of epithelial brush borders but less necrosis than in the vehicle treated mice.

## 7.3 Tregs in the spleen following AT13387 treatment

In the study by Kim *et al*. (2014), which was discussed in Chapter 1, heat preconditioning increased the number of splenic Tregs [224]. In the experiments performed here, Tregs were identified on immunohistochemistry in the spleen in both vehicle and AT13387 treated Balb/c mice (Figure 7.5 and Figure 7.6) but there was no difference in the number of cells identified between the experimental groups (Figure 7.7).

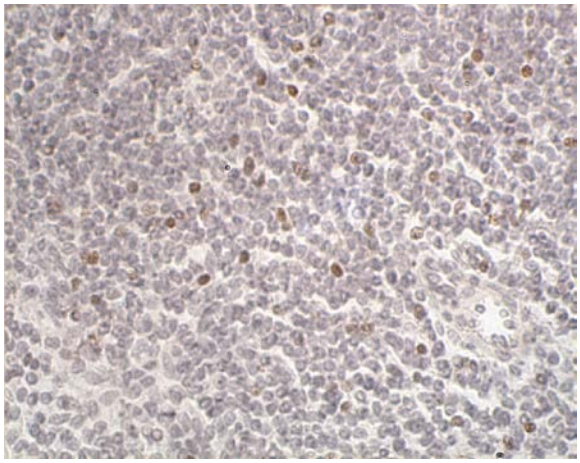

**Figure 7.5 Foxp3 expression on immunohistochemistry in the spleen of Balb/c mice following vehicle treatment**

Balb/c mice were treated with 2HPβC vehicle (n=3). 24 h later, mice were anaesthetised, and the spleen was harvested and placed in methacarn. Sections were later prepared and stained with an antibody to Foxp3. A representative section of the spleen at x 400 magnification is shown. Positive brown staining Tregs are evident.

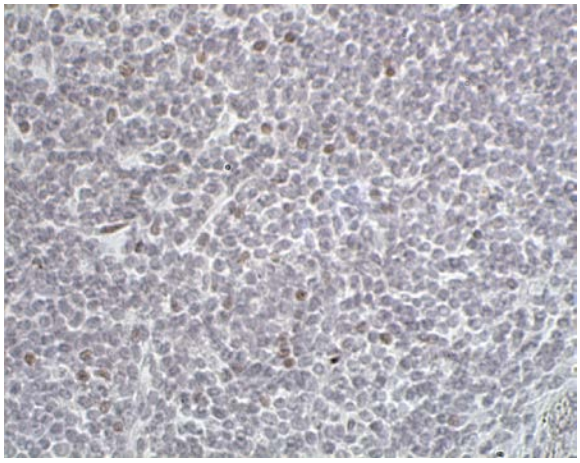

**Figure 7.6 Foxp3 expression on immunohistochemistry in the spleen of Balb/c mice following AT13387 treatment**

Balb/c mice were treated with AT13387 (n=4). 24 h later, mice were anaesthetised, and the spleen was harvested and placed in methacarn. Sections were later prepared and stained with an antibody to Foxp3. A representative section of the spleen at x 400 magnification is shown. Positive brown staining Tregs are evident.

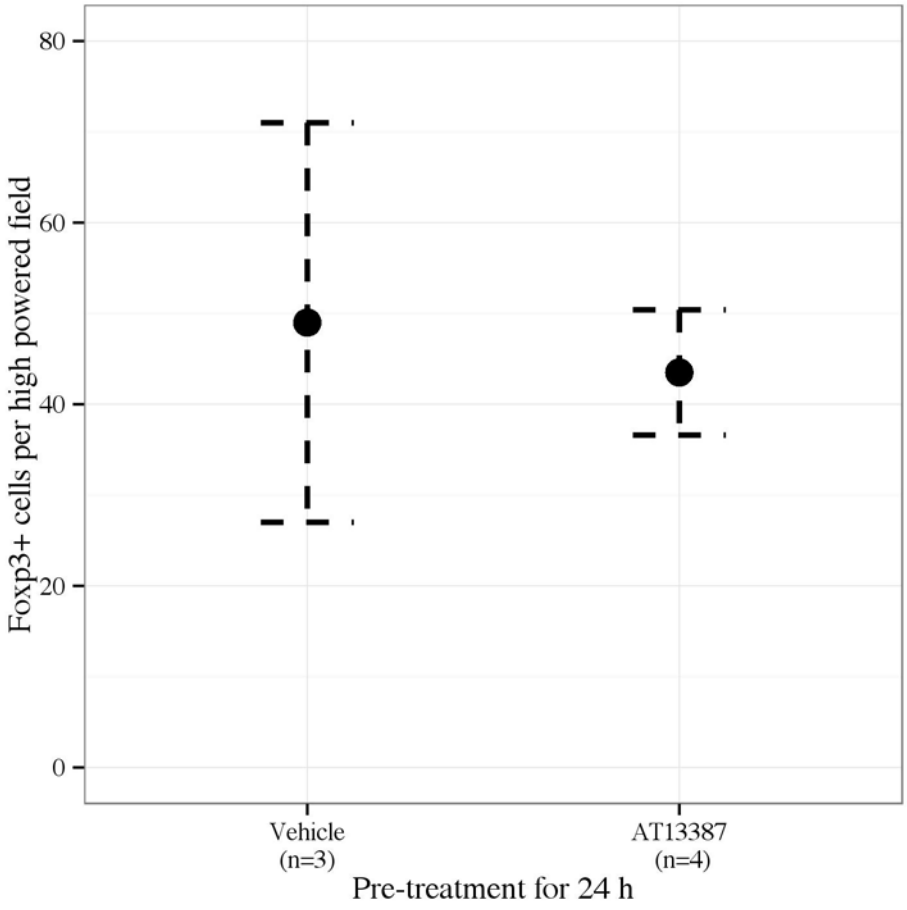


**Figure 7.7 Splenic Foxp3 expression on immunohistochemistry following AT13387 or vehicle treatment in Balb/c mice**

Balb/c mice were treated with AT13387 or 2HPβC vehicle (n=3-4 per group). 24 h later, mice were anaesthetised, and the spleen was harvested and placed in methacarn. Sections were later prepared and stained with an antibody to Foxp3. The average amount of Foxp3+ cells across five non-overlapping random high-powered fields per slide was counted by a blinded observer. Results are presented as mean and standard error of the mean.

## 7.4 T-lymphocytes in the kidney following renal IRI

In the study by Kim *et al*. (2014), increased numbers of Tregs were also detected by flow cytometry in enzyme-dissociated kidneys following renal IRI compared with sham kidneys, indicating localisation of Tregs to the injured kidney. However, following IRI in these experiments, there were no Tregs identified within the injured kidney in either group at 24 h following renal IRI on immunohistochemistry. Since it has been shown elsewhere that NF-κB plays a key role in T cell activation, and T cell-specific NF-κB inhibition provides protection against renal IRI, injured kidneys were also assessed for T-lymphocytes [276]. T-lymphocytes were identified on immunohistochemistry in the injured kidney in both vehicle and AT13387 pre-treated Balb/c mice (Figure 7.8 and Figure 7.9). Again there was no significant difference in the number of cells identified between experimental groups (Figure 7.10).

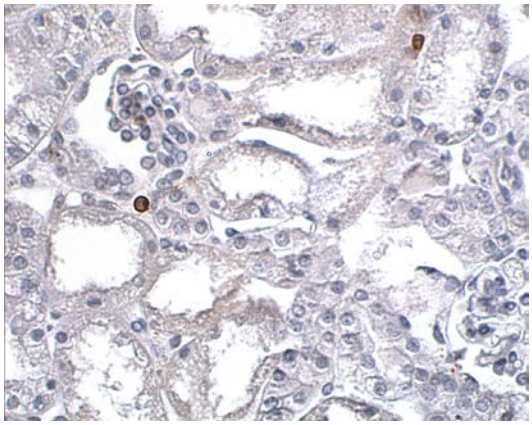

**Figure 7.8 Renal CD3 expression on immunohistochemistry following vehicle pre-treatment and 24 h following renal IRI in Balb/c mice**

Balb/c mice were pre-treated with 2HPβC vehicle (n=9). 24 h later, mice were anaesthetised and underwent right nephrectomy and 30 min of left renal pedicle clamping. Following 24 h of recovery, the left kidney was harvested and placed in methacarn. Sections were later prepared and stained with an antibody to CD3. A representative section of the cortex of the kidney at x 400 magnification is shown. Positive brown staining T-lymphocytes are evident.

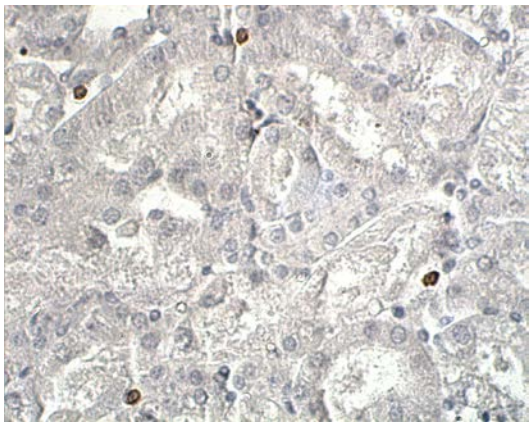

**Figure 7.9 Renal CD3 expression on immunohistochemistry, following AT13387 pre-treatment and 24 h following renal IRI in Balb/c mice**

Balb/c mice were pre-treated with AT13387 (n=9). 24 h later, mice were anaesthetised and underwent right nephrectomy and 30 min of left renal pedicle clamping. Following 24 h of recovery, the left kidney was harvested and placed in methacarn. Sections were later prepared and stained with an antibody to CD3. A representative section of the cortex of the kidney at x 400 magnification is shown. Positive brown staining T-lymphocytes are evident.

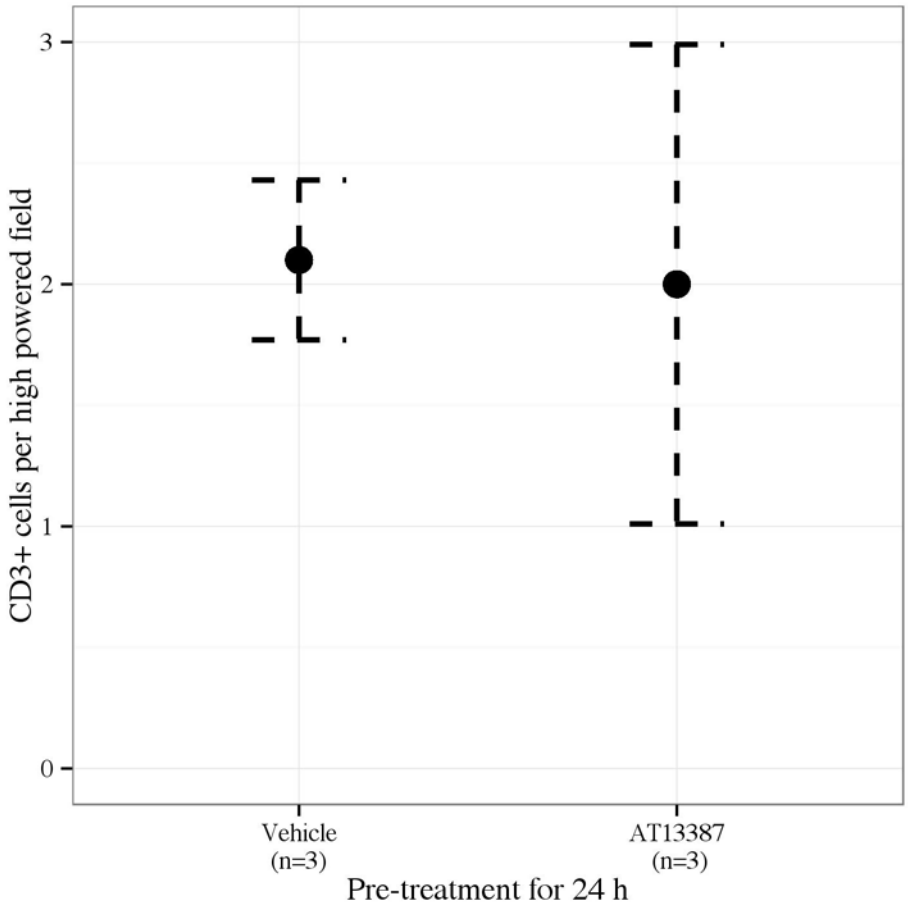


**Figure 7.10 Renal CD3 expression on immunohistochemistry following AT13387 or vehicle pre-treatment and 24 h following renal IRI in Balb/c mice**

Balb/c mice were pre-treated with AT13387 or 2HPβC vehicle (n=9 per group). 24 h later, mice were anaesthetised and underwent right nephrectomy and 30 min of left renal pedicle clamping. Following 24 h of recovery, the left kidney was harvested and placed in methacarn. Sections were later prepared and stained with an antibody to CD3. A blinded observer selected three random samples per group, and the average amount of CD3+ cells across five non-overlapping random high-powered fields per slide was counted. Results are presented as mean and standard error of the mean.

## 7.5 Summary

In this chapter, AT13387 protected kidney function and morphology from renal IRI in Balb/c mice but not Balb/c SCID mice. These two groups of mice are strain matched so the only difference between them should be a lack of an adaptive immune response in the SCID mice. The results of the experiments in this chapter therefore suggest that the protective effect of AT13387 involves the adaptive immune system. This would indicate that the protective effect of AT13387 is at least partially lymphocyte-dependent. However, from the immunohistochemical staining performed, it is currently unclear whether there is Treg or T-lymphocyte involvement, as previously hypothesised on the basis of previous work in this area using heat preconditioning [224].

## 7.6 Discussion

### 7.6.1 Limitations

In the experiments in this chapter Balb/c SCID suffered more severe kidney dysfunction following renal IRI than wild-type Balb/c mice. Following renal IRI the absence of B and T cells has previously been shown to lead to both renal protection [213], and a similar kidney injury to wild type controls [214, 215]. These previous experiments were performed in RAG-1-/- mice as opposed to SCID mice, and also utilised a bilateral ischemia model [213-215]. It is possible that the SCID mice tolerate the unilateral IRI model poorly and suffer worse injury. Further experiments ideally without treatment or vehicle should be performed to clarify this difference between Balb/c and Balb/c SCID in terms of tolerance of renal IRI.

While the immunohistochemistry performed did not identify any differences in T-cell or Treg numbers, this was only preliminary data that was performed on a relatively small number of wild-type mice. The data should therefore be cautiously interpreted, and the sample size of these experiments should be increased. In addition, flow cytometry of blood, spleen and kidneys of wild-type mice should be performed to further elucidate differences in lymphocyte responses following AT13387 treatment. Compared to immunohistochemistry, flow cytometry could also provide more quantitative information on the cell numbers, as well as being more sensitive at detecting cells expressed in relatively low numbers (e.g. Tregs in the kidney) [224]. However, it wouldn't provide detailed information regarding the locality of the cells or the tissue architecture surrounding them.

### 7.6.2 Variability

Less in-group variability was noted for serum creatinine in the renal IRI experiment performed in this chapter, compared to the experiment performed with FVB/n mice in Chapter 6. This may reflect the fact the experiments were performed after the initial experimental learning curve, with less blood loss and better control of temperature [269]. As previously mentioned there is also a plateau in the level of injury with increasing clamp times, which leads to a more consistent level of injury. Therefore it is equally possible that the level of injury induced by 30 minutes of renal pedicle clamping, as performed in this chapter, compared to 20 minutes in the last chapter, was on the plateau and therefore less variable. The higher serum creatinine and tubular necrosis scores in this chapter, compared to Chapter 6, would support this theory. Despite this, there did seem again to be some mice that responded more to AT13387 than others in the Balb/c group. This cannot be explained by performance of surgery on different days, or on different types of mice, as all were from same provider. As previously mentioned, it would be interesting to assess for variation in other markers of kidney function and injury, such as glomerular filtration

rate and kidney injury molecule-1, [270]. Of similar interest would be the levels of p16/p21, which would provide additional information on cellular senescence [271].

### 7.6.3 Reproducibility

In this chapter, the overall pattern of results of the protective effect of AT13387 in Balb/c mice was similar to that seen in the FVB/n mice in Chapter 6. The pattern of the results of the SCID mouse experiment is also replicated in the next chapter, but a longer clamp time (32 minutes) is used in the model. This reflects good reproducibility of experimental data within the thesis. However, the lack of a protective phenotype in SCID mice is at odds with a previous abstract publication by Ferenbach *et al*. (2012) [277]. The possible reasons for this discrepancy are discussed further in Chapter 10.

# Chapter 8: AT13387 reduces lung injury secondary to renal IRI

## 8.1 Background

Secondary lung injury is a known consequence of renal IRI [278]. In Chapter 6 and 7, it was demonstrated that AT13387 pre-treatment leads to functional and morphological protection from renal IRI in FVB/n and Balb/c mice. There could be further systemic benefit of AT13387 treatment by inducing Hsp70 in the lungs of mice in order to reduce secondary lung injury. The kidney protective effect of AT13387 was previously shown in Chapter 7 to be at least partially lymphocyte-dependent, as AT13387 failed to reduce kidney injury following renal IRI in Balb/c SCID mice. It was therefore considered possible to provide the same level of kidney injury from renal IRI to induce secondary lung injury despite AT13387 pre-treatment by using Balb/c SCID mice in a further renal IRI experiment. The experiments in this chapter were performed in conjunction with Duncan Humphries (performed BAL, lung digestion and cytometric analysis) and Ewen Harrison (performed the experiments in Figure 8.1 and Figure 8.2).

## 8.2 Renal IRI causes secondary lung injury

This paragraph contains data that will be reported in Duncan Humphries' thesis. Compared to intervention naive control Balb/c mice, there was no increase in lung injury, in terms of interstitial neutrophil accumulation on flow cytometry of digested lungs or on BAL analysis in Balb/c mice undergoing sham laparotomy or nephrectomy only. In addition, compared to control, sham and nephrectomy only groups, on BAL analysis, cell counts were similar in both Balb/c and Balb/c SCID mice undergoing renal IRI. However, in comparison to control mice, 24 h following

renal IRI in both Balb/c and Balb/c SCID mice, there was a significant increase in interstitial neutrophil accumulation on flow cytometry of digested lungs (Balb/c vs. control, $p<0.05$, Balb/c SCID vs. control, $p<0.01$, t-test), as well as an increase in pulmonary haemorrhage on BAL analysis (Balb/c vs. control, $p<0.05$, Balb/c SCID vs. control, $p<0.05$, t-test). These findings confirm that renal IRI, using the model described in this thesis, causes secondary lung injury in Balb/c and Balb/c SCID mice.

## 8.3 AT13387 increases Hsp70 expression in the lung

AT13387 treatment resulted in a significant dose dependent increase in Hsp70 within the lungs on ELISA 6 h following treatment (AT13387 vs. 2HβC vehicle, $p<0.05$, ANOVA) (Figure 8.1). Levels of Hsp70 remained elevated in the lungs 24 h following AT13387 treatment (AT13387 vs. 2HβC vehicle, $p<0.05$, t-test) (Figure 8.2).

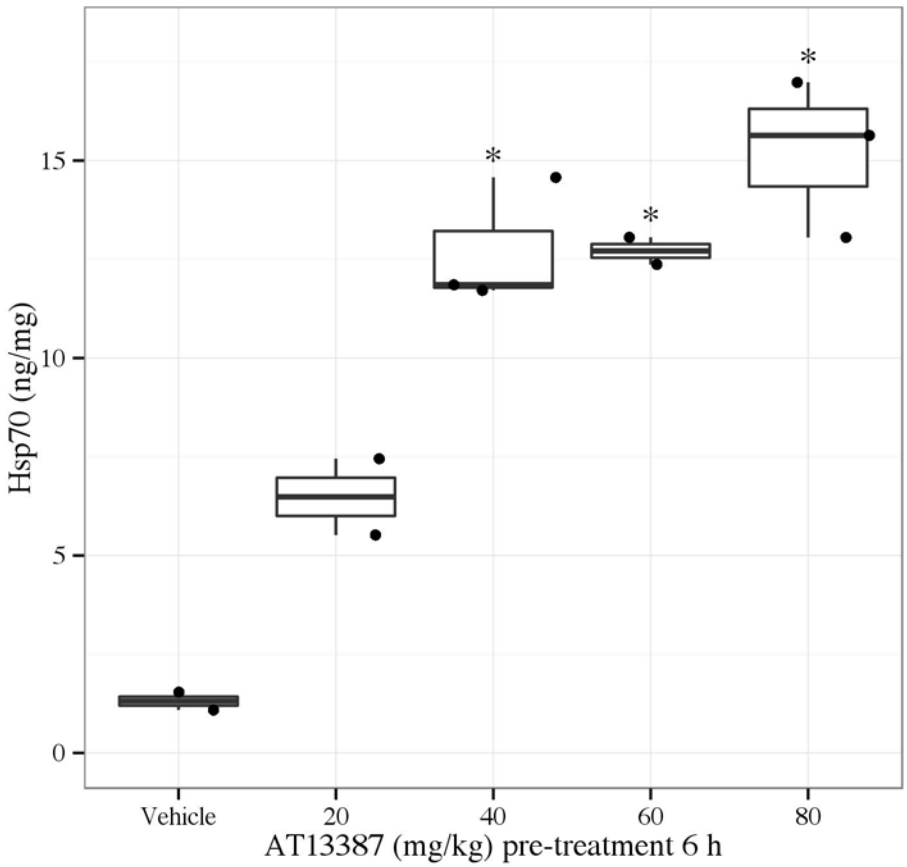


**Figure 8.1 Hsp70 expression in the lung 6 h following AT13387 or vehicle treatment on ELISA in Balb/c mice**

Balb/c mice were treated with AT13387 (20-80 mg/kg) or 2HPβC vehicle 6 h prior to organ harvest (n=2-3 per group). Whole-organ lysates were prepared and analysed by an ELISA for Hsp70. Results are presented in a standard boxplot with individual results jittered. *p<0.05 vs. 2HβC vehicle, ANOVA.

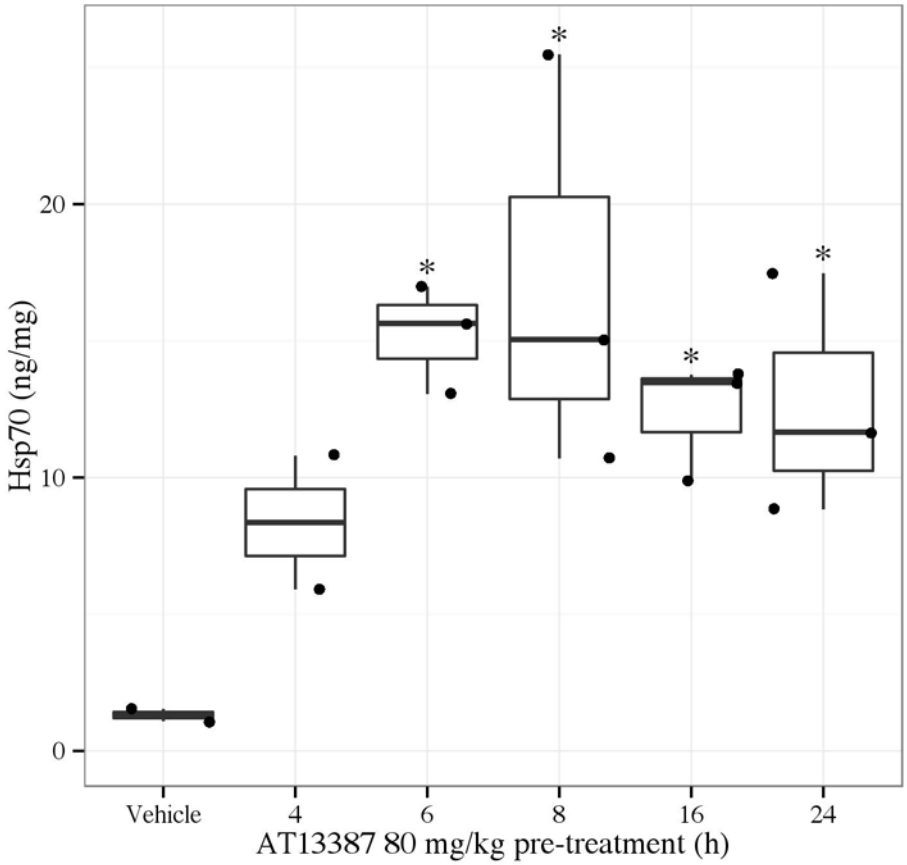


**Figure 8.2 Hsp70 expression in the lung up to 24 h following AT13387 or vehicle treatment on ELISA in Balb/c mice**

Balb/c mice were pre-treated with AT13387 or 2HPβC vehicle at 4, 6, 8, 16 and 24 h prior to organ harvest (n=2-3 per group). Whole-organ lysates were prepared and analysed by an ELISA for Hsp70. Results are presented in a standard boxplot with individual results jittered. *$p<0.05$ vs. 2HβC vehicle, t-test.

## 8.4 Establishing the model for assessing lung injury following pre-treatment with AT13387 and renal IRI

An experimental model was then established using Balb/c SCID mice to assess whether AT13387 could reduce secondary lung injury following renal IRI. The renal pedicle clamp time for this experiment was extended to 32 minutes to maximise renal IRI and thus secondary lung injury. In comparison to pre-treatment with vehicle, significant renal Hsp70 induction on ELISA was again observed in Balb/c SCID mice 24 h following pre-treatment with AT13387 (AT13387 vs. 2HβC vehicle, $p<0.001$, t-test) (Figure 8.3). Compared to vehicle pre-treatment, pre-treatment with AT13387 again did not significantly alter levels of serum creatinine 24 h following renal IRI in Balb/c SCID mice (AT13387 vs. 2HβC vehicle, $p=0.47$, t-test) (Figure 8.4). In addition, compared to vehicle pre-treatment, on BAL analysis, cell counts were similar with AT13387 pre-treatment 24 h following renal IRI in Balb/c SCID mice (Figure 8.5).

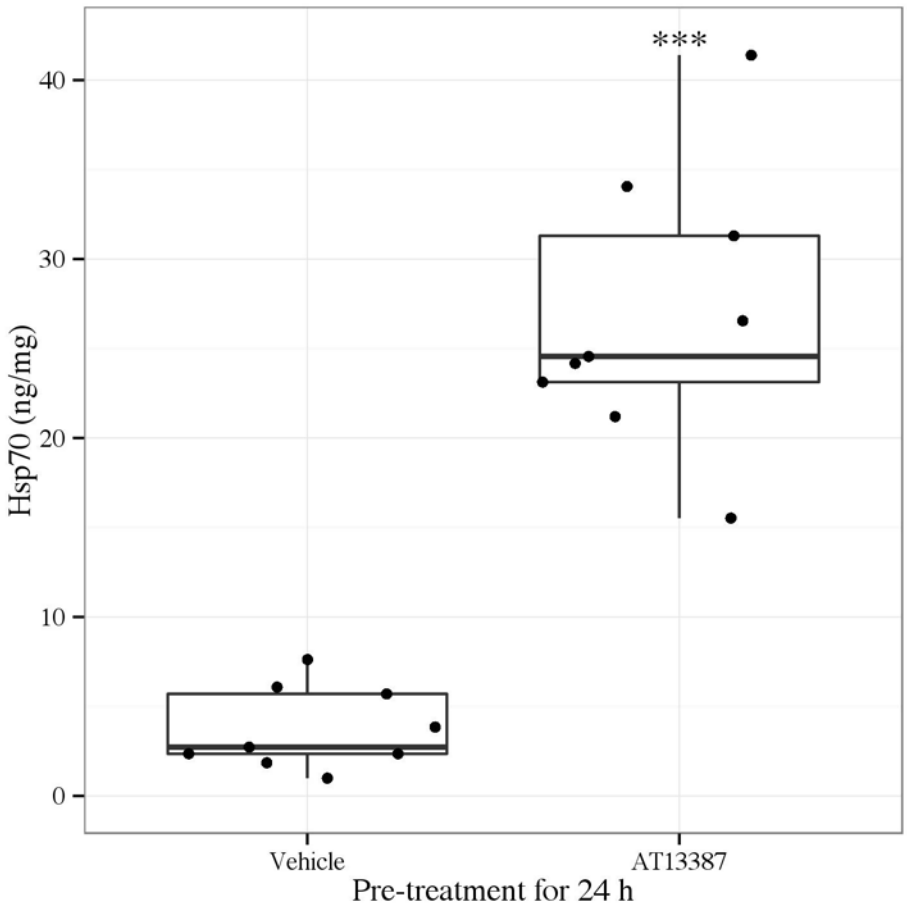


**Figure 8.3 Renal Hsp70 expression following AT13387 or vehicle pre-treatment in the control kidney on ELISA in Balb/c SCID mice**

Mice were pre-treated with AT13387 or 2HβC vehicle (n=9 per group). 24 h later, mice were anaesthetised and underwent right nephrectomy and 32 min of left renal pedicle clamping. Following removal the right (control) kidney was frozen. Whole-organ lysates were later prepared and analysed by an ELISA for Hsp70. Results are presented in a standard boxplot with individual results jittered. ***p<0.001 vs. 2HβC vehicle, t-test.

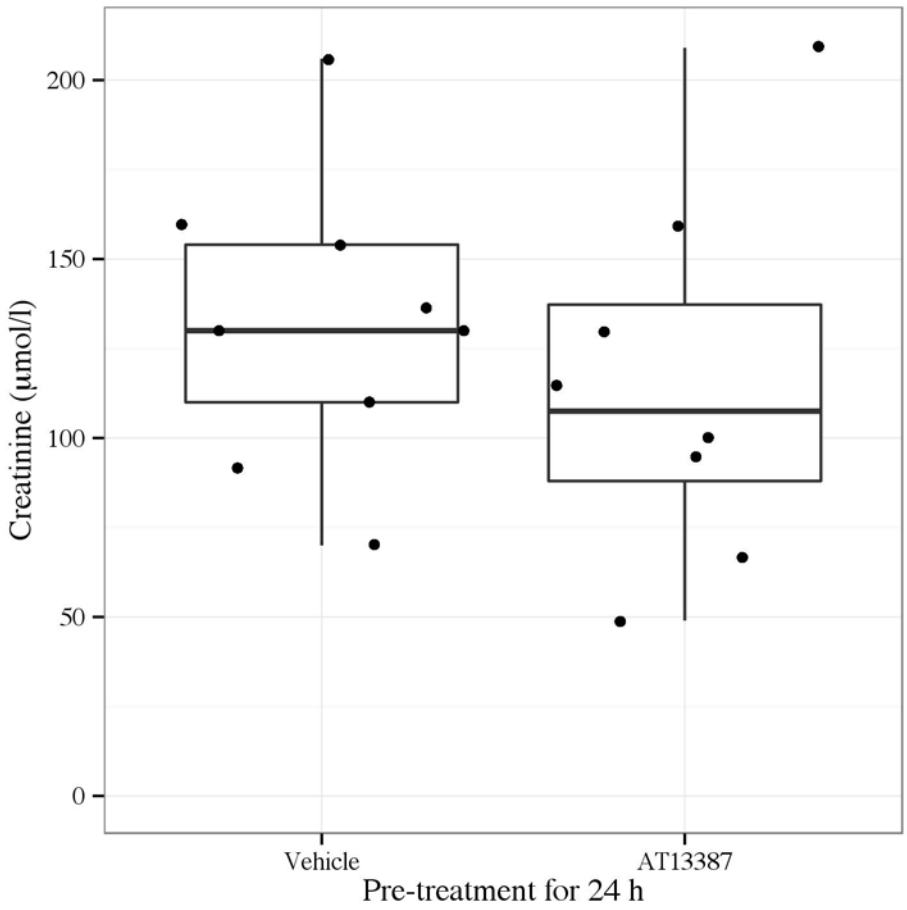


**Figure 8.4 Serum creatinine following AT13387 or vehicle pre-treatment and 24 h following renal IRI in Balb/c SCID mice**

Balb/c SCID mice were pre-treated with AT13387 or 2HβC vehicle (n=9 per group). 24 h later, mice were anaesthetised and underwent right nephrectomy and 32 min of left renal pedicle clamping. Following 24 h of recovery, blood was obtained by intra-cardiac puncture and serum creatinine was determined. Data are displayed for n=8 (instead of 9) in the AT13387 group because of one post-operative mortality. Results are presented in a standard boxplot with individual results jittered.

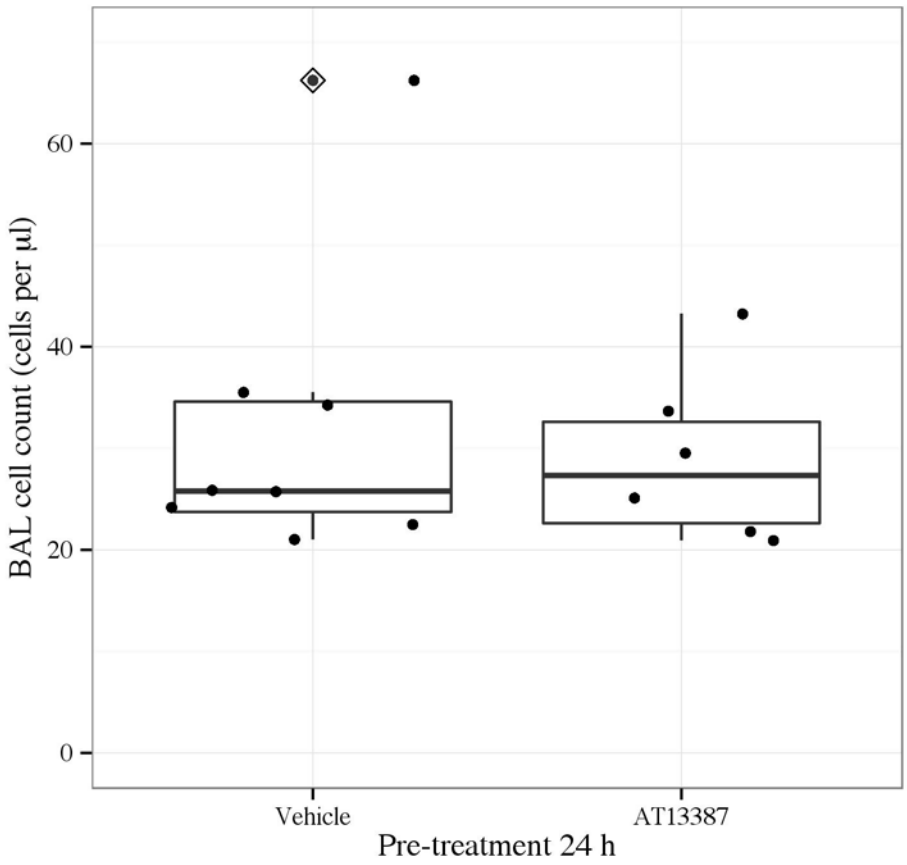


**Figure 8.5 BAL cell count following AT13387 or vehicle pre-treatment and 24 h following renal IRI in Balb/c SCID mice**

Balb/c SCID mice were pre-treated with AT13387 or 2HβC vehicle (n=9 per group). 24 h later, mice were anaesthetised and underwent right nephrectomy and 32 min of left renal pedicle clamping. Following 24 h of recovery, BAL was performed and the fluid underwent cytometric analysis. Data are displayed for n=8 (instead of 9) in the vehicle group and n=6 (instead of 9) in the AT13387 group, because in addition to one post-operative mortality in the AT13387 group; three mice had a low cell yield from the BAL and a total nucleated cell count below the limit of detection. Results are presented in a standard boxplot with individual results jittered. Outlier data are highlighted by a dot with a diamond in the midline.

## 8.5 AT13387 reduces lung injury secondary to renal IRI

Compared to pre-treatment with vehicle, there was protection from secondary lung injury caused by renal IRI in Balb/c SCID mice pre-treated with AT13387. This was evidenced by a significant reduction in interstitial neutrophil accumulation on flow cytometry of digested lungs (AT13387 vs. 2HβC vehicle, $p<0.001$, t-test) (Figure 8.6), as well as a reduction in pulmonary haemorrhage on BAL analysis (AT13387 vs. 2HβC vehicle, $p<0.05$, t-test) (Figure 8.6, Figure 8.7, Figure 8.8, Figure 8.9 and Figure 8.10).

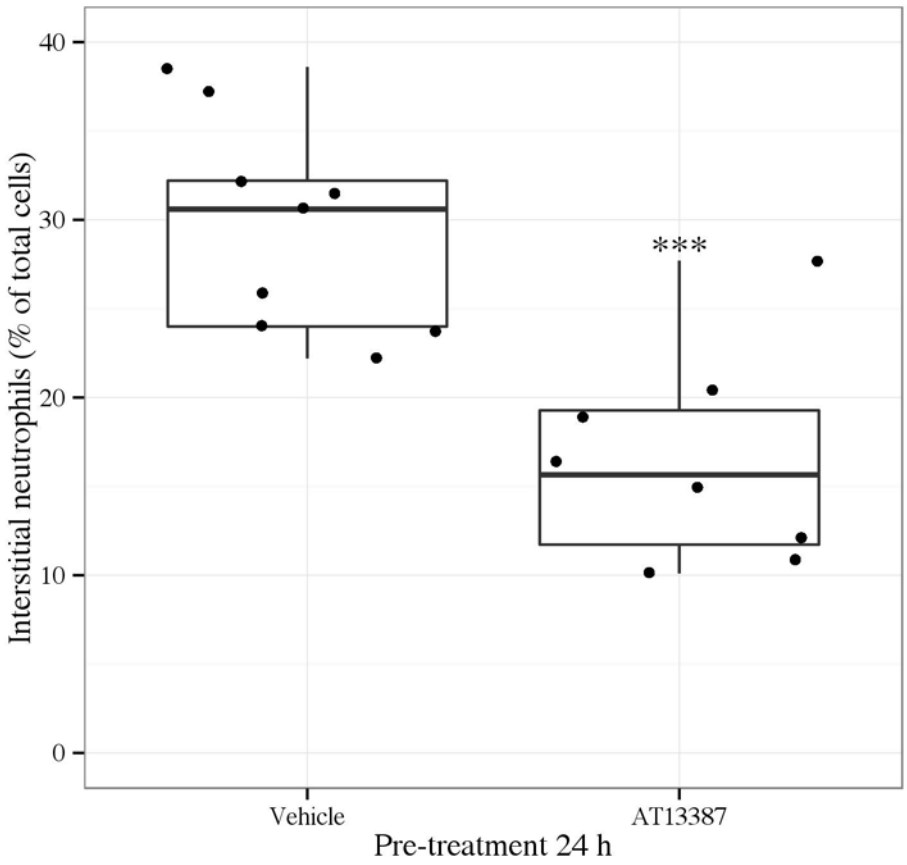


**Figure 8.6 Interstitial neutrophils in the lungs following AT13387 or vehicle pre-treatment and 24 h following renal IRI in Balb/c SCID mice**

Balb/c SCID mice were pre-treated with AT13387 or 2HβC vehicle (n=9 per group). 24 h later, mice were anaesthetised and underwent right nephrectomy and 32 min of left renal pedicle clamping. Following 24 h of recovery, lungs were harvested, digested and underwent cytometric analysis. Data are displayed for n=8 (instead of 9) in the AT13387 group because of one post-operative mortality. Results are presented in a standard boxplot with individual results jittered. ***$p<0.001$ vs. 2HβC vehicle, t-test.

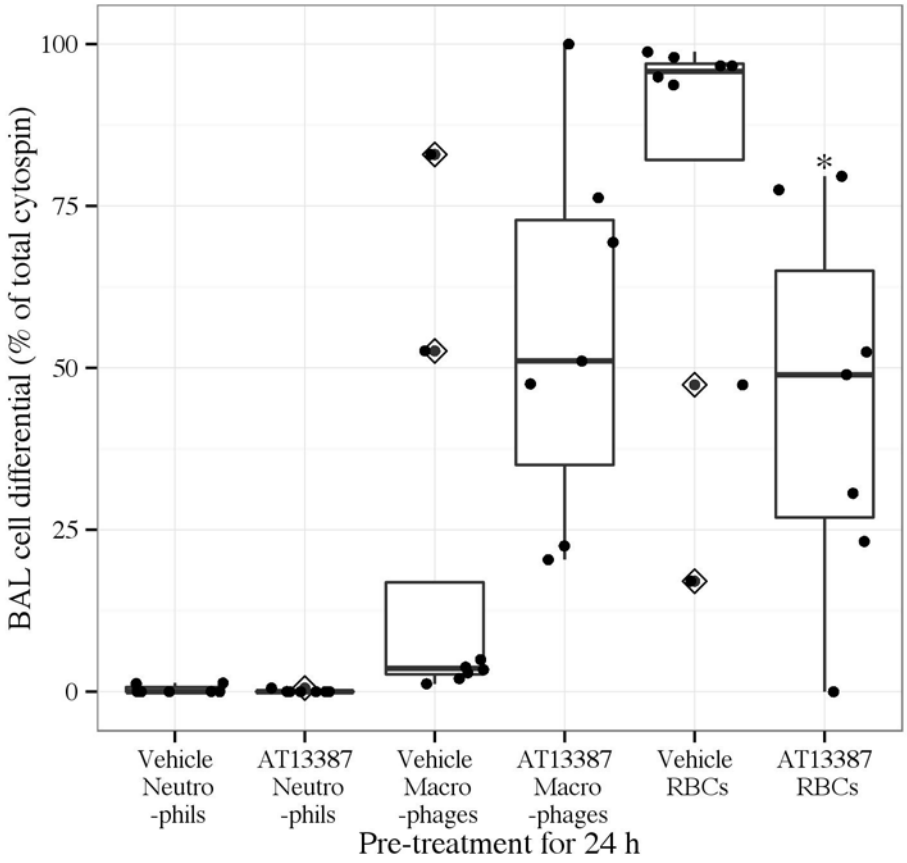


**Figure 8.7 BAL cell differential following AT13387 or vehicle pre-treatment and 24 h following renal IRI in Balb/c SCID mice**

Balb/c SCID mice were pre-treated with AT13387 or 2HβC vehicle (n=9 per group). 24 h later, mice were anaesthetised and underwent right nephrectomy and 32 min of left renal pedicle clamping. Following 24 h of recovery, BAL was performed and the fluid underwent cytometric analysis. Data are displayed for n=8 (instead of 9) is in the vehicle group and n=7 (instead of 9) in the AT13387 group, because in addition to one post-operative mortality in the AT13387 group; two mice had a low cell yield from the BAL and a cell differential below the limit of detection. In one sample with too low a yield for BAL cell count (Figure 8.5); it was still possible to perform a BAL cell differential. Results are presented in a standard boxplot with individual results jittered. Outlier data are highlighted by a dot with a diamond in the midline. *$p<0.05$ vs. 2HβC vehicle, t-test. RBCs=red blood cells.

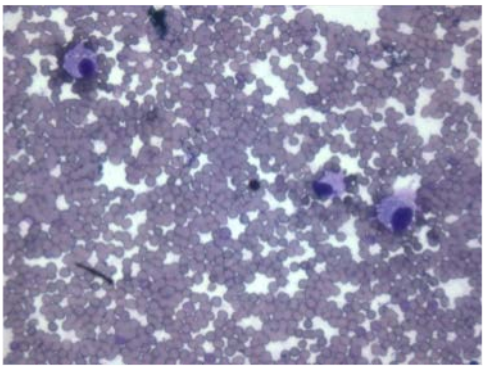

**Figure 8.8 BAL cytospin following vehicle pre-treatment and 24 h following renal IRI in Balb/c SCID mice**

Balb/c SCID mice were pre-treated with 2HβC vehicle (n=9). 24 h later, mice were anaesthetised and underwent right nephrectomy and 32 min of left renal pedicle clamping. Following 24 h of recovery, BAL was performed. A representative cytospin at x 400 magnification is shown. Macrophages are evident amongst numerous red blood cells.

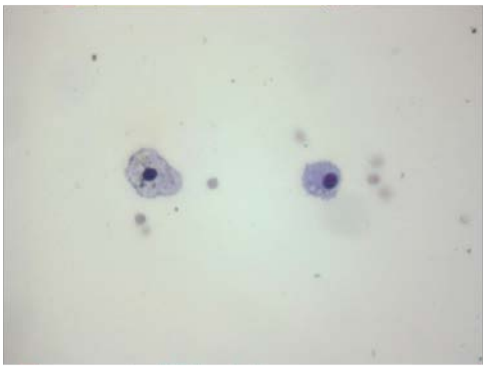

**Figure 8.9 BAL cytospin following AT13387 pre-treatment and 24 h following renal IRI in Balb/c SCID mice**

Balb/c SCID mice were pre-treated with AT13387 (n=9). 24 h later, mice were anaesthetised and underwent right nephrectomy and 32 min of left renal pedicle clamping. Following 24 h of recovery, BAL was performed. A representative cytospin at x 400 magnification is shown. Macrophages are evident but there are minimal red blood cells.

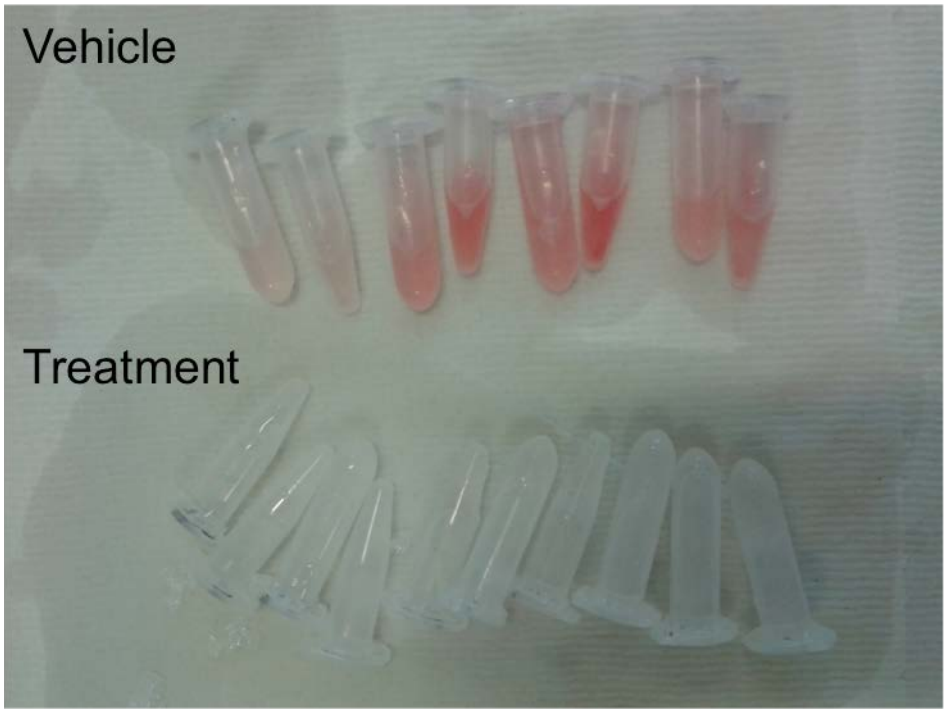


**Figure 8.10 BAL following AT13387 or vehicle pre-treatment and 24 h following renal IRI in Balb/c SCID mice**

Balb/c SCID mice were pre-treated with AT13387 or 2HβC vehicle (n=9 per group). 24 h later, mice were anaesthetised and underwent right nephrectomy and 32 min of left renal pedicle clamping. Following 24 h of recovery, BAL was performed. A photograph of primary and secondary lavages in separate eppendorf tubes is shown for each group (n=4-5 per group shown in photograph). There is blood staining in the lavages of vehicle treated mice but clear lavages for the AT13387 treated mice.

## 8.6 Summary

In this chapter, it was shown that AT13387 induces Hsp70 expression in the lungs of mice. Following pre-treatment with AT13387 there was also a reduction in pulmonary haemorrhage and neutrophil accumulation in the lungs of mice following renal IRI. This was despite equivalent levels of kidney injury, which was made possible by the use of SCID mice. The results of these experiments suggest that AT13387 may have protective properties in the lungs, perhaps involving Hsp70 induction, which reduce secondary lung injury following renal IRI.

## 8.7 Discussion

### 8.7.1 Limitations

It was decided to utilise SCID mice in this chapter, as it was hypothesised from previous experiments in Chapter 7 that there would be similar levels of kidney injury in vehicle and AT13387-treated SCID mice after renal IRI. This in theory would mean that the stimulus for secondary lung injury would be similar between the groups. As per this hypothesis, pre-treatment with AT13387 again did not reduce kidney injury following renal IRI in SCID mice. This could be viewed as strength of the data; since an experiment involving only wild-type mice would have introduced the possibility that changes in secondary lung injury were the result of less damage to the kidney after AT13387 pre-treatment. However, it is also a weakness, as there are no corroborating data from wild-type mice. In the following chapter, lung injury is assessed in wild-type mice following renal IRI caused by kidney transplantation, but this is across a smaller number of animals. The effect of AT13387 on secondary lung injury in wild-type mice should therefore be formally determined in the renal IRI model as well.

### 8.7.2 Variability

In this chapter lung injury was assessed by interstitial neutrophil accumulation on flow cytometry of digested lungs, and pulmonary haemorrhage on BAL analysis. Pulmonary haemorrhage was determined by the percentage of red blood cells in the cytospin of the BAL. The cell count of the BAL was similar but not identical between the groups therefore it was decided to quantify the amount of red blood cells as a percentage of the total cytospin in each BAL, rather than cell number. As the percentage of red blood cells increased, the percentage of the other cells present (i.e. macrophages, as neutrophils did not cross over from the interstitial space to the alveolar space) decreased as a result. This does not reflect a change in macrophage number per se. In terms of flow cytometry of digested lungs to detect interstitial neutrophils, non-adherent cells were removed from the lung vasculature and appropriate staining was performed to ensure specificity in terms of detecting only neutrophils.

### 8.7.3 Reproducibility

The results of the SCID mouse experiment, in terms of renal Hsp70 induction by AT13387, and a lack of functional kidney protection by AT13387 after renal IRI, has been replicated from Chapter 5 and Chapter 7 respectively. Moreover, across both experimental groups, there was a significant increase in interstitial neutrophil accumulation on flow cytometry of digested lungs, as well as an increase in pulmonary haemorrhage on BAL analysis in SCID mice undergoing renal IRI. This was a consistent effect from the initial work performed by Duncan Humphries, which confirmed that secondary lung injury occurred in the renal IRI model with both Balb/c and Balb/c SCID mice (section 8.2). This reflects good reproducibility of data. In the following chapter lung injury is again reduced by AT13387, but this is across a small number of wild-type mice following renal transplantation. The

reproducibility of the lung data in SCID mice following renal IRI with AT13387 pre-treatment is therefore currently unclear, and should be confirmed.

# Chapter 9: Recipient treatment with AT13387 reduces renal IRI in transplantation

## 9.1 Background

In Chapter 7 and 8, the kidney protective effect of AT13387 was shown to be at least partially lymphocyte-dependent. This could mean that the protective effect of AT13387 is systemic and immunomodulatory in nature. As such, it may be feasible to pre-treat recipient mice in order to modify the recipient's immune response to reperfusion. This could reduce the detrimental effects of IRI in the transplanted kidney. However, in Chapter 6 and 7, the renoprotective effect of AT13387 was demonstrated following pre-treatment in a renal IRI model. It is therefore uncertain whether there is any therapeutic potential for using AT13387 in a recipient prior to transplantation or whether treatment needs localised to the kidney prior to the onset of injury. This chapter addresses the hypothesis that recipient treatment with AT13387 reduces renal IRI in transplantation. The experiments in this chapter were performed in conjunction with George Tse (performed renal transplantations) and Duncan Humphries (performed BAL, lung digestion and cytometric analysis).

## 9.2 Recipient treatment with AT13387 is feasible in a renal transplant model

An isograft renal transplantation model involving 4 h of cold ischemia prior to transplantation was used. Compared to pre-treatment of recipient Balb/c mice with vehicle, AT13387 pre-treatment of recipient Balb/c mice resulted in no chenge in tubular necrosis score (AT13387 vs. 2HβC vehicle, p=0.71, Mann-Whitney U test) (Figure 9.1) on histological assessment of the transplanted kidney 24 h following renal transplantation (Figure 9.2 and Figure 9.3).

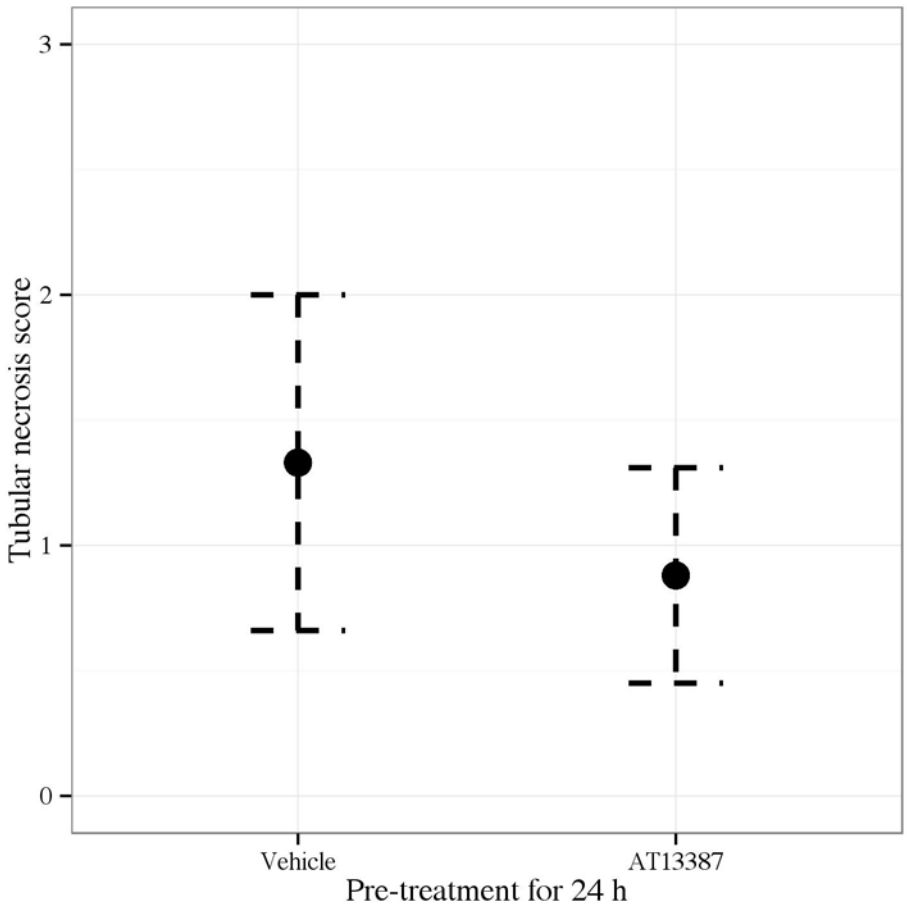


**Figure 9.1 Tubular necrosis score in the transplanted kidney following AT13387 or vehicle pre-treatment of recipient Balb/c mice and 24 h following renal transplantation**

Mice were pre-treated with AT13387 or 2HβC vehicle (n=3-4 per group). 24 h later, mice were anaesthetised and underwent right nephrectomy. This was followed by isograft renal transplantation with a donor kidney that had been harvested from a treatment naive donor mouse and cold stored at 4°C for 4 h. All mice had a single intact native left kidney and the model was not transplant-dependent. Following 24 h of recovery, the transplanted kidney was harvested and placed in methacarn. Sections were later prepared and stained with haematoxylin and eosin. A blinded observer then determined the tubular necrosis score. Results are presented as mean and standard error of the mean.

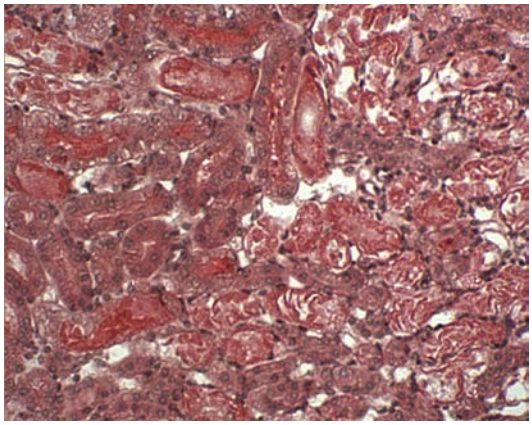

**Figure 9.2 Morphological kidney injury in the transplanted kidney following pre-treatment of recipient Balb/c mice with vehicle and 24 h following renal transplantation**

Mice were pre-treated with 2HβC vehicle (n=3). 24 h later, mice were anaesthetised and underwent right nephrectomy. This was followed by isograft renal transplantation with a donor kidney that had been harvested from a treatment naive donor mouse and cold stored at 4°C for 4 h. All mice had a single intact native left kidney and the model was not transplant-dependent. Following 24 h of recovery, the transplanted kidney was harvested and placed in methacarn. Sections were later prepared and stained with haematoxylin and eosin. A representative section of kidney cortex at x 200 magnification is shown. There are areas of tubular necrosis and significant tubular cell damage.

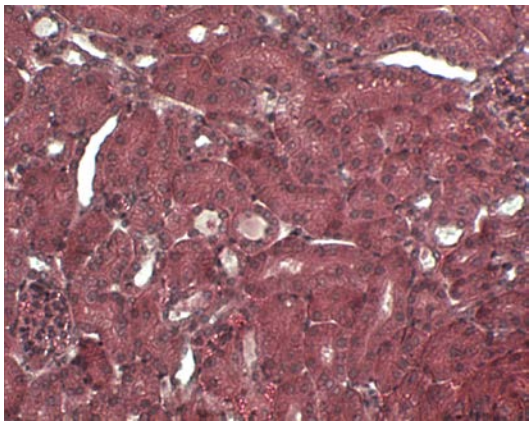

**Figure 9.3 Morphological kidney injury in the transplanted kidney following pre-treatment of recipient Balb/c mice with AT13387 and 24 h following renal transplantation**

Mice were pre-treated with AT13387 (n=4). 24 h later, mice were anaesthetised and underwent right nephrectomy. This was followed by isograft renal transplantation as per Figure 9.2. A representative section of kidney cortex at x 200 magnification is shown. There are areas of tubular necrosis and significant tubular cell damage.

## 9.3 AT13387 reduces secondary lung injury in renal transplantation

Compared to intervention naive control Balb/c mice, in both vehicle and AT13387 pre-treated recipient Balb/c mice, cell counts on BAL analysis were similar 24 h following renal transplantation (Figure 9.4).

However, compared to controls, in both vehicle and AT13387 pre-treated recipient Balb/c mice, 24 h following renal transplantation there was evidence of secondary lung injury. This was demonstrated by a significant increase in pulmonary haemorrhage on BAL analysis (renal transplantation vs. control, <0.05, t-test) (Figure 9.5) and interstitial neutrophil accumulation on flow cytometry of digested lungs (renal transplantation vs. control, <0.05, t-test) (Figure 9.6). This indicates that significant secondary lung injury occurred following renal transplantation in this model.

Compared to pre-treatment of recipient Balb/c mice with vehicle, there was protection from secondary lung injury induced by renal transplantation in recipient Balb/c mice pre-treated with AT13387. This was evidenced by a significant reduction in pulmonary haemorrhage on BAL analysis (AT13387 vs. 2HβC vehicle, $p<0.05$, t-test) (Figure 9.5). However, compared to vehicle, on flow cytometry of digested lungs, there was no reduction in interstitial neutrophil accumulation induced by renal transplantation in Balb/c recipient mice pre-treated with AT13387 (Figure 9.6).

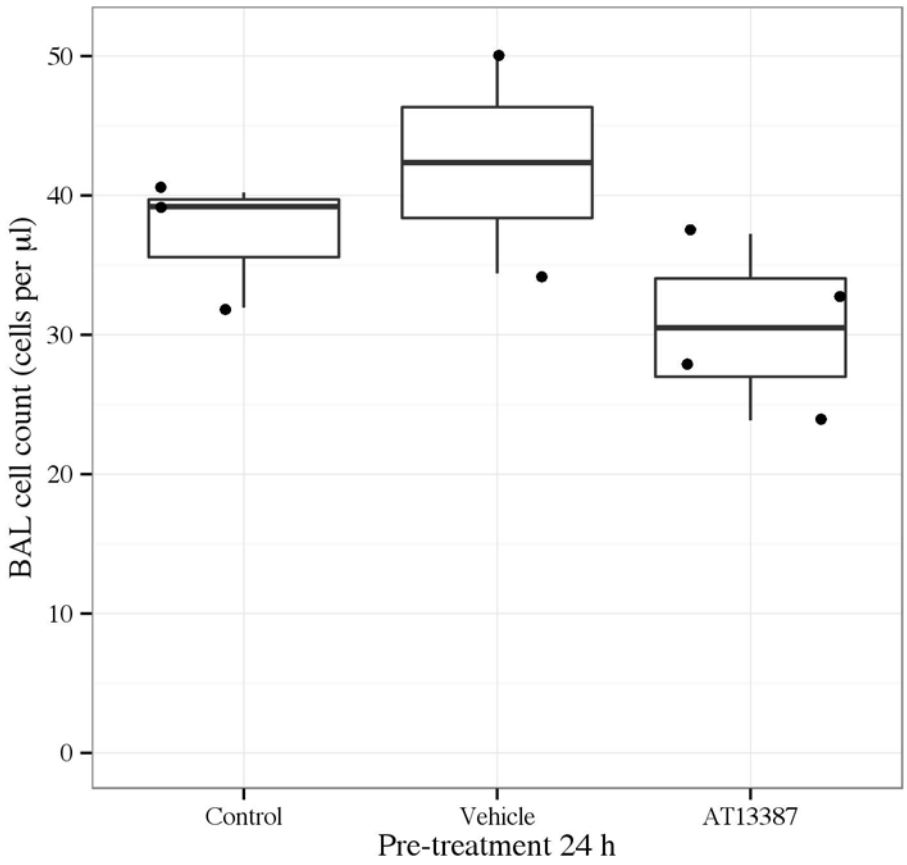


**Figure 9.4 BAL cell count following AT13387 or vehicle pre-treatment and 24 h following renal transplantation in Balb/c mice.**

Balb/c mice were pre-treated with AT13387 or 2HβC vehicle (n=3-4 per group). 24 h later, mice were anaesthetised and underwent right nephrectomy. This was followed by isograft renal transplantation with a donor kidney that had been harvested from a treatment naive donor mouse and cold stored at 4°C for 4 h. All mice had a single intact native left kidney and the model was not transplant-dependent. Following 24 h of recovery, BAL was performed and the fluid underwent cytometric analysis. The negative controls were treatment naive mice that did not undergo renal transplantation or any other intervention (n=3). Data are displayed for n=2 (instead of 3) in the vehicle group because one animal did not have a BAL performed. Results are presented in a standard boxplot with individual results jittered.

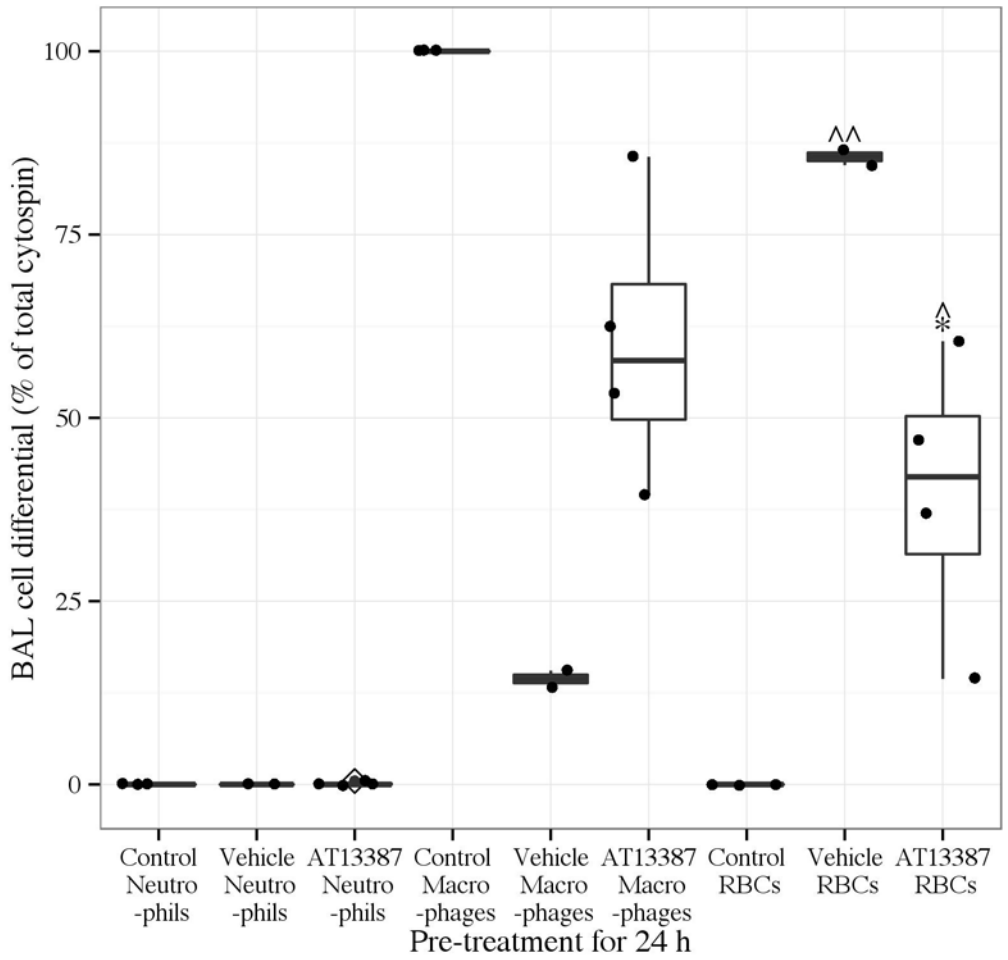


**Figure 9.5 BAL cell differential following AT13387 or vehicle pre-treatment and 24 h following renal transplantation in Balb/c mice**

Balb/c mice were pre-treated with AT13387 or 2HβC vehicle (n=3-4 per group). 24 h later, mice were anaesthetised and underwent right nephrectomy. This was followed by isograft renal transplantation with a donor kidney that had been harvested from a treatment naive donor mouse and cold stored at 4°C for 4 h. All mice had a single intact native left kidney and the model was not transplant-dependent. Following 24 h of recovery, BAL was performed and the fluid underwent cytometric analysis. The negative controls were treatment naive mice that did not undergo renal transplantation or any other intervention (n=3). Data are displayed for n=2 (instead of 3) in the vehicle group because one animal did not have a BAL performed. Results are presented in a standard boxplot with individual results jittered. Outlier data are highlighted by a dot with diamond in the midline. *$p<0.05$ vs. 2HβC vehicle, ^$p<0.05$ vs. control and ^^$p<0.01$ vs. control, t-test. RBCs=red blood cells.

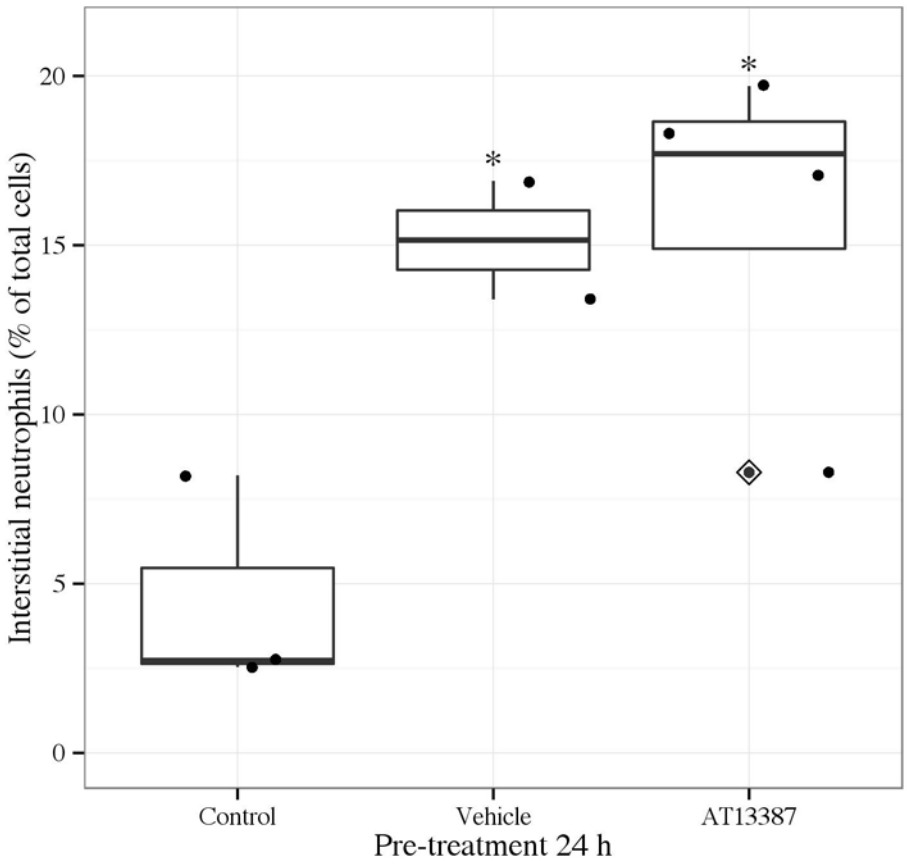


**Figure 9.6 Interstitial neutrophils in the lungs following AT13387 or vehicle pre-treatment and 24 h following renal transplantation in Balb/c mice**

Balb/c mice were pre-treated with AT13387 or 2HβC vehicle (n=3-4 per group). 24 h later, mice were anaesthetised and underwent right nephrectomy. This was followed by isograft renal transplantation with a donor kidney that had been harvested from a treatment naive donor mouse and cold stored at 4°C for 4 h. All mice had a single intact native left kidney and the model was not transplant-dependent. Following 24 h of recovery, lungs were harvested, digested and underwent cytometric analysis. The negative controls were treatment naive mice that did not undergo renal transplantation or any other intervention (n=3). Data are displayed for n=2 (instead of 3) in the vehicle group because one animal did not have lungs harvested. Results are presented in a standard boxplot with individual results jittered. Outlier data are highlighted by a dot with diamond in the midline. *$p<0.05$ vs. control, t-test.

## 9.4 Summary

The experiments in this chapter demonstrate that recipient treatment with AT13387 in a renal transplant model is feasible but not associated with significant protection of kidney morphology across a limited sample size. There does appear to be protection from secondary lung injury in this model following pre-treatment of the recipient mice with AT13387. Again a limited sample size may have negated the full benefit or lack of benefit from this aspect of AT13387 recipient therapy. These issues are discussed further below, and in Chapter 10.

## 9.5 Discussion

### 9.5.1 Limitations

The results in this chapter provide preliminary data about the efficacy of recipient treatment with AT13387 in a renal transplantation model utilising a cold ischemic time of 4 h. In a previous publication that utilised a murine renal transplantation model of IRI, approximately 75% of tubules in the corticomedullary junction showed tubular epithelial necrosis after 4 h of cold ischemia [241]. On the basis of this previous publication and previous in-house data, this cold ischemic time was therefore selected for these experiments as well. The major weakness of this experiment is the low sample size, which could have resulted in the experiment being underpowered to detect differences between the groups. Indeed, such small numbers of animals preclude any meaningful interpretation of the data. Despite this, the experiment is an important step towards translational relevance, and the sample size of this experiment should be increased to build on this preliminary data.

A non-transplant dependent model, which leaves the recipient mouse with a native kidney *in situ*, was selected to aid survival [242]. However, this reduces the utility of certain biochemical markers of kidney injury, such as creatinine, as the native kidney takes on the responsibility of clearing creatinine for the injured kidney graft. Assessment of histological injury markers in the kidney graft remained feasible in the context of this non-transplant dependent model, but it is a more subjectively determined outcome measure. Given that only one blinded observer performed histological scoring, this represents a further weakness of this experiment.

### 9.5.2 Variability

In this chapter there was variation in tubular necrosis score within the groups. This is understandable given the technical demands of the procedure. Translating treatments from IRI models to small animal transplant studies is one of the most challenging steps in the process of drug development in transplantation. Even when technical expertise is available there can be issues with variability and survival at the injury levels required to produce acute tubular necrosis in the kidney graft. One option to reduce variability is to leave the native kidney *in situ* long enough to give the graft time to recover (e.g. 5 days), but this requires a second procedure for the nephrectomy of the native kidney [242].

### 9.5.3 Reproducibility

An interesting finding of this chapter was that lung injury was present following renal transplantation. This is agreeable with the data presented from the renal IRI model in the previous chapter, and suggests that secondary lung injury is consistent consequence of renal IRI. Across a limited sample size, AT13387 also reduced lung injury in terms of reduced pulmonary haemorrhage on BAL. This is similar to the

reduction in lung injury observed in Balb/c SCID mice in Chapter 8. As per the analysis performed of lung injury in Chapter 8, apparent differences in macrophages on BAL between the groups were a reflection of a reduction in red blood cells (i.e. pulmonary haemorrhage), as opposed to a true difference in macrophage number. This is because the result was again expressed as a percentage of the total cytospin. These findings should also be confirmed across a greater sample size.

# Chapter 10: Discussion

## 10.1 Background

In this final chapter, the significance of the findings of this thesis will be discussed in the order they were presented, starting with *in vitro* data before moving on to consider the later *in vivo* results. Then the strengths and weaknesses of the data will be further evaluated, and the future directions of each area of research will be outlined. The results of the experiments performed will also be put in the context of current published evidence on this topic of investigation. The meetings where the data from this thesis have been presented are later described on page 229 and the peer review publications resulting from this work are listed on page 230.

## 10.2 *In vitro* data

### 10.2.1 Chapter 3

In mechanistic work in Chapter 3, a carefully designed *in vitro* model was developed to simulate the sterile inflammatory environment of renal IRI. It was found that Hsp90 inhibition with AT13387 and 17-DMAG resulted in breakdown of IKKα, IKKβ and NEMO, which are the three subunits of the IKK complex. This reduced highly specific TLR4-mediated NF-κB activation by hyaluronan to the level of untreated cells left in basal conditions in normal culture medium. Moreover, it led to a reduction in the release of pro-inflammatory cytokines.

These findings suggest a potent anti-inflammatory effect from AT13387. However, the relevance of reduced inflammatory signalling and cytokine expression in HEK293 cells, which were primarily selected for their ease of use in evaluating TLR4 signalling rather than similarities to human renal epithelial cells, is uncertain. Also, since the cytokine array and Western blot data is displayed for only one experiment; it is difficult to know how reproducible these results are. Albeit, similar results were later observed in Chapter 3 following LPS stimulation.

In experimental renal IRI, transgenic mice that are missing TLR4 [168, 170, 172, 176], or that have been treated with TLR4-blocking agents demonstrate a markedly protected phenotype [173]. Donor TLR4 status is also of critical importance in human transplantation [178]. Furthermore, NF-κB de-activation with small interfering RNAs targeting either IKKβ or NF-κB transcription factor RelB, or *in vivo* transfection with NF-κB decoy oligodeoxynucleotides have previously been shown to protect the kidney from IRI [279-281]. Therefore, despite a lack of data to suggest a definitive pathway of protection, the potential of AT13387 to interrupt TLR4-mediated NF-κB signalling is still highly attractive from a translational perspective since it offers a pharmacological strategy to temporarily de-activate NF-κB. This in contrast to ablation of the IKK complex, which reduces NF-κB mediated inflammation but also prevents subsequent NF-κB mediated protection from apoptosis [137].

In Chapter 3 of this thesis it has also been confirmed, as previously described elsewhere in the literature, that TNFα-mediated NF-κB activity can be reduced by Hsp90 inhibition [131, 132, 134, 135]. Furthermore, in keeping with other studies in human cell lines, it was confirmed that LPS-mediated NF-κB activity could be decreased by Hsp90 inhibition [73, 250, 251]. These combined results suggest that the repressive effect of Hsp90 inhibition on NF-κB activity is not only TLR4-

specific or mediated by sterile DAMPs. Hsp90 may therefore be an integral part of NF-κB activation, primarily at a junction downstream from TLR4.

Although numerous pathways can lead to NF-κB activation, IKK is a common point of convergence [128], and activation of NF-κB occurs nearly universally via IKK-mediated degradation of IκB [129]. Indeed, it has previously been shown in HeLa cells that geldanamycin can prevent the formation of a proposed hetero-complex involving IKK and Cdc37/Hsp90, reducing the size of the complex and preventing activation of NF-κB [133]. It has also been observed in alveolar epithelial cells that treatment with geldanamycin induces dissociation of Hsp90 from the IKK complex, rendering the complex detergent insoluble and the NF-κB system impassive to cytokine stimulation [136].

It therefore seems likely that Hsp90 inhibitors repress TLR4-mediated NF-κB activity primarily through IKK. The breakdown of all the major subunits of IKK by AT13387 and 17-DMAG following hyaluronan or LPS stimulation in this study would support this hypothesis. The hypothesis is also endorsed by partial regain of NF-κB activity following pre-treatment and incubation with AICAR, which is a compound that prevents IKKα degradation by AT13387 and 17-DMAG through inhibition of autophagy [249].

AICAR is an activator of 5' AMP-activated protein kinase (AMPK) but it inhibits autophagy by an AMPK independent mechanism through prevention of class III PI3-kinase binding to beclin-1 [282]. AICAR alone led to partial repression of TLR4-mediated NF-κB activation by hyaluronan, which may have resulted from its ability to stimulate 5' AMPK. This could explain the inability of AICAR to completely reverse NF-κB repression due to Hsp90 inhibition despite its capacity to prevent IKKα degradation. In addition, although a significant regain of NF-κB activity was

observed in 17-DMAG pre-treated cells, it did not have as pronounced an effect in AT13387 pre-treated cells, which could be explained by the increased potency of AT13387.

In keeping with this observation an additional finding of Chapter 3 was that AT13387 appeared more consistently effective at rendering NF-κB unresponsive to cytokine stimulation than 17-DMAG. It was initially noted at 1000 nM doses that AT13387 was more effective at reducing hyaluronan-mediated NF-κB activity, but in subsequent experiments both drugs seemed equivalent at this higher dose. As such, the variability in the 17-DMAG 1000 nM results could represent a batch effect secondary to using different stock solutions of 17-DMAG. Despite this, AT13387 was conclusively more potent in most other experiments at reducing NF-κB activity at lower doses than 17-DMAG, for example, following TNFα, LPS and hyaluronan stimulation. In further *in vitro* experiments AT13387 was also significantly more effective at improving cell survival following oxidative stress than 17-DMAG. Although AT13387 does not appear to act through different mechanisms from 17-DMAG, it is a smaller molecule Hsp90 inhibitor and therefore may be more efficacious in this respect. A final consideration is that AT13387 100 nM and 17-DMAG 500 nM actually increased NF-κB activation on SEAP assay following hyaluronan stimulation. The dose of these drugs could therefore be critical to their effect. Indeed, there could be complex interaction of different molecules resulting in pro-inflammatory effects of Hsp90 inhibitors with lower doses, but anti-inflammatory effects at a higher dose.

#### 10.2.1.1 Future directions

The data gathered in this chapter would be made more robust by replicating the experiments that were performed on only one occasion e.g. the cytokine arrays and Western blots. The results of the experiments performed should also be confirmed in

other cell lines. Particularly since HEK293 cells were primarily selected for their ease of use in evaluating TLR4 signalling rather than similarities to human renal epithelial cells. This could include other established cell lines (e.g. HK2 cells) or primary renal cells. Detailed analysis of the dose effect of AT13387 and 17-DMAG would also be of interest.

Another area of research worth pursuing is the further development of Hsp90 inhibition with AT13387 to establish the relevance *in vivo* of repressing TLR4-mediated NF-κB activation in renal IRI. It was difficult to establish after the *in vivo* experiments described in this thesis, whether potential reductions in TLR4 and NF-κB expression in injured kidneys by AT13387 were the cause of protection or simply "read outs" of less damage to the kidney. As such, enquiries have been made about acquiring TLR4 -/- mice for this line of investigation.

The use of TLR4 -/- mice could provide a better answer to the question of whether repression of TLR4-mediated NF-κB activation is a key to the protection in renal IRI by AT13387. Due to inherent protection from renal IRI observed in TLR4-/- mice, it could be challenging to demonstrate any potential drug or loss of drug effect, and careful titration of the level of injury would be needed [168, 170, 172, 176]. In addition, if there were a loss of protection from renal IRI by AT13387 in TLR4 -/- mice, it is unclear at this stage what the "add back" experiment to show regain of protection by the drug would be. This may mean that pursuing a conditional TLR4 knockout model would be a better option.

### 10.2.2 Chapter 4

The potential lack of similarity between HEK293s and human renal tubular epithelial cells, also calls into question the relevance in Chapter 4 of demonstrating *in vitro*

protection from oxidative stress with Hsp90 inhibition in these cells. The significance of this limitation is lessened considerably by the convincing and reproducible level of *in vivo* protection demonstrated by AT13387 from renal IRI in later chapters.

In experiments that have not been reported in this thesis, there were further difficulties demonstrating the mechanisms of protection from oxidative stress offered by Hsp90 inhibition. In particular, it was not possible to link cytoprotection to either enhanced Hsp70 expression or a reduction in inflammatory signalling in HEK293 cells. This was firstly due to a high background expression of Hsp70 in these cells under basal conditions. This made it difficult to significantly modify Hsp70 expression following Hsp90 inhibition, but might also signify that the protection demonstrated in this model was not Hsp70-mediated.

Secondly, an anticipated reduction in the numbers of viable cells in assays following oxidative stress, which is a cytotoxic insult, made it problematic to demonstrate any differences in NF-κB signalling between experimental conditions. For example, despite starting experiments with equal cell numbers, following oxidative stress, there were a greater number of viable cells after Hsp90 inhibition. It is anticipated that these Hsp90 inhibitor treated cells would probably secrete lower levels of SEAP, which was used to indicate NF-κB activity. However, a smaller number of viable cells after vehicle treatment could conversely secrete high levels of SEAP, which could have led to a balancing out of SEAP levels between experimental groups. The same problem was encountered when assessing NF-κB activity following oxidative stress compared to control conditions.

#### 10.2.2.1 Future directions

The results of the experiments performed in Chapter 4 should also be confirmed in other cell lines, and potentially other models of cellular injury (e.g. chemical insults and hypoxia). It would be useful to adopt a more advanced assay of cell viability (e.g. xCELLigence System) to acquire real-time data on cell viability, rather than a single static result at the end of the experiment. Moreover, it would be interesting to establish if TLR4-mediated NF-κB activation actually leads to cell death. This was not formally assessed in this thesis, but no obvious differences in cell number were identified when performing the cell signalling experiments in Chapter 3. Although it should be noted that these experiments were conducted over a relatively short time frame of 24 h, and perhaps if the experiments were extended there would have been a reduction noted in cell viability.

## 10.3 *In vivo* data

### 10.3.1 Chapter 5

As described in Chapter 1, previous studies have shown that pharmacological inhibition of Hsp90 is protective from experimental renal IRI in mice [84, 85]. However, a drug designed to reduce IRI in renal transplantation has an absolute requirement for low toxicity. Therefore, one of the main challenges going forward is to develop low toxicity drugs that can be safely utilised in human renal transplantation. AT13387 is a novel small molecule Hsp90 inhibitor with a low toxicity profile in phase II human studies in oncology and therefore excellent translational potential in this context [99, 100]. In Chapter 5 of this thesis, AT13387 led to a marked induction of Hsp70 expression in the kidneys of mice.

This up-regulation of Hsp70 was consistent across various strains of mice including FVB/n, Balb/c and Balb/c SCID mice. As AT13387 was being used as a pre-treatment to prevent renal IRI, these experiments were an important step prior to assessing the efficacy of this agent in reducing renal IRI [238]. The results of the ELISA were also validated using immunohistochemistry, which clarified that Hsp70 induction was within renal tubular cells, and maximal in the outer stripe of the outer medulla of the kidney

#### 10.3.1.1 Future directions

The weaknesses of this data were that Hsp70 induction was only assessed at two time points (6 h and 24 h). The experiment performed at 6 h also had a limited sample size (n=3), and therefore caution must be exercised in interpreting the data. A more complete time course experiment, using more animals at each time point, could provide additional data on the kinetics of AT13387. Hsp70 is the most commonly used biomarker of Hsp90 inhibition but it would be useful to explore other indicators of Hsp90 inhibition, particularly if experiments using Hsp70-/- mice are to be considered in future [264].

### 10.3.2 Chapter 6

In Chapter 6, AT13387 pre-treatment resulted in functional and morphological kidney protection following renal IRI in FVB/n mice. Cytokine arrays were used to evaluate CXCL1 and CXCL2 expression, and therefore the NF-κB activation status of the kidneys injured by IRI in AT13387 treated mice, compared to vehicle treated mice [266, 267]. Similar to the human cytokine array panels used in Chapter 3, the arrays also assessed 38 other chemokines and cytokines, many of which are markers

of inflammation. In contrast, the arrays in this chapter were performed on 4 kidney lysates per group, in order to allow for quantitative analysis.

CXCL1 and CXCL2 expression was significantly reduced in the kidney following renal IRI in mice pre-treated with AT13387. CXCL1 is the equivalent of GROα, which had reduced expression following AT13387 pre-treatment in the arrays performed in Chapter 3. The significant reduction in the renal expression of CXCL1 and CXCL2 with AT13387 pre-treatment suggests a reduction in NF-κB-mediated inflammatory signalling within the kidney. This is also suggested by a significant reduction in TLR4 expression on real time PCR analysis of injured kidneys following AT13387 pre-treatment.

#### 10.3.2.1 Future directions

In Chapter 6 there was notable variation in serum creatinine levels, particularly in the AT13387 group, with the unilateral IRI model. By adopting a simpler bilateral ischemia model the variability could be reduced. This wouldn't give information on the induction of Hsp70 in each experimental animal but as Hsp70 is so consistently up-regulated with the 80 mg/kg dose of AT13387, perhaps this isn't a major issue. In the unilateral IRI model, it would be interesting to assess other markers of kidney function, such as glomerular filtration rate, and other markers of kidney injury (e.g. kidney injury molecule-1) or cellular senescence (e.g. p16 or p21) [270, 271]. Furthermore, at just 24 hours following renal IRI, it is likely that protective effect of AT13387 may have involved programmed cell death, so markers of apoptosis (e.g. caspase activation) could also be assessed [159]. Moreover, since injury was assessed at only one time point (24 h after surgery), additional experiments could be performed using a longer recovery period. This could address whether AT13387 is simply delaying the onset of kidney injury, or preventing it from occurring. The unilateral IRI model could also be extended beyond the initial 7 days it takes for

acute tissue injury to resolve. This would assess the impact of AT13387 pre-treatment on eventual kidney regeneration following renal IRI [238].

### 10.3.3 Chapter 7

In Chapter 7, AT13387 pre-treatment resulted in functional and morphological kidney protection following renal IRI in Balb/c mice. Using Balb/c SCID mice, it was demonstrated that the kidney protection from renal IRI afforded by AT13387 is at least partially lymphocyte-dependent. This is similar to the lymphocyte-dependent nature of the protection from renal IRI that is garnered by Hsp70 induction using heat preconditioning [224]. In contrast to previous heat preconditioning studies by Kim *et al*. (2014), there was no evidence found on immunohistochemistry to suggest that the protective effect of AT13387 is either T-cell or more specifically Treg dependent [224]. This data was preliminary, and performed across small numbers of animals; it should therefore be cautiously interpreted. Further work, with increased sample sizes, and potentially involving flow cytometry of blood, spleen and kidneys, needs to be performed to understand what the key subset of lymphocytes or the adaptive immune response involved may be.

There are also additional caveats to the work demonstrating the potentially lymphocyte-dependent nature of the protection from renal IRI exhibited with AT13387. For instance, while the majority of SCID mice lack functional lymphocytes, in a process termed “leakiness” 2-23% appear to develop a limited number of B and T cells [283]. This usually occurs in older SCID mice (> 3 months old) than were used in the experiments described in this thesis (6-8 weeks) but could still represent a limitation of the findings [283].

In addition, in further experiments performed in Edinburgh, it has been reported in an abstract publication by the Ferenbach *et al*. (2012), that compared to Balb/c mice, Balb/c SCID mice have a protective phenotype in renal IRI [277]. This was not observed in either renal IRI experiment performed using SCID mice in Chapter 7 or 8 of this thesis. This variation echoes other inconsistencies in this area that have previously been reported, with renal IRI studies using RAG-1-/- mice (lacking B and T cells) showing both renal protection [213], and a similar kidney injury to wild type controls [214, 215].

In a publication by Day *et al*. (2006), the only study in which RAG-1-/- mice displayed a protective phenotype from renal IRI, the authors address these inconsistent outcomes, and discuss the variations between published studies that could potentially have contributed. These variations include the method of pedicle clamping, use of heparin and anesthetic agents, and degree of injury [213]. In a study by Park *et al*. (2002), the background strains of the RAG-1-/- mice were C57BL/6, and mixed C57BL/6 and B6129. The mice received heparin 1 h prior to surgery and were anesthetized with inhalational isoflurane. The authors used 27.5 min of bilateral renal artery only clamping, and allowed for 30 h of recovery from IRI [215]. Burne-Taney *et al*. (2005) used RAG-1-/- mice with a background strain of C57BL/6, which underwent 30 min of bilateral renal pedicle clamping, and also RAG-1-/- mice on a BALB/c background that underwent 35 min of bilateral clamping. The mice were anesthetized with intra-peritoneal sodium pentobarbital, and were recovered for 72 h [214]. Day *et al*. (2006) used RAG-1-/- mice on a C57BL/6 background. Mice were anesthetized with intra-peritoneal ketamine and xylazine, and intra-muscular acepromazine. They then clamped the renal pedicles bilaterally for 32 min, and allowed for 24 h of recovery [213]. While all these publications using RAG-1 -/- mice adopted bilateral IRI models, Ferenbach *et al*. (2012) used the same unilateral model described in this thesis. A possible reason for the conflicting results presented in this thesis, is that a 20 min clamp time was used by Ferenbach *et al*. (2012), rather than the 30 min and 32 min clamp times used in Chapter 7, and Chapter 8, respectively [277].

There are further discrepancies in this thesis that call into question the link between increased Hsp70 expression and lymphocyte dependency of the protection from renal IRI offered by AT13387. For instance, it is unclear why in Chapter 5 of this thesis, on immunohistochemistry, Hsp70 induction following AT13387 treatment in the kidney was observed mainly in renal tubular cells rather than in interstitial lymphocyte type cells. It is also uncertain why in Chapter 4, *in vitro* protection from oxidative stress was demonstrable with AT13387 despite the obvious absence of lymphocytes in the cell system used. These inconsistencies may just reflect a multimodal mechanism of protection offered by AT13387, which was anticipated at the outset of this thesis and does not necessarily disprove the importance of lymphocytes in the protective effect of this agent.

#### 10.3.3.1 Future directions

It should be highlighted that the experiments in Chapter 7, involving Balb/c and Balb/c SCID mice groups, were not designed to address the specific question of whether SCID mice are inherently protected from renal IRI. As such, mice from each group (Balb/c and Balb/c SCID) were separately randomised based on type of treatment (AT13387 vs. vehicle). In fact, Balb/c mice underwent their operations first, in order to demonstrate kidney protection from renal IRI following pre-treatment with AT13387. At a later date Balb/c SCID were acquired and then experimented on to specifically assess the importance of lymphocytes in the protective effect of AT13387. A true comparison between Balb/c and Balb/c SCID mice would require proper randomisation specifically for this purpose with experiments performed in each group on the same days. This would ensure that experimental conditions (e.g. room temperature) were identical and would provide a more robust answer to the question of whether SCID mice have an innate protection from renal IRI. Although a rectal temperature probe was used to minimise variation in temperature in the experiments reported in this thesis, even 1–2 degree changes in temperature can markedly alter the degree of injury and its long-term consequences

[17]. Therefore it makes sense to have surgery performed in each group of mice on the same day if possible. These additional experiments should be performed using both 20 min and 30 min clamp times, and bilateral and unilateral models of renal IRI. Consideration should also be given to using different background strains of SCID mice.

As previously mentioned, more experiments should be performed to help understand what subset of lymphocytes or the adaptive immune response involved in the effect of AT13387 may be. Flow cytomtery of blood, spleens and kidneys of mice treated by AT13387 could supplement expansion of the initial immunohistochemistry to a larger group of animals. In addition, more targeted depletion of lymphocyte subsets (e.g. by anti-CD25 antibodies) could also be performed.

It is possible that "add back" experiments involving adoptive transfer of Tregs to SCID mice prior to renal IRI could be considered to assess whether the protective effect of AT13387 is restored in the presence of Tregs. This could establish that Tregs are a critical cell type involved in the protective effect of AT13387 and would further complement the findings of Kim *et al*. (2014) [224]. However, in similar experiments recently performed in Edinburgh by Devey *et al*. (2012), it was unexpectedly found that adoptive transfer of Tregs failed to protect mice from liver IRI [284]. This was explained by an inability to transfer sufficient Tregs to ameliorate injury and suggests difficulties with this approach even in the hands of scientists dedicated to lymphocyte research [284].

Before performing challenging adoptive transfer studies there are also other issues to consider. There is the potential involvement of other cell types, such as macrophages, to contemplate. Indeed, one option would be to carry out monocyte/macrophage depletion experiments first to assess the influence of these cells on the protective

effect of AT13387. These experiments could be performed using an in-house colony of CD11b-DTR mice, which express the human diphtheria toxin receptor under the control of the CD11b promoter. Treatment with diphtheria toxin in these mice induces conditional renal and circulating monocyte/macrophage depletion [42, 240, 265]. Importantly, and in contrast to clodronate, this monocyte/macrophage depletion strategy itself should not lead to any protection from renal IRI, eliminating the need for injury titration [265].

### 10.3.4 Chapter 8

Treating transplant donors raises issues regarding the potential for a detrimental impact on other donor organs by systemic treatments. This possibility must be excluded in the context of donor pre-treatment and multi-organ donation, but may not be an issue if organs share pathways of protection [285]. There are therefore organ-specific issues that need resolved before AT13387, can be implemented in transplantation, as there is the possibility that AT13387 may be beneficial to one organ but not to others. Hsp90 inhibition with geldanamycin has previously been shown to induce Hsp70 levels in the lung and reduce secondary lung injury resulting from haemorrhagic shock [138]. In Chapter 8 of this thesis, AT13387 was additionally shown to induce Hsp70 up-regulation in the lungs of mice, which appeared to provide protection from secondary lung injury caused by both renal IRI in Chapter 8 and then renal transplantation in Chapter 9.

#### 10.3.4.1 Future directions

The experiments in Chapter 8 are again limited since they were performed in SCID mice and did not involve wild-type mice. In the Chapter 9, lung injury was assessed in wild type mice following renal IRI caused by renal transplantation, but only in a

small number of renal transplants (n=2 in the vehicle group). The results of both experiments should therefore be verified in wild type mice and across a larger sample of animals. However, the results still highlight that Hsp90 inhibitors may be protective to both kidneys and lungs, which could represent a particular advantage of Hsp90 inhibitors over other agents. Acute lung injury severe enough to require mechanical ventilation occurs in 2.7% of renal transplantations from extended criteria donors, and results in a 5-fold increase in 1-year mortality. Therefore the lung protective properties of AT13387 could be of clinical relevance in renal transplantation [286]. Nevertheless, it is likely that this avenue of research would be better pursued in different models where the clinical need is greater, such as sepsis induced lung injury or sepsis induced lung injury combined with a head injury ("double hit" model [287]). Due to limitations on the material transfer agreement with Astex for use of AT13387, collaborations are on going with Duncan Humphries to investigate generic Hsp90 inhibitors, including 17-DMAG, in this context.

### 10.3.5 Chapter 9

IRI in the context of transplantation deserves special consideration. During the initial warm ischemic period of organ recovery, hypoxia depletes adenosine triphosphate stores, generates reactive oxygen species and leads to failure of cellular ion exchange. Cold storage during organ transportation reduces metabolic activity and slows cell death, but adds to ischemic tissue damage on reperfusion. Following reperfusion, tissue injury is extensive and the innate immune system is aggressively activated. Inflammatory cells infiltrate the graft and release various cytokines, pro-coagulant factors and further free radicals. Microvascular dysfunction and endothelial binding of leucocytes causes capillary obstruction and exacerbates ischemic damage. Rapid cell death ensues with the release of DAMPs that trigger a profound adaptive immune response. Over the following days repair and regeneration processes occur on a background of resolving inflammation [28, 288]. The IRI model used in previous chapters assessed only a warm ischemic insult, while

the transplant-associated IRI model in Chapter 9 incorporated an additional period of cold ischemia. This experiment is therefore an important step towards translational relevance.

Due to the potential systemic and immunomodulatory nature of the protective effect of AT13387, it was hypothesised that it may be feasible to pre-treat recipient mice with the aim of reducing IRI in a transplanted kidney. This hypothesis was driven by a desire to broaden the range of these therapies to a wider group of patients including renal transplant recipients. In Chapter 9, in the experiment designed to address this hypothesis, no difference in tubular necrosis scores was observed following recipient pre-treatment with AT13387 and isograft renal transplantation. Transplants were performed with a kidney graft that had been harvested from a treatment naive mouse and subjected to cold ischemia for a period of 4 h to cause moderate to severe IRI.

Due to the low numbers of animals used, it is not possible to meaningfully interpret this result. In addition, the utility of serum creatinine, which was the primary outcome measure for all the previous IRI experiments, was reduced by the fact that the model was not transplant-dependent (i.e. the transplanted kidney was not a life-supporting organ [242]). The presence of a single intact native kidney capable of creatinine clearance meant serum creatinine was not a valid outcome measure in this experiment. In renal IRI experiments, preservation of kidney function is arguably a more objective indicator of renal protection than kidney morphology and although the two methods tend to correlate, it is probably more relevant to human disease [289, 290].

The murine transplantation model was designed to primarily assess for features of acute and chronic rejection on histology in the transplanted kidney and the presence of a native kidney in the model ensures a higher survival rate [239, 240, 242]. The

peri-operative mortality rate in the experiments in Chapter 9 across both groups was already high at 56% (9/16). As these deaths occurred within 24 h, they were probably due to technical problems, rather than the prolonged cold ischemic time required to induce moderate to severe IRI, which is normally not necessary in the model. Removing both recipient native kidneys prior to transplantation of a severely injured kidney would have been higher risk. Therefore an alternative would be to leave the native kidney *in situ* long enough to give the graft time to recover e.g. 5 days [242].

#### 10.3.5.1 Future directions

The possibility of modulating immune responses to kidney reperfusion by renal transplant recipients is very attractive. Since therapies that mediate protection from renal IRI entirely through renal parenchymal cells, renal tubular cells or resident leucocytes may necessitate earlier localisation of the treatment to the kidney. This could require donor pre-treatment and hence there will be ethical and logistical barriers to clinical implementation. These barriers include lack of legislation and difficulty establishing consent from both donor and recipient. Therefore treatment of transplant recipients using AT13387 has exciting translational potential and is worthy of further exploration.

The variability inherent in the technically challenging murine transplantation model means that despite observing a moderate effect size for reduction in tubular necrosis score by AT13387 (cohen's d= 0.45), a larger sample would be required to pursue this experiment further. As previously mentioned, altering the model so that the native kidney is left *in situ* long enough to give the graft time to recover, is another option to consider [242] In addition, it would be useful to evaluate further experimental groups, such as donor pre-treated mice, as well as treatment of both donor and recipient with AT13387.

Following a recent successful funding application, this treatment strategy will be also be explored in a larger animal porcine transplantation model, which is currently being developed in Edinburgh. A project licence is currently under review and the plan is for AT13387 to be initially tested in an auto-transplantation model. The larger body size of the pig will allow for surgical procedures that are more technically feasible including transplant dependent models, and will facilitate the collection of peripheral blood for determination of serum creatinine on a repeated basis [291]. The input of veterinary anaesthetists and use of invasive monitoring will additionally lead to less haemodynamic instability during prolonged transplantation procedures, which may be a problem leading to variation and peri-operative death in the murine transplantation model.

## 10.4 Published evidence

Over the past 25 years various agents have been tested in RCTs to assess whether renal transplant related IRI could be reduced. In a double-blinded RCT by Schneeberger *et al*. (1989), recipients of deceased donor kidneys were randomised to receive superoxide dismutase (n=81), a free radical scavenger, or placebo (n=96) infused intravenously prior to reperfusion. There was no difference in early graft function between the groups to suggest that superoxide dismutase prevented the early impact of IRI on the kidney graft [29]. The lack of protection provided by this agent was confirmed in a further RCT by Pollak *et al*. (1993) of 116 patients [30]. However, on four-year follow up of the patients included in the study by Schneeberger *et al*. (1989), graft survival was found to be better in those patients who received superoxide dismutase secondary to a lower incidence of rejection [31].

At the beginning of the 1990s, an open label study by Rabl *et al*. (1993) randomised recipients of deceased donor kidneys to receive omnibionta (n=16), an anti-oxidant therapy intravenously prior to reperfusion, or control (n=14). Creatinine levels were

significantly lower in the omnibionta treatment group but only up to day 6 post-operatively [32]. Noel *et al*. (1997) then performed a double blind RCT of intravenous pentoxifylline, an anti-inflammatory agent, at induction of anaesthesia and for 48 hours post-operatively in 140 patients receiving kidney transplants from deceased donors. Pentoxifylline had no demonstrable effect on ischemic graft injury when compared to placebo [33]. Haug *et al*. (1993) performed an initial phase I trial of 18 patients who received deceased donor kidneys at high risk for DGF and showed that use of an anti-ICAM-1 murine monoclonal antibody, enlimomab, reduced DGF [34]. However, it was later found in a multicentre RCT of 262 patients receiving deceased donor kidneys by Salmela *et al*. (1999) that an intravenous injection of enlimomab 3 hours before transplantation, followed by a single dose for the next 5 days did not reduce DGF when compared to placebo [35].

In the last decade, Hladunewich *et al*. (2003) randomised 43 adult recipients of DBD donor kidneys with reduced creatinine clearance 2 h post-transplant to treatment with insulin-like growth factor, within 5 hours after transplant and twice a day for 6 days following transplant, but observed no difference in graft function compared to placebo [36]. In a study by Fontana *et al*. (2005), 26 recipients of deceased donor kidneys were treated with either dopamine or fenoldopam (dopamine-1 receptor agonist) for 48 hours post-transplant, but there were no significant differences in graft function between the groups [37]. In a multicentre open label study with blinded evaluation of endpoints only, Martinez *et al*. (2010) randomised 104 recipients of deceased donor kidneys at increased risk of DGF to high doses of epoetin beta before surgery and at 12 hours, 7 days and 14 days post transplantation, but found that the frequency of DGF was similar to control [38]. Finally, a Cochrane review has evaluated 13 RCTs with 724 patients, comparing calcium channel blockers via various routes of administration in the peri-transplantation period with controls. The review concluded that calcium channel blockers may reduce the incidence of DGF post-transplantation, but that the results should be treated with caution due to the heterogeneity of the trials [39].

More recently, diannexin, a recombinant form of the endogenous human annexin V protein, was tested in a double blind, placebo-controlled Phase II/III RCT of renal transplant recipients. However, during the second part of the clinical trial participant recruitment was suspended (clinical trials.gov identifier: NCT01442337) with further analysis of pre-clinical toxicology data noted as the reason [40]. Further clinical trials are ongoing with various other novel agents [41]. OPN-305 (Opsona Therapeutics Ltd), a Toll-like receptor-specific monoclonal antibody, is currently under investigation in a multicenter RCT of adult deceased donor renal transplant recipients receiving kidneys at high risk for DGF [40]. Eculizumab, a humanized monoclonal antibody directed against the C5 component of the complement cascade (ClinicalTrials.gov Identifier: NCT01756508, NCT01403389), QPI-1002 (also known as I5NP, Quark Pharmaceuticals), a synthetic siRNA (ClinicalTrials.gov Identifier: NCT00802347) and mirococept, a complement inhibitor (International Standard Randomised Controlled Trial Number: 49958194) are also under investigation [28].

## 10.5 Context

With the increasing use of DCD kidneys for renal transplantation the need to develop pharmacological agents to reduce the impact of IRI has never been greater. Producing pharmacological strategies for reducing IRI is highly challenging at every stage of development from initial experiments using cell culture models, to small animal studies, then large animal investigations and eventually clinical trials. There will clearly be various challenges that will occur when attempting to translate AT13387 from these initial pre-clinical studies to a future clinical trial, and these are worth considering when providing context to the findings of this thesis.

For the majority of treatments of IRI tested thus far, the benefits in terms of early outcomes in relation to better early graft function and prevention of DGF have not

been apparent [41]. The question then becomes, why are promising therapies in pre-clinical studies not translating to significant clinical benefit in human trials? The past decade in particular has seen rapid progress in understanding of the pathophysiology of IRI and still there remains a need to gain yet further mechanistic insight into the vast array of molecular events that occur during IRI [22]. As a consequence, perhaps the most efficacious treatments have not been subject to RCTs in humans yet.

There is also a striking disconnect between experimental animal studies that are typically conducted in young, healthy animals with no comorbidities and the renal transplant population in the UK and abroad. For instance, the median age of a patient requiring a renal transplant in England is 45 years of age and on average 16% have diabetes, 5% have pulmonary disease and 3% have had a myocardial infarction [292].

Furthermore, in many animal studies the agent is administered to the donor prior to the ischemic period (pre-conditioning); in humans, discussions regarding the ethics of this are going, but precedents exist in DBD transplantation. Indeed, the optimum management of DBD donors already encompasses the provision of a range of drugs and infusions to preserve organs in a suitable condition for transplantation. In contrast, pre-treatments in the DCD donor to either precondition organs or optimise the donor, may influence the process leading to death and this is rightly considered unacceptable [231]. Current legislation forbids pre-mortem intervention in DCD donors, and with this limitation in place, pharmacological pre-treatment is not currently possible [14]. Despite this, in the setting of DCD organ recovery, normothermic regional perfusion and normothermic *ex-vivo* perfusion are two emerging techniques that could circumvent these barriers and allow earlier treatment of either the donor or kidney graft with pharmacological agents. There is also the issue of the increasing use of multiple drugs in renal transplantation, with recipients potentially exposed to a number of pharmacological agents that might interact with

the protective pathways under manipulation by test agents [293]. Finally, an absence of long-term follow up in these trials could mean that any long-term impact of therapies have been undetected.

It is clear that the clinical trials that have been conducted over the past 25 years have included relatively small number of patients. This may not allow robust statistical analysis of the efficacy of the agents that have been tested thus far [294]. For instance, one may wish to consider the number of participants that would need to be recruited in order to test whether a pharmacological agent has the efficacy to reduce the current 49% incidence of DGF in DCD kidney transplantation to an incidence more typically observed after DBD kidney transplantation (presently 24% in the UK) [15]. In this example, to have a 90% ($\beta = 0.1$) chance of detecting significance at the 5% level ($\alpha = 0.05$), an RCT would have to recruit 146 patients receiving a DCD kidney transplant (73 per arm of trial). This may not initially sound difficult to achieve, but across 24 transplant centres performing DCD kidney transplants during 2013/14 in UK, the median number of DCD kidney transplants performed per centre was only 31 (range 3 - 98) [10].

An obvious solution to this problem is the organisation of larger multicenter RCTs of the most promising agents. However, there are challenges to be overcome with multicenter trials in the context of transplantation. Clinical protocols may differ vastly between units with regards to donor or recipient criteria, kidney discard rates, *ex-vivo* management of organs and use of preservation fluids. These differences may have to be accepted and a more pragmatic attitude to “real-world” comparisons adopted. Nevertheless, intrinsic variability between units will inevitably lead to the need for even larger sample sizes and increased drug effects. When controlling for differences in donor factors, paired kidney allocation studies designs may reduce variability but these studies are difficult to execute [17].

Another issue in the appropriate sizing and powering of trials is the choice of endpoints. In terms of defining DGF, the need for dialysis is subjective with a variation in threshold for dialysis evident across centers [295]. Some patients may be dialysed mainly for hyperkalaemia rather than uraemia so DGF defined on use of dialysis is not exact. The use of biomarkers of graft injury is also problematic. For example, despite being widely used, serum creatinine is considered a relatively poor biomarker of kidney injury since numerous factors may regulate its generation, volume of distribution and excretion [296]. Although urine output is clinically useful and absence can indicate DGF, urinary biomarkers are limited by graft anuria as well as persistent native kidney diuresis [297]. Clear definitions of graft function are therefore required and should be supplemented with circulating biomarkers of graft injury, such as aspartate transaminase, heart-type fatty acid–binding protein and neutrophil gelatinase–associated lipocalin [297].

AT13387 is a promising agent, and mechanistic insight into the protective mode of action in renal IRI has been acquired in this thesis. However, there is still clearly much to learn about this drug, and many barriers to overcome before it can be tested in human patients in the setting of renal transplantation. Despite this, there is patient safety data already available for AT13387. It is therefore possible that if the data presented in this thesis can be taken be forward, then AT13387 could be more rapidly translated into a RCT in recipients of deceased donor kidneys. This is in comparison to other agents that are at a similar pre-clinical stage of development but lack toxicology data. Indeed, the assessment of drugs that are already in clinical use is an area of future opportunity in renal IRI. A recent example is heme arginate, which is already used in patients to treat porphyria. The fact there is patient safety data already available for heme arginate, has meant that only a few years after it was shown to reduce renal IRI in aged mice, it has already been translated into a RCT in recipients of deceased donor kidneys (ClinicalTrials.gov Identifier: NCT01430156) [42].

## 10.6 Summary

In conclusion, this thesis aimed to establish mechanisms of protection offered by Hsp90 inhibitors in renal IRI and investigate a less toxic analogue that has the potential to be safely translated into human studies. These aims have been achieved as the data presented has demonstrated potential mechanisms of protection offered by these drugs and highlighted a new agent in AT13387 that is capable of reducing both functional and morphological kidney injury following renal IRI. These are novel findings that increase the current understanding of IRI. They also highlight AT13387 as a potentially exciting new therapy for reducing renal IRI and secondary lung injury in various clinical settings including transplantation.

# References


1. Abbasi M, Chertow G, Hall Y. End-stage Renal Disease. *Am Fam Physician* 2010; **82:** 1512.
2. US Renal Data System, USRDS 2013 Annual Data Report: Atlas of Chronic Kidney Disease and End-Stage Renal Disease in the United States, National Institute of Health, National Institute of Diabetes and Digestive and Kidney Diseases, Bethesda, MD, 2013.
3. Roderick P, Davies R, Jones C, Feest T, Smith S, Farrington K. Simulation model of renal replacement therapy: predicting future demand in England. *Nephrol Dial Transplant* 2004; **19:** 692-701.
4. Gilg J, Pruthi R, Fogarty D. UK Renal Registry 17th Annual Report: Chapter 1 UK Renal Replacement Therapy Incidence in 2013: National and Centre-specific Analyses. *Nephron* 2015; **129(suppl 1):** 1-29.
5. Rao A, Casula A, Castledine C. UK Renal Registry 17th Annual Report: Chapter 2 UK Renal Replacement Therapy Prevalence in 2013: National and Centre-specific Analyses. *Nephron* 2015; **129(suppl 1):** 31-56.
6. Wolfe RA, Ashby VB, Milford EL, Ojo AO, Ettenger RE, Agodoa LY, et al. Comparison of mortality in all patients on dialysis, patients on dialysis awaiting transplantation, and recipients of a first cadaveric transplant. *N Engl J Med* 1999; **341:** 1725-30.
7. Ojo AO, Hanson JA, Meier-Kriesche H, Okechukwu CN, Wolfe RA, Leichtman AB, et al. Survival in recipients of marginal cadaveric donor kidneys compared with other recipients and wait-listed transplant candidates. *J Am Soc Nephrol* 2001; **12:** 589-97.
8. Chung R, Howard K, Craig JC, Chapman JR, Turner R, Wong G. Economic evaluations in kidney transplantation: frequency, characteristics, and quality-a systematic review. *Transplantation* 2014; **97:** 1027-33.
9. Tonelli M, Wiebe N, Knoll G, Bello A, Browne S, Jadhav D, et al. Systematic Review: Kidney Transplantation Compared With Dialysis in Clinically Relevant Outcomes. *Am J Transplant* 2011; **11:** 2093-109.
10. NHSBT Transplant Activity in the UK. UK Transplant Registry Activity Report 2013-14. http://www.organdonation.nhs.uk/statistics/transplant_activity_report/. Accessed 23rd of February 2015.
11. Thiruchelvam PT, Willicombe M, Hakim N, Taube D, Papalois V. Renal transplantation. *Bmj* 2011; **343:** d7300.
12. NHSBT. Transplant Activity in the UK. UK Transplant Registry Activity Report 2003-4. http://www.organdonation.nhs.uk/statistics/transplant_activity_report/archive_activity_reports/. Accessed 23rd of February 2015.
13. Rojas-Pena A, Sall LE, Gravel MT, Cooley EG, Pelletier SJ, Bartlett RH. Donation After Circulatory Determination of Death: The University of Michigan Experience With Extracorporeal Support. *Transplantation* 2014

14. Oniscu GC, Randle LV, Muiesan P, Butler AJ, Currie IS, Perera MT, et al. In situ normothermic regional perfusion for controlled donation after circulatory death-the United kingdom experience. *Am J Transplant* 2014; **14:** 2846-54.
15. Summers DM, Johnson RJ, Hudson A, Collett D, Watson CJ, Bradley JA. Effect of donor age and cold storage time on outcome in recipients of kidneys donated after circulatory death in the UK: a cohort study. *Lancet* 2013; **381:** 727-34.
16. Hamed MO, Chen Y, Pasea L, Watson CJ, Torpey N, Bradley JA, et al. Early graft loss after kidney transplantation: risk factors and consequences. *Am J Transplant* 2015; **15:** 1632-43.
17. Cavaille-Coll M, Bala S, Velidedeoglu E, Hernandez A, Archdeacon P, Gonzalez G, et al. Summary of FDA workshop on ischemia reperfusion injury in kidney transplantation. *Am J Transplant* 2013; **13:** 1134-48.
18. Summers DM, Watson CJ, Pettigrew GJ, Johnson RJ, Collett D, Neuberger JM, et al. Kidney donation after circulatory death (DCD): state of the art. *Kidney Int* 2015
19. Yarlagadda SG, Coca SG, Formica RN, Jr., Poggio ED, Parikh CR. Association between delayed graft function and allograft and patient survival: a systematic review and meta-analysis. *Nephrol Dial Transplant* 2009; **24:** 1039-47.
20. Summers DM, Johnson RJ, Allen J, Fuggle SV, Collett D, Watson CJ, et al. Analysis of factors that affect outcome after transplantation of kidneys donated after cardiac death in the UK: a cohort study. *Lancet* 2010; **376:** 1303-11.
21. Summers DM, Counter C, Johnson RJ, Murphy PG, Neuberger JM, Bradley JA. Is the increase in DCD organ donors in the United Kingdom contributing to a decline in DBD donors? *Transplantation* 2010; **90:** 1506-10.
22. Eltzschig HK, Eckle T. Ischemia and reperfusion--from mechanism to translation. *Nat Med* 2011; **17:** 1391-401.
23. Aydin Z, van Zonneveld AJ, de Fijter JW, Rabelink TJ. New horizons in prevention and treatment of ischaemic injury to kidney transplants. *Nephrol Dial Transplant* 2007; **22:** 342-6.
24. Lameire NH, Bagga A, Cruz D, De Maeseneer J, Endre Z, Kellum JA, et al. Acute kidney injury: an increasing global concern. *Lancet* 2013; **382:** 170-9.
25. Sharfuddin AA, Molitoris BA. Pathophysiology of ischemic acute kidney injury. *Nat Rev Nephrol* 2011; **7:** 189-200.
26. Murugan R, Kellum JA. Acute kidney injury: what's the prognosis? *Nat Rev Nephrol* 2011; **7:** 209-17.
27. Murry CE, Jennings RB, Reimer KA. Preconditioning with ischemia: a delay of lethal cell injury in ischemic myocardium. *Circulation* 1986; **74:** 1124-36.
28. Ponticelli C. Ischaemia-reperfusion injury: a major protagonist in kidney transplantation. *Nephrol Dial Transplant* 2014; **29:** 1134-40.
29. Schneeberger H, Illner WD, Abendroth D, Bulkley G, Rutili F, Williams M, et al. First clinical experiences with superoxide dismutase in kidney transplantation--results of a double-blind randomized study. *Transplant Proc* 1989; **21:** 1245-6.

30. Pollak R, Andrisevic JH, Maddux MS, Gruber SA, Paller MS. A randomized double-blind trial of the use of human recombinant superoxide dismutase in renal transplantation. *Transplantation* 1993; **55:** 57-60.
31. Land W, Schneeberger H, Schleibner S, Illner WD, Abendroth D, Rutili G, et al. The beneficial effect of human recombinant superoxide dismutase on acute and chronic rejection events in recipients of cadaveric renal transplants. *Transplantation* 1994; **57:** 211-7.
32. Rabl H, Khoschsorur G, Colombo T, Petritsch P, Rauchenwald M, Koltringer P, et al. A multivitamin infusion prevents lipid peroxidation and improves transplantation performance. *Kidney Int* 1993; **43:** 912-7.
33. Noel C, Hazzan M, Coppin MC, Codaccioni MX, Pruvot FR, Labalette M, et al. A randomized controlled trial of pentoxifylline for the prevention of delayed graft function in cadaveric kidney graft. *Clin Transplant* 1997; **11:** 169-73.
34. Haug CE, Colvin RB, Delmonico FL, Auchincloss H, Jr., Tolkoff-Rubin N, Preffer FI, et al. A phase I trial of immunosuppression with anti-ICAM-1 (CD54) mAb in renal allograft recipients. *Transplantation* 1993; **55:** 766-72; discussion 72-3.
35. Salmela K, Wramner L, Ekberg H, Hauser I, Bentdal O, Lins LE, et al. A randomized multicenter trial of the anti-ICAM-1 monoclonal antibody (enlimomab) for the prevention of acute rejection and delayed onset of graft function in cadaveric renal transplantation: a report of the European Anti-ICAM-1 Renal Transplant Study Group. *Transplantation* 1999; **67:** 729-36.
36. Hladunewich MA, Corrigan G, Derby GC, Ramaswamy D, Kambham N, Scandling JD, et al. A randomized, placebo-controlled trial of IGF-1 for delayed graft function: a human model to study postischemic ARF. *Kidney Int* 2003; **64:** 593-602.
37. Fontana I, Germi MR, Beatini M, Fontana S, Bertocchi M, Porcile E, et al. Dopamine "renal dose" versus fenoldopam mesylate to prevent ischemia-reperfusion injury in renal transplantation. *Transplant Proc* 2005; **37:** 2474-5.
38. Martinez F, Kamar N, Pallet N, Lang P, Durrbach A, Lebranchu Y, et al. High dose epoetin beta in the first weeks following renal transplantation and delayed graft function: Results of the Neo-PDGF Study. *Am J Transplant* 2010; **10:** 1695-700.
39. Shilliday IR, Sherif M. Calcium channel blockers for preventing acute tubular necrosis in kidney transplant recipients. *Cochrane Database Syst Rev* 2007**:** Cd003421.
40. Tsapepas DS, Powell JT, Martin ST, Hardy MA, Ratner LE. An update to managing renal transplant ischemia reperfusion injury: novel therapies in the pipeline. *Clin Transplant* 2013; **27:** 647-8.
41. Powell JT, Tsapepas DS, Martin ST, Hardy MA, Ratner LE. Managing renal transplant ischemia reperfusion injury: novel therapies in the pipeline. *Clin Transplant* 2013; **27:** 484-91.
42. Ferenbach DA, Nkejabega NC, McKay J, Choudhary AK, Vernon MA, Beesley MF, et al. The induction of macrophage hemeoxygenase-1 is protective during acute kidney injury in aging mice. *Kidney Int* 2011; **79:** 966-76.

43. Linkermann A, Brasen JH, Himmerkus N, Liu S, Huber TB, Kunzendorf U, et al. Rip1 (receptor-interacting protein kinase 1) mediates necroptosis and contributes to renal ischemia/reperfusion injury. *Kidney Int* 2012; **81:** 751-61.
44. Linkermann A, Stockwell BR, Krautwald S, Anders HJ. Regulated cell death and inflammation: an auto-amplification loop causes organ failure. *Nat Rev Immunol* 2014; **14:** 759-67.
45. Linkermann A, Green DR. Necroptosis. *N Engl J Med* 2014; **370:** 455-65.
46. Dare AJ, Bolton EA, Pettigrew GJ, Bradley JA, Saeb-Parsy K, Murphy MP. Protection against renal ischemia-reperfusion injury in vivo by the mitochondria targeted antioxidant MitoQ. *Redox Biol* 2015; **5:** 163-8.
47. Trieb K, Dirnhofer S, Krumbock N, Blahovec H, Sgonc R, Margreiter R, et al. Heat shock protein expression in the transplanted human kidney. *Transpl Int* 2001; **14:** 281-6.
48. Borkan SC, Gullans SR. Molecular chaperones in the kidney. *Annu Rev Physiol* 2002; **64:** 503-27.
49. Kampinga HH, Hageman J, Vos MJ, Kubota H, Tanguay RM, Bruford EA, et al. Guidelines for the nomenclature of the human heat shock proteins. *Cell Stress Chaperones* 2009; **14:** 105-11.
50. Kelly KJ. Heat shock (stress response) proteins and renal ischemia/reperfusion injury. *Contrib Nephrol* 2005; **148:** 86-106.
51. Ritossa F. Discovery of the heat shock response. *Cell Stress Chaperones* 1996; **1:** 97-8.
52. Jo SK, Ko GJ, Boo CS, Cho WY, Kim HK. Heat preconditioning attenuates renal injury in ischemic ARF in rats: role of heat-shock protein 70 on NF-kappaB-mediated inflammation and on tubular cell injury. *J Am Soc Nephrol* 2006; **17:** 3082-92.
53. Benjamin IJ, McMillan DR. Stress (heat shock) proteins: molecular chaperones in cardiovascular biology and disease. *Circ Res* 1998; **83:** 117-32.
54. Kaarniranta K, Elo M, Sironen R, Lammi MJ, Goldring MB, Eriksson JE, et al. Hsp70 accumulation in chondrocytic cells exposed to high continuous hydrostatic pressure coincides with mRNA stabilization rather than transcriptional activation. *Proc Natl Acad Sci U S A* 1998; **95:** 2319-24.
55. Gerner EW, Schneider MJ. Induced thermal resistance in HeLa cells. *Nature* 1975; **256:** 500-2.
56. Soti C, Nagy E, Giricz Z, Vigh L, Csermely P, Ferdinandy P. Heat shock proteins as emerging therapeutic targets. *Br J Pharmacol* 2005; **146:** 769-80.
57. Tutar Y. Prelude; cellular mechanics. *Protein Pept Lett* 2009; **16:** 570.
58. Kocabiyik S. Essential structural and functional features of small heat shock proteins in molecular chaperoning process. *Protein Pept Lett* 2009; **16:** 613-22.
59. De Maio A. Extracellular heat shock proteins, cellular export vesicles, and the Stress Observation System: a form of communication during injury, infection, and cell damage. It is never known how far a controversial finding will go! Dedicated to Ferruccio Ritossa. *Cell Stress Chaperones* 2011; **16:** 235-49.
60. Beere HM. "The stress of dying": the role of heat shock proteins in the regulation of apoptosis. *J Cell Sci* 2004; **117:** 2641-51.

61. Aufricht C. Heat-shock protein 70: molecular supertool? *Pediatr Nephrol* 2005; **20:** 707-13.
62. Anckar J, Sistonen L. Heat shock factor 1 as a coordinator of stress and developmental pathways. *Adv Exp Med Biol* 2007; **594:** 78-88.
63. Almeida MB, do Nascimento JL, Herculano AM, Crespo-Lopez ME. Molecular chaperones: toward new therapeutic tools. *Biomed Pharmacother* 2011; **65:** 239-43.
64. Voellmy R. On mechanisms that control heat shock transcription factor activity in metazoan cells. *Cell Stress Chaperones* 2004; **9:** 122-33.
65. Ananthan J, Goldberg AL, Voellmy R. Abnormal proteins serve as eukaryotic stress signals and trigger the activation of heat shock genes. *Science* 1986; **232:** 522-4.
66. Csermely P, Schnaider T, Soti C, Prohaszka Z, Nardai G. The 90-kDa molecular chaperone family: structure, function, and clinical applications. A comprehensive review. *Pharmacol Ther* 1998; **79:** 129-68.
67. Tutar L, Tutar Y. Heat shock proteins; an overview. *Curr Pharm Biotechnol* 2010; **11:** 216-22.
68. Buchner J. Hsp90 & Co. - a holding for folding. *Trends Biochem Sci* 1999; **24:** 136-41.
69. Bagatell R, Whitesell L. Altered Hsp90 function in cancer: a unique therapeutic opportunity. *Mol Cancer Ther* 2004; **3:** 1021-30.
70. Chatterjee A, Dimitropoulou C, Drakopanayiotakis F, Antonova G, Snead C, Cannon J, et al. Heat shock protein 90 inhibitors prolong survival, attenuate inflammation, and reduce lung injury in murine sepsis. *Am J Respir Crit Care Med* 2007; **176:** 667-75.
71. Hahn JS. The Hsp90 chaperone machinery: from structure to drug development. *BMB Rep* 2009; **42:** 623-30.
72. Bharadwaj S, Ali A, Ovsenek N. Multiple components of the HSP90 chaperone complex function in regulation of heat shock factor 1 In vivo. *Mol Cell Biol* 1999; **19:** 8033-41.
73. Madrigal-Matute J, Lopez-Franco O, Blanco-Colio LM, Munoz-Garcia B, Ramos-Mozo P, Ortega L, et al. Heat shock protein 90 inhibitors attenuate inflammatory responses in atherosclerosis. *Cardiovasc Res* 2010; **86:** 330-7.
74. Pearl LH, Prodromou C. Structure and mechanism of the Hsp90 molecular chaperone machinery. *Annu Rev Biochem* 2006; **75:** 271-94.
75. Dutta R, Inouye M. GHKL, an emergent ATPase/kinase superfamily. *Trends Biochem Sci* 2000; **25:** 24-8.
76. Neckers L, Workman P. Hsp90 molecular chaperone inhibitors: are we there yet? *Clin Cancer Res* 2012; **18:** 64-76.
77. Zou J, Guo Y, Guettouche T, Smith DF, Voellmy R. Repression of heat shock transcription factor HSF1 activation by HSP90 (HSP90 complex) that forms a stress-sensitive complex with HSF1. *Cell* 1998; **94:** 471-80.
78. Hegde RS, Zuo J, Voellmy R, Welch WJ. Short circuiting stress protein expression via a tyrosine kinase inhibitor, herbimycin A. *J Cell Physiol* 1995; **165:** 186-200.
79. Uehara Y, Hori M, Takeuchi T, Umezawa H. Screening of agents which convert 'transformed morphology' of Rous sarcoma virus-infected rat kidney

cells to 'normal morphology': identification of an active agent as herbimycin and its inhibition of intracellular src kinase. *Jpn J Cancer Res* 1985; **76:** 672-5.
80. Uehara Y, Hori M, Takeuchi T, Umezawa H. Phenotypic change from transformed to normal induced by benzoquinonoid ansamycins accompanies inactivation of p60src in rat kidney cells infected with Rous sarcoma virus. *Mol Cell Biol* 1986; **6:** 2198-206.
81. Whitesell L, Mimnaugh EG, De Costa B, Myers CE, Neckers LM. Inhibition of heat shock protein HSP90-pp60v-src heteroprotein complex formation by benzoquinone ansamycins: essential role for stress proteins in oncogenic transformation. *Proc Natl Acad Sci U S A* 1994; **91:** 8324-8.
82. Trepel J, Mollapour M, Giaccone G, Neckers L. Targeting the dynamic HSP90 complex in cancer. *Nat Rev Cancer* 2010; **10:** 537-49.
83. Kim YS, Alarcon SV, Lee S, Lee MJ, Giaccone G, Neckers L, et al. Update on Hsp90 inhibitors in clinical trial. *Curr Top Med Chem* 2009; **9:** 1479-92.
84. Harrison EM, Sharpe E, Bellamy CO, McNally SJ, Devey L, Garden OJ, et al. Heat shock protein 90-binding agents protect renal cells from oxidative stress and reduce kidney ischemia-reperfusion injury. *Am J Physiol Renal Physiol* 2008; **295:** F397-405.
85. Sonoda H, Prachasilchai W, Kondo H, Yokota-Ikeda N, Oshikawa S, Ito K, et al. The protective effect of radicicol against renal ischemia--reperfusion injury in mice. *J Pharmacol Sci* 2010; **112:** 242-6.
86. Dello Russo C, Polak PE, Mercado PR, Spagnolo A, Sharp A, Murphy P, et al. The heat-shock protein 90 inhibitor 17-allylamino-17-demethoxygeldanamycin suppresses glial inflammatory responses and ameliorates experimental autoimmune encephalomyelitis. *J Neurochem* 2006; **99:** 1351-62.
87. Poulaki V, Iliaki E, Mitsiades N, Mitsiades CS, Paulus YN, Bula DV, et al. Inhibition of Hsp90 attenuates inflammation in endotoxin-induced uveitis. *FASEB J* 2007; **21:** 2113-23.
88. Rice JW, Veal JM, Fadden RP, Barabasz AF, Partridge JM, Barta TE, et al. Small molecule inhibitors of Hsp90 potently affect inflammatory disease pathways and exhibit activity in models of rheumatoid arthritis. *Arthritis Rheum* 2008; **58:** 3765-75.
89. Yun TJ, Harning EK, Giza K, Rabah D, Li P, Arndt JW, et al. EC144, a synthetic inhibitor of heat shock protein 90, blocks innate and adaptive immune responses in models of inflammation and autoimmunity. *J Immunol* 2011; **186:** 563-75.
90. Madrigal-Matute J, Fernandez-Garcia CE, Gomez-Guerrero C, Lopez-Franco O, Munoz-Garcia B, Egido J, et al. HSP90 inhibition by 17-DMAG attenuates oxidative stress in experimental atherosclerosis. *Cardiovasc Res* 2012; **95:** 116-23.
91. Geller R, Taguwa S, Frydman J. Broad action of Hsp90 as a host chaperone required for viral replication. *Biochim Biophys Acta* 2012; **1823:** 698-706.
92. Wirk B. Heat shock protein inhibitors for the treatment of fungal infections. *Recent Pat Antiinfect Drug Discov* 2011; **6:** 38-44.

93. Peterson LB, Blagg BS. To fold or not to fold: modulation and consequences of Hsp90 inhibition. *Future Med Chem* 2009; **1:** 267-83.
94. Gartner EM, Silverman P, Simon M, Flaherty L, Abrams J, Ivy P, et al. A phase II study of 17-allylamino-17-demethoxygeldanamycin in metastatic or locally advanced, unresectable breast cancer. *Breast Cancer Res Treat* 2012; **131:** 933-7.
95. Ramanathan RK, Egorin MJ, Erlichman C, Remick SC, Ramalingam SS, Naret C, et al. Phase I pharmacokinetic and pharmacodynamic study of 17-dimethylaminoethylamino-17-demethoxygeldanamycin, an inhibitor of heat-shock protein 90, in patients with advanced solid tumors. *J Clin Oncol* 2010; **28:** 1520-6.
96. Soga S, Akinaga S, Shiotsu Y. Hsp90 inhibitors as anti-cancer agents, from basic discoveries to clinical development. *Curr Pharm Des* 2013; **19:** 366-76.
97. Samuni Y, Ishii H, Hyodo F, Samuni U, Krishna MC, Goldstein S, et al. Reactive oxygen species mediate hepatotoxicity induced by the Hsp90 inhibitor geldanamycin and its analogs. *Free Radic Biol Med* 2010; **48:** 1559-63.
98. Duerfeldt AS, Peterson LB, Maynard JC, Ng CL, Eletto D, Ostrovsky O, et al. Development of a Grp94 inhibitor. *J Am Chem Soc* 2012; **134:** 9796-804.
99. Graham B, Curry J, Smyth T, Fazal L, Feltell R, Harada I, et al. The heat shock protein 90 inhibitor, AT13387, displays a long duration of action in vitro and in vivo in non-small cell lung cancer. *Cancer Sci* 2012; **103:** 522-7.
100. Mahadevan D, Shapiro G, Kurtin SE, Cleary JM, Lyons JF, Rodriguez-Lopez A, et al. Activity of AT13387, a novel, non-ansamycin inhibitor of heat shock protein 90, against gastrointestinal stromal tumors (GIST). *Journal of Clinical Oncology* 2013; **31:** abstr 105.
101. Woodhead AJ, Angove H, Carr MG, Chessari G, Congreve M, Coyle JE, et al. Discovery of (2,4-dihydroxy-5-isopropylphenyl)-[5-(4-methylpiperazin-1-ylmethyl)-1,3-dihydrois oindol-2-yl]methanone (AT13387), a novel inhibitor of the molecular chaperone Hsp90 by fragment based drug design. *J Med Chem* 2010; **53:** 5956-69.
102. Zhang PL, Lun M, Schworer CM, Blasick TM, Masker KK, Jones JB, et al. Heat shock protein expression is highly sensitive to ischemia-reperfusion injury in rat kidneys. *Ann Clin Lab Sci* 2008; **38:** 57-64.
103. Perdrizet GA, Heffron TG, Buckingham FC, Salciunas PJ, Gaber AO, Stuart FP, et al. Stress conditioning: a novel approach to organ preservation. *Curr Surg* 1989; **46:** 23-6.
104. Perdrizet GA, Kaneko H, Buckley TM, Fishman MS, Pleau M, Bow L, et al. Heat shock and recovery protects renal allografts from warm ischemic injury and enhances HSP72 production. *Transplant Proc* 1993; **25:** 1670-3.
105. Wagner M, Cadetg P, Ruf R, Mazzucchelli L, Ferrari P, Redaelli CA. Heme oxygenase-1 attenuates ischemia/reperfusion-induced apoptosis and improves survival in rat renal allografts. *Kidney Int* 2003; **63:** 1564-73.
106. Redaelli CA, Tien YH, Kubulus D, Mazzucchelli L, Schilling MK, Wagner AC. Hyperthermia preconditioning induces renal heat shock protein expression, improves cold ischemia tolerance, kidney graft function and survival in rats. *Nephron* 2002; **90:** 489-97.

107. Redaelli CA, Wagner M, Kulli C, Tian YH, Kubulus D, Mazzucchelli L, et al. Hyperthermia-induced HSP expression correlates with improved rat renal isograft viability and survival in kidneys harvested from non-heart-beating donors. *Transpl Int* 2001; **14:** 351-60.
108. Suzuki S, Maruyama S, Sato W, Morita Y, Sato F, Miki Y, et al. Geranylgeranylacetone ameliorates ischemic acute renal failure via induction of Hsp70. *Kidney Int* 2005; **67:** 2210-20.
109. Fuller TF, Rose F, Singleton KD, Linde Y, Hoff U, Freise CE, et al. Glutamine donor pretreatment in rat kidney transplants with severe preservation reperfusion injury. *J Surg Res* 2007; **140:** 77-83.
110. Zhang Y, Zou Z, Li YK, Yuan HB, Shi XY. Glutamine-induced heat shock protein protects against renal ischaemia-reperfusion injury in rats. *Nephrology (Carlton)* 2009; **14:** 573-80.
111. Yang CW, Kim BS, Kim J, Ahn HJ, Park JH, Jin DC, et al. Preconditioning with sodium arsenite inhibits apoptotic cell death in rat kidney with ischemia/reperfusion or cyclosporine-induced Injuries. The possible role of heat-shock protein 70 as a mediator of ischemic tolerance. *Exp Nephrol* 2001; **9:** 284-94.
112. Yang CW, Ahn HJ, Han HJ, Kim WY, Li C, Shin MJ, et al. Pharmacological preconditioning with low-dose cyclosporine or FK506 reduces subsequent ischemia/reperfusion injury in rat kidney. *Transplantation* 2001; **72:** 1753-9.
113. Yeh CH, Hsu SP, Yang CC, Chien CT, Wang NP. Hypoxic preconditioning reinforces HIF-alpha-dependent HSP70 signaling to reduce ischemic renal failure-induced renal tubular apoptosis and autophagy. *Life Sci* 2010; **86:** 115-23.
114. Kim YO, Li C, Sun BK, Kim JS, Lim SW, Choi BS, et al. Preconditioning with 1,25-dihydroxyvitamin D3 protects against subsequent ischemia-reperfusion injury in the rat kidney. *Nephron Exp Nephrol* 2005; **100:** e85-94.
115. Yang CW, Li C, Jung JY, Shin SJ, Choi BS, Lim SW, et al. Preconditioning with erythropoietin protects against subsequent ischemia-reperfusion injury in rat kidney. *FASEB J* 2003; **17:** 1754-5.
116. Park KM, Kramers C, Vayssier-Taussat M, Chen A, Bonventre JV. Prevention of kidney ischemia/reperfusion-induced functional injury, MAPK and MAPK kinase activation, and inflammation by remote transient ureteral obstruction. *J Biol Chem* 2002; **277:** 2040-9.
117. Stacchiotti A, Bonomini F, Favero G, Rossini C, Rodella LF, Rezzani R. Stress proteins in experimental nephrotoxicity: a ten year experience. *Ital J Anat Embryol* 2010; **115:** 153-8.
118. Wang Z, Gall JM, Bonegio RG, Havasi A, Hunt CR, Sherman MY, et al. Induction of heat shock protein 70 inhibits ischemic renal injury. *Kidney Int* 2011; **79:** 861-70.
119. Hayden MS, Ghosh S. NF-kappaB in immunobiology. *Cell Res* 2011; **21:** 223-44.
120. Jing H, Lee S. NF-kappaB in cellular senescence and cancer treatment. *Mol Cells* 2014; **37:** 189-95.
121. Zhang H, Burrows F. Targeting multiple signal transduction pathways through inhibition of Hsp90. *J Mol Med (Berl)* 2004; **82:** 488-99.

122. Furuichi K, Wada T, Yokoyama H, Kobayashi KI. Role of Cytokines and Chemokines in Renal Ischemia-Reperfusion Injury. *Drug News Perspect* 2002; **15:** 477-82.
123. Chen F, Castranova V, Shi X. New insights into the role of nuclear factor-kappaB in cell growth regulation. *Am J Pathol* 2001; **159:** 387-97.
124. Lee JI, Burckart GJ. Nuclear factor kappa B: important transcription factor and therapeutic target. *J Clin Pharmacol* 1998; **38:** 981-93.
125. Salminen A, Paimela T, Suuronen T, Kaarniranta K. Innate immunity meets with cellular stress at the IKK complex: regulation of the IKK complex by HSP70 and HSP90. *Immunol Lett* 2008; **117:** 9-15.
126. Isaacs JS, Xu W, Neckers L. Heat shock protein 90 as a molecular target for cancer therapeutics. *Cancer Cell* 2003; **3:** 213-7.
127. Israel A. The IKK complex, a central regulator of NF-kappaB activation. *Cold Spring Harb Perspect Biol* 2010; **2:** a000158.
128. Li Q, Verma IM. NF-kappaB regulation in the immune system. *Nat Rev Immunol* 2002; **2:** 725-34.
129. Hayden MS, Ghosh S. Signaling to NF-kappaB. *Genes Dev* 2004; **18:** 2195-224.
130. Brandt GE, Blagg BS. Alternate strategies of Hsp90 modulation for the treatment of cancer and other diseases. *Curr Top Med Chem* 2009; **9:** 1447-61.
131. Lewis J, Devin A, Miller A, Lin Y, Rodriguez Y, Neckers L, et al. Disruption of hsp90 function results in degradation of the death domain kinase, receptor-interacting protein (RIP), and blockage of tumor necrosis factor-induced nuclear factor-kappaB activation. *J Biol Chem* 2000; **275:** 10519-26.
132. Malhotra V, Shanley TP, Pittet JF, Welch WJ, Wong HR. Geldanamycin inhibits NF-kappaB activation and interleukin-8 gene expression in cultured human respiratory epithelium. *Am J Respir Cell Mol Biol* 2001; **25:** 92-7.
133. Chen G, Cao P, Goeddel DV. TNF-induced recruitment and activation of the IKK complex require Cdc37 and Hsp90. *Mol Cell* 2002; **9:** 401-10.
134. Broemer M, Krappmann D, Scheidereit C. Requirement of Hsp90 activity for IkappaB kinase (IKK) biosynthesis and for constitutive and inducible IKK and NF-kappaB activation. *Oncogene* 2004; **23:** 5378-86.
135. Lee KH, Jang Y, Chung JH. Heat shock protein 90 regulates IkappaB kinase complex and NF-kappaB activation in angiotensin II-induced cardiac cell hypertrophy. *Exp Mol Med* 2010; **42:** 703-11.
136. Pittet JF, Lee H, Pespeni M, O'Mahony A, Roux J, Welch WJ. Stress-induced inhibition of the NF-kappaB signaling pathway results from the insolubilization of the IkappaB kinase complex following its dissociation from heat shock protein 90. *J Immunol* 2005; **174:** 384-94.
137. Chen LW, Egan L, Li ZW, Greten FR, Kagnoff MF, Karin M. The two faces of IKK and NF-kappaB inhibition: prevention of systemic inflammation but increased local injury following intestinal ischemia-reperfusion. *Nat Med* 2003; **9:** 575-81.
138. Pittet JF, Lu LN, Geiser T, Lee H, Matthay MA, Welch WJ. Stress preconditioning attenuates oxidative injury to the alveolar epithelium of the lung following haemorrhage in rats. *J Physiol* 2002; **538:** 583-97.

139. Hendrick JP, Hartl FU. Molecular chaperone functions of heat-shock proteins. *Annu Rev Biochem* 1993; **62:** 349-84.
140. Riordan M, Sreedharan R, Wang S, Thulin G, Mann A, Stankewich M, et al. HSP70 binding modulates detachment of Na-K-ATPase following energy deprivation in renal epithelial cells. *Am J Physiol Renal Physiol* 2005; **288:** F1236-42.
141. Marber MS, Mestril R, Chi SH, Sayen MR, Yellon DM, Dillmann WH. Overexpression of the rat inducible 70-kD heat stress protein in a transgenic mouse increases the resistance of the heart to ischemic injury. *J Clin Invest* 1995; **95:** 1446-56.
142. Trost SU, Omens JH, Karlon WJ, Meyer M, Mestril R, Covell JW, et al. Protection against myocardial dysfunction after a brief ischemic period in transgenic mice expressing inducible heat shock protein 70. *J Clin Invest* 1998; **101:** 855-62.
143. Nanasi PP, Jednakovits A. Multilateral in vivo and in vitro protective effects of the novel heat shock protein coinducer, bimoclomol: results of preclinical studies. *Cardiovasc Drug Rev* 2001; **19:** 133-51.
144. Lubbers NL, Polakowski JS, Wegner CD, Burke SE, Diaz GJ, Daniell KM, et al. Oral bimoclomol elevates heat shock protein 70 and reduces myocardial infarct size in rats. *Eur J Pharmacol* 2002; **435:** 79-83.
145. Jednakovits A, Ferdinandy P, Jaszlits L, Banyasz T, Magyar J, Szigligeti P, et al. In vivo and in vitro acute cardiovascular effects of bimoclomol. *Gen Pharmacol* 2000; **34:** 363-9.
146. Richter K, Haslbeck M, Buchner J. The heat shock response: life on the verge of death. *Mol Cell* 2010; **40:** 253-66.
147. Feinstein DL, Galea E, Aquino DA, Li GC, Xu H, Reis DJ. Heat shock protein 70 suppresses astroglial-inducible nitric-oxide synthase expression by decreasing NFkappaB activation. *J Biol Chem* 1996; **271:** 17724-32.
148. Yoo CG, Lee S, Lee CT, Kim YW, Han SK, Shim YS. Anti-inflammatory effect of heat shock protein induction is related to stabilization of I kappa B alpha through preventing I kappa B kinase activation in respiratory epithelial cells. *J Immunol* 2000; **164:** 5416-23.
149. Tang D, Kang R, Xiao W, Wang H, Calderwood SK, Xiao X. The anti-inflammatory effects of heat shock protein 72 involve inhibition of high-mobility-group box 1 release and proinflammatory function in macrophages. *J Immunol* 2007; **179:** 1236-44.
150. Ran R, Lu A, Zhang L, Tang Y, Zhu H, Xu H, et al. Hsp70 promotes TNF-mediated apoptosis by binding IKK gamma and impairing NF-kappa B survival signaling. *Genes Dev* 2004; **18:** 1466-81.
151. Weiss YG, Bromberg Z, Raj N, Raphael J, Goloubinoff P, Ben-Neriah Y, et al. Enhanced heat shock protein 70 expression alters proteasomal degradation of IkappaB kinase in experimental acute respiratory distress syndrome. *Crit Care Med* 2007; **35:** 2128-38.
152. Russo GL, Russo M, Spagnuolo C, Tedesco I, Bilotto S, Iannitti R, et al. Quercetin: a pleiotropic kinase inhibitor against cancer. *Cancer treatment and research* 2014; **159:** 185-205.

153. Borges TJ, Wieten L, van Herwijnen MJ, Broere F, van der Zee R, Bonorino C, et al. The anti-inflammatory mechanisms of Hsp70. *Front Immunol* 2012; **3:** 95.
154. Kaushal GP. Autophagy protects proximal tubular cells from injury and apoptosis. *Kidney Int* 2012; **82:** 1250-3.
155. Yang Y, Fiskus W, Yong B, Atadja P, Takahashi Y, Pandita TK, et al. Acetylated hsp70 and KAP1-mediated Vps34 SUMOylation is required for autophagosome creation in autophagy. *Proc Natl Acad Sci U S A* 2013; **110:** 6841-6.
156. Eleftheriadis T, Lawson BR. Toll-like receptors and kidney diseases. *Inflamm Allergy Drug Targets* 2009; **8:** 191-201.
157. Tominaga K. The emerging role of senescent cells in tissue homeostasis and pathophysiology. *Pathobiol Aging Age Relat Dis* 2015; **5:** 27743.
158. Elmore S. Apoptosis: a review of programmed cell death. *Toxicol Pathol* 2007; **35:** 495-516.
159. Price PM, Safirstein RL, Megyesi J. The cell cycle and acute kidney injury. *Kidney Int* 2009; **76:** 604-13.
160. Lanneau D, Brunet M, Frisan E, Solary E, Fontenay M, Garrido C. Heat shock proteins: essential proteins for apoptosis regulation. *J Cell Mol Med* 2008; **12:** 743-61.
161. Fagone P, Di Rosa M, Palumbo M, De Gregorio C, Nicoletti F, Malaguarnera L. Modulation of heat shock proteins during macrophage differentiation. *Inflamm Res* 2012; **61:** 1131-9.
162. Robson MG. Toll-like receptors and renal disease. *Nephron Exp Nephrol* 2009; **113:** e1-7.
163. Medzhitov R, Preston-Hurlburt P, Janeway CA, Jr. A human homologue of the Drosophila Toll protein signals activation of adaptive immunity. *Nature* 1997; **388:** 394-7.
164. Verstrepen L, Bekaert T, Chau TL, Tavernier J, Chariot A, Beyaert R. TLR-4, IL-1R and TNF-R signaling to NF-kappaB: variations on a common theme. *Cell Mol Life Sci* 2008; **65:** 2964-78.
165. Johnson GB, Brunn GJ, Platt JL. Activation of mammalian Toll-like receptors by endogenous agonists. *Crit Rev Immunol* 2003; **23:** 15-44.
166. Anders HJ, Banas B, Schlondorff D. Signaling danger: toll-like receptors and their potential roles in kidney disease. *J Am Soc Nephrol* 2004; **15:** 854-67.
167. Kim BS, Lim SW, Li C, Kim JS, Sun BK, Ahn KO, et al. Ischemia-reperfusion injury activates innate immunity in rat kidneys. *Transplantation* 2005; **79:** 1370-7.
168. Wu H, Chen G, Wyburn KR, Yin J, Bertolino P, Eris JM, et al. TLR4 activation mediates kidney ischemia/reperfusion injury. *J Clin Invest* 2007; **117:** 2847-59.
169. Wolfs TG, Buurman WA, van Schadewijk A, de Vries B, Daemen MA, Hiemstra PS, et al. In vivo expression of Toll-like receptor 2 and 4 by renal epithelial cells: IFN-gamma and TNF-alpha mediated up-regulation during inflammation. *J Immunol* 2002; **168:** 1286-93.

170. Pulskens WP, Teske GJ, Butter LM, Roelofs JJ, van der Poll T, Florquin S, et al. Toll-like receptor-4 coordinates the innate immune response of the kidney to renal ischemia/reperfusion injury. *PLoS One* 2008; **3:** e3596.
171. Lorne E, Dupont H, Abraham E. Toll-like receptors 2 and 4: initiators of non-septic inflammation in critical care medicine? *Intensive Care Med* 2010; **36:** 1826-35.
172. Chen J, Hartono JR, John R, Bennett M, Zhou XJ, Wang Y, et al. Early interleukin 6 production by leukocytes during ischemic acute kidney injury is regulated by TLR4. *Kidney Int* 2011; **80:** 504-15.
173. Liu M, Gu M, Xu D, Lv Q, Zhang W, Wu Y. Protective effects of Toll-like receptor 4 inhibitor eritoran on renal ischemia-reperfusion injury. *Transplant Proc* 2010; **42:** 1539-44.
174. Leemans JC, Stokman G, Claessen N, Rouschop KM, Teske GJ, Kirschning CJ, et al. Renal-associated TLR2 mediates ischemia/reperfusion injury in the kidney. *J Clin Invest* 2005; **115:** 2894-903.
175. Shigeoka AA, Holscher TD, King AJ, Hall FW, Kiosses WB, Tobias PS, et al. TLR2 is constitutively expressed within the kidney and participates in ischemic renal injury through both MyD88-dependent and -independent pathways. *J Immunol* 2007; **178:** 6252-8.
176. Rusai K, Sollinger D, Baumann M, Wagner B, Strobl M, Schmaderer C, et al. Toll-like receptors 2 and 4 in renal ischemia/reperfusion injury. *Pediatr Nephrol* 2010; **25:** 853-60.
177. Goligorsky MS. TLR4 and HMGB1: partners in crime? *Kidney Int* 2011; **80:** 450-2.
178. Kruger B, Krick S, Dhillon N, Lerner SM, Ames S, Bromberg JS, et al. Donor Toll-like receptor 4 contributes to ischemia and reperfusion injury following human kidney transplantation. *Proc Natl Acad Sci U S A* 2009; **106:** 3390-5.
179. Lu CY, Penfield JG, Kielar ML, Vazquez MA, Jeyarajah DR. Hypothesis: is renal allograft rejection initiated by the response to injury sustained during the transplant process? *Kidney Int* 1999; **55:** 2157-68.
180. Asea A, Rehli M, Kabingu E, Boch JA, Bare O, Auron PE, et al. Novel signal transduction pathway utilized by extracellular HSP70: role of toll-like receptor (TLR) 2 and TLR4. *J Biol Chem* 2002; **277:** 15028-34.
181. Ohashi K, Burkart V, Flohe S, Kolb H. Cutting edge: heat shock protein 60 is a putative endogenous ligand of the toll-like receptor-4 complex. *J Immunol* 2000; **164:** 558-61.
182. Vabulas RM, Ahmad-Nejad P, Ghose S, Kirschning CJ, Issels RD, Wagner H. HSP70 as endogenous stimulus of the Toll/interleukin-1 receptor signal pathway. *J Biol Chem* 2002; **277:** 15107-12.
183. Zou N, Ao L, Cleveland JC, Jr., Yang X, Su X, Cai GY, et al. Critical role of extracellular heat shock cognate protein 70 in the myocardial inflammatory response and cardiac dysfunction after global ischemia-reperfusion. *Am J Physiol Heart Circ Physiol* 2008; **294:** H2805-13.
184. Henderson B, Calderwood SK, Coates AR, Cohen I, van Eden W, Lehner T, et al. Caught with their PAMPs down? The extracellular signalling actions of

molecular chaperones are not due to microbial contaminants. *Cell Stress Chaperones* 2010; **15:** 123-41.
185. de Jong PR, Schadenberg AW, Jansen NJ, Prakken BJ. Hsp70 and cardiac surgery: molecular chaperone and inflammatory regulator with compartmentalized effects. *Cell Stress Chaperones* 2009; **14:** 117-31.
186. Tsan MF, Gao B. Heat shock proteins and immune system. *J Leukoc Biol* 2009; **85:** 905-10.
187. Shi Y, Rock KL. Cell death releases endogenous adjuvants that selectively enhance immune surveillance of particulate antigens. *Eur J Immunol* 2002; **32:** 155-62.
188. Asea A. Heat shock proteins and toll-like receptors. *Handb Exp Pharmacol* 2008; **183:** 111-27.
189. Goh YC, Yap CT, Huang BH, Cronshaw AD, Leung BP, Lai PB, et al. Heat-shock protein 60 translocates to the surface of apoptotic cells and differentiated megakaryocytes and stimulates phagocytosis. *Cell Mol Life Sci* 2011; **68:** 1581-92.
190. Cahill CM, Waterman WR, Xie Y, Auron PE, Calderwood SK. Transcriptional repression of the prointerleukin 1beta gene by heat shock factor 1. *J Biol Chem* 1996; **271:** 24874-9.
191. Asea A. Mechanisms of HSP72 release. *J Biosci* 2007; **32:** 579-84.
192. Zhu J, Quyyumi AA, Wu H, Csako G, Rott D, Zalles-Ganley A, et al. Increased serum levels of heat shock protein 70 are associated with low risk of coronary artery disease. *Arterioscler Thromb Vasc Biol* 2003; **23:** 1055-9.
193. Dulin E, Garcia-Barreno P, Guisasola MC. Extracellular heat shock protein 70 (HSPA1A) and classical vascular risk factors in a general population. *Cell Stress Chaperones* 2010; **15:** 929-37.
194. Zhang X, Xu Z, Zhou L, Chen Y, He M, Cheng L, et al. Plasma levels of Hsp70 and anti-Hsp70 antibody predict risk of acute coronary syndrome. *Cell Stress Chaperones* 2010; **15:** 675-86.
195. Oehler R, Pusch E, Zellner M, Dungel P, Hergovics N, Homoncik M, et al. Cell type-specific variations in the induction of hsp70 in human leukocytes by feverlike whole body hyperthermia. *Cell Stress Chaperones* 2001; **6:** 306-15.
196. Schroder O, Schulte KM, Ostermann P, Roher HD, Ekkernkamp A, Laun RA. Heat shock protein 70 genotypes HSPA1B and HSPA1L influence cytokine concentrations and interfere with outcome after major injury. *Crit Care Med* 2003; **31:** 73-9.
197. Temple SE, Cheong KY, Ardlie KG, Sayer D, Waterer GW. The septic shock associated HSPA1B1267 polymorphism influences production of HSPA1A and HSPA1B. *Intensive Care Med* 2004; **30:** 1761-7.
198. Matzinger P. Tolerance, danger, and the extended family. *Annu Rev Immunol* 1994; **12:** 991-1045.
199. Srivastava P. Interaction of heat shock proteins with peptides and antigen presenting cells: chaperoning of the innate and adaptive immune responses. *Annu Rev Immunol* 2002; **20:** 395-425.

200. Ferenbach DA, Bonventre JV. Mechanisms of maladaptive repair after AKI leading to accelerated kidney ageing and CKD. *Nat Rev Nephrol* 2015; **11:** 264-76.
201. Franceschi C, Campisi J. Chronic inflammation (inflammaging) and its potential contribution to age-associated diseases. *J Gerontol A Biol Sci Med Sci* 2014; **69 Suppl 1:** S4-9.
202. Tchkonia T, Zhu Y, van Deursen J, Campisi J, Kirkland JL. Cellular senescence and the senescent secretory phenotype: therapeutic opportunities. *J Clin Invest* 2013; **123:** 966-72.
203. Njemini R, Lambert M, Demanet C, Kooijman R, Mets T. Basal and infection-induced levels of heat shock proteins in human aging. *Biogerontology* 2007; **8:** 353-64.
204. Njemini R, Bautmans I, Onyema OO, Van Puyvelde K, Demanet C, Mets T. Circulating heat shock protein 70 in health, aging and disease. *BMC Immunol* 2011; **12:** 24.
205. Ramirez V, Uribe N, Garcia-Torres R, Castro C, Rubio J, Gamba G, et al. Upregulation and intrarenal redistribution of heat shock proteins 90alpha and 90beta by low-sodium diet in the rat. *Cell Stress Chaperones* 2004; **9:** 198-206.
206. Ramirez V, Mejia-Vilet JM, Hernandez D, Gamba G, Bobadilla NA. Radicicol, a heat shock protein 90 inhibitor, reduces glomerular filtration rate. *Am J Physiol Renal Physiol* 2008; **295:** F1044-51.
207. Barrera-Chimal J, Perez-Villalva R, Ortega JA, Uribe N, Gamba G, Cortes-Gonzalez C, et al. Intra-renal transfection of heat shock protein 90 alpha or beta (Hsp90alpha or Hsp90beta) protects against ischemia/reperfusion injury. *Nephrol Dial Transplant* 2014; **29:** 301-12.
208. Bonventre JV, Yang L. Cellular pathophysiology of ischemic acute kidney injury. *J Clin Invest* 2011; **121:** 4210-21.
209. Kinsey GR, Okusa MD. Role of leukocytes in the pathogenesis of acute kidney injury. *Crit Care* 2012; **16:** 214.
210. Linfert D, Chowdhry T, Rabb H. Lymphocytes and ischemia-reperfusion injury. *Transplant Rev (Orlando)* 2009; **23:** 1-10.
211. Burne MJ, Daniels F, El Ghandour A, Mauiyyedi S, Colvin RB, O'Donnell MP, et al. Identification of the CD4(+) T cell as a major pathogenic factor in ischemic acute renal failure. *J Clin Invest* 2001; **108:** 1283-90.
212. Satpute SR, Park JM, Jang HR, Agreda P, Liu M, Gandolfo MT, et al. The role for T cell repertoire/antigen-specific interactions in experimental kidney ischemia reperfusion injury. *J Immunol* 2009; **183:** 984-92.
213. Day YJ, Huang L, Ye H, Li L, Linden J, Okusa MD. Renal ischemia-reperfusion injury and adenosine 2A receptor-mediated tissue protection: the role of CD4+ T cells and IFN-gamma. *J Immunol* 2006; **176:** 3108-14.
214. Burne-Taney MJ, Yokota-Ikeda N, Rabb H. Effects of combined T- and B-cell deficiency on murine ischemia reperfusion injury. *Am J Transplant* 2005; **5:** 1186-93.
215. Park P, Haas M, Cunningham PN, Bao L, Alexander JJ, Quigg RJ. Injury in renal ischemia-reperfusion is independent from immunoglobulins and T lymphocytes. *Am J Physiol Renal Physiol* 2002; **282:** F352-7.

216. Burne-Taney MJ, Ascon DB, Daniels F, Racusen L, Baldwin W, Rabb H. B cell deficiency confers protection from renal ischemia reperfusion injury. *J Immunol* 2003; **171:** 3210-5.
217. Renner B, Strassheim D, Amura CR, Kulik L, Ljubanovic D, Glogowska MJ, et al. B cell subsets contribute to renal injury and renal protection after ischemia/reperfusion. *J Immunol* 2010; **185:** 4393-400.
218. Gandolfo MT, Jang HR, Bagnasco SM, Ko GJ, Agreda P, Satpute SR, et al. Foxp3+ regulatory T cells participate in repair of ischemic acute kidney injury. *Kidney Int* 2009; **76:** 717-29.
219. Monteiro RM, Camara NO, Rodrigues MM, Tzelepis F, Damiao MJ, Cenedeze MA, et al. A role for regulatory T cells in renal acute kidney injury. *Transpl Immunol* 2009; **21:** 50-5.
220. Lai LW, Yong KC, Lien YH. Pharmacologic recruitment of regulatory T cells as a therapy for ischemic acute kidney injury. *Kidney Int* 2012; **81:** 983-92.
221. Kinsey GR, Sharma R, Huang L, Li L, Vergis AL, Ye H, et al. Regulatory T cells suppress innate immunity in kidney ischemia-reperfusion injury. *J Am Soc Nephrol* 2009; **20:** 1744-53.
222. Kinsey GR, Huang L, Vergis AL, Li L, Okusa MD. Regulatory T cells contribute to the protective effect of ischemic preconditioning in the kidney. *Kidney Int* 2010; **77:** 771-80.
223. de Zoeten EF, Wang L, Butler K, Beier UH, Akimova T, Sai H, et al. Histone deacetylase 6 and heat shock protein 90 control the functions of Foxp3(+) T-regulatory cells. *Mol Cell Biol* 2011; **31:** 2066-78.
224. Kim MG, Jung Cho E, Won Lee J, Sook Ko Y, Young Lee H, Jo SK, et al. The heat-shock protein-70-induced renoprotective effect is partially mediated by CD4(+)CD25(+)Foxp3(+) regulatory T cells in ischemia/reperfusion-induced acute kidney injury. *Kidney Int* 2014; **85:** 62-71.
225. Kinsey GR, Huang L, Jaworska K, Khutsishvili K, Becker DA, Ye H, et al. Autocrine adenosine signaling promotes regulatory T cell-mediated renal protection. *J Am Soc Nephrol* 2012; **23:** 1528-37.
226. de Zoeten EF, Wang L, Sai H, Dillmann WH, Hancock WW. Inhibition of HDAC9 increases T regulatory cell function and prevents colitis in mice. *Gastroenterology* 2010; **138:** 583-94.
227. Wever KE, Menting TP, Rovers M, van der Vliet JA, Rongen GA, Masereeuw R, et al. Ischemic preconditioning in the animal kidney, a systematic review and meta-analysis. *PLoS One* 2012; **7:** e32296.
228. Zimmerman RF, Ezeanuna PU, Kane JC, Cleland CD, Kempananjappa TJ, Lucas FL, et al. Ischemic preconditioning at a remote site prevents acute kidney injury in patients following cardiac surgery. *Kidney Int* 2011; **80:** 861-7.
229. Gurusamy KS, Kumar Y, Sharma D, Davidson BR. Ischaemic preconditioning for liver transplantation. *Cochrane Database Syst Rev* 2008**:** CD006315.
230. Hosgood SA, van Heurn E, Nicholson ML. Normothermic machine perfusion of the kidney: better conditioning and repair? *Transpl Int* 2014

231. McNally SJ, Harrison EM, Wigmore SJ. Ethical considerations in the application of preconditioning to solid organ transplantation. *J Med Ethics* 2005; **31:** 631-4.
232. Gandolfo MT, Jang HR, Bagnasco SM, Ko GJ, Agreda P, Soloski MJ, et al. Mycophenolate mofetil modifies kidney tubular injury and Foxp3+ regulatory T cell trafficking during recovery from experimental ischemia-reperfusion. *Transpl Immunol* 2010; **23:** 45-52.
233. Bidmon B, Kratochwill K, Rusai K, Kuster L, Herzog R, Eickelberg O, et al. Increased immunogenicity is an integral part of the heat shock response following renal ischemia. *Cell Stress Chaperones* 2012; **17:** 385-97.
234. Hoste EA, De Corte W. Clinical consequences of acute kidney injury. *Contrib Nephrol* 2011; **174:** 56-64.
235. Keijzer C, Wieten L, van Herwijnen M, van der Zee R, Van Eden W, Broere F. Heat shock proteins are therapeutic targets in autoimmune diseases and other chronic inflammatory conditions. *Expert Opin Ther Targets* 2012; **16:** 849-57.
236. van Eden W, van Herwijnen M, Wagenaar J, van Kooten P, Broere F, van der Zee R. Stress proteins are used by the immune system for cognate interactions with anti-inflammatory regulatory T cells. *FEBS Lett* 2013; **587:** 1951-8.
237. Harrison EM, McNally SJ, Devey L, Garden OJ, Ross JA, Wigmore SJ. Insulin induces heme oxygenase-1 through the phosphatidylinositol 3-kinase/Akt pathway and the Nrf2 transcription factor in renal cells. *FEBS J* 2006; **273:** 2345-56.
238. Hesketh EE, Czopek A, Clay M, Borthwick G, Ferenbach D, Kluth D, et al. Renal ischaemia reperfusion injury: a mouse model of injury and regeneration. *J Vis Exp* 2014
239. Tse GH, Hesketh EE, Clay M, Borthwick G, Hughes J, Marson LP. Mouse kidney transplantation: models of allograft rejection. *J Vis Exp* 2014**:** e52163.
240. Qi F, Adair A, Ferenbach D, Vass DG, Mylonas KJ, Kipari T, et al. Depletion of cells of monocyte lineage prevents loss of renal microvasculature in murine kidney transplantation. *Transplantation* 2008; **86:** 1267-74.
241. Farrar CA, Zhou W, Lin T, Sacks SH. Local extravascular pool of C3 is a determinant of postischemic acute renal failure. *FASEB J* 2006; **20:** 217-26.
242. Tse GH, Hughes J, Marson LP. Systematic review of mouse kidney transplantation. *Transpl Int* 2013; **26:** 1149-60.
243. Borner U, Szasz G, Bablok W, Busch EW. [A specific fully enzymatic method for creatinine: reference values in serum (author's transl)]. *J Clin Chem Clin Biochem* 1979; **17:** 679-82.
244. Schneider CA, Rasband WS, Eliceiri KW. NIH Image to ImageJ: 25 years of image analysis. *Nat Methods* 2012; **9:** 671-5.
245. Faul F, Erdfelder E, Lang AG, Buchner A. G*Power 3: a flexible statistical power analysis program for the social, behavioral, and biomedical sciences. *Behav Res Methods* 2007; **39:** 175-91.
246. Hughes MA, Green CS, Lowchyj L, Lee GM, Grippe VK, Smith MF, Jr., et al. MyD88-dependent signaling contributes to protection following Bacillus

anthracis spore challenge of mice: implications for Toll-like receptor signaling. *Infect Immun* 2005; **73:** 7535-40.
247. Thomas P, Smart TG. HEK293 cell line: a vehicle for the expression of recombinant proteins. *Journal of pharmacological and toxicological methods* 2005; **51:** 187-200.
248. Meldrum KK, Zhang H, Hile KL, Moldower LL, Dong Z, Meldrum DR. Profibrotic effect of interleukin-18 in HK-2 cells is dependent on stimulation of the Toll-like receptor 4 (TLR4) promoter and increased TLR4 expression. *J Biol Chem* 2012; **287:** 40391-9.
249. Qing G, Yan P, Xiao G. Hsp90 inhibition results in autophagy-mediated proteasome-independent degradation of IkappaB kinase (IKK). *Cell Res* 2006; **16:** 895-901.
250. Kastelic T, Schnyder J, Leutwiler A, Traber R, Streit B, Niggli H, et al. Induction of rapid IL-1 beta mRNA degradation in THP-1 cells mediated through the AU-rich region in the 3'UTR by a radicicol analogue. *Cytokine* 1996; **8:** 751-61.
251. Hsu HY, Wu HL, Tan SK, Li VP, Wang WT, Hsu J, et al. Geldanamycin interferes with the 90-kDa heat shock protein, affecting lipopolysaccharide-mediated interleukin-1 expression and apoptosis within macrophages. *Mol Pharmacol* 2007; **71:** 344-56.
252. Ryan MJ, Johnson G, Kirk J, Fuerstenberg SM, Zager RA, Torok-Storb B. HK-2: an immortalized proximal tubule epithelial cell line from normal adult human kidney. *Kidney Int* 1994; **45:** 48-57.
253. Pfaller W, Gstraunthaler G. Nephrotoxicity testing in vitro--what we know and what we need to know. *Environ Health Perspect* 1998; **106 Suppl 2:** 559-69.
254. Valente MJ, Henrique R, Costa VL, Jeronimo C, Carvalho F, Bastos ML, et al. A rapid and simple procedure for the establishment of human normal and cancer renal primary cell cultures from surgical specimens. *PLoS One* 2011; **6:** e19337.
255. Gresch O, Altrogge L. Transfection of difficult-to-transfect primary mammalian cells. *Methods Mol Biol* 2012; **801:** 65-74.
256. Galvao J, Davis B, Tilley M, Normando E, Duchen MR, Cordeiro MF. Unexpected low-dose toxicity of the universal solvent DMSO. *FASEB J* 2014; **28:** 1317-30.
257. Noiri E, Nakao A, Uchida K, Tsukahara H, Ohno M, Fujita T, et al. Oxidative and nitrosative stress in acute renal ischemia. *Am J Physiol Renal Physiol* 2001; **281:** F948-57.
258. Ryter SW, Kim HP, Hoetzel A, Park JW, Nakahira K, Wang X, et al. Mechanisms of cell death in oxidative stress. *Antioxid Redox Signal* 2007; **9:** 49-89.
259. Gulden M, Jess A, Kammann J, Maser E, Seibert H. Cytotoxic potency of H2O2 in cell cultures: impact of cell concentration and exposure time. *Free Radic Biol Med* 2010; **49:** 1298-305.
260. Nortcliffe A, Ekstrom AG, Black JR, Ross JA, Habib FK, Botting NP, et al. Synthesis and biological evaluation of nitric oxide-donating analogues of sulindac for prostate cancer treatment. *Bioorg Med Chem* 2014; **22:** 756-61.

261. Davies J. Engineered renal tissue as a potential platform for pharmacokinetic and nephrotoxicity testing. *Drug discovery today* 2014; **19:** 725-9.
262. Kipari T, Cailhier JF, Ferenbach D, Watson S, Houlberg K, Walbaum D, et al. Nitric oxide is an important mediator of renal tubular epithelial cell death in vitro and in murine experimental hydronephrosis. *Am J Pathol* 2006; **169:** 388-99.
263. Eiseman JL, Lan J, Lagattuta TF, Hamburger DR, Joseph E, Covey JM, et al. Pharmacokinetics and pharmacodynamics of 17-demethoxy 17-[[(2-dimethylamino)ethyl]amino]geldanamycin (17DMAG, NSC 707545) in C.B-17 SCID mice bearing MDA-MB-231 human breast cancer xenografts. *Cancer Chemother Pharmacol* 2005; **55:** 21-32.
264. Whitesell L, Bagatell R, Falsey R. The stress response: implications for the clinical development of hsp90 inhibitors. *Current cancer drug targets* 2003; **3:** 349-58.
265. Ferenbach DA, Sheldrake TA, Dhaliwal K, Kipari TM, Marson LP, Kluth DC, et al. Macrophage/monocyte depletion by clodronate, but not diphtheria toxin, improves renal ischemia/reperfusion injury in mice. *Kidney Int* 2012; **82:** 928-33.
266. Tian B, Nowak DE, Jamaluddin M, Wang S, Brasier AR. Identification of direct genomic targets downstream of the nuclear factor-kappaB transcription factor mediating tumor necrosis factor signaling. *J Biol Chem* 2005; **280:** 17435-48.
267. Zhou A, Scoggin S, Gaynor RB, Williams NS. Identification of NF-kappa B-regulated genes induced by TNFalpha utilizing expression profiling and RNA interference. *Oncogene* 2003; **22:** 2054-64.
268. Burne MJ, Haq M, Matsuse H, Mohapatra S, Rabb H. Genetic susceptibility to renal ischemia reperfusion injury revealed in a murine model. *Transplantation* 2000; **69:** 1023-5.
269. Delbridge MS, Shrestha BM, Raftery AT, El Nahas AM, Haylor JL. The effect of body temperature in a rat model of renal ischemia-reperfusion injury. *Transplant Proc* 2007; **39:** 2983-5.
270. Charlton JR, Portilla D, Okusa MD. A basic science view of acute kidney injury biomarkers. *Nephrol Dial Transplant* 2014; **29:** 1301-11.
271. McGlynn LM, Eller K, MacDonald AI, Macintyre A, Russell D, Koppelstaetter C, et al. Pathfinder cells provide a novel therapeutic intervention for acute kidney injury. *Rejuvenation Res* 2013; **16:** 11-20.
272. Wang E, Meier DJ, Sandoval RM, Von Hendy-Willson VE, Pressler BM, Bunch RM, et al. A portable fiberoptic ratiometric fluorescence analyzer provides rapid point-of-care determination of glomerular filtration rate in large animals. *Kidney Int* 2012; **81:** 112-7.
273. Wang E, Sandoval RM, Campos SB, Molitoris BA. Rapid diagnosis and quantification of acute kidney injury using fluorescent ratio-metric determination of glomerular filtration rate in the rat. *Am J Physiol Renal Physiol* 2010; **299:** F1048-55.
274. Miura M, Fu X, Zhang QW, Remick DG, Fairchild RL. Neutralization of Gro alpha and macrophage inflammatory protein-2 attenuates renal ischemia/reperfusion injury. *Am J Pathol* 2001; **159:** 2137-45.

275. Koo GC, Hasan A, O'Reilly RJ. Use of humanized severe combined immunodeficient mice for human vaccine development. *Expert review of vaccines* 2009; **8:** 113-20.
276. Xue C, Liu Y, Li C, Li Y, Yang T, Xie L, et al. Powerful protection against renal ischemia reperfusion injury by T cell-specific NF-kappaB inhibition. *Transplantation* 2014; **97:** 391-6.
277. Ferenbach DA, Kluth DC, Hughes J. Involvement of IgM natural antibodies in renal ischaemia reperfusion injury: a potential new therapeutic target? *Transplant International* 2012; **25:** 1-34.
278. Doi K, Ishizu T, Fujita T, Noiri E. Lung injury following acute kidney injury: kidney-lung crosstalk. *Clin Exp Nephrol* 2011; **15:** 464-70.
279. Feng B, Chen G, Zheng X, Sun H, Zhang X, Zhang ZX, et al. Small interfering RNA targeting RelB protects against renal ischemia-reperfusion injury. *Transplantation* 2009; **87:** 1283-9.
280. Cao CC, Ding XQ, Ou ZL, Liu CF, Li P, Wang L, et al. In vivo transfection of NF-kappaB decoy oligodeoxynucleotides attenuate renal ischemia/reperfusion injury in rats. *Kidney Int* 2004; **65:** 834-45.
281. Wan X, Fan L, Hu B, Yang J, Li X, Chen X, et al. Small interfering RNA targeting IKKbeta prevents renal ischemia-reperfusion injury in rats. *Am J Physiol Renal Physiol* 2011; **300:** F857-63.
282. Viana R, Aguado C, Esteban I, Moreno D, Viollet B, Knecht E, et al. Role of AMP-activated protein kinase in autophagy and proteasome function. *Biochem Biophys Res Commun* 2008; **369:** 964-8.
283. Bosma GC, Fried M, Custer RP, Carroll A, Gibson DM, Bosma MJ. Evidence of functional lymphocytes in some (leaky) scid mice. *J Exp Med* 1988; **167:** 1016-33.
284. Devey LR, Richards JA, O'Connor RA, Borthwick G, Clay S, Howie AF, et al. Ischemic preconditioning in the liver is independent of regulatory T cell activity. *PLoS One* 2012; **7:** e49647.
285. de Rougemont O, Lehmann K, Clavien PA. Preconditioning, organ preservation, and postconditioning to prevent ischemia-reperfusion injury to the liver. *Liver Transpl* 2009; **15:** 1172-82.
286. Yuan H, Tuttle-Newhall JE, Dy-Liacco M, Schnitzler MA, Dzebisashvili N, Xiao H, et al. Clinical correlates, outcomes and healthcare costs associated with early mechanical ventilation after kidney transplantation. *Am J Surg* 2013; **206:** 686-92.
287. Mascia L. Acute lung injury in patients with severe brain injury: a double hit model. *Neurocrit Care* 2009; **11:** 417-26.
288. Kosieradzki M, Rowinski W. Ischemia/reperfusion injury in kidney transplantation: mechanisms and prevention. *Transplant Proc* 2008; **40:** 3279-88.
289. Rosen S, Heyman SN. Difficulties in understanding human "acute tubular necrosis": limited data and flawed animal models. *Kidney Int* 2001; **60:** 1220-4.
290. Parekh DJ, Weinberg JM, Ercole B, Torkko KC, Hilton W, Bennett M, et al. Tolerance of the human kidney to isolated controlled ischemia. *J Am Soc Nephrol* 2013; **24:** 506-17.

291. Giraud S, Favreau F, Chatauret N, Thuillier R, Maiga S, Hauet T. Contribution of large pig for renal ischemia-reperfusion and transplantation studies: the preclinical model. *J Biomed Biotechnol* 2011; **2011:** 532127.
292. Karim A, Farrugia D, Cheshire J, Mahboob S, Begaj I, Ray D, et al. Recipient age and risk for mortality after kidney transplantation in England. *Transplantation* 2014; **97:** 832-8.
293. McCafferty K, Byrne C, Yaqoob MM. Ischaemic conditioning strategies for the nephrologist: a promise lost in translation? *Nephrol Dial Transplant* 2014; **29:** 1827-40.
294. Callaghan CJ, Charman SC, Muiesan P, Powell JJ, Gimson AE, van der Meulen JH. Outcomes of transplantation of livers from donation after circulatory death donors in the UK: a cohort study. *BMJ open* 2013; **3:** e003287.
295. Daly PJ, Power RE, Healy DA, Hickey DP, Fitzpatrick JM, Watson RW. Delayed graft function: a dilemma in renal transplantation. *BJU Int* 2005; **96:** 498-501.
296. Jo SK, Rosner MH, Okusa MD. Pharmacologic treatment of acute kidney injury: why drugs haven't worked and what is on the horizon. *Clin J Am Soc Nephrol* 2007; **2:** 356-65.
297. Jochmans I, Lerut E, van Pelt J, Monbaliu D, Pirenne J. Circulating AST, H-FABP, and NGAL are early and accurate biomarkers of graft injury and dysfunction in a preclinical model of kidney transplantation. *Ann Surg* 2011; **254:** 784-91; discussion 91-2.

# Abbreviations

ESRD – End-stage renal disease

DBD - Donation after brain death

DCD – Donation after circulatory death

IRI - Ischemia-reperfusion injury

DGF – Delayed graft function

RCT - Randomised controlled trials

Hsp90 - Heat shock protein 90

HSF1 - Heat shock transcription factor 1

17-AAG - 17-allylamino-17-demethoxygeldanamycin

17-DMAG - 17-dimethylamino-ethylamino-17-demethoxygeldanamycin

IKK - IkappaB (IκB) kinase

NF-κB - NF-kappaB

TNFα - Tumour necrosis factor-alpha

TLR4 - Toll-like receptor 4

LPS – Lipopolysaccharide

HMGB1 - High mobility group box 1

IL – Interleukin

INF-γ - interferon-γ

Tregs – Regulatory T cell

HEK293 - Human embryonic kidney cells 293

SCID – Severe combined immunodeficient

DMSO - Dimethyl sulfoxide

2HβC - (2-Hydroxypropyl)-β-cyclodextrin

AICAR - 5-aminoimidazole-4-carboxyamideribonucleoside

BSA - Bovine serum albumin

FITC - Fluorescein isothiocyanate

RFUs - Relative fluorescence units

GAPDH - glyceraldehyde 3-phosphate dehydrogenase

PBS - Phosphate buffered saline

BAL - Broncho-alveolar lavage

RPMI - Roswell park memorial institute medium

ACK - Ammonium-chloride-potassium

TBS - Tris buffered saline

ANOVA - Analysis of variance

CXCL1 - chemokine (C-X-C motif) ligand 1

CXCL2 - chemokine (C-X-C motif) ligand 2

RBCs – red blood cells

# Presentations of data from this thesis

The Role of Heat Shock Protein 90 in Modulating Ischemia-Reperfusion Injury in the Kidney. Edinburgh School of Surgery Prize Day Chiene Medal Session Winner. Edinburgh - November 30th 2012.

Heat Shock Protein 90 inhibition abrogates TLR4-mediated NF-κB activity and reduces renal ischemia-reperfusion injury. International Surgical Congress. Association of Surgeons of Great Britain and Ireland (ASGBI). Moynihan Prize Session Winner. Glasgow – May 2nd 2013.

Heat shock protein 90 inhibition with AT13387 abrogates TLR4-mediated NF-κB activity and protects from oxidative stress. 2nd International Meeting on Ischemia Reperfusion Injury in Transplantation. Poitiers – April 24th 2014.

# Publication of data from this thesis

Publications

1. O'Neill S, Ross JA, Wigmore SJ, Harrison EM. The role of heat shock protein 90 in modulating ischemia-reperfusion injury in the kidney. *Expert Opinion on Investigational Drugs* 2012; **21** (10): 1535-1548.
2. O'Neill S, Hughes J. Heat-shock protein-70 and regulatory T cell-mediated protection from ischemic injury. *Kidney International* 2014; **85** (1): 5-7.
3. O'Neill S, Harrison EM, Ross JA, Wigmore SJ, Hughes J. Heat-Shock Proteins and Acute Ischaemic Kidney Injury. *Nephron Experimental Nephrology* 2014; **126** (4): 167-174.
4. O'Neill S, Gallagher K, Hughes J, Wigmore SJ, Ross JA, Harrison EM. Challenges in early clinical drug development for ischemia-reperfusion injury in kidney transplantation. *Expert Opinion on Drug Discovery* 2015; **10** (7): 753-762.
5. O'Neill S, Humphries D, Tse GH, Marson LP, Dhaliwal K, Hughes J, Ross JA, Wigmore SJ, Harrison EM. Heat shock protein 90 inhibition abrogates TLR4-mediated NF-κB activity and reduces renal ischemia-reperfusion injury. *Scientific Reports* 2015; **7** (5): 12958.

Abstracts

1. O'Neill S, Hughes J, Ross JA, Wigmore SJ, Harrison EM. Heat shock protein 90 inhibition abrogates TLR4-mediated NF-κB activity and reduces renal ischemia-reperfusion injury. *British Journal of Surgery* 2013; **100** (S7): 2.
2. O'Neill S, Hughes J, Ross JA, Wigmore SJ, Harrison EM. Heat shock protein 90 inhibition with AT13387 abrogates TLR4-mediated NF-κB activity and protects from oxidative stress. *Transplant International* 2014; **27** (S1): 4.